

INcreasing Safety in NPPs by Covering Gaps in Environmental Fatigue Assessment

INCEFA-PLUS findings on Environmental Fatigue



INCEFA-PLUS Consortium, 2020



This project has received funding from the Euratom Research & Training Programme 2014-2018 under grant agreement n° 662320.

**INCEFA-PLUS: INcreasing Safety in NPPs by Covering Gaps in Environmental Fatigue
Assessment**

INCEFA-PLUS FINDINGS ON ENVIRONMENTAL FATIGUE

Copyright Notice:

©INCEFA-PLUS Consortium, 2020.

ISBN: 978-84-09-24496-6

<https://incefaplus.unican.es/>

Edited by INCEFA-PLUS Project.

Editors:

- Sergio Cicero
- Isabela Procopio
- Sergio Arrieta



INCEFA-PLUS findings on Environmental Fatigue by INCEFA-PLUS Consortium is licensed under CC BY-NC-ND 4.0. To view a copy of this license, visit <https://creativecommons.org/licenses/by-nc-nd/4.0>

Reproduction of this document and its content, in part or in whole, is authorised, provided the source is acknowledged, save where otherwise stated.



This project has received funding from the Euratom Research & Training Programme 2014-2018 under grant agreement n° 662320.

Foreword

This document constitutes a Reference Book compiling the research developed within the INCEFA-PLUS Project¹. It provides a comprehensive overview of the tasks performed, and it also presents the background and the assumptions taken to develop the INCEFA-PLUS experimental and analytical works.

The document compiles and orders documents and contributions from INCEFA-PLUS partners. Therefore, it constitutes a joint effort. The main contributors in the different chapters are conveniently acknowledged at the beginning of the corresponding sections.

Authors/Contributors (alphabetical order):

Arrieta, Sergio (CIEMAT/University of Cantabria)
Austin, Tim (JRC)
Bruchhausen, Matthias (JRC)
Chitty, Walter-John (IRSN)
Cicero, Román (Inesco)
Cicero, Sergio (University of Cantabria)
Cuvilliez, Sam (EDF)
De Baglion, Laurent (Framatome)
Dundulis, Gintautas (LEI)
Gourdin, Cédric (CEA)
Huotilainen, Caitlin (VTT)
Le Roux, Jean-Christophe (EDF)
Mann, Jonathan (Rolls-Royce)
Mayinger, Wolfgang (PreussenElektra)
McLennan, Alec (Jacobs)
Métais, Thomas (EDF)
Miroslava, Ernestova (UJV-Rez)
Mottershead, Kevin (Jacobs)
Novotny, Radek (JRC)
Perosanz López, Francisco Javier (CIEMAT)
Platts, Norman (Jacobs)
Procopio, Isabela (University of Cantabria)
Prompt, Nicolas (EDF)
Spätig, Philippe (PSI)
Twite, Marius (Rolls-Royce)
Vankeerberghen, Marc (SCK-CEN)

¹ CORDIS: <https://cordis.europa.eu/project/id/662320>.

Editor's note:

The analysis and conclusions contained in this document are based on the data available in June 2020. For the latest updates until the end of the INCEFA-PLUS Project (October 2020), please consult:

- MDPI Metals 2020, Special Issue "Environmental Fatigue Assessment of Metallic Materials and Components".
- INCEFA-SCALE Project (<https://incefascal.unican.es/>).

Manuscript completed in October 2020.

1st edition.

NCEFA-PLUS: Increasing Safety in NPPs by Covering Gaps in Environmental Fatigue Assessment

Index:

Chapter 1	Introduction to INCEFA-PLUS Project.....	9
1.1	Overview	9
1.2	Concept and objectives	10
	References	13
Chapter 2	Previous situation: existing methods for analysing EAF.....	15
2.1	Overview	15
2.2	Review of existing methods for analysing fatigue database and resulting fatigue models in the Nuclear Industry	16
2.2.1	Former fatigue curves	16
2.2.2	NUREG/CR-6909.....	18
2.2.3	ASME Code-Cases.....	20
2.2.4	EN-13445	21
2.2.5	RCC-M Approach	24
2.2.6	DCFS Approach.....	25
2.2.7	KTA approach	27
2.2.8	Summary of existing methods.....	28
2.3	New possible approaches	30
2.3.1	Data fitting equation	30
2.3.2	Fatigue curve	30
2.3.3	Gap between laboratory and component.....	31
2.3.4	Mean stress	31
2.3.5	Environmental effects	31
2.4	Conclusions	32
	References	32
Chapter 3	INCEFA-PLUS experimental programme	35
3.1	Ensuring data quality: Testing Protocol, Expert Panel and MatDB.....	35
3.2	Experimental phases and results	36
3.2.1	Phase I	38
3.2.2	Phase II	39
3.2.3	Phase III	41
	References	46

Chapter 4	Statistical analysis.....	49
4.1	Introduction	49
4.2	Approach #1: analysing the data using a statistical linear model.....	50
4.2.1	Data used.....	50
4.2.2	Description of the model used	52
4.2.3	Discussion of the main programme data	57
4.2.4	Analysis of low F_{en} data	58
4.2.5	Conclusion for approach #1	61
4.3	Approach #2: analysing the data using residual plots and null hypothesis testing	62
4.3.1	Manual examination of the fatigue data obtained on the common material	62
4.3.2	Two-samples hypothesis testing for assessing statistical significance of surface finish effect	74
4.4	Bringing both approaches on a comparable basis	78
4.4.1	Best-fit curve	79
4.4.2	Surface roughness correction	79
4.4.3	Environmental effects	80
4.4.4	Conclusion	81
4.5	Analysis of the data generated during specific complementary testing campaigns ..	81
4.5.1	Analysis of the data generated during the mean stress programme	81
4.5.2	Analysis of the data generated during the hold time programme	89
4.5.3	Fatigue data contributed by PreussenElektra.....	95
4.6	Conclusions of statistical analysis	97
4.7	Impact of using fatigue data generated from multiple specimen geometries	98
4.7.1	Methodology	99
4.7.2	Results and discussion.....	103
4.8	Quantifying lab-to-lab scatter for solid specimen data	110
	References	112
Chapter 5	INCEFA-PLUS data evaluation againsts existing fatigue assessment procedures...	115
5.1	Introduction	115
5.2	Theoretical background of the $F_{en-threshold}$ Code-Case proposal.....	116
5.3	Quantification of the $F_{en-threshold}$ using the INCEFA-PLUS PWR data generated on rough specimens.....	121
5.4	Conclusion	126
	References	127

Chapter 6	Conclusions.....	129
6.1	Test campaing	129
6.2	Statistical treatment.....	130
6.3	Data scattering impact	132
6.4	INCEFA-PLUS data evaluation against NUREG/CR-6909	133
	References	133
Annexes	135

This page intentionally left blank.

CHAPTER 1 INTRODUCTION TO INCEFA-PLUS PROJECT

This Chapter is based on the document “Increasing Safety in NPPs by Covering gaps in Environmental Assessment“ [1.1], developed by the INCEFA Consortium.

1.1 OVERVIEW

The nuclear industry faces many important challenges. Among them, the long-term operation (LTO) of existing Nuclear Power Plants (NPPs), ensuring safety issues, and the development of new safe efficient NPPs, are surely two of the most relevant ones. Safety is therefore a common objective in both scenarios, and this requires an adequate management of in-service components and innovative designs for the new ones.

In this sense, when dealing with safety issues in NPPs, fatigue of materials is always a key issue. Moreover, concerning this phenomenon, it has been observed that there are currently several significant gaps when performing fatigue assessments, with empirical observations and theoretical questions that have not been properly addressed. The effect of factors such as the mean stress, hold time periods or surface roughness are of particular relevance. Current knowledge of these factors and their corresponding effects on fatigue performance provide uncertain results in some cases, with non-well defined load conditions, and over-conservative assessments in other cases, none failure due to low cycle fatigue has been reported in existing light water reactors [1.2].

The fatigue ageing of the materials used in NPPs is caused by transients that produce variable stresses and strains in the structural components. Due to the intrinsic characteristics of these transients, loading conditions are often subjected to hold periods and/or take place with a given level of mean stress/mean strain. Also, the lower roughness found in laboratory specimens when compared to that existing in the real components of NPPs, suggests that it might be useful to offset the corresponding under-conservatism in the material data by using a correction (constant) factor. The effects of all these parameters had not been studied sufficiently when the INCEFA-PLUS Project started in 2015, and the data available at that time suggested that they could play a vital role in the material behaviour and, therefore, in the safe management and license renewal of NPPs.

The INCEFA-PLUS Project analysed the effects of all these factors, considering the typical environment existing in NPPs, and provided an updated and upgraded body of knowledge concerning Environmental Fatigue Assessment (EFA) in NPPs.

The members of the project are:

- Centro de Investigaciones Energéticas, Medioambientales y Tecnológicas (CIEMAT) – Spain.
- Commissariat à l’Energie Atomique et aux Energies Alternatives (CEA) – France.
- Electricité de France (EDF) – France.
- European Commission, Joint Research Centre (JRC) – The Netherlands.

- Framatome (FRM) – France.
- Inesco Ingenieros (INI) – Spain.
- Institut de Radioprotection et de Sûreté Nucléaire (IRSN) – France.
- Jacobs (JCB) – United Kingdom.
- Lithuanian Energy Institute (LEI) – Lithuania.
- Paul Scherrer Institute (PSI) – Switzerland.
- PreussenElektra (PEL) – Germany.
- Rolls-Royce (RR) – United Kingdom.
- Studiecentrum voor Kernenergie - Centre d'Études Nucléaire (SCK-CEN) – Belgium.
- Teknologian Tutkimuskeskus VTT Oy (VTT) – Finland.
- UJV-Rez, a.s. (UJV) – Czech Republic.
- University of Cantabria (UC) – Spain.

Originally, the two main objectives of the project were:

- To characterize the effect of the actual parameters of nuclear plants on the fatigue behaviour of the most significant materials, considering the degradation mechanisms involved in the process, and (based on this).
- To develop a harmonized procedure for computing the fatigue ageing of materials, allowing the long-term safe operation of nuclear power plants.

In agreement with these two objectives, the project was divided in two main parts:

- The first one was focused on the characterization of a typical alloys employed in NPPs (mostly stainless steel 304L), analysing the effects of the following vital parameters representing realistic conditions in NPPs: mean strain, hold time periods and surface roughness. These three parameters were analysed at two strain ranges under a typical nuclear environment (Light Water Reactor, LWR) and also in air. The results allowed the material ageing under realistic conditions to be better understood.
- The second part of the project involved the development of an innovative procedure for estimating the fatigue degradation of the materials based on the obtained experimental results.

In short, the project promoted the development of a better characterization of the fatigue ageing of a common 304L structural material relevant to current European NPPs and, based on such knowledge, provide insights in fatigue assessments.

1.2 CONCEPT AND OBJECTIVES

Fatigue accounts for almost 25% of all reported failures in domestic operating NPPs [1.3], and for this reason this ageing mechanism has been extensively analysed historically. However, the data obtained in laboratory fatigue tests has not reflected accurately in-plant observations. The lack of correlation between the laboratory test data and the in-plant operating experience compromises somewhat the confidence in the corrosion fatigue assessments performed in LWR environments, thus impeding total safety management of the NPPs from being developed.

One of the most relevant reasons for the discrepancy between laboratory data and plant experience can be the different loading conditions of the laboratory samples and the actual structural components in NPPs. There is a considerable amount of laboratory data generated with the aim of investigating different parameters that may have an influence on the fatigue life of nuclear components. However, most of these investigated parameters are related with the LWR environment (e.g. temperature, oxygen dissolved concentration), and not with the loading conditions (except for the strain rate parameter) or with the real conditions of the material (e.g. surface roughness).

It is essential, therefore, to identify the most influential loading parameters in the material fatigue ageing, and to perform laboratory tests that accurately reproduce the normal operating conditions in NPPs. There are three gaps in EFA understanding related to loading conditions that are considered to be essential for an effective and safe management of structural components [1.4]:

- **Mean strain:** defined as the mean value of the maximum and minimum strains, it can have significant effects on fatigue performance. Most laboratory tests (outside the INCEFA-PLUS Project) are carried out under strain control with fully reverse loading (strain ratio $R=-1$) (i.e. no mean strain is considered). However, it is extremely difficult to find a fatigue process in a nuclear component without mean strain, due to the existence of static loads (e.g. weight load) that produce constant strain on the component, or to industrial processes such as machining, welding and heat treatments, which are typical in nuclear components and may induce both pre-hardening and residual strains. It is well known that a compressive mean stress (and hence, also strain) is beneficial to fatigue life, whereas a tensile mean stress is detrimental to fatigue life. There is however data that contradict this general assumption and reveal certain beneficial effect of a mean tensile stress on the fatigue life of 304L under high temperature (300 °C) in PWR environment [1.5]. Therefore, mean stress or strain must be taken into account when predicting the fatigue life. This issue was addressed in the project.
- **Hold time periods:** cyclic loading in NPPs takes place at very low frequency, but with a special characteristic: the existence of hold time periods. The frequency of the cycles is generally low (except in thermal shocks), but between the different cycles there may be a long period of time where the operational conditions are constant. One of the few fatigue test programmes [1.6] acquired with hold time periods in a common stainless steel showed that the corresponding fatigue life in air was higher than that observed under monotonic cycling periods. However, no data were available (by the beginning of the project) concerning this effect in a Light Water Reactor (LWR) environment and in other steels or alloys. Other loading conditions, such as variable amplitude or frequency, are considered to have less influence on the fatigue damage and were not considered within the scope of INCEFA-PLUS.
- **Surface roughness:** some available data on 316NG and 304 stainless steels [1.7] show that the fatigue life in air of roughened specimens is approximately three times lower than that observed in smooth specimens. However, limited experimental data (e.g. Argonne National Laboratory on Low Alloy Steel for Boiling Water Reactors [1.7]) suggest that the effect of surface roughness in high temperature water is lower than

that observed in a high temperature air environment. This suggests that there may be an excessive conservatism when multiplying the surface roughness factor (1.5-3.5 in NUREG/CR-6909 [1.7]) by the F_{en} factor [1.4]. Thus, further SN tests have been performed in the INCEFA-PLUS Project to study the apparently different influence of surface roughness in air and water environments. This could justify a reduction in the design margin applicable for components in water environments.

As a consequence of all this, the INCEFA-PLUS Project contained four main scientific and technical issues, with their corresponding work packages (Figure 1.1), that were designed to fill these identified gaps:

- Issue 1) The gathering of relevant information to develop a strong state of the art about fatigue ageing mechanisms. This information covered the test data available at the beginning of the project, damage mechanisms, typical loading conditions in plant, the most common materials used in NPPs (and those that would be used in the future) and detailed analysis of fatigue failures that have occurred in Europe. The intention was to collect the experience and results of previous studies performed in European countries and also abroad. These data were useful not only for taking certain decisions (e.g. type of stainless steel to be tested), but also to compare them with the results obtained during the development of the project. This issue was covered in an in-kind project named INCEFA, led by Jacobs (formerly Amec, during the in-kind project). This partner also led the management of INCEFA-PLUS Project (Work Package 1, WP1).
- Issue 2) The definition and development of an exhaustive fatigue test programme covering a typical alloy subjected to different loading conditions. This issue represented a key task of the project and was covered in Work Package 2 (WP2), led by the Joint Research Centre (JRC).
- Issue 3) The analysis of the data obtained and their corresponding treatment were presented as important activities for the development of an accurate procedure and for the understanding of the fatigue behaviour of the material. The experience and the expertise provided by the members of the consortium guaranteed the success of such a complex task. This third issue was also focused on the development of an innovative Fatigue Assessment Procedure (FAP), taking into account the results obtained and observed in the project. The starting point was the methodologies that were being applied when the project started. The FAP provides the corresponding recommendations, corrections or modifications to those methodologies. This issue was covered in Work Package 3 (WP3), led by EDF.
- Issue 4) Dissemination and Training played a key role in this project, with the aim of obtaining the maximum added value for INCEFA-PLUS. This issue covers development of the project webpage, the participation in social and scientific networks, the participation in international scientific events, the publication of the experimental results and their corresponding analysis in scientific journals and conference proceedings, the dissemination of the INCEFA-PLUS outcomes, the development of this document, and the organisation of training seminars for experts and for young scientists based on the knowledge and experience gained during the project. A final international event was organised (October 2020) for discussion and dissemination of results among

industry, end-users and academia. This fourth issue was covered in Work Package 4 (WP4), led by University of Cantabria.

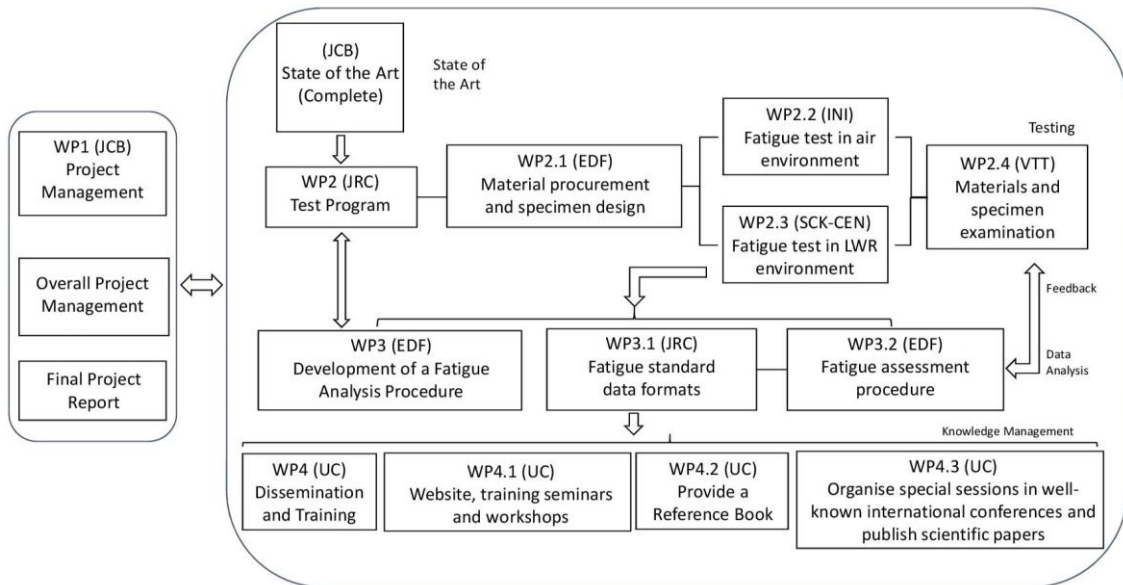


Figure 1.1 Work Packages INCEFA-PLUS Project.

REFERENCES

- [1.1] K. Mottershead, INcreasing Safety in NPPs by Covering gaps in Environmental Fatigue Assessment, Horizon 2020, Call NFRP-2014-2015, Topic: NFRP-01-2014, Proposal number: 662320, (2014).
- [1.2] D. Tice, A. McLennan, P. Gill, Environmentally assisted fatigue (EAF) knowledge gap analysis: Update and revision of the EAF knowledge gaps, Palo Alto, CA, 2018.
- [1.3] O. Cronvall, I. Männistö, Applications concerning OECD Pipe Failure Database OPDE, 2011.
- [1.4] EPRI, Environmentally Assisted Fatigue Gap Analysis and Roadmap for Future Research: Roadmap; Technical Report 1026742, Palo Alto, CA, 2011.
- [1.5] H. Solomon, C. Amzallag, A. Vallee, R. Lair, Influence of Mean Stress on the Fatigue Behavior of 304L SS in Air and PWR Water; PVP2005-71064, 2005. doi:10.1115/PVP2005-71064.
- [1.6] J.P. Solin, S. Reese, W. Mayinger, Long Life Fatigue Performance of Stainless Steel; PVP2011-57942, in: ASME PVP2011, 2011.
- [1.7] O.K. Chopra, G.L. Stevens, NUREG/CR-6909, Rev.1; Effect of LWR Water Environments on the Fatigue Life of Reactor Materials. Final Report, 2018.

This page intentionally left blank.

CHAPTER 2 PREVIOUS SITUATION: EXISTING METHODS FOR ANALYSING EAF

This Chapter is based on the document “Summary of methods for analysing fatigue databases and resulting fatigue models” [2.1], developed by Thomas Métais and Nicolas Prompt (EDF).

2.1 OVERVIEW

As mentioned in Chapter 1, WP3 was concerned with developing a sensible fatigue model from the data obtained through the testing campaigns (WP2). This work-package was divided into two parts: a first part focusing on standardizing fatigue data formats and thus facilitating exchange of data between partners (WP3.1) and a second part focusing on the data analysis and the fatigue curves in order to build a fatigue model integrating the various detrimental effects of the environment (WP3.2).

Since there are various ways to start defining a new fatigue model, a summary of the existing methodologies used before INCEFA-PLUS started its activities was done.

The most straightforward way to define a new fatigue model is to consider former methods and expand on this basis. Section 2.2 will therefore remind the main existing methods found at the beginning of the project and details the aspects that could be improved.

Another way is to start from a blank sheet and explore the various possibilities open to the definition of a new fatigue methodology. This is considered in Section 0.

When selecting a methodology, there are also arguments outside of the purely statistical and technical aspects that need to be included in the decision process, for instance:

- One main advantage of former methodologies is to be able to compare approaches on a common basis and save from departing from other international approaches, hence making the new approach more easily accepted by national safety authorities.
- One has to also bear in mind how the new method will be used in order to make it easily applicable to the end user.
- It is important to consider the current status of the various methodologies (in discussion, validated, used already in stress reports, etc.) and how they have been used in industrial calculations for Nuclear Steam Supply System components.
- Finally, the domain of definition of a new methodology needs also to be defined upfront.

Some of these aspects will also be discussed in the subsequent sections.

2.2 REVIEW OF EXISTING METHODS FOR ANALYSING FATIGUE DATABASE AND RESULTING FATIGUE MODELS IN THE NUCLEAR INDUSTRY

The development of a new fatigue model encompasses not only the corresponding fatigue curves but also the incorporation of environmental effects and other effects into fatigue assessments. The following sections summarise the different solutions found over the years before the INCEFA-PLUS Project started.

These sections also add a discussion about the status of the various methodologies and how they have been used in industrial calculations for nuclear components.

2.2.1 FORMER FATIGUE CURVES

The main former fatigue curves (ASME 2007 [2.2], RCC- M 2007 [2.3], etc.) do not include the effect of the Pressurized Water Reactor (PWR) environment on fatigue but include an effect of the mean stress. The curves were built using a database of experimental data points in air and defining a mean air curve to which the Goodman mean stress correction is applied. Finally, factors to include effects unaccounted for in laboratory testing are also applied.

The basic fatigue equation that is used to fit the data has the following form:

$$\ln(N) = A - B \ln(\varepsilon_a - C) \quad \text{eq. 2.1}$$

where A, B and C are three constants to be determined, N is the number of cycles and ε_a is the strain amplitude.

Here, eq. 2.1 will be referred to as the "Langer curve" [2.4]. Other fatigue models can be used, such as the Basquin model, which is:

$$\varepsilon_a = AN^B \quad \text{eq. 2.2}$$

where A and B are constants to adjust, N is the number of cycles and ε_a is the strain amplitude.

The mean air curve (Langer curve) was determined with a standard statistical regression method (least squares) based on the fatigue equation given above. When using this methodology, an issue arises related to the unbalance between the non-comparable magnitudes of the x and y axes (strain amplitudes vs. number of cycles). A balancing through a coefficient can be performed, but no reference was found as to what was selected in the case of the Langer curve.

The Goodman mean stress correction is applied in the following rule, obtained by writing mathematically the intersection of the material yield limit and the Goodman curve on a Haigh diagram (see Figure 2.1), and solving for S_a :

$$S_a' = S_a \left(\frac{\sigma_u - \sigma_y}{\sigma_u - S_a} \right) \quad \text{for } S_a < \sigma_y \quad \text{eq. 2.3}$$

$$S_a' = S_a \quad \text{for } S_a > \sigma_y \quad \text{eq. 2.4}$$

where S_a is the alternating stress before correction, S_a' is the alternating stress after mean stress correction, σ_u is the ultimate strength and σ_y is the cyclic yield strength.

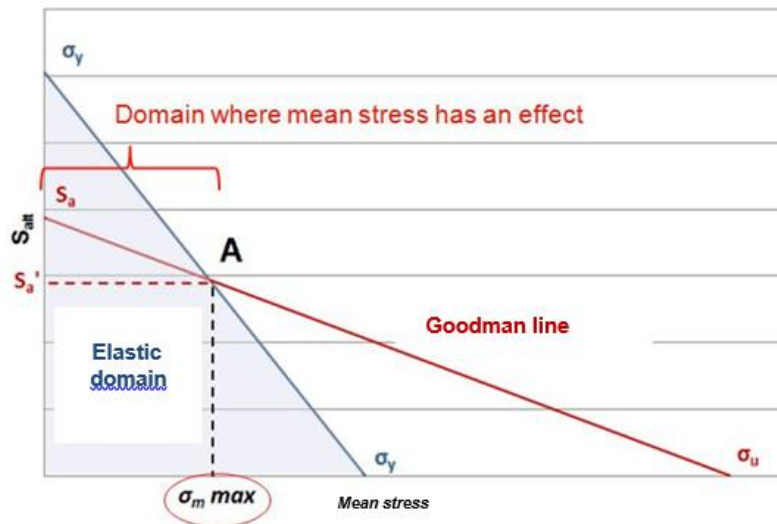


Figure 2.1 Goodman line and yield domain in the mean stress vs. alternating stress coordinate system [2.1].

It may be noted that if the alternating stress is above the cyclic yield stress value, then there is no level of mean stress to account for in the analysis. It can be considered that the mean stress simply redistributes in the structure. It may also be noted that this relationship does not involve knowing the level of mean stress at a given time of the life of the component: it offers to cover a maximum allowable level of mean stress allowed in the structure without redistribution through local plasticity.

This maximum level of mean stress covered can be calculated by solving for σ_m (mean stress) instead of S_a when writing mathematically the intersection of the material yield limit and the Goodman curve on a Haigh diagram. For the former ASME curve (curve C) for instance, it is possible to calculate the level of mean stress covered by the fatigue curve (Figure 2.2). It can be observed that at a high number of cycles, the maximum level of mean stress covered is around 110-120 MPa.

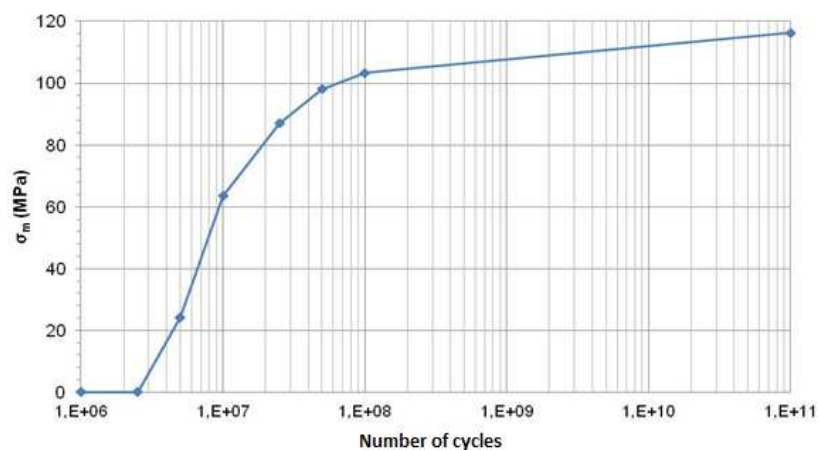


Figure 2.2 Level of mean stress covered by ASME C former fatigue curve [2.1].

This methodology is based on a mathematical representation of the effect of mean stress on fatigue and not on any experimentation specific to the nuclear industry and nuclear grade materials.

The factors that were used to transition from the mean air curve to the design curve were determined essentially on literature reviews. For both factors on life and on strain amplitude, the final factors are a multiplication of single sub-factors. The overall approach is summarized in Table 2.1:

Data fitting equation	Langer fatigue model
Fatigue curve	Mean air curve determined from air tests using the total least-squares method
Gap between laboratory and component	Translation coefficients (lab vs. industrial environment, size effect and data scatter) based on the multiplication of single sub-factors determined through literature review
Mean stress	Goodman correction
Environmental effects	N/A

Table 2.1 Summary of the approach for ASME fatigue model [2.1,2.2].

The weak point of this approach is the little amount of data that supports the sub-factors to transition from the mean air curve to the design curve. This weakness is subsequently amplified by the definition of single sub-factors to represent life and strain amplitude reduction: fatigue data is highly scattered and it is a difficult task to determine a single representative factor. The same comment applies to the Goodman mean stress correction, which is essentially theoretical and based on the Goodman diagram.

These fatigue curves have been used widely over the past 50 years. Most of the NPPs operating or in construction today in the USA, France, China, Finland, Germany and other countries have been designed using this fatigue curve.

2.2.2 NUREG/CR-6909

The NUREG/CR-6909 [2.5,2.6] was developed as an improvement of the previous fatigue methodology, although the construction of the fatigue curve is very similar. The main difference with the previous methodology is the inclusion of PWR environment effects through a F_{en} (environmental) factor.

The mean air curve that was defined uses the Langer fatigue equation (see Section 2.2.1) and fits the data with the total least-square methodology. In [2.7], the following weighting is applied to cover the unbalance between the large values for life and the small strain amplitude values:

$$D = [(x - x')^2 + k((x - x')^2)] \quad \text{eq. 2.5}$$

where D is the experimental distance between a data point and the proposed model, x is the horizontal coordinate of the experimental data point obtained (number of life cycles), x' is the predicted horizontal coordinate using the fatigue model (assuming $y = y'$), y is the vertical coordinate of the experimental data point obtained (strain amplitude), y' is the predicted vertical coordinate using the fatigue model (assuming $x = x'$), and k is a factor to account for the unbalance between the strain amplitude and the number of cycles ($k = 20$ in [2.7]).

The mean stress correction is the same as the original fatigue curve (i.e. the Goodman mean stress correction).

One significant improvement of this approach is on the factors enabling transition from the mean air curve to the design curve. Concerning the factor on life, different sub-factors were identified, but the most extensive effort was put on determining the coefficient on data scatter and material variability. The approach was based on [2.8]. The sub-factors were all given as a range and not a single number. These sub-factor ranges were then combined together using a Monte-Carlo analysis to obtain the global factor on life.

Concerning the factor on strain amplitude, the approach is different as it was recognized that in the high-cycle domain, the aggravating effects could not be combined but the most aggravating one should be taken. As a result, a literature review was performed to evaluate the maximum strain amplitude reduction factors associated with the different effects and the highest one was selected.

The environmental effects were studied through the results of testing campaigns in PWR environment. The environmental factor (F_{en}) expressions were simply established through study of the data trends. The various effects were listed (surface finish, PWR environment, temperature, hold times, etc.) and conclusions were based on result sensitivity to single parameter, with no multiple dependencies considered [2.5,2.6].

The overall approach is summarized in Table 2.2:

Data fitting equation		Langer fatigue model
Fatigue curve		Mean air curve determined from air tests using the total least-squares method (with weights applied)
Gap between laboratory and component	Factor on life	Translation coefficients (surface roughness, size effect, data scatter and loading history) based on the Monte-Carlo combination of sub-factor ranges
	Factor on strain amplitude	Highest coefficient between all aggravating effects identified through literature review
Mean stress		Goodman correction
Environmental effects		F_{en} factor determined through study of data trends in comparison to one aggravating effect

Table 2.2 Summary of the approach for NUREG/CR-6909 fatigue model [2.1].

Although this methodology was a significant step forward from the former methodology, there is still room for improvement, as detailed in an EPRI report [2.9]. The main possible improvements are related to the still high degree of reliance on literature review to determine some sub-factors, and an unbalanced use of statistical analyses to predict the factor on life and the factor on strain amplitude.

Moreover, the environmental factors account well for the effect of PWR environment in a laboratory environment, with clean polished push-pull specimens, but are not representative of an industrial component [2.9]. Additionally, the calculation of the F_{en} factor requires taking into account the strain rate, which is a quantity that was not historically considered in fatigue calculations. This adds extra complexity to the fatigue calculations.

Compared to the previous fatigue curve, the NUREG/CR-6909, Rev.1 [2.6] has not yet been used in so many cases. Nevertheless, in practical terms, it is the new fatigue curve since Addendum 2009 of the ASME 2007 version of the code [2.2] and is destined to be used in all future fatigue calculations using more recent versions of the ASME. It has been used for instance in the USA for the license extension beyond 40 years of operation of some NPPs.

2.2.3 ASME CODE-CASES

Two Code-Cases were submitted to ASME to include Environmentally Assisted Fatigue (EAF) into fatigue calculations: Code-Case N-761 [2.10] and Code-Case N-792-1 [2.11]. The latter relates to the NUREG/CR-6909 method (see Section 2.2.2) to incorporate EAF, while the former is a different method based on a set of multiple fatigue curves that include the effect of temperature and strain rate.

The Code-Case N-761 presents the specificity of proposing one fatigue curve to cover all effects, including PWR environmental effects. The rationale for this decision is that analysts are faced in practice with the difficulty of transients with different strain rates and temperatures: one fatigue curve proposal that covers all configurations enables to prevent hesitations in the choice of an adequate strain rate or temperature to take for the calculation. Another reason put forward in [2.12] is that modern FEA methods allow a higher degree of refinement of the analyses which gradually makes the margins of the ASME code shrink. In this context, implementing one fatigue curve enables to maintain an adequate level of margin.

The construction of the fatigue curve is based on the same method as the NUREG/CR-6909 curve. Factors of up to 5 on the number of cycles are then added to account for environmental effects. These factors are determined from experimental results in PWR environment.

As seen in Figure 2.3, the factor for environmental effects is applied on life only. The argument put forward in [2.12] is that for low number of cycles, once a crack has initiated, the crack propagation can occur very fast so there should be extra margin in that domain. The overall approach is summarized in Table 2.3.

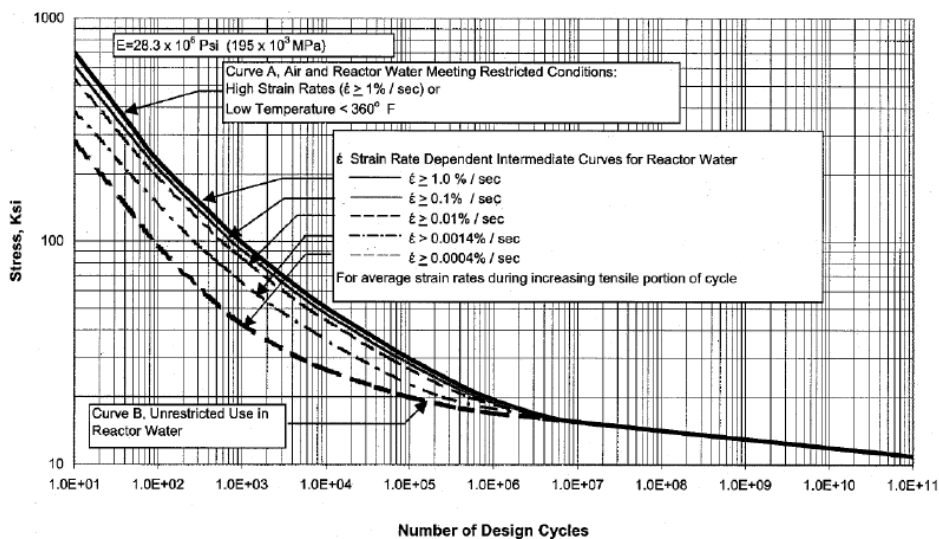


Figure 2.3 Fatigue curve proposal form Code-Case N-761 [2.10].

Data fitting equation		Same as NUREG/CR-6909
Fatigue curve		Same as NUREG/CR-6909
Gap between laboratory and component	Factor on life	Same as NUREG/CR-6909
	Factor on strain amplitude	Same as NUREG/CR-6909
Mean stress		Same as NUREG/CR-6909
Environmental effects		Integrated as part of the fatigue curve through a factor on life

Table 2.3 Summary of the approach for Code-Case N-761 model [2.1].

The obvious advantage of the approach is its simplicity. On the other hand, this method can be very conservative, as in case of difficulties to determine the strain rate of combined transients, it will end up being the lowest fatigue curve that will be prescribed. Moreover, as in NUREG/CR-6909, this approach does not take into account the competition between the detrimental effects.

This set of fatigue curves has not been used today even though it has been integrated to an ASME Code-Case.

2.2.4 EN-13445

The European standard EN-13445 [2.13] presents a different approach to define a fatigue model. This approach does not include EAF for the time being, but proposals are currently underway in this direction [2.14].

The design fatigue curve is built from a mean air curve to which the factors of 10 on life and 1.3 on the number of cycles are applied. The mean air curve does not relate to the ASME fatigue curve but is the result of "testing in air on a large range of steels" (including non-nuclear grades) [2.13]. The main references for building the mean air fatigue curves are the German AD-Merkblatt S2 [2.15] and work from the 1970 led by MPA-Stuttgart. For non-welded components, it is not explicitly indicated in the EN-13445 how the mean air model was derived (from which fatigue equation (Langer, Basquin, etc.) and with which fit (total least squares or another method), although it seems that the fitting equation is built with a specific fit that includes the ultimate tensile strength (UTS) (Figure 2.4).

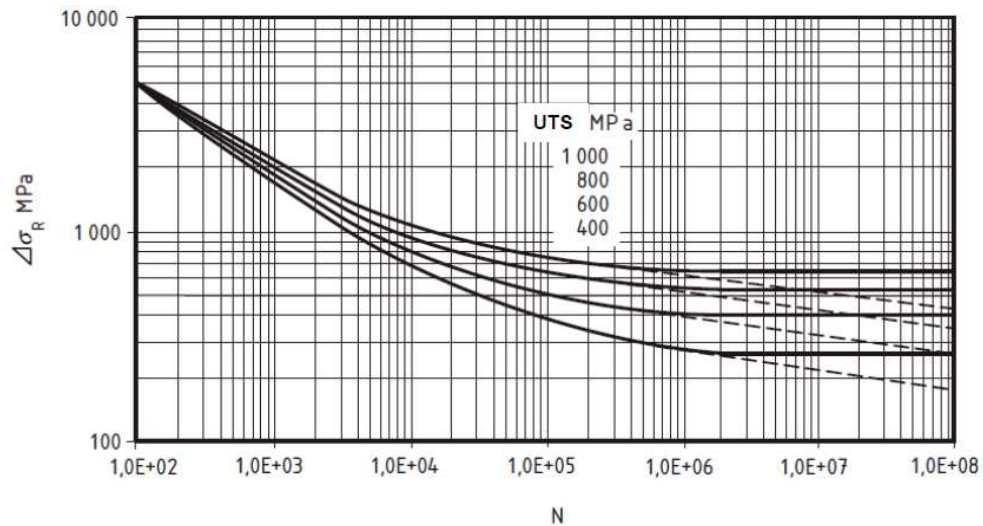


Figure 2.4 Fatigue curves for non-welded components¹ in EN-13445 [2.13].

Concerning the fatigue curves for welded components, and since these curves are straight lines in a log-log domain (Figure 2.5), it seems the Basquin model was selected.

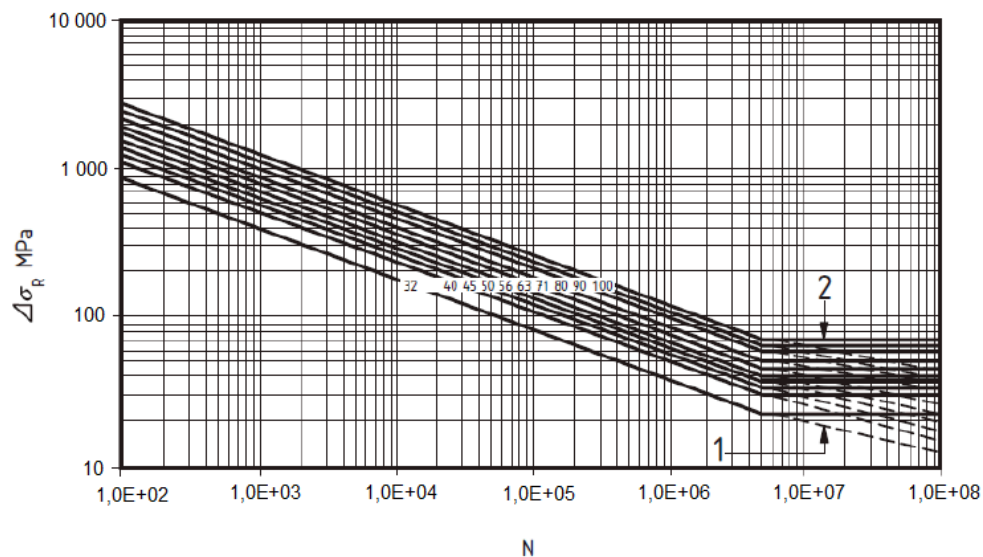


Figure 2.5 Fatigue curves for welded components² in EN-13445 [2.13].

The factors of 10 and 1.3 can be explained in two ways. According to a note in EN-13445, they seem to be linked to data scatter only: it is indeed stated that the design curves are located at three standard deviations from the mean air curve, where the standard deviations seem to be evaluated on data scatter only. On the other hand, some sources describe the factors of 10 and 1.3 as "safety factors" to obtain the design curve. They are inherited from the AD-Merkblatt S2 [2.15].

¹ The different fatigue curves each correspond to a different UTS level. The dashed lines correspond to fatigue endurance limits in the case of variable amplitude loads.

² Numbers from 32 to 100 correspond to the class of the fatigue curve. Numbers 1 and 2 indicate the two ways for determining the endurance limit.

Once this design curve is obtained, the EN-13445 explains that additional coefficients need to be applied to the curve to account for effects that are linked to the components or the loads being applied:

- For welded components, the fatigue curve needs to be further corrected for temperature and thickness effects. In addition, different classes of fatigue curves are given depending on the nature of the analysed weld. These can be comparable to the stress indices given in ASME Section NB-3600 for welds.
- For non-welded parts, the fatigue curve needs correction for temperature, mean stress, thickness and surface roughness. It is nevertheless not very clear today how these coefficients were determined. They could emanate from various sources such as AD-Merkblatt S2 [2.15], Eurocode 3 [2.16], or TWI test results. The coefficients to be applied have essentially an effect on the strain amplitude.

The fatigue curves endurance limits are determined depending whether the loadings have variable amplitude or not. In the case of non-variable amplitude loadings, the endurance limit is constant and given in EN-13445. The constant value of the fatigue endurance limit is given as a fraction (≈ 0.45) of the ultimate strength, which is an approach developed since the first Wohler curves were derived. In the case of variable amplitude loadings, a fatigue curve equation is given. The Miner-Haibach approach [2.17] with a modified slope of the fatigue curve is used to account for this effect.

Concerning environmental effects, reference [2.14] puts forward a concept that could be applicable in conjunction with fatigue curves from the EN-13445. It introduces coefficients depending on temperature and on strain rate that are to be included in the fatigue curve directly. The overall approach is summarized in Table 2.4 and Table 2.5.

Data fitting equation	Langer fatigue model
Fatigue curve	Best fit of fatigue data points in air + endurance limit depending on variable or non-variable loading
Gap between laboratory and component	Factors on life of 10 and 1.3 (safety factors or 3 standard deviation of the data scatter) + factors on temperature (f_{T^*}), surface roughness (f_s) and thickness (f_e)
Mean stress	Factor f_m to account for mean stress
Environmental effects	N/A

Table 2.4 Summary of the approach in the EN-13445 model for non-welded components [2.1].

Unlike other methods, it can be seen here that the EN-13445 advocates generating different fatigue curves depending on the analytical case considered. This is a complicated approach for analysts who are more used to performing fatigue calculations with one single curve as an input.

This method has the advantage of being very detailed on welded components in comparison to other international codes and standards.

Data fitting equation	Basquin fatigue model
Fatigue curve	Best fit of fatigue data points in air + endurance limit depending on variable or non-variable loading
Gap between laboratory and component	Factors on life of 10 and 1.3 (safety factors or 3 standard deviation of the data scatter) + factors on temperature (f_{T^*}), and thickness (f_e) + class of the fatigue
Mean stress	N/A (mean stress redistributes itself through the thickness of the weld)
Environmental effects	N/A

Table 2.5 Summary of the approach in the EN-13445 model for welded components [2.1].

The EN-13445 has been used widely in other industries (petrochemical, welding, oil and gas, etc.), and it has also been used in some cases for some conventional island components on the European Pressurized Reactor (EPR®). However, in practical terms, it has not been applied to Nuclear Steam Supply System (NSSS) components.

2.2.5 RCC-M APPROACH

Two proposals to modify the RCC-M code (or Requests for Modification – RM) were submitted late 2014 and were incorporated to the 2016 version of the RCC-M code [2.3]. This so-called RCC-M approach encompassed not only a proposal for a fatigue curve but also a dedicated method to incorporate environmental effects.

The mean air curve specified in this document is identical to the one in NUREG/CR-6909. This conclusion was reached [2.18] based on a statistical comparison between the air data available and the NUREG/CR-6909.

The coefficients on life and on strain amplitude were determined as the combination of international research and the results from French experimental campaigns [2.19]. Concerning the factor on life, it was calculated as the statistical combination of aggravating parameters linked to the component effect, the loading effect and data scatter. These three categories recall the ones in NUREG/CR-6909 (surface roughness, loading history, size effect and data scatter) but each intends to cover a much wider range of effects than NUREG/CR-6909. For instance, the component effect covers the surface roughness, the size effect and the effect of a strain gradient through the thickness. The objective of covering a wider range of effects was to acknowledge the overlap or competition between effects [2.19] as well as to leave room for other effects that are unaccounted for. The final coefficients were given as ranges, which were combined through statistical methods, as in NUREG/CR-6909. This leads to a final coefficient of 10.

Concerning the factor on strain amplitude, as in NUREG/CR-6909, it was recognized that the combination of the aggravating effect was not applicable and that the greatest aggravating effect was applicable. In this case, the largest value is the one associated to data scatter and was calculated through the application of four statistical evaluation [2.20]. It was finally fixed as 1.4.

Relative to the mean stress, the method is identical to NUREG/CR-6909 and consists in the Goodman mean stress correction.

Finally, regarding EAF, the proposal is a combination of the NUREG/CR-6909 approach with the introduction of the $F_{en-integrated}$ criteria. The quantity $F_{en-integrated}$ translates the part of environmental effects, which is considered to be already covered, or “integrated”, into the design fatigue curve. The general idea is to calculate EAF and evaluate the F_{en} factor using the NUREG/CR-6909 approach and then compare the F_{en} value with the $F_{en-integrated}$. If the F_{en} is greater than the $F_{en-integrated}$, then the usage factor needs to include EAF; if the F_{en} is smaller than the $F_{en-integrated}$, the environmental effects are already covered by the design fatigue curve and no additional effort is required. This $F_{en-integrated}$ criterion was established thanks to French experimental campaigns [2.19] and a statistical calculation similar to NUREG/CR-6909. A summary of the methodology is in Table 2.6.

Data fitting equation		Same as NUREG/CR-6909
Fatigue curve		Same as NUREG/CR-6909
Gap between laboratory and component	Factor on life	Translation coefficients (data scatter, component effect and loading effect) based on the Monte-Carlo combination of sub-factor ranges
	Factor on strain amplitude	Highest coefficient between all aggravating effects identified as being data scatter – Evaluation of its value through statistical approaches
Mean stress		Same as NUREG/CR-6909
Environmental effects		F_{en} factor identical to NUREG/CR-6909, Rev.1 (Draft Report) + $F_{en-integrated}$ criteria determined through statistical calculation from French testing campaigns

Table 2.6 Summary of the approach in the RCC-M [2.1].

It is worth noting that this approach is exclusively applicable to stainless steels grades that are in conformance with the RCC-M specifications. The methodology has been used for the license extension of the French NPP 900 MWe fleet.

2.2.6 DCFS APPROACH

The DCFS (Design Committee on Fatigue Strength) in Japan has been working on updating the fatigue curves in the JSME code [2.21]. This committee was put together in 2011 by the Japan Welding Engineering Society to develop a fatigue evaluation method and is currently approaching the final stage of the work and issuing proposals [2.18].

The construction of the fatigue methodology started with a best fit curve that was established through the total least-squares fitting methods and using the same fatigue equation as the NUREG/CR-6909 (Langer form) [2.22].

Once this curve was obtained, the curve is corrected in two ways, on stress or on cycles (Figure 2.6), and the number of cycles taken for the analysis is the smallest between the two lives obtained. The correction on cycles starts by correcting for mean stress. The mean stress correction proposal is the Smith-Watson-Topper (SWT) correction [2.23]:

$$S'_a = \sqrt{S_a(S_a + S_{mean})} \quad \text{eq. 2.6}$$

where S_a is the alternating stress before correction, S'_a is the alternating stress after mean stress correction and S_{mean} is the mean stress level.

Unlike the Goodman correction, this correction requires to evaluate the level of mean stress in the calculation. In this proposal, the decision to use the Smith-Watson-Topper (SWT) model was based on comparison between the corrections existing nowadays (Goodman, SWT, etc.) and the experimental data [2.24].

The effect of surface finish is then included into the model through a coefficient (fatigue strength reduction factor, K_{sf} [2.25]) determined through the analysis of experimental data, as a function of the maximum height of the profile (R_z), as defined in ISO 4287:1996 [2.26]. It should be noted though that the effect of surface roughness is found to be negligible in the case of austenitic stainless steels [2.24], which is very different from the ASME and RCC-M approaches.

Finally, a coefficient to cover data scatter on life was then applied. This coefficient was determined as the 95% percentile of the whole data set analysed and not obtained through the NUREG/CR-6909 methodology.

Concerning the correction on stress, the coefficient on data scatter is first applied before the mean stress and surface finish effects.

It should be noted that no coefficient on size effect is applied, unlike other approaches.

Concerning the fatigue endurance limit, the approach is comparable to the one in EN-13445 where the endurance limit is determined separately from the rest of the data fit and depends whether the loading studied is variable or not. Concerning non-variable amplitude loadings, [2.18] indicates that a constant value equal to $0.4\sigma_u$ (where σ_u is the material ultimate strength) may be used for austenitic stainless steels. Concerning variable amplitude loadings, the DCFS is hinting in [2.18] that the choices in EN-13445 seem acceptable but that further work is needed.

The environmental effects will seemingly be taken into account through the JNES proposal [2.27], which was determined based on experimental data. The Japanese proposal was one of the first proposals to account for EAF in fatigue calculations. The environmental factor (F_{en}) expressions were simply established through study of the data trends, which was an approach that was subsequently followed in NUREG/CR-6909. The overall approach is summarized in Table 2.7.

As for NUREG/CR-6909, one main comment on the EAF methodology is that it does not include the possible existing competing effects between the aggravating parameters. This approach is still under discussion among the DCFS committee. The conclusion of the work is destined to be integrated into the JSME code.

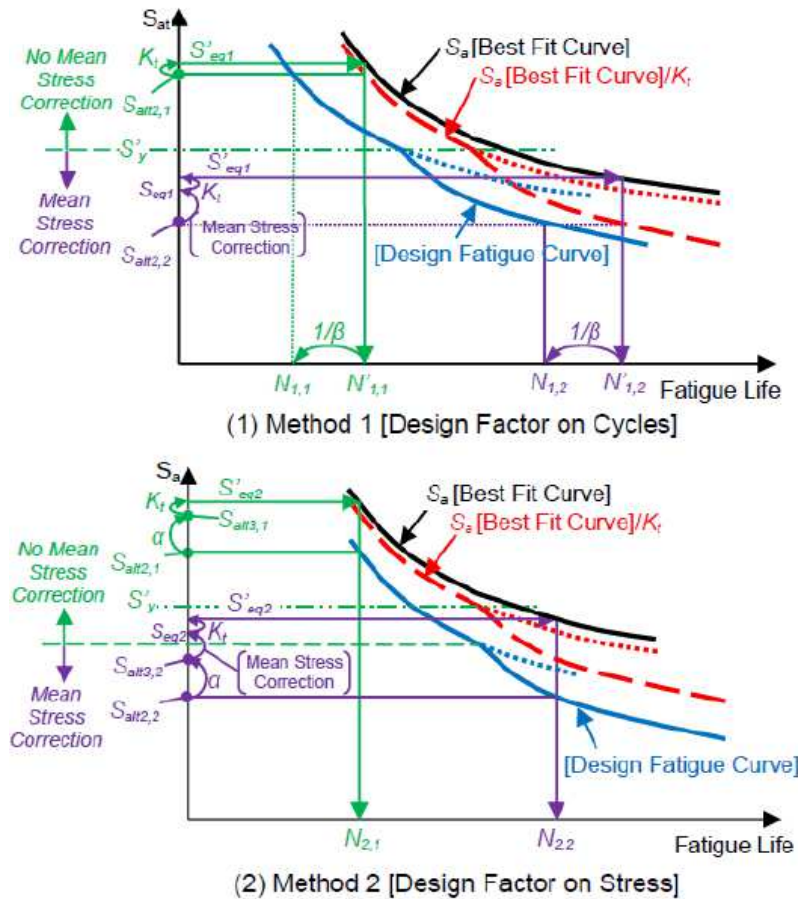


Figure 2.6 Fatigue curve construction according to the DCFS proposal [2.18].

Data fitting equation		Langer fatigue model
Fatigue curve		Mean air curve determined from air test using the total least-squares method + endurance limit depending on variable or non-variable loading
Gap between laboratory and component	Factor on life	Factors for data scatter (β on cycles) + factor surface roughness
	Factor on strain amplitude	Factors for data scatter (α on stress) + factor surface roughness
Mean stress		Mean stress correction through Smith-Watson-Topper approach
Environmental effects		F_{en} factor determined through study of data trends in comparison to one aggravating effects

Table 2.7 Summary of the approach in the DCFS (Japan) model [2.1].

2.2.7 KTA APPROACH

The KTA approach [2.28] includes a fatigue curve as well as a method for incorporating environmental calculations. The KTA air data fit is based on a Langer fatigue equation with a total least-square method [2.29]. It is worthwhile noting that two fits for high or low

temperature are carried out, as a clear temperature effect was shown on Titanium-stabilized austenitic stainless steels [2.29,2.30].

Based on these mean air models, factors on life and on strain amplitude were applied. Concerning the factor on life, the same approach as NUREG/CR-6909 was applied [2.29] (factor of 12). Concerning the factor on strain amplitude, the factor of 1.79 was obtained as the result of the multiplication of the EN-13445 factors for surface roughness (f_s), thickness (f_e) and mean stress (f_m) and a coefficient on data scatter of 1.27. The factors from EN-13445 correspond to values of surface finish of 20 μm , a thickness of 40 mm and a mean stress of 100 MPa [2.29]. It is not indicated how the coefficient on data scatter was derived.

Finally, concerning EAF, the specificity of the German approach is the introduction of thresholds on fatigue usages (e.g. 0.4 for austenitic stainless steels [2.31]). Under these thresholds, no action is deemed necessary to deal with EAF while, beyond these thresholds, action has to be taken. These thresholds were calculated by evaluating representative F_{en} factor values for the Reactor Cooling System (RCS) and dividing the fatigue criteria of 1 by the F_{en} factor. The actions encompass online monitoring, experimental testing as well as analytical calculations. In the case of analytical calculations, the NUREG/CR-6909 method can be used in conjunction with realistic boundary conditions [2.29]: these include approaches such as the one in the RCC-M or the introduction of a transferability factor determined on experimental work [2.32], which includes beneficial and aggravating effects (hold times, transients, etc.). The overall approach is summarized in Table 2.8:

Data fitting equation		Langer fatigue model
Fatigue curve		Mean air curve determined from air test using the total least-squares method (different curves for different temperatures)
Gap between laboratory and component	Factor on life	Same as NUREG/CR-6909
	Factor on strain amplitude	Coefficient from EN-13445 for a mean stress of 100 MPa
Mean stress		Same as NUREG/CR-6909
Environmental effects		EAF thresholds on the usage factor – In the case of EAF calculations, use of F_{en} factor with a transferability factor to include realistic conditions

Table 2.8 Summary of the approach in the KTA [2.1].

The specificity of the KTA approach is the differentiation between temperature levels which has resulted in the definition of multiple fatigue curves. In practice, it can always be difficult to decide which curve to apply when combining peaks and valleys occurring at different temperatures. These modifications were integrated to the KTA code rule 3201.2 from its version 2014 onwards. It is currently being used in fatigue monitoring programs in Germany.

2.2.8 SUMMARY OF EXISTING METHODS

A summary of the results of the existing methodologies can be seen in Table 2.9:

Codes & Standards (Red = Not approved; Green = Approved; Orange = In process) ¹		Former fatigue curves	NUREG/CR-6909	CC N-761	EN-13445 (non-welded)	EN-13445 (welded)	RCC-M (in probationary period)	DCFS (Japan)	KTA	Other methods
Cases used or future use		Over past 50 years to design PWR NPP	For license extension in USA	N/A	Non-nuclear industries & some conventional island components		For EDF NPP life extension	N/A	Fatigue monitoring in Germany	N/A
Data fitting equation		Langer equation			Specific fitting equation including UTS	Basquin equation	Langer equation			Bastenaire equation
Fatigue curve		Mean air curve with total least squares fit			Mean air curve with total least square fit and endurance determined separately		Mean air curve with total least squares fit	Mean air curve with total least squares fit and endurance determined separately	Mean air curve with total least squares fit	Maximum likelihood or quantile regression
Gap between laboratory and component	On life	Factor on life and cycles (safety factor or 3 standard deviation of data scatter) + explicit factor for aggravating parameters	Aggravating effects ranges with statistical combination		Factor on life and cycles (safety factor or 3 standard deviation of data scatter) + explicit factor for aggravating parameters	Aggravating effects ranges with statistical combination	Factor for data scatter (β on cycles) + factor surface roughness	Aggravating effects ranges with statistical combination		Fitting parameters including multiple effects and not a single aggravating effect
	On strain amplitude		Highest coefficient identified through literature review			Highest coefficient identified as being data scatter – Evaluation of its value through statistical approaches	Factor for data scatter (α on stress) + factor surface roughness	Multiplication of factors taken from EN-13445 and coefficient on data scatter		
Mean stress		Goodman correction			Factor f_m to account for mean stress	N/A	Goodman correction	Smith-Watson-Topper corrections	Factor from EN-13445	Use of other methods such as Gerber model
Environmental effects		N/A	F_{en} factor determined through study of data trends	Integrated as part of the fatigue curve through a factor on life	N/A		F_{en} NUREG/CR-6909, Rev.1 (Draft) + $F_{en-integrated}$ criteria determined through French testing campaigns	F_{en} factor determined through study of data trends (JNES)	EAF thresholds on the usage factor + use of F_{en} factor with a transferability factor to include realistic conditions	F_{en} factor designed to bridge gaps identified (hold times, surface roughness, etc....)

Table 2.9 Summary of existing methodologies [2.1].

¹ “Approved” implicitly means approve by a national safety authority (ex.: NUREG/CR-6909 by US NRC)

2.3 NEW POSSIBLE APPROACHES

As seen in the previous section, various fatigue models were built using a wide range of methodologies.

The choices that can be made can be classified into five categories:

1. Choice of the data fitting equation: Langer equation or other, such as the Basquin model.
2. Construction of a fatigue curve: which method and data are used for the fitting.
3. Accounting for discrepancy between laboratory and industrial environment based on the mean air curve: the design curve is built through the application of transfer factors from the mean air curve to the design curve.
4. Accounting for mean stress effects: through the Goodman relationship or another methodology (SWT).
5. Including EAF.

The main steps above were all applied for the various existing international fatigue models and some discrepancies have been revealed at each of these steps. From the INCEFA-PLUS project perspective, it could nevertheless be possible to consider completely new approaches at each of these steps. The various proposals are given in the following sub-sections.

2.3.1 DATA FITTING EQUATION

The Langer and the Basquin equations have been used up to today. The Langer equation is probably the most commonly used model in the nuclear industry. Nevertheless, other fatigue equations have been used throughout history. Among the most famous models, the Bastenaire model could be an option to consider.

The Bastenaire model [2.33] has the following form:

$$N = \frac{A}{(\varepsilon_a - C)} e^{-\left[\frac{(\varepsilon_a - C)}{B}\right]^D} \quad \text{eq. 2.7}$$

where A, B, C and D are constants to adjust, N is the number of cycles and ε_a is the strain amplitude.

Although this model is the most recently developed (1972), it may be more difficult to compare it with other models.

In addition to simply performing a fit of the model, it could be envisaged to use statistical methods (likelihood ratios, Aikake Information Criterion (AIC), etc.) to quantify the adequacy of the statistical model to the set of data.

2.3.2 FATIGUE CURVE

Concerning the way of fitting the data, most commercial softwares use the total least-square regression methods. There are other methods that have been used by EDF for fitting data such as the maximum likelihood [2.34] or the quantile regression method [2.35].

The maximum likelihood has the advantage of being able to include the run-out data in an adequate way. When performing other types of fits, the run-out data is usually considered simply as another failed data point, which can become an issue in the high cycle domain.

The quantile regression, on the other hand, has the clear advantage of skipping the step of building a mean air curve and then applying a factor to account for data scatter. This method enables to fit a curve on data that represents directly an estimation of a given quantile. For instance, in the case of fatigue, the curve corresponding to the 95% percentile could directly be determined based on the data accumulated.

It should also be noted that the data generated by INCEFA-PLUS Project could be divided into sub-sets to analyse the different behaviours separately. For instance, the fatigue behaviour in the high cycle fatigue (HCF) domain and the low cycle fatigue (LCF) domains are significantly different and it is reasonable to consider analysing data separately.

2.3.3 GAP BETWEEN LABORATORY AND COMPONENT

To bridge the gap between laboratory and component, the most straightforward method would be to carry out representative testing on component-like structures, but this is not the aim of the INCEFA-PLUS Project.

Nevertheless, INCEFA-PLUS aims at studying the links between the different aggravating effects, which implies that it may not be easy to establish coefficients linked to one single effect. In this case, the idea would be to establish coefficients based on statistical analyses that would cover more than one aggravating effect. The only issue with this approach will be to develop an adequate amount of testing to cover all links between effects.

In order to achieve this goal, the INCEFA-PLUS Project investigated the use of software such as JMP®, which can directly fit a fatigue curve equation based on the interactions between multiple parameters. The test plan (see Chapter 3) that was derived for the INCEFA-PLUS Project was designed to support such kind of study and was an innovative route that project participants agreed to follow.

2.3.4 MEAN STRESS

It has been seen that there are different proposals to take mean stress into account: the Goodman modified relationship, the Smith-Watson-Topper (SWT) method and through a corrective factor for mean stress (EN-13445).

Other mathematical expressions exist to account for mean stress in fatigue such as the Gerber model. These methods could be compared to the experimental results obtained in order to decide which model seems the most accurate.

2.3.5 ENVIRONMENTAL EFFECTS

Up to now, the NUREG/CR-6909 methodology has been the reference document as far as EAF is concerned. When analysing the document, one finds out that the F_{en} factors were essentially

established based on the analysis of data trends of aggravating parameters analysed separately, followed by the adjustment of the constants of an assumed model.

Another more rigorous approach could be adopted within the INCEFA-PLUS Project. Since the links between the aggravating or beneficial parameters are to be studied, a methodology including all the significant factors in the EAF calculation could be proposed. For instance, a F_{en} integrating a factor for hold times [2.32] and a reduction of the effect as surface roughness increases [2.19] could be put together.

2.4 CONCLUSIONS

The purpose of this chapter was to summarise different options that were open to the INCEFA-PLUS Project for the definition of an EAF assessment methodology. It therefore recalls all the different options that the INCEFA-PLUS members had to pick and choose from to develop a new fatigue methodology including EAF.

REFERENCES

- [2.1] T. Métais, N. Prompt, F. Beaud, Summary of Methods for Analyzing Fatigue Databases and Resulting Fatigue Models, 2017.
- [2.2] ASME, Nuclear Boiler and Pressure Vessel Code - Section III, (2007) edition with 2009 Addendum.
- [2.3] RCC-M, Règles de Construction et de Conception des matériel Mécaniques de l'îlot nucléaires REP, (2007) avec addenda 2008,2009 et 2010.
- [2.4] B. Langer, Design of Pressure Vessels for Low-Cycle Fatigue, J. Basic Eng. (1962). doi:10.1115/1.3657332.
- [2.5] O.K. Chopra, W.J. Shack, NUREG/CR-6909; ANL-06/08, Effect of LWR Coolant Environments on the Fatigue Life of Reactor Materials. Final Report, 2007.
- [2.6] O.K. Chopra, G.L. Stevens, NUREG/CR-6909,Rev.1; Effect of LWR Water Environments on the Fatigue Life of Reactor Materials. Final Report, 2018.
- [2.7] J.M. Keisler, O.K. Chopra, W.J. Shack, Statistical models for estimating fatigue strain-life behavior of pressure boundary materials in light water reactor environments, Nucl. Eng. Des. 167 (1996) 129–154. doi:10.1016/S0029-5493(96)01293-9.
- [2.8] A. Hald, Statistical Theory with Engineering applications, John Wiley and Sons, 1967.
- [2.9] EPRI, Environmentally Assisted Fatigue Gap Analysis and Roadmap for Future Research: Roadmap; Technical Report 1026742, Palo Alto, CA, 2011.
- [2.10] Code-Case ASME N-761, Fatigue Design Curves for Light Water Reactor (LWR) Environments Section III, Division 1, 2010.
- [2.11] Code-Case ASME N-792-1, Fatigue Evaluation Including Environmental Effects, Section III, Division 1, 2010.
- [2.12] W.J. O'Donnell, W.J. O'Donnell, T.P. O'Donnell, Proposed New Fatigue Design Curves for Austenitic Stainless Steels, Alloy 600 and Alloy 800; PVP2005-71409, in: 2005.

doi:10.1115/PVP2005-71409.

- [2.13] EN 13445-3 version V1, Unfired Pressure Vessels - Part 3: Design, (2014).
- [2.14] P. Wilhelm, P. Steinmann, J. Rudolph, Fatigue strain-life behavior of austenitic stainless steels in pressurized water reactor environments, in: 2015. doi:10.1115/PVP2015-45011.
- [2.15] DIN, Analysis for cyclic loading, Merkblatt AD S2. (2012).
- [2.16] EN 1993-1-1, Eurocode 3: Design of steel structures - Part 1-1: General rules and rules for buildings, 2005.
- [2.17] E. Haibach, Betriebsfestigkeit: Verfahren und Daten zur Bauteilberechnung, 3., korrig., Springer, Berlin, 2006.
- [2.18] T. Métais, S. Courtin, P. Genette, L. De Baglion, C. Gourdin, J.-C. Le Roux, Overview of French Proposal of Updated Austenitic SS Fatigue Curves and of a Methodology to Account for EAF; PVP2015-45158, in: Vol. 1A Codes Stand., 2015. doi:10.1115/PVP2015-45158.
- [2.19] J. a Le Duff, A. Lefrançois, J.P. Vernot, D. Bossu, A. Lefrancois, Effect of loading signal shape and of surface finish on the low cycle fatigue behavior of 304L stainless steel in PWR environment; PVP2010-26027, in: Proc. ASME PVP 2010, 2010. doi:10.1115/PVP2010-26027.
- [2.20] G. Blatman, T. Métais, J.-C. Le Roux, S. Cambier, Statistical analyses of high cycle fatigue French data for austenitic SS; PVP2014-28409, in: 2014. doi:10.1115/PVP2014-28409.
- [2.21] JSME, Codes for Nuclear Power Generation Facilities, Rules on Design and Construction for Nuclear Power Plants, The First Part : Light Water Reactor Structural Design Standard, JSME S NC1-2008Ed. through 2011 Ad., JSME. (n.d.).
- [2.22] H. Kanasaki, M. Higuchi, S. Asada, M. Yasuda, T. Sera, Proposal of Fatigue Life Equations for Carbon & Low-Alloy Steels and Austenitic Stainless Steels As a Function of Tensile Strength; PVP2013-97770, in: 2013. doi:10.1115/PVP2013-97770.
- [2.23] S. Asada, T. Hirano, T. Sera, Study On A New Design Fatigue Evaluation Method; PVP2015-45089, in: 2015. doi:10.1115/PVP2015-45089.
- [2.24] Y. Fukuta, H. Kanasaki, S. Asada, T. Sera, Proposal of Surface Finish Factor on Fatigue Strength; PVP2014-28601, in: 2014. doi:10.1115/PVP201428601.
- [2.25] S. Asada, S. Zhang, M. Takanashi, Y. Nomura, Study on incorporation of a new design fatigue curve into the JSME environmental fatigue evaluation method, Am. Soc. Mech. Eng. Press. Vessel. Pip. Div. PVP. 3 (2019). doi:10.1115/PVP2019-93273.
- [2.26] ISO, Geometrical Product Specifications (GPS) - Surface Texture: Profile Method - Terms, Definitions and Surface Texture Parameters, (1997).
- [2.27] JNES, Environmental Fatigue Evaluation Method for Nuclear Power Plants; JNES-SS-1005, 2011.
- [2.28] KTA, Safety Standards of the Nuclear Safety Standards Commission. Components of the Reactor Coolant Pressure Boundary of Light Water Reactors. Part 2: Design and Analysis; KTA 3201.2 (201, GRS, 2017).
- [2.29] X. Schuler, K.-H. Herter, J. Rudolph, Derivation of Design Fatigue Curves for Austenitic Stainless Steel Grades 1.4541 and 1.4550 Within the German Nuclear Safety Standard KTA 3201.2; PVP2013-97138, in: 2013. doi:10.1115/PVP2013-97138.
- [2.30] J.P. Solin, S.H. Reese, H.E. Karabaki, W. Mayinger, Fatigue of stainless steel in simulated operational conditions: Effects of PWR water, temperature and holds; PVP2014-28465, in: ASME 2014 Press. Vessel. Pip. Conf., 2014. doi:10.1115/PVP201428465.

- [2.31] S.H. Reese, J. Rudolph, Environmentally Assisted Fatigue (EAF) Rules And Screening Options In The Context Of Fatigue Design Rules Within German Nuclear Safety Standards; PVP201545022, in: ASME 2015 Press. Vessel. Pip. Conf., 2015. doi:10.1115/PVP201545022.
- [2.32] J.P. Solin, S.H. Reese, H.E. Karabaki, W. Mayinger, Research on hold time effects in fatigue of stainless steel: Simulation of normal operation between fatigue transients; PVP2015-45098, in: ASME 2015 Press. Vessel. Pip. Conf., 2015. doi:10.1115/PVP2015-45098.
- [2.33] F.A. Bastenaire, New Method for the Statistical Evaluation of Constant Stress Amplitude Fatigue-Test Results, in: R.A. Heller (Ed.), Probabilistic Asp. Fatigue, ASTM International, West Conshohocken, PA, 1972: pp. 3–28. doi:10.1520/STP35402S.
- [2.34] R. Millar, Maximum Likelihood Estimation and Inference: With Examples in R, SAS and ADMB, John Wiley and Sons, 2011. doi:10.1002/9780470094846.
- [2.35] R. Koenker, G. Bassett, Regression Quantiles, *Econometrica*. (1978). doi:10.2307/1913643.

CHAPTER 3 INCEFA-PLUS EXPERIMENTAL PROGRAMME

This Chapter includes a description of the different phases of the experimental programme developed by the INCEFA-PLUS Project and its corresponding results. It includes the different measures that were taken to ensure data quality and completeness and the analysis of the impact of using different specimen geometries and lab facilities.

The contents are mainly extracted from the documents:

- INCEFA PLUS Testing Protocol [3.1,3.2].
- Expert Panel tool proposal [3.2,3.3].
- INCEFA-PLUS Management Report (Month 60) [3.4].
- Testing programme matrix [3.5–3.7] and results [3.8–3.10] for different project phases.

3.1 ENSURING DATA QUALITY: TESTING PROTOCOL, EXPERT PANEL AND MATDB

To ensure data quality, a series of measures were taken, including the definition of a Testing Protocol, an evaluation activity developed by an Expert Panel, and the use of MatDB for data management.

First, a Testing Protocol was designed with the aim that all partners would perform their tests in comparable (or as similar as possible) laboratory and specimen conditions. The protocol for the three experimental phases of the project can be found in Annex A [3.1]. Here, sufficient is to say that it covers rules and recommendations for testing specimens, apparatus, testing conditions in air and PWR environment, stressing, testing procedure and test report, among others.

Additionally, an Expert Panel was created to review the data obtained during the different tests and to assess the quality and completeness of each test carried out within INCEFA-PLUS [3.3]. In this sense, some parameters can suggest the quality of the experimental data. For example, the shape of the maximum/minimum stress vs. number of cycles, or more in detail, the shape of the hysteresis loops and their evolution. The review of these data was confirmed as an important point to be considered in the INCEFA-PLUS Project, looking for reliable SN curves. The huge amount of work to be developed by the Expert Panel, especially if a detailed revision was done manually, made it necessary to create a reporting macro to help in this reviewing task (see Annex B for details [3.3]). The aim of this tool was to calculate automatically some parameters that helped the Expert Panel to determine the quality of the tests data. The main capacities or features of this tool are:

1. To be able to upload data (binary and/or excel format): time, strain and stress from the different tests.
2. To automatically detect all the cycles.
3. Screening max. stress and min. stress vs. cycles.
4. Screening max. strain and min. strain vs. cycles.
5. Screening plastic strain vs. cycles.
6. Screening different hysteresis loops (for an easy assessment).
7. Other parameters: number of cycles based on different criteria (N_{15} , N_{25} , N_{50}).

The detailed review of the data implied an analysis of the hysteresis loops. For that reason, the screening of different hysteresis loops (feature nº 6 in the list above) helped noticeably to this task.

In many cases, the Expert Panel asked for additional information or recommended adding more information to the test records.

With all this, the Expert Panel checked the main outputs of each individual test (e.g. stress/strain waveform, stress/strain values, hysteresis loop, etc.), and the corresponding general values (e.g. temperature, chemistry, etc.). Finally, the Panel provided rates for the tests quality and completeness.

MatDB is another tool used by the consortium to ensure quality of data. In order to generate a harmonized data format and a common database, a CEN Workshop (FATEDA - FATigue TEST DATA) [3.11] was planned for the development of technologies for representing and reporting data generated in accordance with the ISO 12106 standard for fatigue testing [3.12]. The technologies provided the basis for the automated transfer of test data to the MatDB database hosted by JRC¹.

The members of the project were very active in promoting the project in order to convince international organisations (e.g. MHI – Japan, NRC – USA, etc.) to contribute fatigue data to MatDB. This objective was of high importance since the more data were collected, the more robust the fatigue analysis procedure.

3.2 EXPERIMENTAL PHASES AND RESULTS

Current guidance for the assessment of environmentally assisted fatigue (EAF) such as NUREG/CR-6909,Rev.1 [3.13] leads to high usage factors for some components in nuclear power plants (NPPs). From these high usage factors, one would expect component failures attributed to EAF to occur in existing light water reactors (LWRs). However no such failures have been observed in practice [3.14]. Consequently, much effort has been invested to improve understanding of EAF in LWR conditions [3.15–3.19].

In that context, the INCEFA-PLUS Project was started to study the influences of the parameters strain range, mean strain, surface roughness, hold time and environment on the fatigue life of stainless steels of relevance for European LWRs.

NUREG/CR-6909,Rev.1 defines an environmental correction factor (F_{en}) relating the fatigue life in the water environment at service temperature to the fatigue life in air at room temperature:

$$\ln(F_{en}) = \ln(N_{f,RTair}) - \ln(N_{f,water}) \quad \text{eq. 3.1}$$

¹ <http://odin.jrc.ec.europa.eu>

For austenitic stainless steels, F_{en} can be calculated as:

$$F_{en} = \exp(T^* \cdot \dot{\epsilon}^* \cdot O^*) \quad \text{eq. 3.2}$$

where T , $\dot{\epsilon}$ and O are parameters related to temperature, strain rate and oxygen content in the water environment, respectively. For the INCEFA-PLUS (Table 3.1, Table 3.2) relevant parameter ranges are defined as [3.13]:

$$T^* = (T - 100)/250 \quad \text{for } 100 \text{ }^\circ\text{C} \leq T \leq 325 \text{ }^\circ\text{C} \quad \text{eq. 3.3}$$

$$\dot{\epsilon}^* = \ln(\dot{\epsilon}/7) \quad \text{for } 0.004\%/s \leq \dot{\epsilon} \leq 7\%/s \quad \text{eq. 3.4}$$

$$O^* = 0.29 \quad \text{for } \text{DO} < 0.1 \text{ ppm} \quad \text{eq. 3.5}$$

The INCEFA-PLUS test programme has been organized in three consecutive phases which each lasted approximately one year. Dividing the programme in different phases allowed slight reorientation of the later phases when the data from earlier phases became available. In each phase, the test matrix was optimized using the Design of Experiments method [3.20].

Parameter	Low level	Middle level	High level	Comment
Strain range (%)	0.6		1.2	
Mean strain (%)	0		0.5	Only for Phase I
Surface roughness R_t (μm)	0.76	approx. 20	> 40	$R_t > 40$ for Phase II only
Hold time (h)	0		72	0 or 3 holds of 72 h per test; cycles depend on condition
Strain rate (%/s)	0.01		0.1	rising strain rate in PWR env., falling strain rate and air tests may vary $e = 0.1$ %/s in some test of phase III only
Temperature T ($^\circ\text{C}$)	230		300	T = 230 $^\circ\text{C}$ in some tests of phase III only

Table 3.1 Summary of test conditions.

Each test record is uploaded to a materials database (MatDB) operated by the European Commission-JRC and can be accessed by all project partners. A panel of fatigue experts from within the consortium considers every test on the basis of data like the cyclic stress and hysteresis curves. Only data that has been approved by the Expert Panel can be used in the final evaluation [3.2]. Furthermore, most of the laboratories testing solid specimens in LWR conditions use shoulder extensometer to apply strain control. Since the strain to be applied during the test is defined at the gauge section, the displacement measured at the shoulder needs to be converted to the displacement of the gauge section [3.21].

The experimental programme was composed of three phases, whose main results are gathered below.

Parameter	Value
Temperature	300 °C ± 3 °C
Pressure	high enough to avoid boiling; reporting mandatory for hollow specimens
Li content	2 ± 0.2 ppm as LiOH
B content	1000 ± 100 ppm as boric acid
Dissolved hydrogen	25 ± 5 cc(STP)H ₂ /kg (standard temperature and pressure (STP): 1 bar, 25 °C)
pH @ 300 °C	≈ 6.95 (calculated)
pH @ 25 °C	≈ 6.41 (calculated)
Conductivity @ 25 °C	≈ 30 μS/cm (calculated)
Anionic contamination	< 10 ppb (any specific, not total; grab samples)
Oxygen	< 5 ppb
Cationic contamination	< 100 ppb (any specific, not total; grab samples)
Total organics carbon (TOC)	< 200 ppb (grab samples)

Table 3.2 INCEFA-PLUS PWR reference environment.

Parameter	Value
K content (as KOH) (ppm)	16.4
Ammonia content (NH ₃) (ppm)	9.7
B content (as B(OH) ₃) (ppm)	1189
Dissolved oxygen (outlet) (ppb)	5
Dissolved hydrogen (outlet) (cc/kg)	30
Conductivity (outlet, ambient temperature) (mS/cm)	0.9
pH (outlet, ambient temperature)	7
Redox (platinum) potential (mV (SHE))	-700
Redox potential (outlet) (mV)	-700

Table 3.3 VVER environment tested on UJV national material.

3.2.1 PHASE I

The Phase I [3.5] testing matrix consisted of 34 air and 43 PWR (LWR environment) tests, with different temperatures (room temperature and 300 °C), surface finishes (smooth, rough), specimen types (hollow, solid), strain amplitudes (0.3% and 0.6%), different mean strain (0% and

0,5%) and with or without hold time. The specific conditions of each test can be seen in the Phase I test matrix in Annex C.

It is important to note that almost 90% of tests were on a common batch of 304L structural material (the chemical composition of which is indicated in Table 3.4) relevant to current European nuclear power plants.

C	Cr	Cu	Mn	Mo	N	Ni	P	S	Si
0.029	18	0.02	1.86	0.04	0.056	10	0.029	0.004	0.37

Table 3.4 Chemical composition of INCEFA-PLUS 304L common material: batch XY182, sheet 23201 produced by Creusot Loire Industries (wt. %, Fe bal.).

The results (fatigue life) of Phase I are shown graphically for air and PWR conditions in Figure 3.1. The environmental effect is obvious. Note that the tests with the same strain amplitude and environment are not all the same as there are differences e.g. in surface finish and hold time periods. Besides, no significant variability between laboratories was seen.

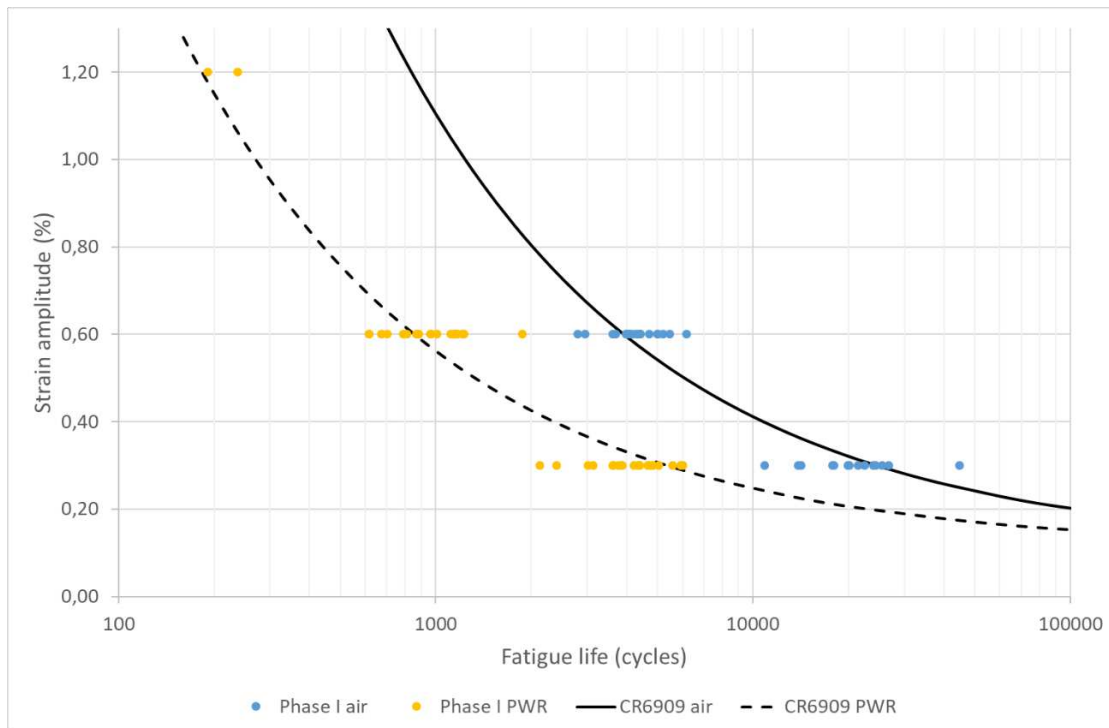


Figure 3.1 Phase I results in air and PWR (data from [3.8]).

3.2.2 PHASE II

The Phase II [3.6] testing matrix consisted of 30 air and 62 PWR tests.

The testing in Phase II were split in two parts. The first part (“main test campaign”) was an extension of the Phase I testing without the factor "mean strain" but considering three different surface roughness values as described below. This part included the major share of tests. A smaller number of tests was dedicated to the exploration of a possible mean stress effect (“mean stress testing”).

3.2.2.1 MAIN TEST CAMPAIGN

To obtain information on the impact of higher surface roughness, IRSN carried out some of their tests in Phase II on the common material and UJV performed tests on their national material with very rough surface finishes ($R_t > 40 \mu\text{m}$).

In order to increase the number of partners being able to test the specimens with the very rough surface finish, Framatome obtained $R_t > 40 \mu\text{m}$ for the next smaller LWR specimen diameter, i.e. for the specimens from Jacobs (6.35 mm) and JRC (6 mm). Due to limitations in the specimen manufacturing process, this surface finish was only achieved in the specimens with the largest gauge diameter [3.22]. For the purpose of establishing the test plan, it was assumed that it was possible to obtain reproducibly very rough surface finishes for these specimens. For the specimens with smaller diameters the surface roughness values remained the same as for Phase I (smooth or rough).

Given these boundary conditions the test matrix was established in an approach similar to Phase I [3.9,3.20]. The environment (air or PWR) together with the actual test conditions where:

- Strain range: 0.6%; 1.2% (same as in Phase I).
- Surface roughness: smooth (polished/honed); rough ($R_t \approx 20 \mu\text{m}$)²; very rough ($R_t > 40 \mu\text{m}$).
- Hold time: no hold; maximum 3 hold periods; cycles with holds depend on environment and strain range (same as Phase I).

The results of Phase II are shown graphically for air and PWR conditions in Figure 3.2:

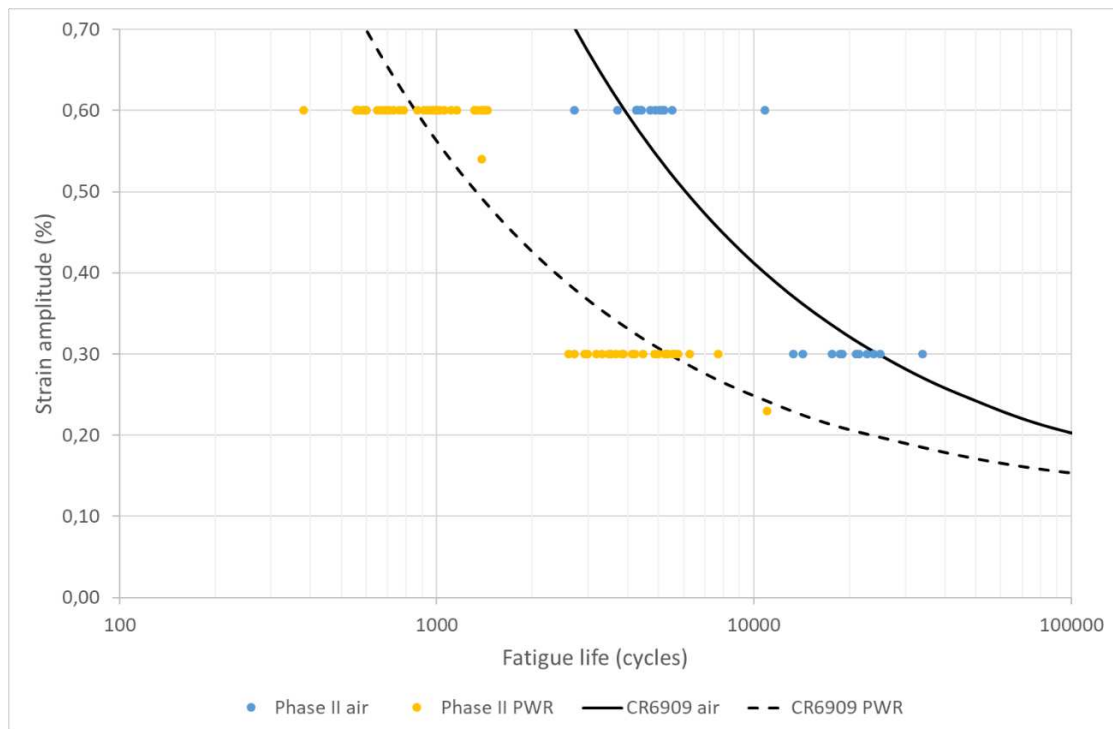


Figure 3.2 Phase II results in air and PWR (data from [3.9]).

² This measure corresponds to the rough specimen from Phase I.

3.2.2.2 MEAN STRESS SUB-PROGRAM

One of the aims of the INCEFA-PLUS Project was to carry out laboratory tests under conditions as close as possible to actual plant conditions. The fatigue tests in INCEFA-PLUS were all carried out in strain control because the fatigue curves in the relevant documents are provided as strain amplitude vs. fatigue life (e.g. [3.13]). However, these fatigue curves are normally established under fully reversed conditions which are not representative for service conditions where components are exposed to an average non-zero load. In the test Phase I the mean load was added as a mean strain because that is the easiest approach from an experimental point of view. It was nevertheless recognized that the test conditions of a mean strain under strain control were not very close to actual plant conditions. Additionally, it was argued that the stresses initially introduced through constant mean strain would quickly relax and, hence, no mean strain effect should be expected. And indeed, the first phase of testing did not reveal any impact of mean strain on the fatigue life.

The stress state in typical plant components is often defined by mean stresses caused by internal pressure or constant weights on to which thermally induced, varying strains are superposed. In order to obtain more realistic test conditions, it was agreed to reserve a limited number of tests to study the impact of strain controlled tests under mean stress conditions. These tests experimentally require an additional feedback loop as the upper and lower strains need to be adjusted regularly to maintain the mean strain at constant level.

EDF and PSI agreed to carry out a series of tests focusing on possible mean stress effects in PWR environment. For fixing the test conditions, a balance had to be struck: a too low stress level would show no effect and would lead to very long tests whereas a too high stress level would lead to ratcheting.

During this study, PSI carried out tests under stress control whereas EDF carried out tests under strain control. To reduce the testing time, the tests were carried out at a frequency so that $d\varepsilon/dt \geq 0.1 \text{ \%}/s$ (i.e. a higher strain rate than the general INCEFA-PLUS testing program).

Once the reference tests established approximately equivalent test conditions (in terms of N_f) between stress and strain control, both EDF and PSI performed a test similar to their respective reference tests but with an added mean stress of 50 MPa. It was decided that if these tests showed a clear mean stress effect the same procedure (reference tests without mean stress followed by tests with mean stress) would be repeated in LWR conditions. These LWR tests were carried out at reduced frequency but otherwise identical conditions to the tests in air.

As this sub-program extended to Phase III, the results are shown in Figure 3.6.

3.2.3 PHASE III

At Phase III [3.7], a program quite similar to those composing Phase I and Phase II was performed, but at a reduced F_{en} factor. The F_{en} reduction could either be achieved by reducing the temperature or by increasing the strain rate.

Phase III was divided in three sub-programs, namely:

1. A sub-program with similar parameters as those used in Phase I and Phase II for surface finish but aiming at a lower F_{en} factor of 2.5.
2. A sub-program to explore variations in hold time to help elucidate why the hold times as defined in the INCEFA-PLUS Project did not reveal major impact of hold times on fatigue life, whereas other projects have reported such effects. For that purpose, a number of tests were carried out to reproduce the test conditions used outside INCEFA-PLUS.
3. A continuation of the sub-program on strain and stress control at mean stress. The aim of this program was to suggest a method for carrying out laboratory tests under conditions which were closer to mechanical loading conditions seen by actual plant components than either stress controlled tests with mean stress or strain controlled tests with mean strain.

3.2.3.1 LOW F_{EN} FACTOR SUB-PROGRAM

The INCEFA-PLUS test conditions of Phases I and II ($T = 300\text{ °C}$, $\dot{\epsilon} = 0.01\%/s$, $DO < 10\text{ ppb}$) yield $F_{en} = 4.57$. The easiest way to reduce the F_{en} would be to either reduce the temperature or increase the strain rate. Although transients at lower temperature occur in plants their impact on fatigue life seemed to be relatively limited. Consequently, only a limited number of tests at low temperature were planned in Phase III [3.7]. These were carried out at the lower strain range (0.6%), where most impact is expected.

The same F_{en} was targeted by reducing T and by increasing $\dot{\epsilon}$ ³. Taking into account the hardware limits for increasing strain rate and the target to change F_{en} as much as possible to obtain a larger effect, the following second (lower) temperature T and second (higher) strain rate, $\dot{\epsilon}$ were selected:

- 1) $T = 230\text{ °C} \rightarrow F_{en} = 2.69$ (with $\dot{\epsilon} = 0.01\%/s$ and $DO < 0.1\text{ ppm}$).
- 2) $\dot{\epsilon} = 0.1\%/s \rightarrow F_{en} = 2.68$ (with $T = 230\text{ °C}$ and $DO < 0.1\text{ ppm}$).

The parameters for this sub-program were strain range, temperature, strain rate and surface roughness which all have two levels. The surface roughness was either polished or rough, ($R_t \approx 20\text{ }\mu\text{m}$), temperature either 230 °C or 300 °C , the strain rate $0.01\%/s$ or $0.1\%/s$, and the strain range was of 0.6% or 1.2%.

The results for reduced F_{en} are shown in Figure 3.3 for reduced temperature in air and in PWR environment respectively, whilst in Figure 3.4 for increased strain rate in air and in PWR environment respectively.

³ Positive strain rate used in NUREG/CR-6909. For technical reasons the negative strain rate (towards compression) can vary.

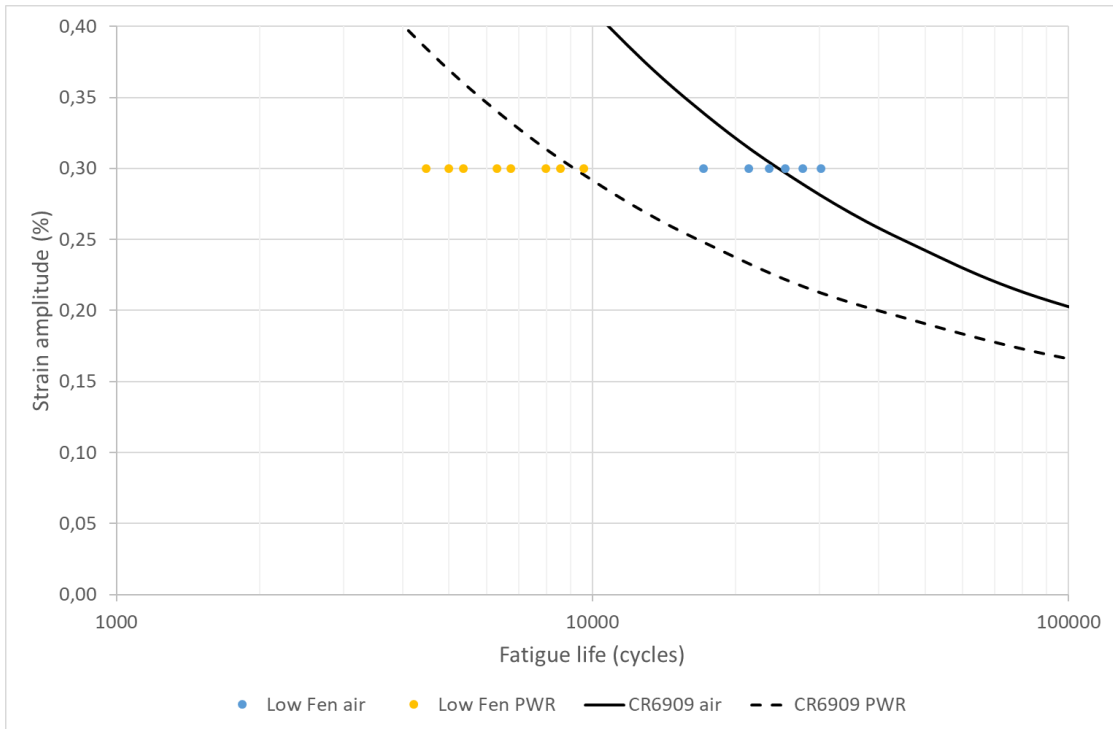


Figure 3.3 Phase III low F_{en} sub-program (by reducing temperature). Results in air and PWR (data from [3.10]).

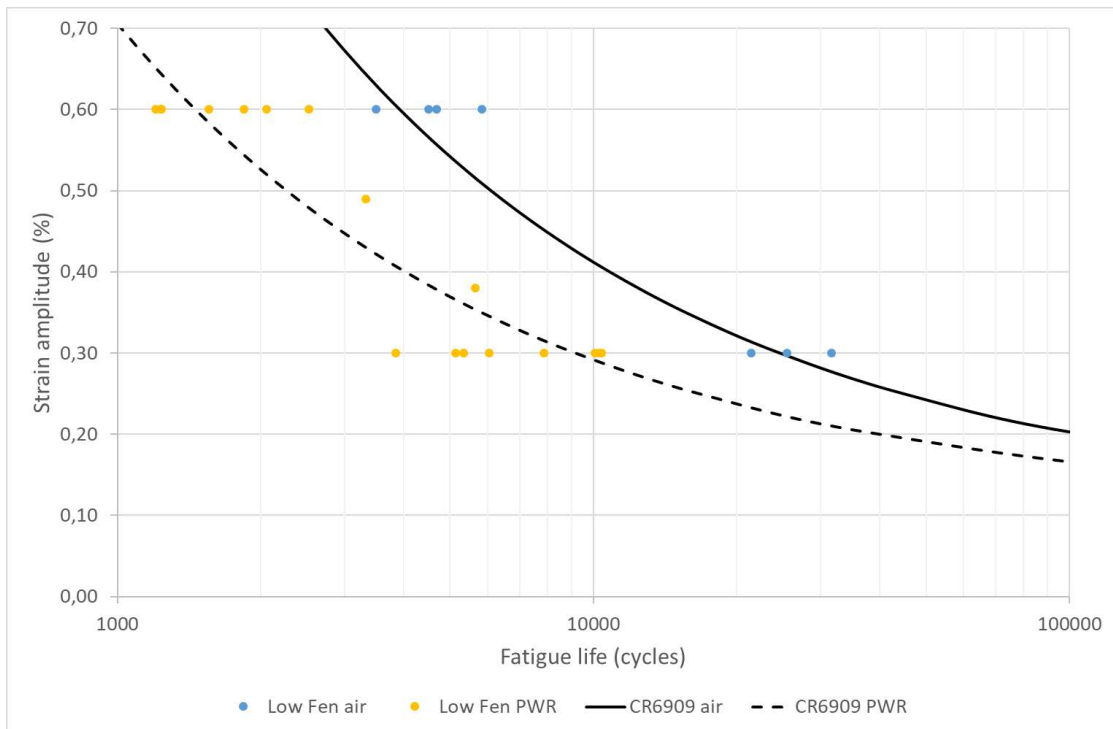


Figure 3.4 Phase III low F_{en} sub-program (by increasing strain rate). Results in air and PWR (data from [3.10]).

3.2.3.2 HOLD TIME SUB-PROGRAM

As mentioned above, testing from Phases I and II did not show a strong effect of hold-times on fatigue endurance lifetimes. Due to the limited number of tests that could be performed in

Phase III [3.7], and the lack of observed effects so far, it was decided to refocus the priorities of the programme onto other factors and limit the further investigation of hold time effects to a limited number of tests. Additionally, by keeping these tests as plant relevant as possible they could clarify if a future test programme investigating any potential benefit of hold times is worthwhile.

To increase the probability of observing a hold time effect [3.15], the strain range was reduced to 0.4% and holds were performed under zero load control (rather than strain control). The hold times consisted of three off 72 hours holds at 350 °C at 10,000 cycle intervals starting from the 10,000th cycle. As EDF were in possession of data from air tests on the common material at a strain range of 0.4%, this allowed for a proper evaluation of the results without increasing the need for further baseline air tests. Some of the proposed tests featured cycling at an elevated temperature and other group featured cycling at room temperature. The latter was included since it should provide a more definitive answer for the effect of holds on 304L material with respect to hold time experiments conducted in the literature. Given that some codes and standards have made provision for a future hold time effect, it was important that the INCEFA-PLUS programme developed a robust and defensible position on hold times to disseminate to the international community.

The results of hold time sub-program are plotted in Figure 3.5:

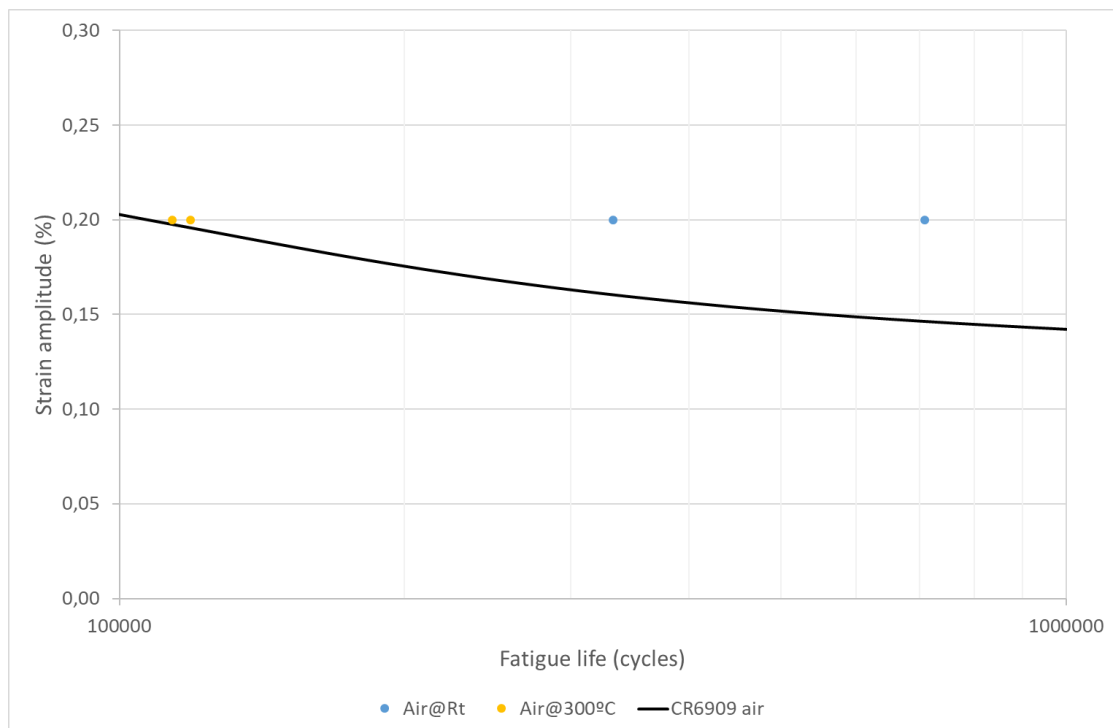


Figure 3.5 INCEFA-PLUS hold time sub-program results (data from [3.10]).

3.2.3.3 MEAN STRESS UNDER STRAIN CONTROL SUB-PROGRAM

Within Phase II, a small program was introduced into to the project to find a way of applying a mean load (in the general meaning of the term) to a specimen in a laboratory experiment which is considered more plant relevant than the two options of strain control with mean strain and stress control with mean stress. The approach was based on strain controlled test with mean

stress. Stress controlled tests with mean stress and the same fatigue life were performed as a benchmark. Tests with mean strain were considered irrelevant since Phase I tests did not show any mean stress effect which is understandable because shake down quickly annihilates stresses from the mean strain.

The Phase II tests indicated that for this type of test there was no interaction between mean stress and environment; i.e. the detrimental effect of applying a mean stress was the same in air and in PWR environment (at least at the conditions used in Phase II). In Phase III [3.7] this observation was checked at different test conditions. The following modifications were considered:

- A change of the applied mean stress level: An increase of the mean stress was discarded because it would lead to unrealistically high stress levels. A decrease of the mean stress would likely lead to lower mean stress effects within the scatter band.
- A change of strain amplitude with mean stress: An increase of strain amplitude increases the risk of ratcheting for tests with mean stress, whereas a decrease would lead to longer tests and larger scatter when approaching the fatigue limit.
- A change of strain/stress rate: Increasing the rates would reduce the environmental effects while reducing it would lead to longer tests.

From these options reducing the strain amplitude was considered the most promising approach. For Phase III a fatigue life of $5 \cdot 10^5$ cycles was targeted for the reference tests in strain controlled mode (compared to 10^5 cycles in Phase II). This should be reached with a strain amplitude of 0.16% for the reference test without mean loading. In stress-controlled mode, a stress amplitude of 155 MPa was applied leading to an expected fatigue life around $5 \cdot 10^4$ cycles. Figure 3.6 shows the outcomes from mean stress sub-programme in Phase II and Phase III together:

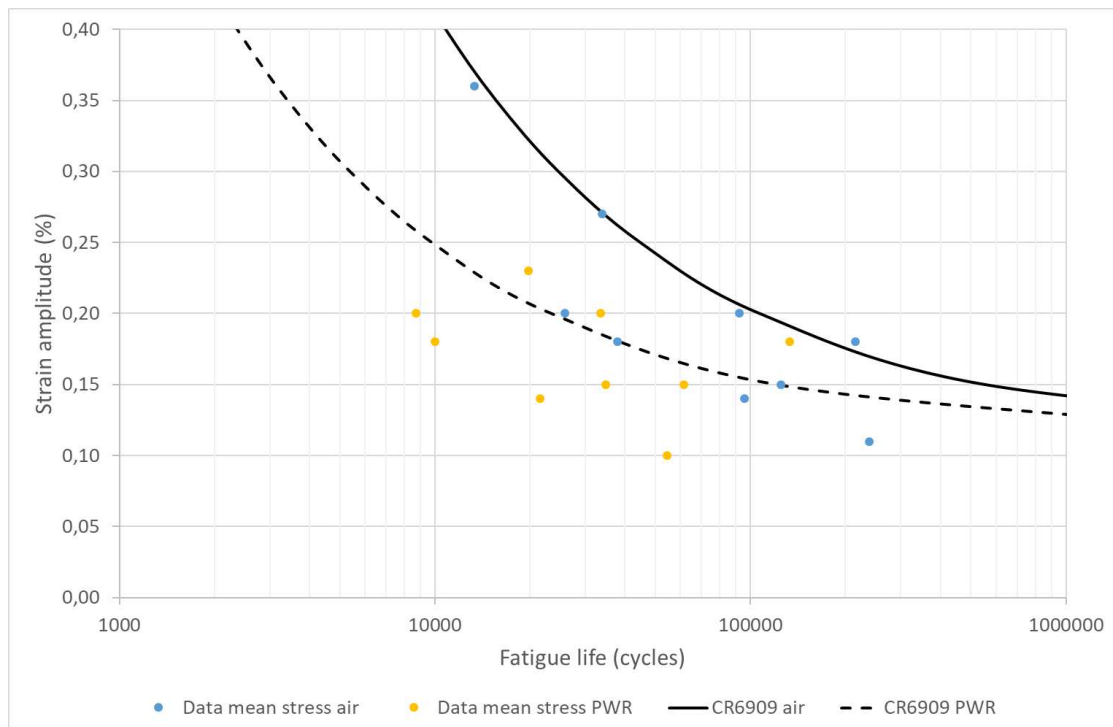


Figure 3.6 INCEFA-PLUS mean stress sub-program. Results in air and PWR (data from [3.9,3.10]).

REFERENCES

- [3.1] M. Vankeerberghen, M. Bruchhausen, Information Pack INCEFA+ Phase II; INCEFA-PLUS Internal Report, 2018.
- [3.2] M. Vankeerberghen, L. Doremus, P. Spätig, M. Bruchhausen, J.-C. Le Roux, M. Twite, R. Cicero, N. Platts, K. Mottershead, Ensuring data quality for environmental fatigue – INCEFA-Plus testing procedure and data evaluation; PVP2018-84081, Am. Soc. Mech. Eng. Press. Vessel. Pip. Div. PVP. 1A-2018 (2018). doi:10.1115/PVP201884081.
- [3.3] R. Cicero, Expert Panel Tool Proposal; INCEFA-PLUS Internal Report, 2017.
- [3.4] K. Mottershead, M. Bruchhausen, S. Cuvilliez, S. Cicero, Management Report (Month 60) (D1.10); INCEFA-PLUS Internal Report, 2020.
- [3.5] M. Bruchhausen, Test matrix for testing Phase I (air and LWR) (D2.07 and 14); INCEFA-PLUS Internal Report, 2016.
- [3.6] M. Bruchhausen, Test matrix for testing Phase II (air and LWR) (D2.09 and 16); INCEFA-PLUS Internal Report, 2018.
- [3.7] M. Bruchhausen, Test matrix for testing Phase III (air and LWR) (D2.11 and 18); INCEFA-PLUS Internal Report, 2019.
- [3.8] M. Bruchhausen, Test data from testing Phase I in MatDB (D2.08 and 15); INCEFA-PLUS Internal Report, 2019.
- [3.9] M. Bruchhausen, Test data from testing Phase II in MatDB (D2.10 and 17); INCEFA-PLUS Internal Report, 2019.
- [3.10] M. Bruchhausen, Test data from testing Phase III in MatDB (D2.12 and 19); INCEFA-PLUS Internal Report, 2020.
- [3.11] European Committee for Standardization, Engineering materials - Electronic data interchange - Formats for fatigue test data, (2017) 1–57.
- [3.12] ISO, Metallic materials - Fatigue testing - Axial-strain-controlled method; ISO/FDIS 12106:2016(E), 2016 (2016).
- [3.13] O.K. Chopra, G.L. Stevens, NUREG/CR-6909,Rev.1; Effect of LWR Water Environments on the Fatigue Life of Reactor Materials. Final Report, 2018.
- [3.14] D. Tice, A. McLennan, P. Gill, Environmentally assisted fatigue (EAF) knowledge gap analysis: Update and revision of the EAF knowledge gaps, Palo Alto, CA, 2018.
- [3.15] M. Herbst, A. Roth, J. Rudolph, Study on hold-time effects in environmental fatigue lifetime of low-alloy steel and austenitic stainless steel in air and under simulated PWR primary water conditions, in: Miner. Met. Mater. Ser., 2019: pp. 987–1006. doi:10.1007/978-3-030-04639-2_62.
- [3.16] K. Tsutsumi, T. Kanasaki, T. Umakoshi, T. Nakamura, S. Urata, H. Mizuta, Nomoto S., Fatigue Life Reduction in PWR Water Environment for Stainless Steels, Assess. Methodol. Prev. Fail. Serv. Exp. Environ. Considerations. 2 (2000) 23–34.

- [3.17] H.T. Harrison, R. Gurdal, Comparison Between ASME Code-Case N-761, NUREG/CR-6909 and Stainless Steel Component Fatigue Test Results; PVP2014-28883, (2014). doi:10.1115/pvp2014-28883.
- [3.18] M. Kamaya, Mean stress effect on fatigue properties of type 316 stainless steel (part II: In PWR primary water environment); PVP2017-65136, Am. Soc. Mech. Eng. Press. Vessel. Pip. Div. PVP. 1A-2017 (2017). doi:10.1115/PVP2017-65136.
- [3.19] T. Métais, D. Tice, A. Morley, G.L. Stevens, L. de Baglion, S. Cuvilliez, Explicit quantification of the interaction between the PWR environment and component surface finish in environmental fatigue evaluation methods for austenitic stainless steels; PVP2018-84240, Am. Soc. Mech. Eng. Press. Vessel. Pip. Div. PVP. 1A-2018 (2018). doi:10.1115/PVP201884240.
- [3.20] M. Bruchhausen, K. Mottershead, C. Hurley, T. Métais, R. Cicero, M. Vankeerberghen, J.-C. Le Roux, Establishing a Multi Laboratory Test Plan for Environmentally Assisted Fatigue, in: Z. Wei, K. Nikbin, P. McKeighan, D. Harlow (Eds.), *Fatigue Fract. Test Planning, Test Data Acquis. Anal.*, ASTM International, West Conshohocken, PA, 2017: pp. 1–18. doi:10.1520/STP159820160047.
- [3.21] M. Vankeerberghen, A. McLennan, I. Simonovski, G. Barrera, S. Arrieta, M. Ernestova, N. Platts, M. Scibetta, M. Twite, Strain Control Correction for Fatigue Testing in LWR Environments; PVP2020-21373, Am. Soc. Mech. Eng. Press. Vessel. Pip. Div. PVP. (2020).
- [3.22] J.-C. Le Roux, Specimen Manufacturing Instructions (D2.1); INCEFA-PLUS Internal Report, 2016.

This page intentionally left blank.

CHAPTER 4 STATISTICAL ANALYSIS

This Chapter includes statistical analysis from the data obtained during INCEFA-PLUS Project. It is based in “Final Work Package 3.2 Report” [4.1], developed by INCEFA-PLUS Consortium, “INCEFA-PLUS Project: Review of the test programme”, by Matthias Bruchhausen et al. [4.2], and “INCEFA-PLUS Project: The impact of using fatigue data generated from multiple specimen geometries on the outcome of a regression analysis”, by Alec McLennan et al. [4.3].

4.1 INTRODUCTION

As shown in Chapter 3, the programme focussed on the effects of the parameters strain rate, mean strain, surface roughness, hold time and environment as well as their interactions on the fatigue life in strain controlled LCF tests. The three test phases had slightly different foci:

1. During the first test phase, two values of each of parameters were considered. A single $F_{en} = 4.57$ was considered for Phase I and Phase II.
2. Since Phase I did not show indications of an effect of mean strain on fatigue life, this parameter was dropped from the main test programme in Phase II and a third surface roughness was introduced. In parallel a limited test programme on the effects of mean stress under strain and stress control was carried out.
3. The results from Phases I and Phase II did not show any hold time effect – in contrast to what was observed elsewhere [4.4]. A likely reason for this discrepancy is differences between the application of the hold time during the fatigue cycle. Consequently, no tests with hold times were included in the main programme during Phase III but a limited programme on hold time effects was added. A reduced environmental factor $F_{en} = 2.68$ was introduced for the main test programme in this phase. The reduction of the F_{en} was achieved by either reducing the temperature or increasing the rising strain rate during the test. The programme on strain and stress controlled testing with mean stress started in Phase II was extended in Phase III.

Some additional effects also needed to be considered:

- Specimen type: While all air tests and most tests in LWR environment were carried on full cylindrical specimens, some of the tests in environment were performed using hollow specimens. The internal pressure in these specimens leads to a different stress state which can have an impact on fatigue life [4.5]. However, no strain range correction was applied to the hollow specimen data used in this work. This decision has been taken consistently with the conclusions further drawn in this Chapter (Section 4.7.2.3). Furthermore, the final surface preparation processes varied depending on the type of specimen and desired surface roughness: polishing and grinding for full specimens and honing for hollow specimens. In the current work the specimen surfaces are characterized exclusively by their roughness value R_t although there may be other differences (like cold work) introduced during the final surface preparation.

- Material: Most tests were carried out on a single batch of 304L austenitic steel. But some data contributed from national programmes are on different heats of 304, 304L, 316L, or 321 Ti-stabilized austenitic stainless steel used in VVERs (X6 CrNiTi 18 10).
- Laboratory: The tests were carried out in different laboratories across Europe. To reduce inter-laboratory scatter as far as possible, a detailed test protocol was defined to harmonize the test procedures for the project [4.6].

4.2 APPROACH #1: ANALYSING THE DATA USING A STATISTICAL LINEAR MODEL

4.2.1 DATA USED

The data¹ used to build the statistical linear model are those generated during the main testing campaign of the project (parameters described in Table 3.1, Table 3.2, and Table 3.3) and accessible through MatDB [4.7]. It consists of strain controlled fatigue tests, and a description of this dataset is given in Figure 4.1 (in terms of material tested, specimen type and surface roughness) and Figure 4.2 (in terms of tested environment, applied strain range, applied mean strain and applied hold times). The data generated during the limited testing programme on mean stress are discussed in Section 4.5.1.

The fatigue life for the solid specimens is characterized as N_{25} , i.e. the cycle during which the maximum stress during a cycle drops by 25% compared to the extrapolation of the quasi-linear part of the maximum cyclic stress vs. cycle curve. If other values are reported, N_{25} is calculated from N_x by means of eq. 4.1 from NUREG/CR-6909,Rev.1 [4.8]:

$$N_{25} = \frac{N_x}{0.947 + 0.00212X} \quad \text{eq. 4.1}$$

where X is the failure criterion in percentage of force drop (e.g. $X = 10$). For hollow specimens N_f is defined by the cycle at which leakage occurs. This is generally considered as a rough equivalent for N_{25} .

¹ INCEFA-PLUS database of experimental test results. Retrieved 16 June 2020 from <https://doi.org/10.5290/50>.

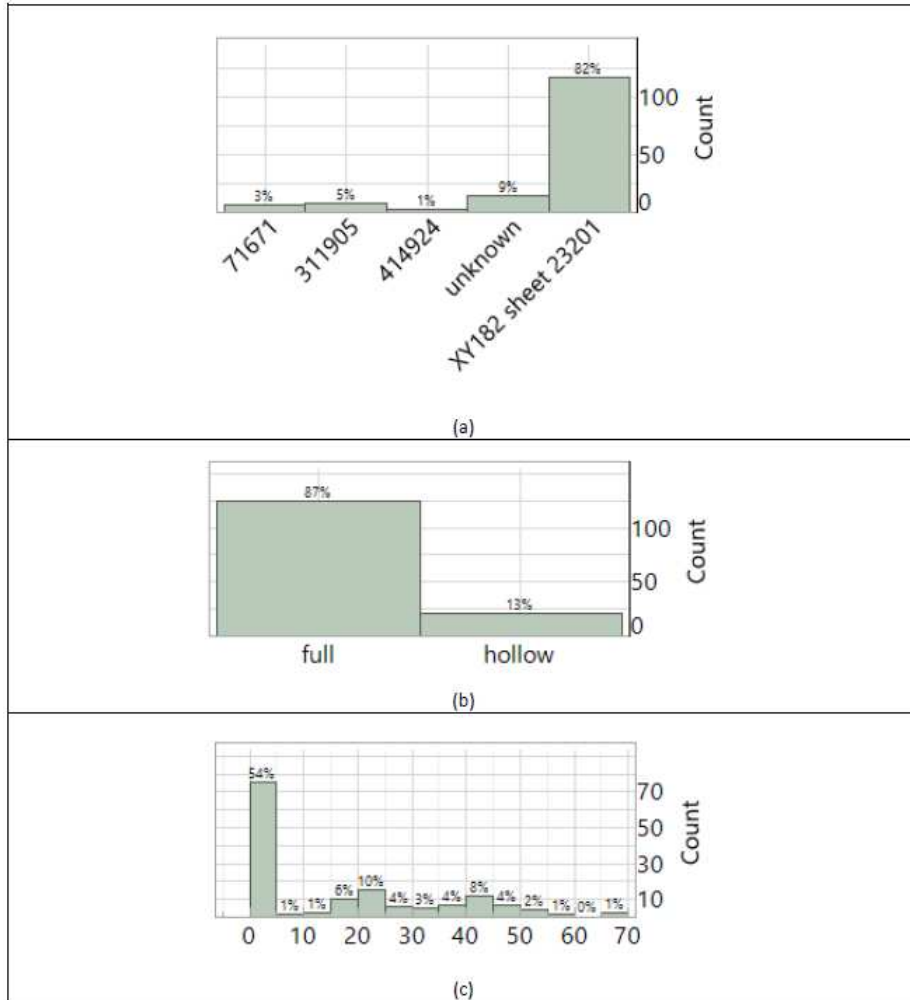


Figure 4.1 Description of the dataset considered in terms of: (a) batch number of the material tested: 71671 is 304, 311905 is 316L, 414924 and 23201 are 304L, “unknown” refers to the UJV national material (X6 CrNiTi 18 10) (b) specimen type (full or hollow) and (c) surface roughness (R_a) of the specimens. The left vertical bar in (c) corresponds to polished specimens [4.1].

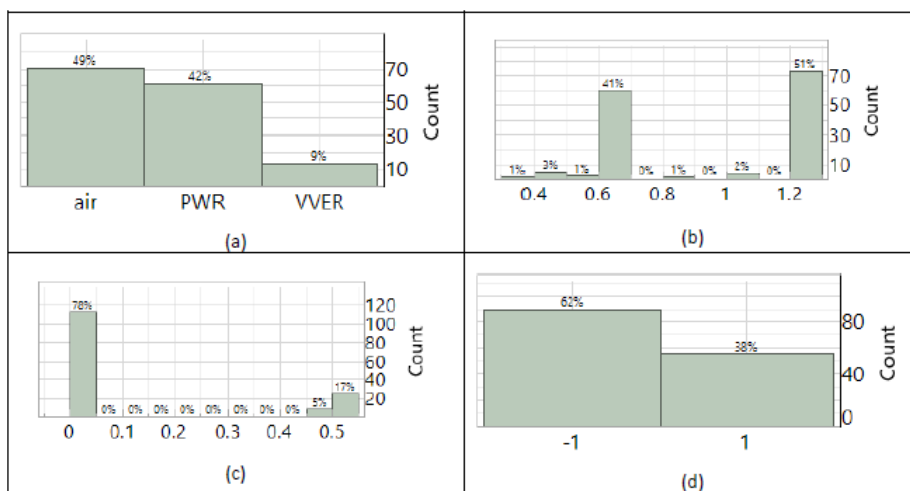


Figure 4.2 Description of the dataset considered in terms of: (a) tested environment, (b) applied strain range, (c) applied mean strain and (d) applied hold times (-1 = no hold, +1 = with holds) [4.1].

4.2.2 DESCRIPTION OF THE MODEL USED

This approach is based on a linear model of the form:

$$\ln(N_f) = \sum_i \alpha_i x_i + \sum_{i < j} \alpha_{i,j} x_i x_j + I \quad \text{eq. 4.2}$$

The x_i and x_j are the input parameters (factors), such as strain range, and I is the intercept. The α_i and $\alpha_{i,j}$ are the model coefficients for the individual effects and the second order interactions, i.e. the situations where the impact of one factor depends on the value of another factor.

The values of the model coefficients α_i and $\alpha_{i,j}$ depend on the units that are being used. Normalizing the ranges of the factors to the interval [-1; 1] allows to directly compare the impact of the different effects in the model by comparing the corresponding model coefficients α_i and $\alpha_{i,j}$. Table 4.1 provides some details on how the different factors have been normalized (e.g. a normalized value of -1 for strain range corresponds to a test with a strain range of 0.6%). It is also important to highlight that the environment is a binary factor: -1 corresponds to air data and +1 to LWR data. More precisely, this means that at this stage of the analysis, for LWR data, only the test conditions that correspond to a $F_{en} = 4.57$ ($T = 300$ °C and rising $\dot{\epsilon} = 0.01\%/s$) are used. LWR data generated with test conditions that corresponds to lower theoretical F_{en} values (≈ 2.68) are discussed in Section 4.2.4.

Factor	Low value (-1)	High value (1)	Comment
Strain range (%)	0.6	1.2	min. and max. values according to test matrix
Mean strain (%)	0	0.5	min. and max. values according to test matrix
Surface roughness R_t (μm)	0.26	65.5	-
Hold time	no hold	incl. holds	nominal variable indicating if test had holds
Environment	air	LWR	nominal variable indicating the environment

Table 4.1 Normalized factors (independent variables).

Before studying the effects of the factors of interest on fatigue life, one should check for correlations between the factors amongst each other. Correlations between the input parameters can easily lead to wrong conclusions. The test matrix for the present study was optimized using the Design of Experiments (DoE) method so that correlations between the input parameters have been minimized from the outset. However, experimental constraints when setting up the test matrix, changes in priorities between the successive test phases, invalid tests and additional data brought into the project may have changed the initial optimization.

Table 4.2 lists the correlations between the factors (i.e. independent variables) strain range, mean strain, surface roughness, hold time and environment. All entries on the main diagonal are 1 which reflects the obvious fact that all factors are perfectly correlated with themselves. The next highest absolute value (-0.119) is the anti-correlation between surface roughness and mean strain. There was a change of focus from Phase I to Phase II when the tests with mean

strain were dropped and a third, rougher surface finish was included (very rough surface finishing). Consequently, tests without mean strain tend to have a higher R_t value. All other correlations have much lower absolute values.

	Strain range	Mean strain	R_t	Hold time	Environment
Strain range	1.0000	0.0306	0.1000	-0.0135	-0.0265
Mean strain	0.0306	1.0000	-0.1119	-0.0232	0.0071
R_t	0.1000	-0.1119	1.0000	0.0926	-0.0278
Hold time	-0.0135	-0.0232	0.0926	1.0000	0.0125
Environment	-0.0265	0.0071	-0.0278	0.0125	1.0000

Table 4.2 Correlations between the independent variables.

The data evaluation was carried out with a commercial statistics software package (JMP®) which has a platform for the evaluation of lifetime data that allows runouts to be considered. As suggested by the ISO 12107:2012 standard for statistical analysis of fatigue data, a lognormal distribution of N_f was assumed [4.9].

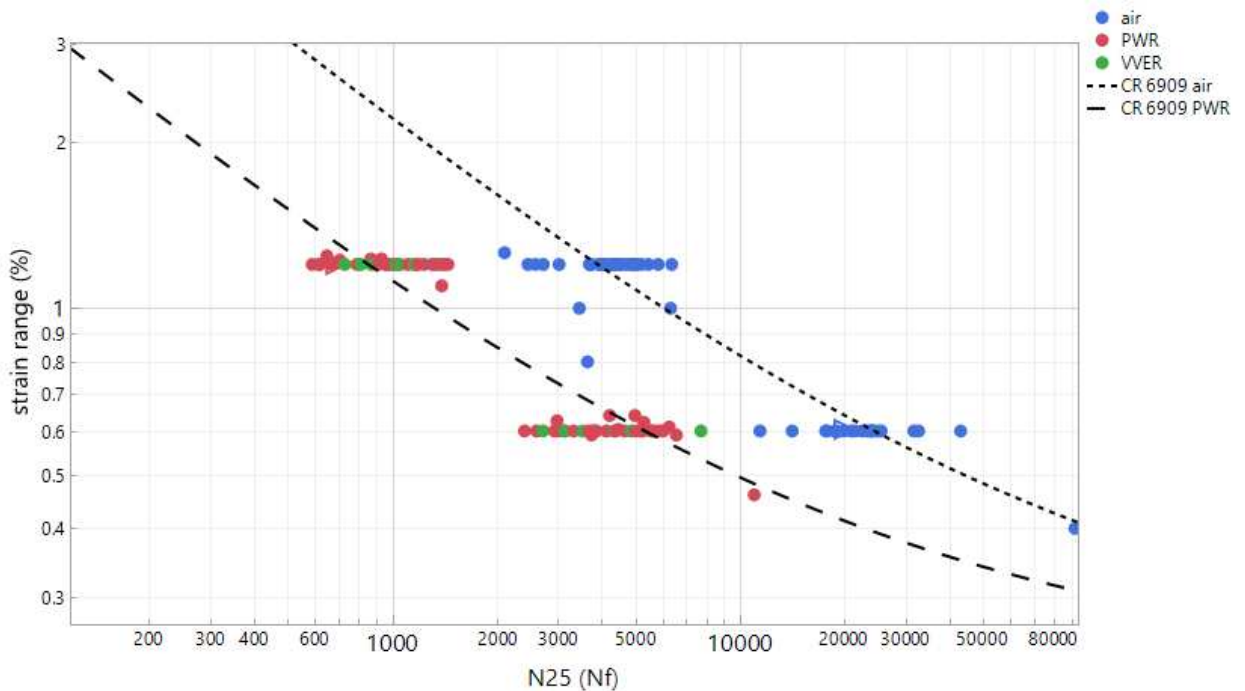


Figure 4.3 Plot of the data considered in Section 4.2. The NUREG/CR-6909 mean curves for air and LWR ($F_{en} = 4.57$) are added for reference. The “D” indicate runout tests [4.1].

The strategy for determining the model describing the fatigue data shown in Figure 4.3 has the following steps:

- 1) Create an initial model including all 5 factors and all 10 possible two-way interactions plus the intercept I (i.e. 16 parameters in total).
- 2) Successively eliminate from the initial model those effects that are not statistically significant i.e. effects that have a high probability to be random. Several statistical measures can be used to decide whether to keep or remove an effect based on its statistical significance. The measures used here are:

- a. p-value: The p-value gives the probability that the variations of the independent variable described by a certain factor are purely random. The p-value is essentially the signal-to-noise ratio. A high p-value means the related parameter can be removed from the model.
 - b. AICc and BIC: The corrected Akaike's Information Criterion (AICc) and Bayesian Information Criterion (BIC) are criteria that can be used to compare different models for the same data set. The model with the lower AICc or BIC is normally preferred. Both are quite similar concepts but vary in so far that the BIC penalizes models with more parameters more than the AICc. More details can be found in the literature [4.10]. In this study BIC is used as the principle measure to arrive at a model that is as simple as possible, i.e. which contains as few terms as possible.
- 3) Eliminate effects that are statistically significant but not "practically relevant". This refers to effects that have a statistically significant effect on fatigue life, but where the impact is relatively small, so that reference is given to a simpler model even at the price of a limited loss of accuracy. The practical relevance of the different model terms is given by the model coefficients α_i and $\alpha_{i,j}$ in eq. 4.2.

Table 4.3 lists the effects in the initial, full model and their respective p-values. The LogWorth that is reported is defined as:

$$\logWorth = -\log_{10}(p - value) \tag{eq. 4.3}$$

It is equivalent to the p-value but better suited for plotting.

Source	LogWorth	PValue
norm strain range	248.350	0.00000
norm env.	225.186	0.00000
norm Rt	4.869	0.00001
norm strain range*norm env.	4.248	0.00006
norm strain range*norm Rt	2.300	0.00501
norm strain range*norm mean strain	1.876	0.01330
norm mean strain	1.451	0.03543
norm hold time	1.004	0.09899
norm Rt*norm env.	0.410	0.38908
norm strain range*norm hold time	0.401	0.39710
norm mean strain*norm Rt	0.369	0.42744
norm hold time*norm env.	0.198	0.63444
norm mean strain*norm env.	0.196	0.63626
norm mean strain*norm hold time	0.133	0.73699
norm Rt*norm hold time	0.128	0.74498

Time to event: N25 (Nf)	AICc	2366.782	Observation Used	139
Distribution: Lognormal	BIC	2411.610	Uncensored Values	136
Censored By: Test status	-2*LogLikelihood	2327.724	Right Censored Values	3

Table 4.3 List of the parameters in the initial, second order factorial model.

After removing all insignificant factors, with p-values higher than 0.05, the model with the terms listed in Table 4.4 remains. Note that mean strain is included in the model although the p-value is larger than 0.05 because there is an interaction term including mean strain which has a lower p-value (principle of effect heredity).

The profiler in Figure 4.4 allows studying the impact the different model factors have on fatigue life. In case of interactions, the slopes in the diagrams for the different factors depend on the settings of some of the other factors. Figure 4.4 shows the situation where the sensitivity of N_f with respect to mean strain is at its maximum (that is the case for the minimum strain range). The plot shows that mean strain has only a very weak impact on N_f (the line is almost horizontal). Furthermore, the error bars include the horizontal red dashed line almost entirely, showing the effect is hardly significant.

It is therefore reasonable to remove also the factor mean strain from the model. The terms of the further reduced model (5 parameters) are then listed in Table 4.5. The corresponding model coefficients are listed in Table 4.6; the normalized factors (Table 4.1) need to be used for the model.

Source	LogWorth	PValue
norm strain range	68.316	0.00000
norm env.	65.568	0.00000
norm Rt	5.215	0.00001
norm strain range*norm env.	3.882	0.00013
norm strain range*norm Rt	2.392	0.00406
norm strain range*norm mean strain	1.706	0.01967
norm mean strain	1.285	0.05184 ^

Time to event: N25 (N_f)	AICc	2352.153	Observation Used	139
Distribution: Lognormal	BIC	2377.168	Uncensored Values	136
Censored By: Test status	-2*LogLikelihood	2332.758	Right Censored Values	3

Table 4.4 Model after removal of all non-significant terms.

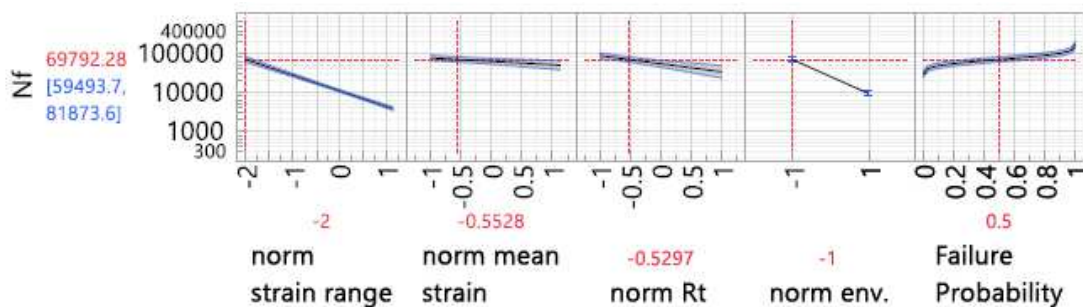


Figure 4.4 Profiler for the model including mean strain (in Table 4.4).

Source	LogWorth	PValue
norm strain range	66.980	0.00000
norm env.	63.815	0.00000
norm Rt	4.829	0.00001
norm strain range*norm env.	3.654	0.00022
norm strain range*norm Rt	2.161	0.00690

Time to event: N25 (Nf)	AICc	2356.467	Observation Used	139
Distribution: Lognormal	BIC	2376.153	Uncensored Values	136
Censored By: Test status	-2*LogLikelihood	2341.612	Right Censored Values	3

Table 4.5 List of the parameters in the reduced model with 5 parameters.

The model contains three main effects (strain range, environment and surface roughness) and two interactions (strain range and surface roughness as well as strain range and environment). Since the factors have been normalized, their impacts can be compared directly by looking at the corresponding model coefficients in Table 4.6.

Term	Estimate	Std.error
Intercept	8.33729754	0.0365404
norm strain range	-0.8480011	0.025482
norm Rt	-0.2124297	0.0473514
norm env.	0.82049209	0.0261416
(norm strain range-0.02554)*(norm Rt+0.52969)	0.12757241	0.0465945
(norm strain range-0.02554)*norm env.	-0.0961237	0.0254511
σ	0.30450252	0.0184764

Table 4.6 Coefficients for model in Table 4.5. σ is the standard deviation of $\ln(N_f)$.

Comparing the coefficients for the two interactions shows that the interaction between strain range and environment has less impact than the interaction between strain range and surface roughness. One could therefore consider further reducing the model by removing the interaction between strain range and environment. The resulting model terms are listed in Table 4.7 and Table 4.8.

However, it is important to note that as the size of the database was increasing during the project, the interactions between effects that were detected varied between successive evaluations. That might mean that the model is at the very limit of what could possibly be detected in terms of interactions between effects. On the other hand, the main individual effects detected were always the same [4.2,4.11].

Source	LogWorth	PValue
norm strain range	64.306	0.00000
norm env.	61.292	0.00000
norm Rt	5.174	0.00001
norm strain range*norm Rt	2.145	0.00717

Time to event: N25 (Nf)	AICc	2367.885	Observation Used	139
Distribution: Lognormal	BIC	2384.855	Uncensored Values	136
Censored By: Test status	-2*LogLikelihood	2355.249	Right Censored Values	3

Table 4.7 List of the parameters in the reduced model with 4 parameters.

Term	Estimate	Std.error
Intercept	8.32523099	0.0381479
norm strain range	-0.8461263	0.0266985
norm Rt	-0.2309967	0.0493917
norm env.	0.82033366	0.0273955
(norm strain range-0.02554)*(norm Rt+0.52969)	0.13307949	0.0488383
σ	0.31938017	0.0193931

Table 4.8 Coefficients for model in Table 4.7.

4.2.3 DISCUSSION OF THE MAIN PROGRAMME DATA

The plot in Figure 4.5 compares the model predictions with the observed fatigue lives. The abscissa contains the 50% quantile of the fatigue life predicted by the model with 4 parameters, i.e. the cycle at which 50% of the specimens are expected to fail for a given combination of experimental conditions. On the ordinate, the same quantity is reported for the two models together with the experimental observations. The difference between the two models is very small, so it seems justified to use the simpler model with just four effects.

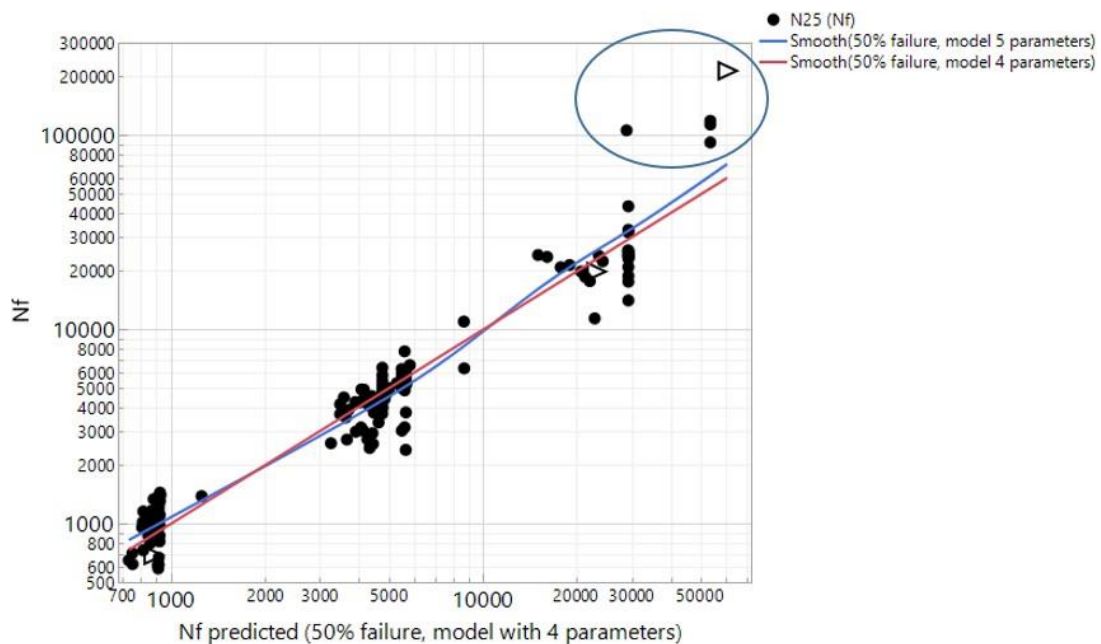


Figure 4.5 Comparison of the observed fatigue lives with the model estimates [4.1].

Comparing the model predictions to the experimental data there are some data points that are not well covered by the model (see circle in Figure 4.5). One point is the runout indicated by the “▷” at the upper right corner of the graph. In the overview plot in Figure 4.3 this is the test with a strain range of 0.359%. Since it is a runout test at a low strain range compared to the bulk of the test data, it is not surprising that this data point is not well covered by the model. The point on the left side of the circle is a test at 0.6% strain range on a national batch of 304L which is known to have a high fatigue limit. So, it is also understandable that it is less well represented by the model. The remaining tests in the circle have been tested at lower strain ranges than the majority of tests, so they do not have a big impact on the model. Furthermore, they lie in a region of the fatigue curve where the NUREG/CR-6909 curves have a notable curvature (on a log-log plot), indicating the vicinity of the fatigue limit. They cannot be expected to be very well described by the extrapolation of a linear model optimized for larger strain ranges².

4.2.4 ANALYSIS OF LOW F_{EN} DATA

Part of the Phase III testing has been dedicated to testing at a reduced F_{en} . Reducing the F_{en} was achieved by increasing the positive strain rate to 0.1%/s (compared to 0.01%/s for the main programme) or by reducing the temperature to 230 °C (compared to 300 °C for the main programme). According to [4.8] both changes lead to a reduced $F_{en} = 2.68$, while, for the main programme, $F_{en} = 4.57$.

When analysing the low F_{en} data some points need to be considered:

- Temperature and positive strain rate are parameters that were not varied in the main programme.
- In Phase III, no tests with holds or mean strain have been carried out.
- Air tests were often carried out at higher strain rates than tests in LWR environment because strain rate has no impact on fatigue life in air.

These points make it difficult to include the low F_{en} data in the analysis of the data from the main programme since not all interactions could be analysed and some effects would be confounded (like positive strain rate and environment) and their impacts could not be separated.

This subsection therefore analyses the low F_{en} data in LWR environment taken with a strain range of 0.6% separately.

4.2.4.1 DATA SET WITH REDUCED F_{EN}

An overview plot of the data is provided in Figure 4.6; note that the low F_{en} data are indicated by a “v” symbol on the plot. The distributions of the main test conditions are given in Figure 4.7. The entire data set includes 50 tests of which 15 are at the reduced F_{en} .

² Because of calibration issues, the data sets from one laboratory had to be reevaluated which led to higher strain ranges and strain rates. It was not possible to update this complete section and all dependent sections before the editorial deadline. However, the analysis itself was repeated with the revised data sets and the conclusions were essentially the same. The main difference was that in the new analysis, the coefficients for the two interaction effects listed in Table 4.6 were very close together, so there is no reason to prefer one over the other (Table 4.7 and Table 4.8). A detailed analysis will be published later [4.30].

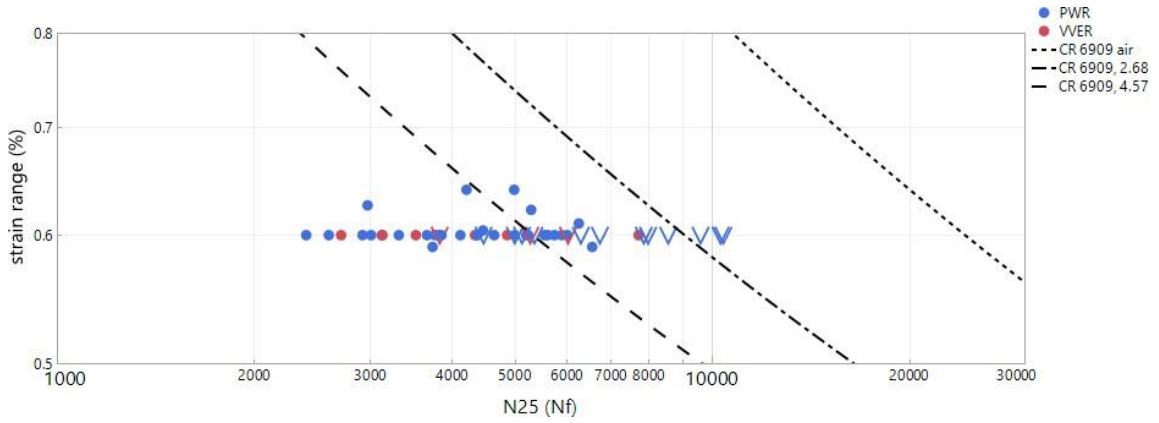


Figure 4.6 Plot of the data analysed in the present subsection [4.1].

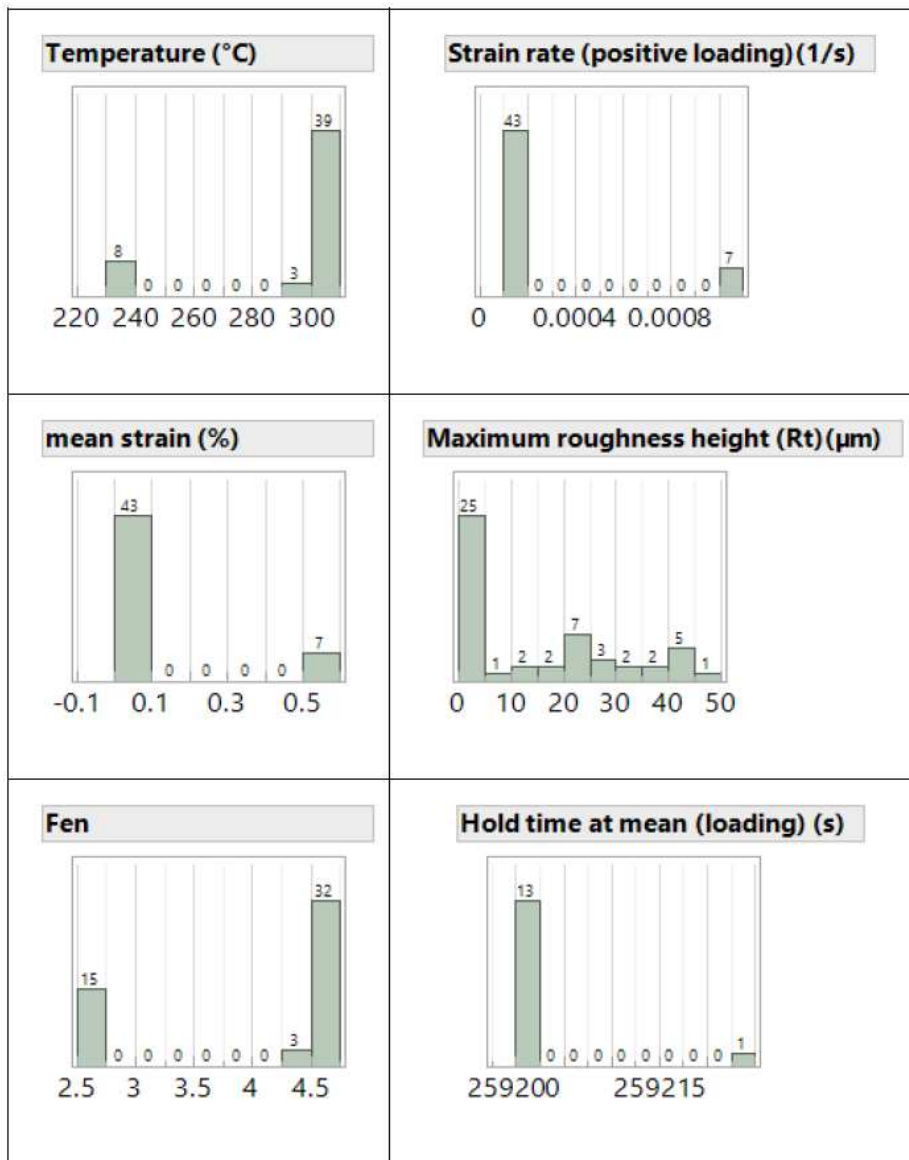


Figure 4.7 Distribution of test condition (low F_{en} sub-program) [4.1].

4.2.4.2 MODEL FOR A REDUCED F_{EN}

The initial model includes the factors and interactions listed in Table 4.9. The interactions not listed in the table (e.g. norm temp * norm pos strain rate) are not included in the initial model as there are not data to estimate these effects.

Parameter	Physical-quantity	Comment
norm Rt	surface roughness R_t	Normalized between 0.355 μm (-1) and 49.75 μm (+1)
norm temp	Temperature T	Normalized between 230 $^{\circ}\text{C}$ (-1) and 302 $^{\circ}\text{C}$ (+1)
norm pos strain rate	positive strain rate $\dot{\epsilon}$ (%s/1)	Normalized between 0.01%/s (-1) and 0.1%/s (+1)
norm mean strain	mean strain	Normalized between 0% (-1) and 0.5% (+1)
norm hold time	hold time	-1 \rightarrow no holds; +1 \rightarrow with holds
norm mean strain * norm Rt	-	-
norm Rt * norm hold time	-	-
norm Rt * norm temp	-	-
norm mean strain * norm hold time	-	-
norm Rt * norm temp	-	-

Table 4.9 List of effects included in the initial model.

Starting from this initial model, the not significant terms were removed as described above in Section 4.2.2 for the data from the main program. The effects included in the final (reduced) model are listed in Table 4.10 and Table 4.11.

Source	LogWorth	PValue
norm Rt	6.029	0.00000
norm temp	4.415	0.00004
norm pos strain rate	4.164	0.00007

Table 4.10 Terms included in the (final and reduced) model for the low F_{en} data.

Term	Estimate	Std.error
Intercept	8.64314293	0.0633828
norm Rt	-0.2866101	0.0515637
norm pos strain rate	0.20421897	0.0472907
norm temp	-0.2084559	0.0464134
σ	0.22784855	0.0227849

Table 4.11 Coefficients for the model in Table 4.10.

Only the main effects surface roughness, positive strain rate and temperature remain in the final model. This outcome is consistent with the analysis of the data from the main programme. The main effects included in the model for the main programme are environment, strain range and surface roughness. Of these, only surface roughness is considered here. The effects of positive strain rate and temperature were not considered in the main programme. Furthermore, all interactions in the 4 and 5 parameters models discussed for the main test campaign (Section 4.2.2) contained a parameter not included here.

Table 4.12 lists the fatigue life from the model N_f and the corresponding F_{en} model for a number of selected cases. Cases 1 and 2 correspond to the “standard” INCEFA-PLUS LWR test conditions (mean testing programme) for polished and ground specimens with the maximum R_t . Similarly, cases 3 and 4 compare the surface roughness at 230 °C and cases 5 and 6 at increased strain rate. In all cases, the F_{en} model was calculated as $N_f(\text{model})/N_f(\text{CR-6909})$, where $N_f(\text{CR-6909})$ corresponds to the mean air curve provided in NUREG/CR-6909,Rev.1.

Case	R_t (μm)	T (°C)	$\dot{\epsilon}$ (%/s)	$N_f(\text{model})$	$F_{en}(\text{model})$	$F_{en}(\text{CR-6909})$	$F_{en}(\text{model})/F_{en}(\text{CR-6909})$
1	0.36	300	0.01	4999	4.87	4.57	1.07
2	49.75	300	0.01	2818	8.64	4.57	1.89
3	0.36	230	0.01	7585	3.21	2.68	1.20
4	49.75	230	0.01	4276	5.70	2.68	2.13
5	0.36	300	0.1	7521	3.24	2.68	1.21
6	49.75	300	0.1	4240	5.74	2.68	2.14

Table 4.12 Fatigue lives and F_{en} factors for selected cases based on the model parameters in Table 4.11.

Basis for the F_{en} values is the mean air curve in CR-6909,Rev.1 which yields 24341 cycles for 0.6% strain range.

For case 1, the F_{en} predicted by the model is quite close to the F_{en} (CR-6909); the difference is less than 7%. The life reducing effect of high surface roughness is not explicitly included in NUREG/CR-6909, but it appears in the INCEFA-PLUS data. Consequently, the F_{en} (model) for the high R_t case is much larger than the corresponding F_{en} (CR-6909).

For the low F_{en} cases with polished specimens (cases 3 and 5) F_{en} (model) is 20% higher than F_{en} (CR-6909). As for case 2, the effect of high R_t in cases 4 and 6 is not explicitly taken into account in the NUREG/CR-6909 which explains why in these cases F_{en} (model) is significantly larger than F_{en} (CR-6909).

It should be noted that the F_{en} reduction by reducing the temperature or increasing the strain rate lead to the same F_{en} (model), which is in complete agreement with the NUREG/CR-6909 predictions³.

4.2.5 CONCLUSION FOR APPROACH #1

4.2.5.1 CONCLUSION FOR THE MODEL BASED ON THE MAIN PROGRAMME DATA

Starting from an initial model with 5 main effects and 10 interactions two reduced models with 5 and 4 effects respectively have been formulated. These models describe the bulk of the data

³ The erroneous calibration detected late in the project, required a reassessment of the data from one laboratory. A repetition of the analysis was carried out and no major differences were found. In particular, the fatigue lives for the cases listed in Table 4.2 re-calculated with the revised model differ less than 6% from the values in most cases. The only exception is case 5 where a difference of 16% was found. It was not possible to update the book before the editorial deadline. The final analysis with the revised data set is going to be published elsewhere [4.30].

very well with only a few outliers at lower strain ranges. The main factors influencing fatigue life are the strain range and the environment as well as the surface roughness as expressed by R_t .

It is not obvious how to deal with the interactions (between strain range and surface roughness as well as between strain range and environment) that have been identified as being statistically significant. Indeed, the interactions that were detected varied between successive evaluations of the data during the project. This may indicate that the model used is at the very limit of what could possibly be detected in terms of interactions between effects.

4.2.5.2 CONCLUSION FOR THE MODEL FOR LOW F_{en} DATA

The project has carried out a number of tests in a low F_{en} programme, where the F_{en} (CR-6909) was reduced by approximately a factor 2 compared to the tests in the main programme. This was achieved by either reducing the temperature from 300 °C to 230 °C or by increasing the strain rate from 0.01%/s to 0.1%/s.

Based on all LWR data at 0.6% strain range, a descriptive model was developed that includes the main factors R_t , temperature and strain range. In the case of polished specimens, the environmental factor F_{en} (model) calculated from this model agrees fairly well with the NUREG/CR-6909 predictions. However, the life reducing effect of high surfaces roughness (corresponding to an increase of F_{en} by 77%) is not reflected in NUREG/CR-6909.

The temperature reduction and the increase of the stain rate lead to the same reduction of F_{en} (model) which is in complete agreement with NUREG/CR-6909 predictions.

4.3 APPROACH #2: ANALYSING THE DATA USING RESIDUAL PLOTS AND NULL HYPOTHESIS TESTING

4.3.1 MANUAL EXAMINATION OF THE FATIGUE DATA OBTAINED ON THE COMMON MATERIAL

To further increase the understanding of the data gathered during the INCEFA-PLUS Project, the JMP® analysis was supplemented by a manual examination of the data using standard analytical methods that have previously been applied in analysing this type of data.

This section describes a review of the data using the engineering methods associated with the ANL report NUREG/CR-6909, namely a Langer format description of best-fit behaviour in an air environment, along with the use of environmental factor (F_{en}) as described in [4.8].

The overall process described in this section can be summarised as follows:

1. Derivation of a material specific best-fit curve based on a Langer equation.
2. Derivation of expressions describing the effects of surface roughness in both air and water environments.
3. Normalisation of the data using these surface roughness expressions in order to investigate for the effects of other testing parameters.
4. Use of statistical tests to identify significant effects in relevant subsets of the database.

The following analyses were performed using a bespoke script written in the open source programming language Python 3.

4.3.1.1 DATA USED

As discussed in Section 4.2.5, analysis of a complex multi-variate dataset is a complicated task, and throughout the project conclusions were found to be sensitive to the choice of data that was included in any given model.

The manual approach described in this section aimed to limit potential misinterpretations of the data by focusing on smaller subsets of the overall database. These represented self-consistent datasets that could be compared to already-established engineering descriptions of the fatigue behaviour of austenitic stainless steels in air and PWR water environments, in order to gradually develop an understanding of the dataset.

The following analyses made use of the same database as that described in Section 4.2.1 with the following modifications:

1. The analysis focused solely on XY182 material (common material) to reduce possible sources of scatter between different materials.
2. Additional data representing air fatigue tests on XY182 material were included in some parts of the analysis. These data were sourced from previous PhD projects ([4.12–4.14]) led in France and are not formally contained in the INCEFA-PLUS database.
3. Low F_{en} data were included in the analysis.
4. Given the observed uncertainties surrounding the treatment of data from tests on hollow specimens (Section 4.7), these were not included in the main analysis.
5. Data collected at strain amplitudes less than or equal to 0.25% were not included.

In order to interrogate the different models in this section, a residuals analysis type approach has been adopted. This approach offers a useful way of measuring the accuracy of a given model for individual data points and visualising overall trends as a function of different test parameters. Within this section, residuals are defined as:

$$Residuals = \log_{10}(experimental\ life) - \log_{10}(predicted\ life) \quad eq. 4.4$$

Given that fatigue data is typically log-normally distributed, the residuals are calculated based on logarithms to the base 10. In this formulation, positive residuals (i.e. > 0) represent data where the fatigue life was longer than that predicted by the applied model, and negative residuals represent shorter than predicted lives. A residual of 0 shows perfect agreement between experiment and model. Residuals of 0.3 and -0.3 represent factors of 2 above and below predictions respectively.

4.3.1.2 DERIVATION OF MATERIAL SPECIFIC BEST-FIT CURVE

The ANL best-fit curve and F_{en} methods described in NUREG/CR-6909 were based on a large study that incorporated data from multiple sources and included a relatively large number of different heats and types of material. As such, the methods represent a description of the average fatigue behaviour of austenitic stainless steels and individual materials can exhibit different mechanical and environmental responses. Previous experience within national testing

programmes has shown that improved descriptions of fatigue behaviour can be obtained by using material-specific best-fit curves in analytical models.

The best-fit curves in NUREG/CR-6909 are based on results collected under the test conditions listed in Table 4.13.

Strain-controlled loading
Fully-reversed loading (R = -1)
Simple waveforms (i.e. no hold times)
Polished surface
Air environment

Table 4.13 Test conditions used in the generation of best-fit curves.

Figure 4.8 (a) shows the available XY182 data corresponding to these conditions in both air and PWR water environments. The ANL best-fit curve can be seen to generally underestimate the fatigue life of the XY182 data points in air across the full range of strain amplitudes, which shows that XY182 has a superior fatigue life in air when compared to the ANL model.

In order to compare the PWR data to the ANL model these data were normalised by multiplying the fatigue lifetimes by the relevant F_{en} factor for those test conditions. Throughout this analysis the F_{en} expressions given in NUREG/CR-6909, Rev.1 Final Report have been used. Figure 4.8 (b) shows these normalised results, with the ANL best-fit curve generally providing a good description of the data at strain amplitudes of 0.3%, but slightly under-predicting the observed lives at an amplitude of 0.6%.

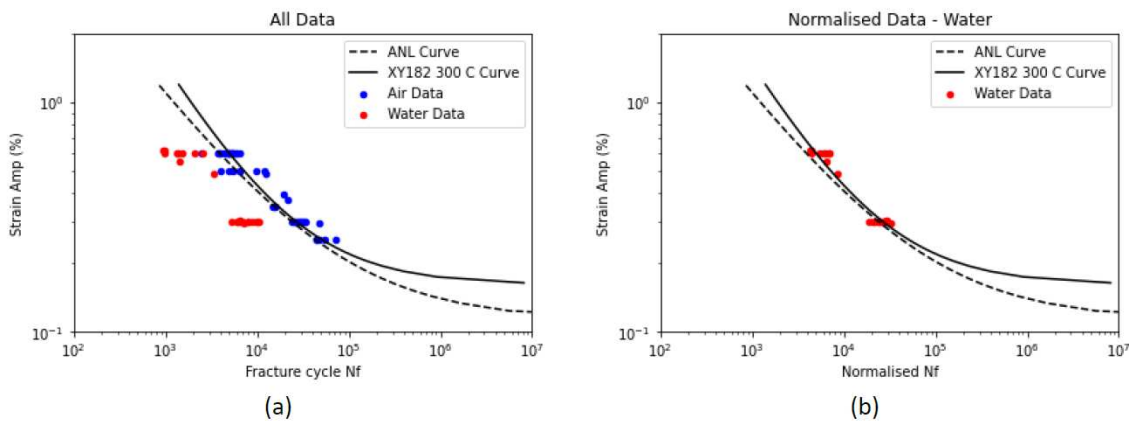


Figure 4.8 (a) XY182 data in air and PWR environments corresponding to conditions in Table 4.13 compared to different best-fit air curves. (b) PWR data normalised according to F_{en} [4.1].

It should be noted that overall, the ANL best-fit curve and F_{en} factors do provide a reasonably good estimate (within expected scatter factors of 2) of the fatigue lifetimes of XY182 for these conditions that are directly comparable to the data used to derive that method (Figure 4.9).

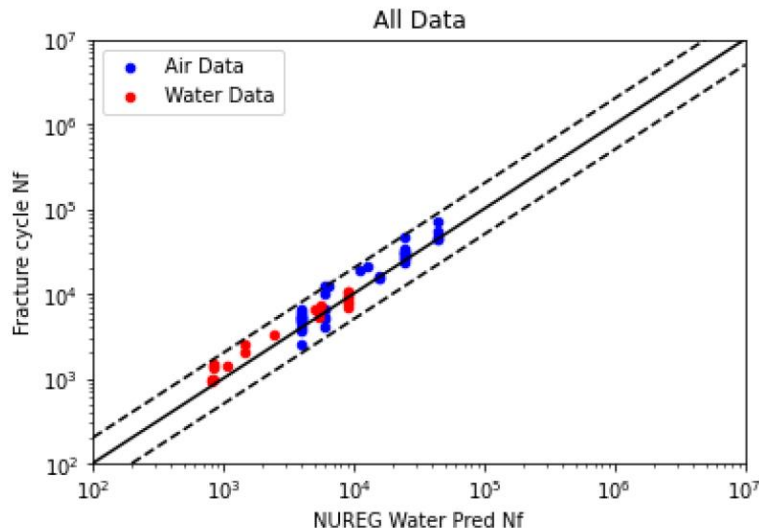


Figure 4.9 XY182 data in air and PWR environments corresponding to conditions in Table 4.13 compared to predictions using the ANL best-fit curve and F_{en} expressions [4.1].

Given that the fatigue behaviour of XY182 is not perfectly described by the ANL curve, a revised best-fit model was independently derived for this material. The model was based on high temperature (300 °C) data on XY182 that conformed to the test conditions given in Table 4.13, and included additional proprietary data that was made available by EDF for the purposes of this activity, but not more generally within the project. The data used has been obtained for applied strain amplitudes between 0.6% and 0.2%. A Langer form of best-fit curve was fitted to the data using a Maximum Likelihood Estimation method and is given by:

$$\ln(N) = 7.295 - 1.483 \ln(\varepsilon_a - 0.160) \quad \text{eq. 4.5}$$

where N is the fatigue lifetime, and ε_a is the strain amplitude (%). This curve is also shown in Figure 4.8, where in each case it can be observed to provide an improved description of the fatigue lives of XY182 across the full range of strain amplitudes.

Unless explicitly stated otherwise, throughout the remaining analyses air best-fit predictions have been based on the use of eq. 4.5. PWR water predictions were based on eq. 4.5 multiplied by the ANL F_{en} model calculated for the relevant test conditions.

4.3.1.3 ACCOUNTING FOR THE EFFECTS OF SURFACE ROUGHNESS

To facilitate an examination of the less pronounced effects (i.e. mean strain and hold times) expressions describing the effects of surface roughness in each environment were defined and incorporated into the models to normalise the data.

The JMP® analysis described in Section 4.2.2 identifies a significant effect of surface roughness on fatigue behaviour. Previous versions of that analysis using different datasets [4.2] had suggested that the effects of surface roughness varied in air and water environments. The JMP® model presented in Section 4.2.2 suggests that the effects of surface roughness are approximately equal in each environment, but that there is a difference in the magnitude of the effect at different strain amplitudes (varying between 0.3% and 0.6% with a greater effect being

observed at 0.3%). In the current analysis for XY182 material, the effects of surface roughness were found to vary by environment.

A dataset based on the conditions listed in Table 4.13, but also including specimens with a roughened surface, were examined in both air and PWR water environments. The additional French air data ([4.12–4.14]) were not included in the main dataset but have also been analysed to show the impact that a larger database has on the results. The residual plots using models with no correction for surface roughness effects are shown in Figure 4.10. Figure 4.10 (a) shows residuals as a function of ϵ_a which indicates that there is a small difference in the mean fatigue lifetimes at different strain amplitudes. Figure 4.10 (b) shows a relatively consistent decrease in the residuals (i.e. reduction in fatigue life) as the surface roughness increases for specimens tested in a PWR environment. A linear trend through the data appears to show a much less pronounced effect in air, although the residuals corresponding to roughened surface conditions are predominantly negative. The statistical significance of these effects is discussed further in Section 4.3.2.

Figure 4.10 (c) shows an equivalent residuals plot as a function of surface roughness for a dataset that includes the additional French air data. In this case, there is a more pronounced trend between fatigue life and surface roughness in air, with the magnitude of the effect being approximately half of that displayed by the water data.

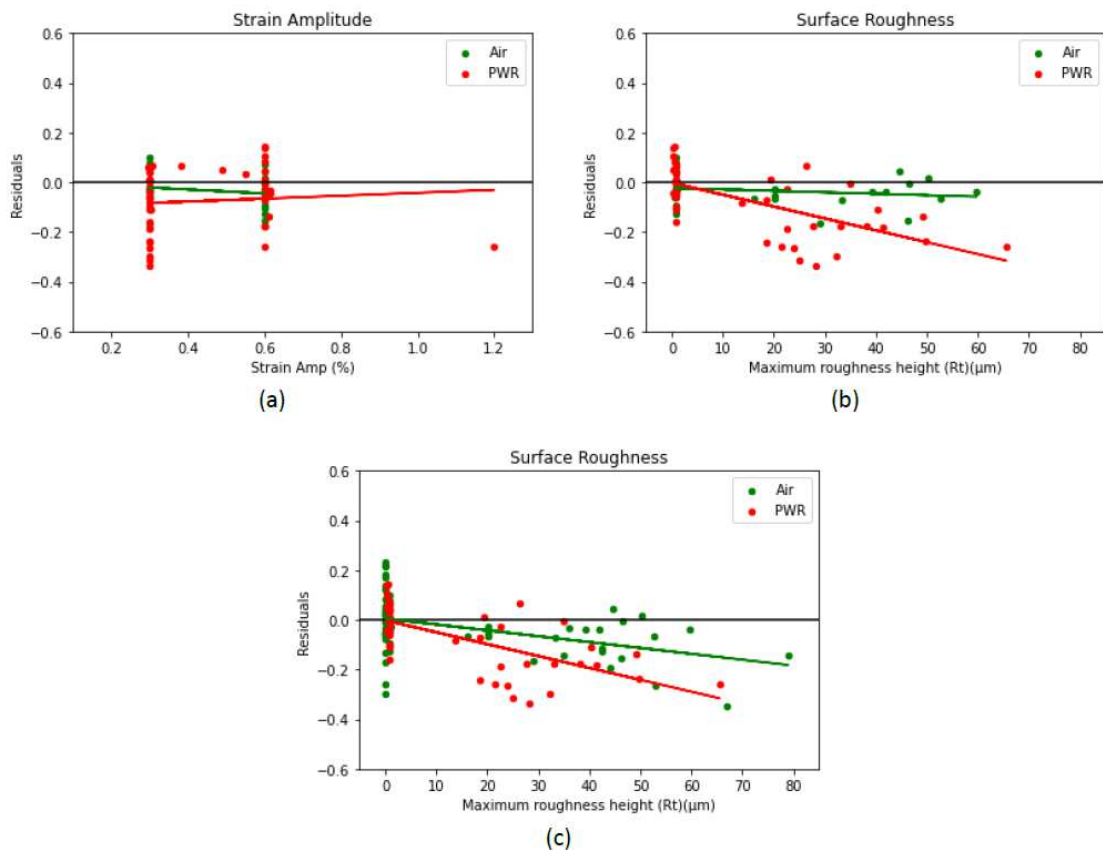


Figure 4.10 Residual plots for XY182 polished and roughened data using material-specific best-fit curve (a) excluding additional French air data, (b) excluding additional French air data and (c) including additional French air data [4.1].

For each of the figures in Figure 4.10, simple linear best-fit models were fitted to the data in order to provide a description of the effects of surface roughness in each environment. These were given by:

$$\text{Air (excluding additional French air data): } F_{rough} = 10^{-0.0006R_t} \quad \text{eq. 4.6}$$

$$\text{Air (including additional French air data): } F_{rough} = 10^{-0.00236R_t} \quad \text{eq. 4.7}$$

$$\text{PWR water: } F_{rough} = 10^{-0.00478R_t} \quad \text{eq. 4.8}$$

where R_t is the maximum roughness height in microns.

These expressions were incorporated into the models by multiplying the previously predicted lives for polished specimens by the factor F_{rough} . For air data gathered during the INCEFA-PLUS programme, Figure 4.10 (b) shows that the polished air residuals have a small negative offset. In deriving each of the F_{rough} expressions, only the gradient term from the best-fit lines was used to prevent any inappropriate over-correction of the data.

Figure 4.11 shows residual plots for the polished and roughened data without any mean strain or hold times (excluding additional French air data) using the models that incorporate the surface roughness corrections. Using the corrected expressions leads to flat residual plots in terms of surface roughness across the range of examined values, indicating that the effects of surface roughness have been normalised in this dataset. Subsequent plots based on the corrected models would also be expected to show a flat response for similar roughness effects. Figure 4.11 (b) indicates that the polished PWR residuals have a higher mean value than the model would predict.

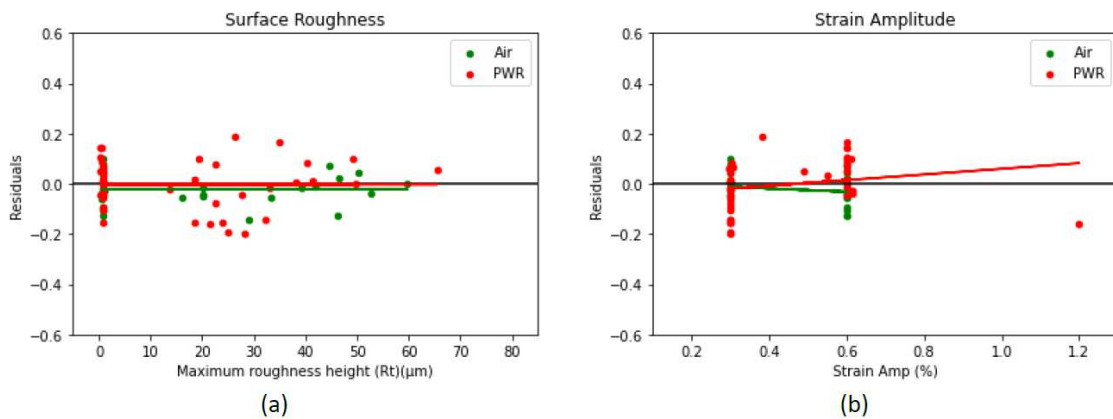


Figure 4.11 Residual plots for the XY182 polished and roughened data without any mean strain or hold times (excluding additional French air data) using surface roughness corrected models. (a) Surface roughness. (b) Strain amplitude [4.1].

4.3.1.4 INVESTIGATION OF MEAN STRAIN AND HOLD TIME EFFECTS

The normalised models that incorporate environment-specific surface roughness effects were used to predict the lifetimes of an expanded dataset, based on the previous data along with those corresponding to tests that included mean strains and/or hold times. A small number of outliers (defined as having a residual > 0.4 or < -0.4) were removed from the analysis to aid interpretation of the results.

Residual plots for a range of relevant test parameters are shown in Figure 4.12 (excluding additional French air data) and Figure 4.13 (including additional French air data). In each set of graphs, the air surface roughness correction that corresponded to the data that were included in the graph was used. The same water model was used in both graphs. A summary of the relevant statistics for each model fit are provided in Table 4.14.

Model	p, Shapiro Normality Test	Standard Deviation, SD	Mean of residuals
Air (excluding additional French air data)	0.09	1.22	-0.0043
Air (including additional French air data)	0.23	1.27	-0.008
PWR water	0.18	1.24	0.0046

Table 4.14 Summary of statistical fitting parameters for different models incorporating a surface roughness correction.

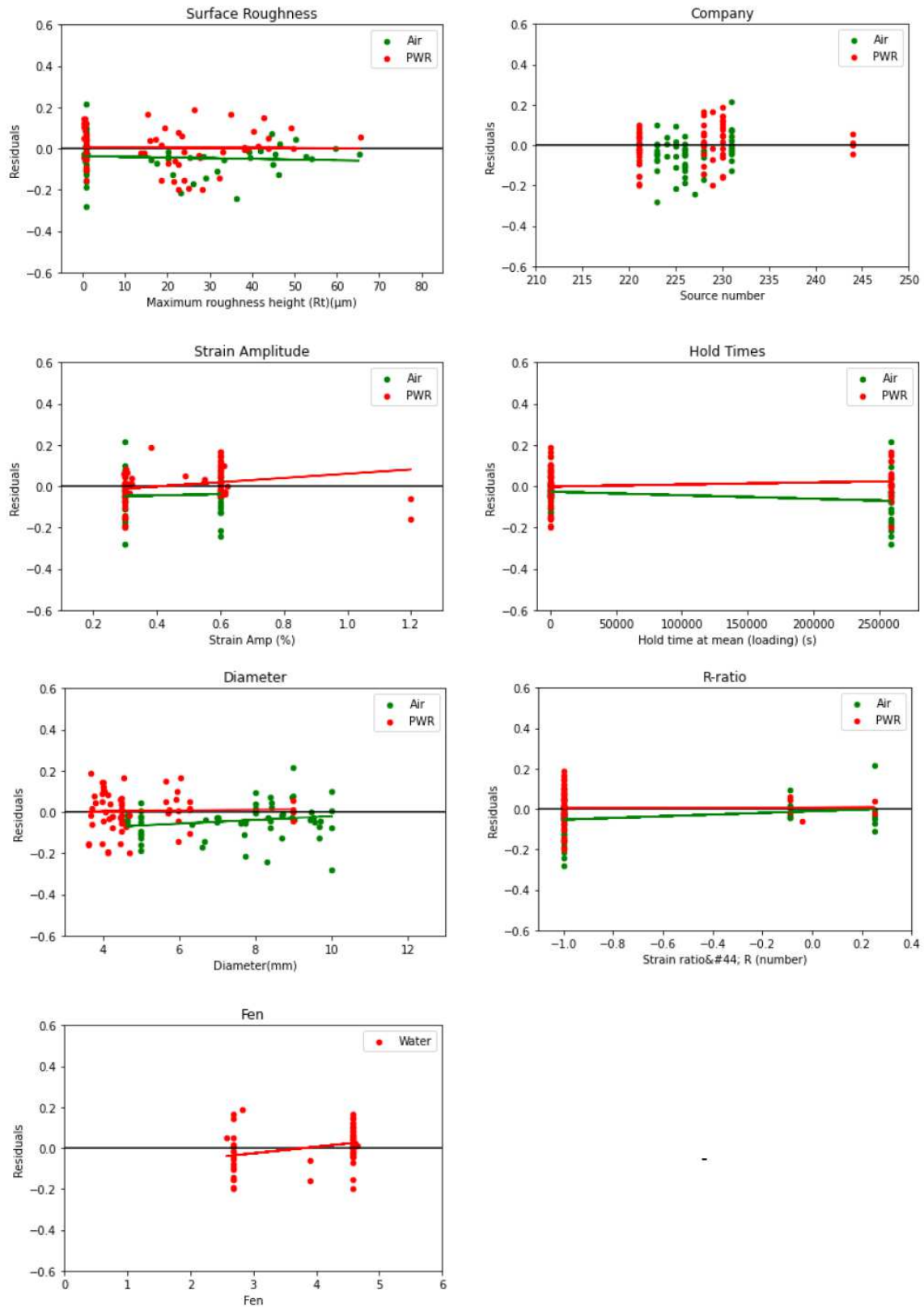


Figure 4.12 Residual plots for a range of test parameters. XY182 dataset excluding additional French air data. Air model featuring eq. 4.6 [4.1].

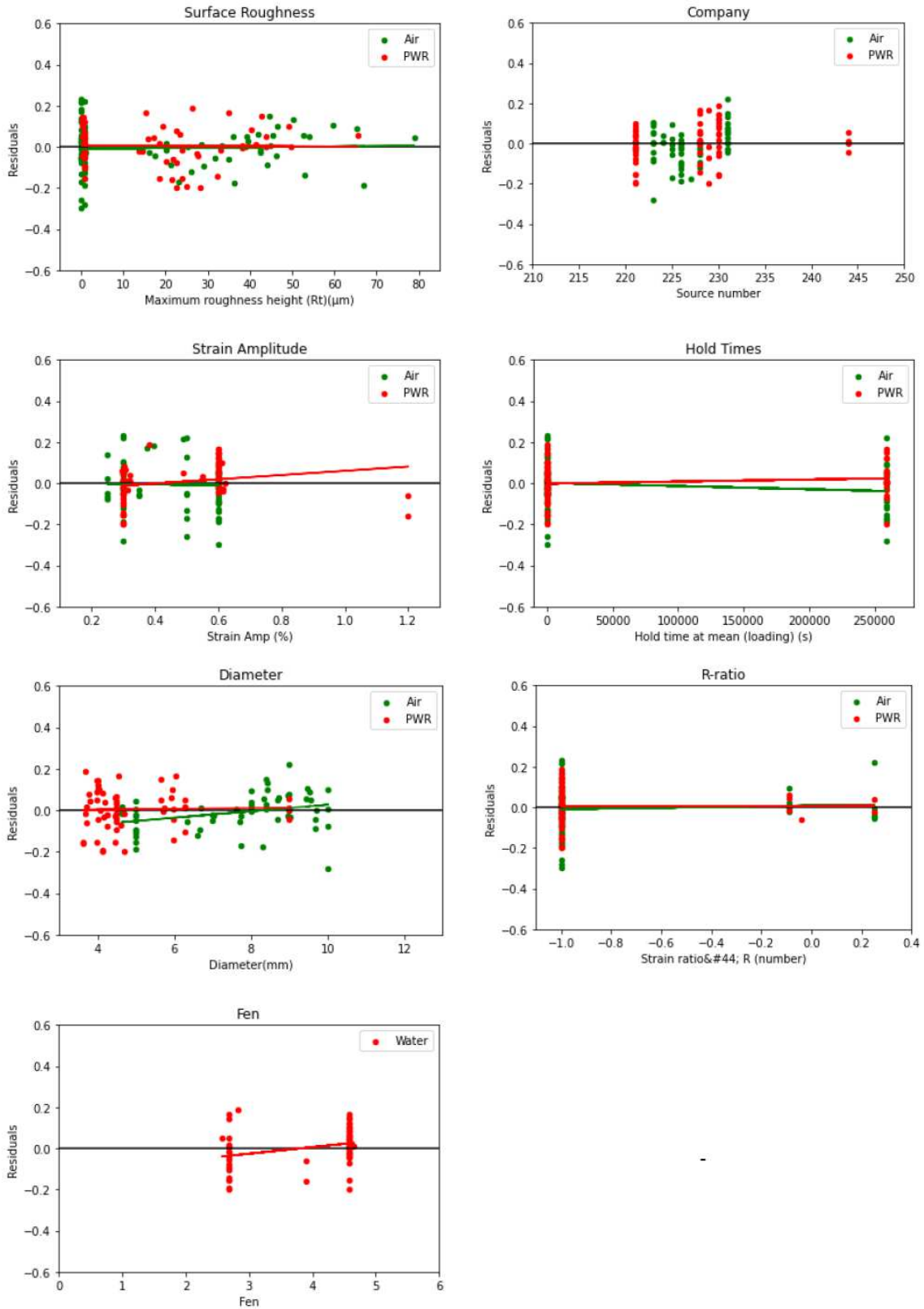


Figure 4.13 Residual plots for a range of test parameters. XY182 dataset including additional French air data. Air model featuring eq. 4.7 [4.1].

4.3.1.5 DISCUSSION

The surface roughness residual plots in both datasets are flat and the residuals display an even spread around the origin, with a similar overall range of scatter for polished and roughened tests. This suggests that the surface roughness effects in specimens that featured hold times and mean strains are similar in the specimens without these effects. The good agreement of this additional data provides further support for the validity of those expressions. A more detailed statistical analysis of this data is presented in Section 4.3.2.

With regards to hold times and mean strains, the residual plots are relatively flat indicating that there is no clear effect of these variable within the range of conditions that were examined during the project. A slight negative trend is visible in both sets of air results, along with a positive trend in the R-ratio plots for air results excluding the additional French air data. However, these are small relative to the scatter that is present in the data and the JMP® analysis in Section 4.2.2 confirmed that any possible effects are most likely not to be statistically significant. For mean strains, the absence of effects is most likely due to early plastic relaxation of any mean stresses that are present at the start of the test. Under strain-controlled loading conditions, the tests could be considered to be analogous to testing a material that has received a relatively mild level of cold work prior to testing, which would not be expected to have a large effect on fatigue lifetimes.

For hold times, it has been suggested that the absence of any significant effects might be due to the initial selection of test parameters [4.15] within the programme. These differed from previous test results that did identify a significant effect of hold times when they were applied to tests performed at lower strain amplitudes. As described in [4.15] additional tests that were more similar to those used in the AdFaM [4.4] programme were included in Phase III of the project. Due to long test times, the data from those tests has not been analysed within this analysis (see Section 4.5.2).

The residual plots for different laboratories show that overall the level of scatter within any given laboratory is relatively similar, and that the means can vary. For the air data modelled using eq. 4.6 (i.e. no significant effect of roughness in air), the air residuals for each laboratory are mainly negative and this is reflected in the lower mean value displayed most clearly in the surface roughness residuals plot. Applying the model based on eq. 4.7 improves the residual fits for laboratories 223, 224 and 225 but overcorrects 231. Testing at different laboratories complicates the interpretation of the results since the effects of surface roughness then become confounded with normal scatter between different facilities. An additional confounding factor is the use of different specimen diameters by different laboratories. The residual plots for specimen diameter show no clear trend for tests performed in PWR water. There appears to be a possible small trend that is visible in the air results, however the magnitude of the trend depends on the assumed surface roughness behaviour. In both cases the residuals for the specimen with the smallest diameter are consistently negative, but they are also within the scatter of the wider dataset. Additional analysis (not reported here) suggested that it was not possible to claim that the observed trend is statistically significant, and given the confounded nature of the database it is difficult to say for certain if this effect is real. Further discussion on these effects in the context of the JMP® analyses was provided in Section 4.7.2.2.

Phase III of the testing programme introduced a small number of tests that were performed using a lower F_{en} value. This was achieved by either increasing the strain rate of the test or decreasing the temperature by suitable amounts so as to achieve the same lower F_{en} . Whilst the results collected at the higher F_{en} value show good agreement with the NUREG/CR-6909 model, the residual plots in Figure 4.12 and Figure 4.13 indicate that the lower F_{en} results have shorter fatigue lives than those predicted by the same model. This is in agreement with the observations made in Section 4.2.4 which focused on results collected at a strain amplitude of 0.3%.

Given that the JMP[®] analysis in Section 4.2.2 attributed different effects of surface roughness to different strain amplitudes, separate residual plots for each strain amplitude were examined. These are shown in Figure 4.14 for the model based on eq. 4.7 (i.e. surface roughness effect in air). The two amplitudes display different overall mean values which mirrors the strain amplitude residual plots in Figure 4.12 and Figure 4.13. However, for both strain amplitudes the corrected models lead to flat residual responses in terms of surface roughness, and this is apparent in both environments. This would suggest that the observed surface roughness effects are not dependent on strain amplitude. The PWR data at a strain amplitude of 0.3% does appear to show a less evenly distributed level of scatter across the range of roughness values (lower lives at intermediate roughness and higher lives at higher roughness) but overall the corrected results are within the scatter of the polished data. The apparent mismatch with the observations in Section 4.2.2 is most likely due to differences in the databases that were used to generate the models, which is further compounded by the small amount of available data collected under directly comparable test conditions and the relatively small effect size that is being investigated. The relative differences between the models are discussed in more detail in Section 4.4.

Figure 4.14 also shows residual plots for F_{en} conditions at each strain amplitude. The results indicate that at a strain amplitude of 0.6% the relative difference between both conditions is well described by the F_{en} model. The mean of the residuals at 0.6% is slightly higher (approximately 10-15%) than the air predictions. It is not clear why these residuals are higher although it is noted that laboratory 230 reports higher than average residuals for tests at 0.6% and this laboratory also completed a larger number of tests at that strain amplitude. It should be noted that within Phase III of the testing, tests at this higher strain amplitude only decreased F_{en} by increasing the strain rate. At a strain amplitude of 0.3%, where lower F_{en} values were also achieved by lowering the test temperature, the F_{en} model appears to under-predict the low F_{en} results by approximately 25% when compared to the higher F_{en} results. It is not clear why the F_{en} model is over-predicting the observed lifetimes at the lower strain amplitude, but given the relatively small amount of data, it is considered that this is likely due to a combination of test scatter and the material specific environmental response. The low F_{en} results sit within the scatter of the higher F_{en} values and the overall decrease is considered to be small compared to the usual interpretation of test and material scatter (i.e. a factor of 2). At the lower strain amplitude, the results based on higher strain rates were in reasonable agreement with those based on a lower temperature. These observations support those made in Section 4.2.4.

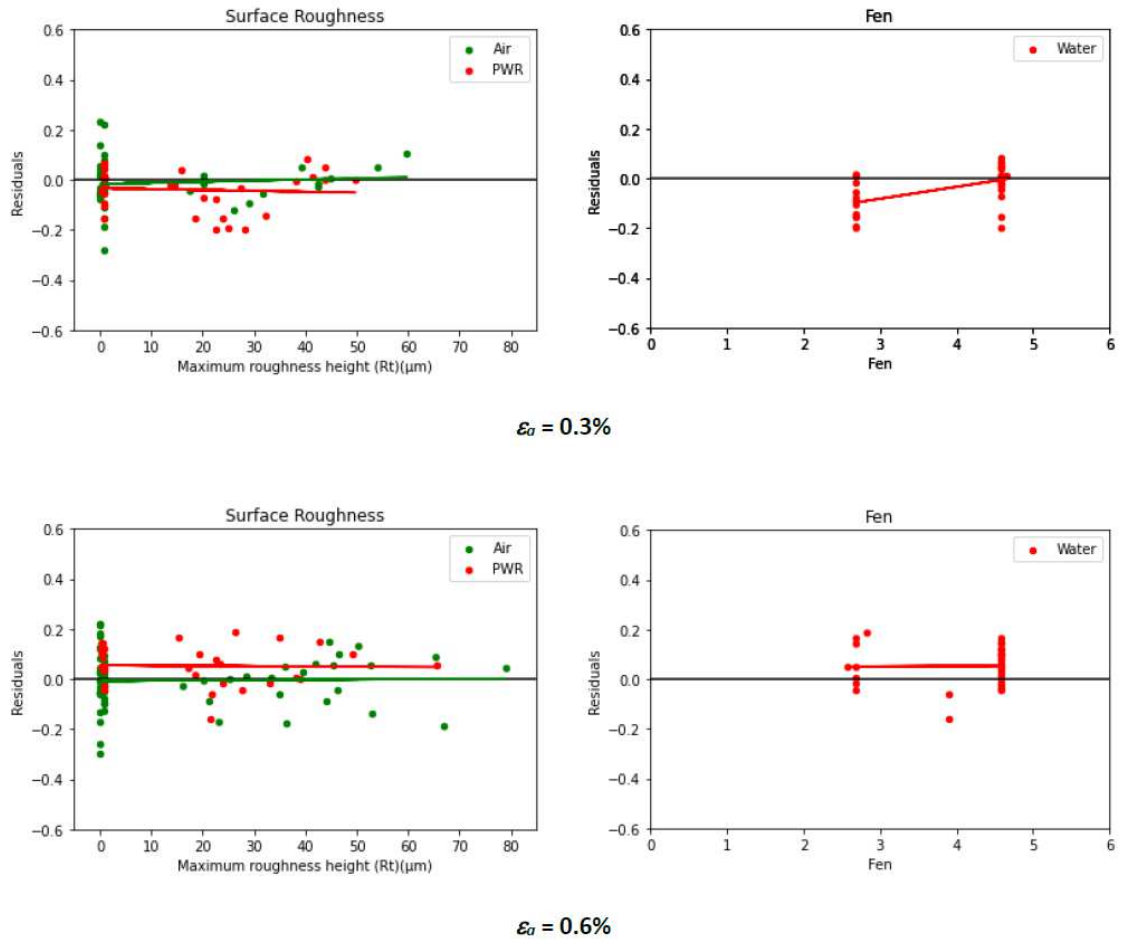


Figure 4.14 Residual plots for XY182 dataset including additional French air data separated by strain amplitude [4.1].

4.3.1.6 CONCLUSIONS

The main conclusions from this section of the analysis are as follows:

- The XY182 common material data that were collected during the INCEFA-PLUS programme are in good agreement with the NUREG/CR-6909 models that describe the fatigue endurance behaviour of austenitic stainless steels in air and PWR water environments. The use of a material-specific best-fit air curve further improves the agreement between predictions and experimental results.
- A detrimental effect of surface finish was observed in data collected from testing in PWR water. A minimal effect was observed for the equivalent INCEFA-PLUS data collected in air, however an effect (approximately half as penalising as in water) was observed when additional common material sourced from outside the project was included in the analyses. In both cases, the effects of surface roughness were much smaller than those assumed in NUREG/CR-6909.
- The data were normalised for the effects of surface finish based on linear descriptions of those effects in each environment. Analysis of a wider database using these models did not indicate any significant effects of mean strain or hold-times within the range of values that were tested in the project.

- No significant differences were found at different strain amplitudes other than a general small change in the mean position of the residuals which might be attributed to laboratory scatter. Several of the analytical parameters are confounded with each other which complicates the analysis, especially for small effects.
- Data collected at lower F_{en} values are well described by the F_{en} expressions at a strain amplitude of 0.6% and have lifetimes approximately 25% lower than predicted at a strain amplitude of 0.3%. Lower F_{en} data at the lower strain amplitude were achieved by either increasing the strain rate or lowering the temperature and the results from each approach were comparable.
- The differences between the current analysis on XY182 material and the JMP® model presented in Section 4.2.2 are attributed to differences in the datasets that were used to formulate the models. The observed trends are small and data interpretation is very sensitive to the choice of input data.

4.3.2 TWO-SAMPLES HYPOTHESIS TESTING FOR ASSESSING STATISTICAL SIGNIFICANCE OF SURFACE FINISH EFFECT

In order to supplement the analysis performed in Section 4.3.1, two-sample hypothesis testing has been implemented to assess the statistical significance of surface finish effect, based on the data generated during the main programme. These tests, shortly described hereafter, have been applied to the data generated on the common material only so as to remove potential source of additional scatter due to the inclusion of national materials (18% of the data represented in Figure 4.1 (a)). The data used in this subsection comprises data points generated with or without mean strain, as well as with or without hold times. Since the analyses presented in the previous sections (4.2 and 4.3.1) concluded that these two parameters (as tested during the project) have no effects, it is then possible to consider larger samples for analysing the effect of surface roughness.

4.3.2.1 BRIEF DESCRIPTION OF THE STATISTICAL TESTS USED

The three tests that were used are all statistical hypothesis tests that allow a side-by-side comparison of two samples of the considered set of data points (which correspond in our case to two different values of the studied parameter). In each of these tests, the null hypothesis H_0 assumes that there is no effect of the studied parameter. Each of these tests returns a p-value, which represents the probability of observing a test statistic at least as large as that obtained if H_0 is true. The p-value is then compared with a significance level α (set to 0.05), under which H_0 has to be rejected. In our case, the value of α quantifies the risk of falsely deciding that the parameter has an effect. The following descriptions of the tests used are very concise (see [4.16] for more details).

4.3.2.1.1 TWO-SAMPLE KOLMOGOROV-SMIRNOV TEST

The Kolmogorov–Smirnov (KS) test is based on the direct comparison between the empirical Cumulative Distribution Functions (CDF) of two samples. It is a non-parametric test, in the sense that it does not rely on any a priori hypothesis on the sample distribution (normality or homoscedasticity for instance), which might be convenient because these hypotheses can sometimes be difficult to verify.

The following hypotheses are investigated:

- Null hypothesis H_0 : the two samples are drawn from the same distribution.
- Alternative hypothesis H_a : the two samples are not drawn from the same distribution.

$$\begin{cases} H_0: F_1 = F_2 \\ H_a: F_1 \neq F_2 \end{cases} \quad \text{eq. 4.9}$$

F_1 and F_2 being respectively the CDFs of samples 1 and 2. The null hypothesis is rejected when the maximum distance D_{n_1, n_2} (which is the test statistic in this two-tailed version) reaches “high” values.

$$D_{n_1, n_2} = \max_x |F_{1, n_1}(x) - F_{2, n_2}(x)| \quad \text{eq. 4.10}$$

with n_1 and n_2 the sizes of samples 1 and 2 respectively, F_{1, n_1} and F_{2, n_2} the empirical CDFs of samples 1 and 2 respectively. An illustration of D_{n_1, n_2} is given in .

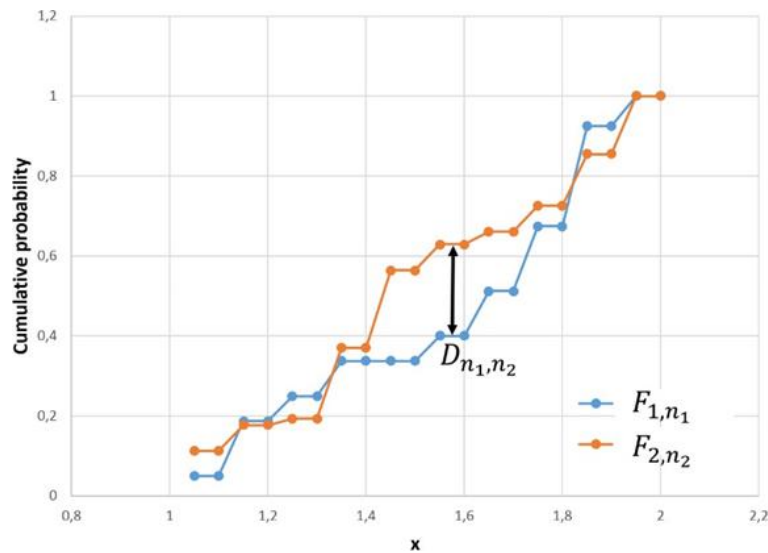


Figure 4.15 Illustration of the two-samples KS statistic [4.1].

It is important to note that the two-sample KS test only verifies whether the two samples are drawn from the same distribution. If the null hypothesis H_0 is rejected, it does not give any indication on the potential sources of the observed differences. The two following complementary tests can provide further information: the Mann-Whitney U test (MWU) indicates whether the two distributions are different in terms of central tendency, while the Mood rank test for dispersion indicates if they are different in their degree of dispersion.

4.3.2.1.2 MANN-WHITNEY U TEST

The following hypotheses are investigated:

$$\begin{cases} H_0: F_1 = F_2 + \theta, \theta = 0 \\ H_a: F_1 = F_2 + \theta, \theta \neq 0 \end{cases} \quad \text{eq. 4.11}$$

where θ is the translation parameter, which represents the shift between both CDFs F_1 and F_2 , or equivalently the difference between the medians of both populations. The MWU test is a

nonparametric test based on the ranks of each sample elements, determined against the union of both samples. By considering ranks rather than observed values, the data becomes symmetrically distributed and the impact of atypical points is considerably diminished. The procedure for the test involves pooling the observations from the two samples into one combined sample, keeping track of which sample each observation comes from, and then ranking lowest to highest from 1 to $n = n_1 + n_2$, respectively.

4.3.2.1.3 MOOD RANK TEST FOR DISPERSION

The following hypotheses are investigated:

$$\begin{cases} H_0: F_1(x) = F_2(x/\tau), \tau = 1 \\ H_a: F_1(x) = F_2(x/\tau), \tau \neq 1 \end{cases} \quad \text{eq. 4.12}$$

with τ the scale parameter, which indicates the dispersion in the samples. τ is not necessarily a standard deviation, as this test is also a nonparametric test.

4.3.2.2 IMPLEMENTATION

These tests have been implemented using Python language, and existing functions of the open-source SciPy library⁴. To allow for reproducibility of this analysis, Table 4.15 provides the names of the functions used in this library. KS and MWU tests were used in their two-sided versions.

Test	scipy.stats function used
Two-sample Kolmogorov-Smirnov test (KS)	scipy.stats.ks_2samp
Mann-Whitney U test (MWU)	scipy.stats.mannwhitneyu
Mood rank test for dispersion (Mood)	scipy.stats.mood

Table 4.15 scipy.stats function used for the tests.

The strain-controlled fatigue database available on the common material has been first split into two distinct groups: air and PWR data. PWR data comprises all the test conditions achieved in terms of temperature and positive strain rate, that is to mean “high” and “reduced” F_{en} conditions. Then, these two groups have been further split into two subgroups: polished and ground specimens. Note that for PWR data, hollow specimens are included in the subgroup that corresponds to smooth (polished) specimens (the inner wall of these specimens has a honed finish). In order to remove the strain amplitude dependency, \log_{10} residual has been calculated for each data point (either in air or PWR environment), according to eq. 4.4, where the prediction uses the XY182 best fit-curve and the NUREG/CR-6909, Rev.1 F_{en} expression (when needed). The samples used as input data for statistical hypothesis testing are the following:

- \log_{10} residuals for air/polished specimens data (30 data points), and \log_{10} residuals for air/ground specimens data (28 data points) in order to assess the significance of surface finish effect in air. These two samples are plotted in Figure 4.16 (as a function of strain amplitude, for information purposes only).
- \log_{10} residuals of PWR/polished specimens data (43 data points) and \log_{10} residuals of PWR/ground specimens data (36 data points) in order to assess the significance of

⁴ <https://scipy.org/>

surface finish effect in PWR environment. These two samples are plotted in Figure 4.17 (as a function of strain amplitude, for information purposes only).

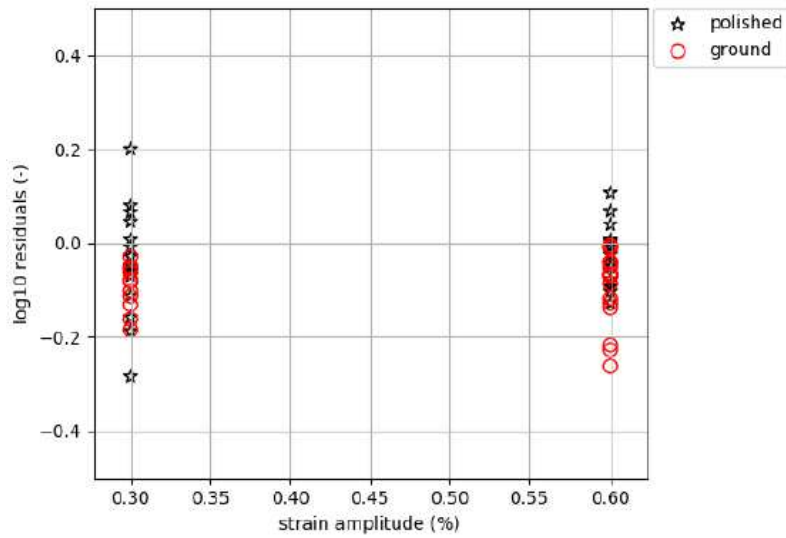


Figure 4.16 : Log₁₀ residuals for strain-controlled fatigue data generated in air on the common material, and calculated according to eq. 4.4 [4.1].

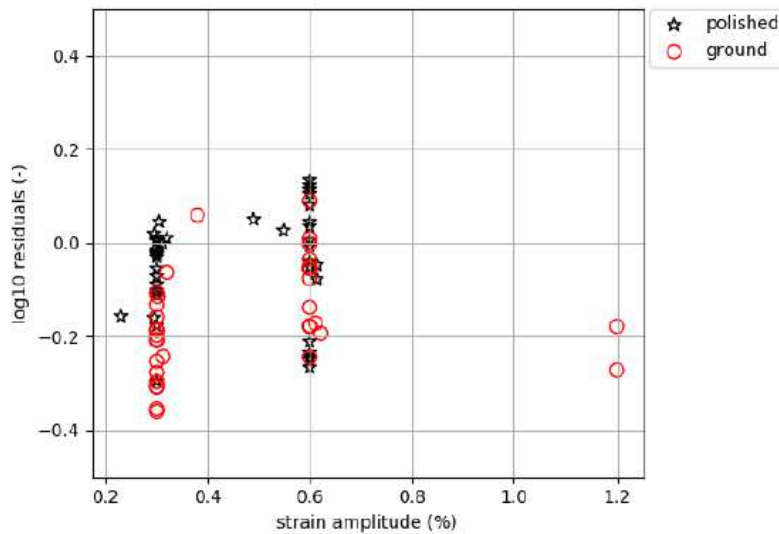


Figure 4.17 Log₁₀ residuals for strain-controlled fatigue data generated in PWR environment on the common material, and calculated according to eq. 4.4 [4.1].

The results of the statistical tests are presented in Table 4.16 and Table 4.17, respectively for air and PWR data. In both cases, the conclusion of the KS test is that there is a significant (in a statistical sense) difference between the tests conducted on polished specimens and ground specimens.

Furthermore, for both air and PWR groups, the MWU test indicates that this difference can be attributed to differences in central tendencies (negative shift of the mean of the residuals for ground specimens).

However, the Mood rank test for dispersion provides a high p-value that does not allow rejecting H_0 (that is to say, there are no clear differences in scatter), here again for both air and PWR groups.

type of test	p-value	statistical significance ($\alpha = 0.05$)
KS	6.1546e-03	Y
MWU	4.5142e-03	Y
Mood	1.2085e-01	N

Table 4.16 Results of the three statistical tests implemented for two-sample comparisons of the subgroups: air/polished specimens and air/ground specimens.

type of test	p-value	statistical significance ($\alpha = 0.05$)
KS	8.7438e-05	Y
MWU	2.8076e-05	Y
Mood	9.1542e-01	N

Table 4.17 Results of the three statistical tests implemented for two-sample comparisons of the subgroups: PWR/polished specimens and PWR/ground specimens.

Complementary tests (not reported here) such as for instance Levene's test for equality of variances and two-sample t-test (for equality of means) were also implemented and led to the same conclusion (differences in means, no evidences for variances). Since it seems that the effect of surface roughness (in both air and PWR environment) highlighted here seems to be explained by differences in central tendencies, one can give an estimate of the magnitude calculating the distance between the means of the two samples (in air and in PWR environment). This distance can be easily converted into a factor on life, which is 1.15 in air and 1.31 in PWR environment. It should be noted that these factors are average values for the dataset that was collected, and the actual life reduction factor varies with surface roughness (e.g. as shown in Figure 4.10). For typical plant surface finishes, the factors are much smaller than those assumed in the derivation of NUREG/CR-6909 (i.e. 1.5 - 3.5) and the implications of this are discussed further in Chapter 5.

4.4 BRINGING BOTH APPROACHES ON A COMPARABLE BASIS

This section compares individual model parameters for several factors from the models presented in Sections 4.7.2.1 and 4.3.1. The Section 4.7.2.1 model is very similar to the Section 4.3.1 model, however the former has been used in this section to minimise the effects of material scatter since it was based solely on XY182 material.

4.4.1 BEST-FIT CURVE

Figure 4.18 shows a comparison between the different best-fit curves from each of the models. The blue and green lines show the ANL air best-fit curve and the Section 4.3.1 XY182 material-specific curve respectively. The equivalent information for the JMP® model was inferred by calculating the difference in predicted lives at each strain amplitude based on the Intercept term in Table 4.25. In this graph, the JMP® lifetimes have been multiplied by a single factor so as to make the 0.3% strain amplitude data point coincident with the XY182 curve at that same strain amplitude. The relative difference in predicted lifetimes (lifetime at 0.6% divided by lifetime at 0.3% strain amplitude) values are given in Table 4.18. The JMP® and Section 4.3.1 models show good agreement with each other which is expected given that they were both based on XY-182 data and the material specific curve provides a better representation of baseline fatigue life for this material.

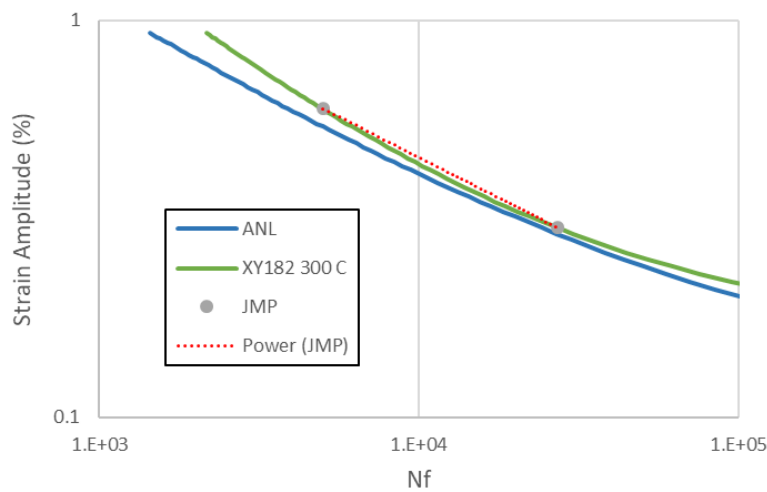


Figure 4.18 Comparison between descriptions of best-fit baseline behaviour between the different models [4.1].

Model	Factor between 0.3% and 0.6%
ANL	6.24
XY182 (300 °C)	5.46
JMP®	5.48

Table 4.18 Difference in factors of life between 0.3% and 0.6% strain amplitude by different models.

4.4.2 SURFACE ROUGHNESS CORRECTION

Ratios on life (calculated as rough life divided by polished life) were calculated for each of the different surface roughness correction factors in the models. The Section 4.3.1 F_{rough} air term is based on eq. 4.7 (i.e. the larger surface roughness effect) whereas the JMP® expressions were inferred from Table 4.25, taking into account both of the relevant terms. In each case, the effects were normalized to give the relative decrease between the parameters listed in Table 4.1.

Curiously, the relative effect of surface roughness that was identified in PWR within Section 4.3.1 is in very good agreement with the JMP® model based on a strain amplitude of 0.3%. The Section 4.3.1 air response is more onerous than the JMP® model term for strain amplitudes of 0.6%, which is attributed to the inclusion of the additional French air data (sourced from [4.12–4.14]) in deriving that term which was not used in the JMP® analysis. The equivalent Section 4.3.1 model that excludes the additional French air data would predict an almost negligible effect of surface roughness, so it makes sense that the JMP® model (which used an intermediary dataset) would contain predictions between these two extremes. Despite this, the predicted responses are broadly similar.

A previous analysis based on [4.2] showed similar results and relationships to those shown in Figure 4.19, however in that paper the effect of surface roughness was linked to environment in the same way as the Section 4.3.1 model has been implemented here. Overall it appears that both models include similar terms for representing the effect of surface roughness in PWR, however it is not clear why the controlling criteria are different in each case and this warrants further investigation.

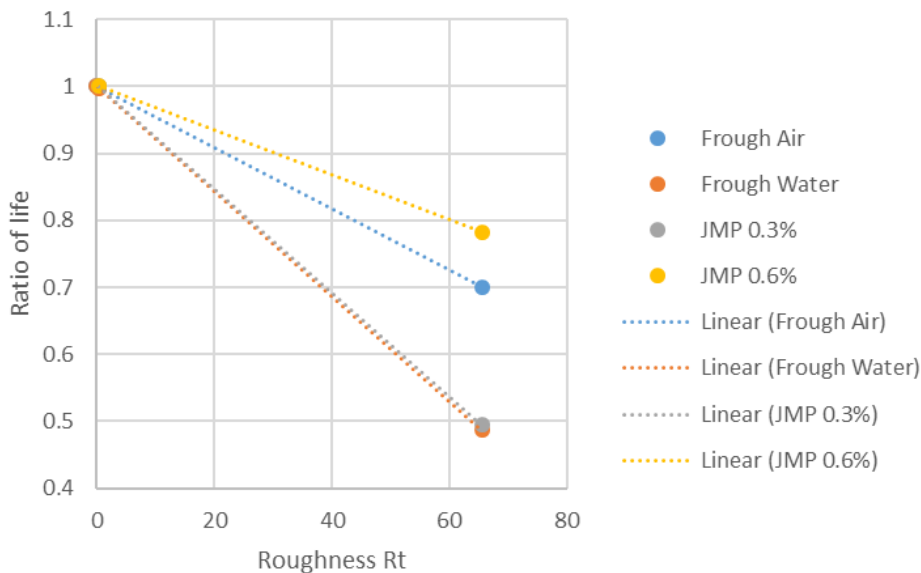


Figure 4.19 Comparison between different surface roughness corrections used in the models [4.1].

4.4.3 ENVIRONMENTAL EFFECTS

The majority of testing that was performed during the INCEFA-PLUS programme was collected under conditions corresponding to a $F_{en} = 4.57$. Based on the ‘env’ term in Table 4.25, the JMP® model for high F_{en} conditions would predict a higher equivalent F_{en} factor of 5.11 (approximately 12% higher than NUREG/CR-6909). The Section 4.3.1 analysis showed that for high F_{en} conditions, the NUREG/CR-6909 F_{en} provided a good description of the data at a strain amplitude of 0.3%, and was approximately 10-15% lower (i.e. conservative) for 0.6%.

For low F_{en} conditions, the Section 4.3.1 model indicated that F_{en} was similarly conservative at a strain amplitude of 0.6% and approximately 25% non-conservative at 0.3%. Section 4.2.4.2

showed that F_{en} was approximately 20% non-conservative at a strain amplitude of 0.3% and for polished conditions. These results are again in good agreement with each other.

4.4.4 CONCLUSION

Overall, the individual comparisons between the models show that they are in good agreement with each other and are capturing the same effects. This might be expected since both were derived from datasets that featured a majority of the same material and test conditions. Residual differences are attributed to the remaining variation in test data that was included in the model derivations (most significantly the use of hollow test data and the additional French air data).

Both models are also in good agreement with the NUREG/CR-6909 model, especially when material-specific factors are taken into account.

It is not clear why the models arrive at different interpretations of the interaction between surface roughness and either strain amplitude or environment. As discussed in Section 4.2.2, throughout the project analyses on different data sets have resulted in different interpretations of the smaller magnitude effects that have been observed. The difference in interpretation is considered to be most likely related to minor differences in the utilized datasets that subtly change the statistical significance of certain effects when all the data is considered as a complete set.

4.5 ANALYSIS OF THE DATA GENERATED DURING SPECIFIC COMPLEMENTARY TESTING CAMPAIGNS

4.5.1 ANALYSIS OF THE DATA GENERATED DURING THE MEAN STRESS PROGRAMME

This subsection presents the small testing program dedicated to the study of a mean stress effect on the fatigue life of austenitic stainless steel that was decided at the end of the INCEFA-PLUS testing Phase I. As expected, no effect of 0.5% mean strain on the fatigue life was observed with the strain-controlled fatigue tests carried out at 0.3% and 0.6% of strain amplitude in air and in primary water environment. It was then decided to explore another way to test a mean load (in the general meaning of the term) to a specimen in a laboratory experiment. Thus, a small testing program was set up and completed in the Phases II and III to investigate possible effects of mean stress (see Sections 3.2.3.2 and 3.2.3.3). The tests were to be performed by EDF and PSI partners. It was decided to carry out tests at 300 °C in air and PWR environment with and without mean stress of 50 MPa, which is considered as representative of static stress in real pressurized pipes.

4.5.1.1 EXPERIMENTAL PROCEDURES

Since it is not possible to impose a 50 MPa mean stress with standard strain-controlled fatigue tests, it was agreed to run two other types of fatigue tests. The first one was proposed by EDF and consisted in performing tests with an imposed strain amplitude and a continuously increasing mean strain to keep the mean stress level constant, which would be otherwise be

relaxed near to zero. The second type of tests were done by PSI and consisted in pure load-controlled tests, where the stress amplitude and mean stress can be arbitrarily chosen. The main drawback of these two types of tests is that ratcheting unavoidably occurs during the experiments. Furthermore, the strain amplitude is not constant during the load-controlled tests and the mean stress is not really constant for the first part of the strain controlled tests. Nonetheless, these proposed tests were recognized to be two straightforward procedures to control the mean stress level. To minimize the ratcheting effect and to have a chance to see any effect of the mean stress, it was agreed to perform the tests at relatively low strain amplitude, namely around 0.2%, which corresponds to a fatigue life of about 10^5 cycles in air.

The tests were performed in the same environments (air and PWR) as the other tests of INCEFA-PLUS except for the strain rate. Indeed, strain rate was chosen at 0.1%/s, to reduce the time of testing. This corresponds to a frequency of 0.125 Hz for 0.2% of strain amplitude, which is the frequency selected for the load-controlled tests. The F_{en} calculated with the NUREG/CR-6909 formula corresponding to 0.1%/s is equal to 2.68, which is well defined for the strain-controlled tests run by EDF. For the load-controlled tests, the F_{en} were estimated after the tests, based on the average strain rate over all the cycles of an experiment. This leads to a rather modest range of F_{en} from 2.59 to 3.05, or equivalently an estimated $F_{en} = 2.82 \pm 0.23$.

4.5.1.2 EXPERIMENTAL RESULTS

The results of all tests carried out in the frame on the program on mean stress effects, 21 in total, are summarized in Table 4.19, where we report the strain amplitude, the mean stress, and σ_{max} at half-life ($\tilde{\sigma}_{max}$) for the tests in strain-control; and the stress amplitude, the mean stress and the strain amplitude at half-life ($\tilde{\epsilon}_a$) for the load-control tests. The half-life values are reported as they are used later in the analysis to correlate the fatigue life determined with and without mean stress and for both control modes.

Testing mode	N_f (cycles)	ϵ_a (%)	$\tilde{\epsilon}_a$ (%)	σ_{mean} (MPa)	$\tilde{\sigma}_{max}$ (MPa)	σ_a (MPa)
strain-control air	10500	0.497	0.497	0	195	-
strain-control air	92000	0.2	0.2	0	153	-
strain-control air	215000 (runout)	0.18	0.18	0	153	-
strain-control air	25864	0.2	0.2	50	232	-
strain-control air	37872	0.18	0.18	50	219	-
strain-control PWR	132850	0.18	0.18	0	153	-
strain-control PWR	358019 (runout)	0.18	0.18	0	159	-
strain-control PWR	33752	0.2	0.2	0	151	-
strain-control PWR	10015	0.18	0.18	50	227	-

strain-control PWR	8724	0.2	0.2	50	230	-
load-control air	13336	-	0.36	0	169	169
load-control air	124613	-	0.14	0	150	150
load-control air	33801	-	0.27	0	159	159
load-control air	238439	-	0.11	50	200	150
load-control air	95900	-	0.136	50	210	160
load-control PWR	61632	-	0.15	0	150	150
load-control PWR	180760 (runout)	-	0.13	0	153	153
load-control PWR	34800	-	0.15	0	155	155
load-control PWR	19800	-	0.23	0	157	157
load-control PWR	21500	-	0.14	50	205	155
load-control PWR	54500	-	0.11	50	200	150

Table 4.19 Fatigue data obtained with different control modes and mean stresses.

The fatigue life of austenitic stainless steels is typically characterized by the succession of:

1. Primary cyclic hardening.
2. Softening.
3. Stabilization or secondary hardening.

The details of the hardening/softening sequence depend in particular on strain-amplitude, strain-rate, and temperature so that the hardening/softening/hardening can occur at different stages of the fatigue life. In strain-controlled experiments, cyclic hardening and softening are simply manifested by an increase or a decrease of the stress amplitude during the fatigue life. Hardening followed by softening occurs between 10 and 100 cycles as we can observe on the left of Figure 4.20, which corresponds to a test without mean stress in strain-controlled mode. For the test with a 50 MPa mean stress, due to the Bauschinger effect of the material, the desired value of the mean stress can only be reached after around 1000 cycles as illustrated on the right figure. This is possible thanks to a continuous increase of the mean strain that reaches around 8% for the tests at 0.2% of strain amplitude and 6.5% for 0.18%. It should be noted that there are no differences of behaviours in water in comparison to the air.

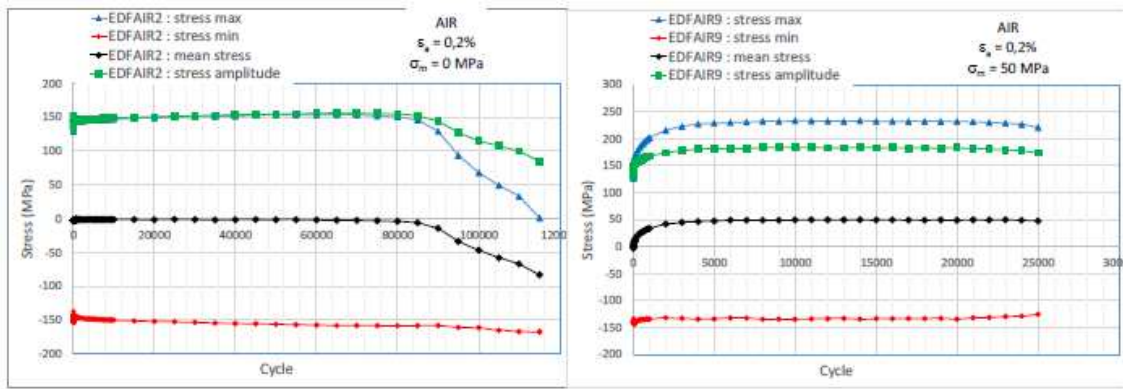


Figure 4.20 Stresses (min., max., and amplitude) and mean stress evolution versus cycle at a nominal strain amplitude of 0.2 % in air with $\sigma_m = 0$ MPa (left) and $\sigma_m = 50$ MPa (right); strain-control mode [4.1].

The results of the strain-controlled tests on the effect of the environment on fatigue life are illustrated in Figure 4.21. As expected, the PWR environment has a detrimental effect on the fatigue life of the 304L austenitic stainless steel at 0.2% of strain amplitude. In addition, the decrease of the fatigue life is well predicted by the environmental factor F_{en} given by the NUREG/CR-6909 for the strain rate tested i.e. 0.1%/s. This is true for the tests without mean stress but also for the tests with a 50 MPa mean stress. One can also observe from this figure that a mean stress has a detrimental effect on the fatigue life both in air and in water environment, whatever the strain amplitude is (0.2% or 0.18%). The three tests performed at 0.18% of strain amplitude without mean stress are not sufficient to conclude on the effect of the environment. It seems that no effect of the environment occurs in these conditions of temperature and strain rate at this level of strain amplitude, when no mean stress is applied. On the contrary, when a mean stress is applied, the fatigue life in water environment is again lower than the one in air and the difference can be well estimated by the NUREG/CR-6909 prediction.

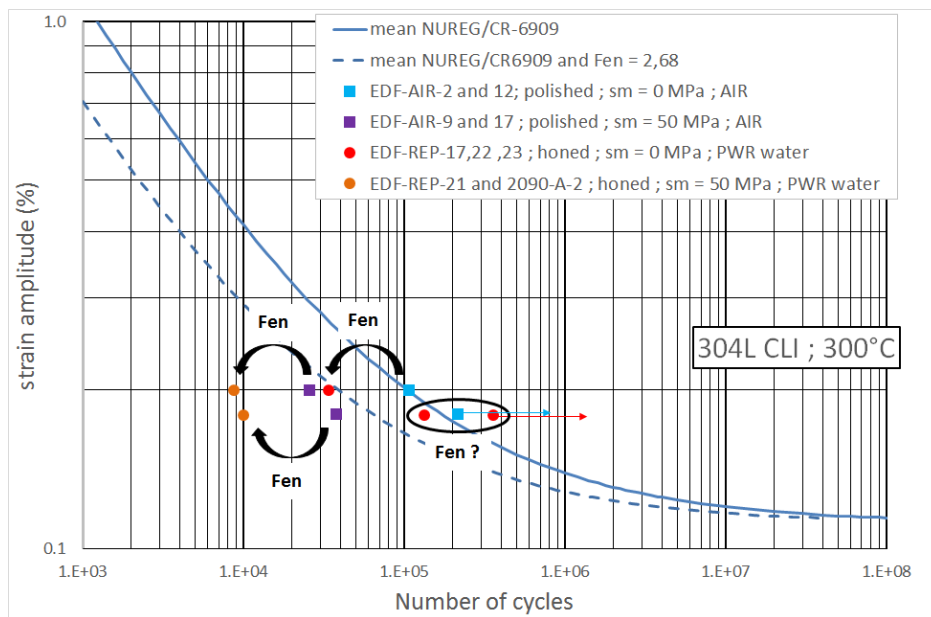


Figure 4.21 Strain-life data obtained from the strain-controlled tests [4.1].

In load-controlled experiments, the cyclic hardening and softening sequence appears as a variation of the strain amplitude, where a decrease of the strain amplitude evidently represents

the hardening behaviour, while an increase reflects the softening. The evolution of the strain amplitude and mean strain for some of our experiments is illustrated in Figure 4.22 and Figure 4.23. We can clearly see in Figure 4.22 for the tests without mean stress (left figure) that the strain amplitude decreases slightly during most of the fatigue life reflecting a persistent cyclic hardening. It has also to be emphasized that, for a similar stress amplitude, the tests with $\sigma_m = 50$ MPa have a smaller strain amplitude than that of the test with zero mean stress. The behaviour is specific of the austenitic steel and explains the increase of the fatigue life with mean stress at a given stress amplitude (compare the left and right plots in in Figure 4.22 and Figure 4.23). Note also the difference in the mean strain evolution during the fatigue life. As can be seen, the mean strain is of the order of few percent in the stabilized region and the ratcheting remains limited. The mean strain is attained after several cycles at the beginning of the experiment to reach the imposed with σ_{max} .

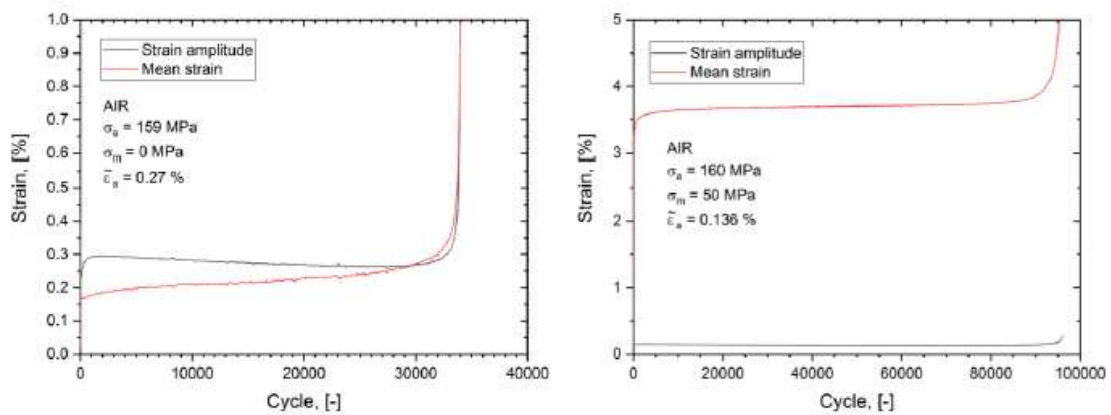


Figure 4.22 Strain amplitude and mean strain evolution versus cycle at a nominal stress amplitude of 160 MPa in air with $\sigma_m = 0$ MPa (left) and $\sigma_m = 50$ MPa (right) [4.1].

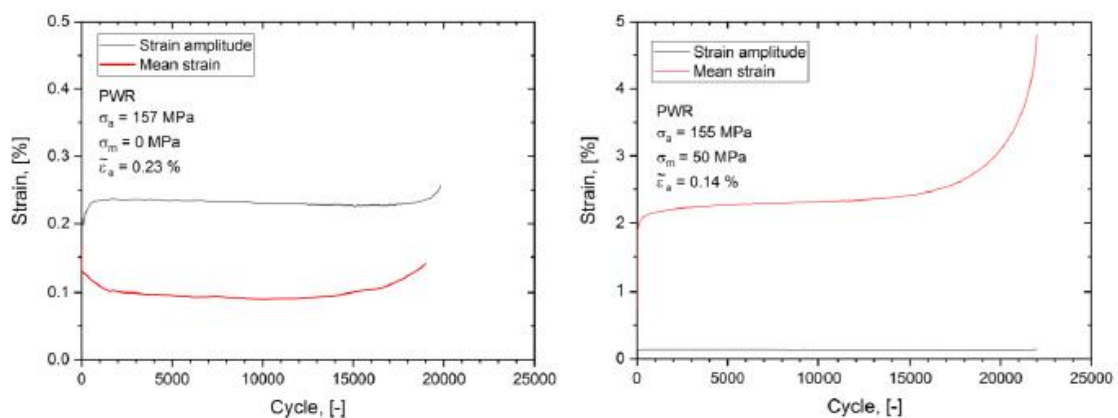


Figure 4.23 Strain amplitude and mean strain evolution versus cycle at a nominal stress amplitude of 156 MPa in PWR environment with $\sigma_m = 0$ MPa (left) and $\sigma_m = 50$ MPa (right) [4.1].

Figure 4.24 presents the fatigue life of the load-controlled experiments. One observes a clear increase of the fatigue life with mean stress for the tests performed in air. On the contrary, the effect seems to much less marked in PWR environment.

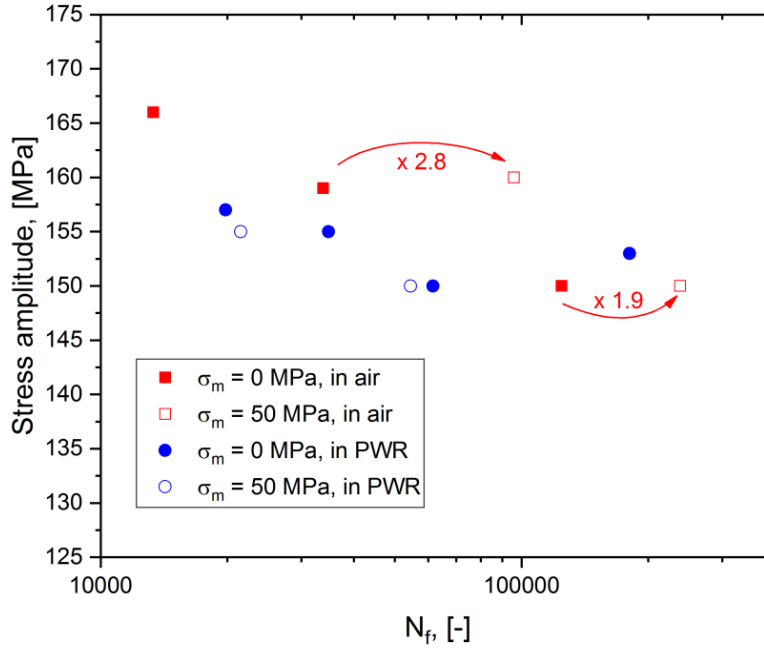


Figure 4.24 Stress-life data obtained from the load-controlled tests [4.1].

An attempt to correlate all fatigue data with zero and non-zero mean stress in air and PWR environment and for both testing modes was done. For austenitic steels, it has already been shown that the fatigue life can be predicted with the approach proposed by Smith, Watson and Topper (SWT) and based upon a maximum stress–strain amplitude function. The SWT function between strain-amplitude, stress-amplitude, mean stress and fatigue life has the form:

$$SWT = \sqrt{(\sigma_a + \sigma_{mean})\varepsilon_a E} = \sqrt{\sigma_{max}\varepsilon_a E} \quad \text{eq. 4.13}$$

where E is the Young’s modulus and σ_{max} is the value determined at half-life. Already in the original paper of SWT, various forms, albeit similar, of the stress-strain function were suggested. In our analysis, we have selected the values at half-life ($N_f/2$) for σ_{max} and ε_a and noted them $\tilde{\sigma}_{max}$ and $\tilde{\varepsilon}_a$. Note that these values are very close to the imposed values σ_{max} and ε_a in load-control and strain-control respectively. So in the following, SWT is calculated as:

$$SWT = \sqrt{\tilde{\sigma}_{max}\tilde{\varepsilon}_a E} \quad \text{eq. 4.14}$$

SWT is calculated with the data summarized in Table 4.19. In order to use the SWT parameter in a practical way for fatigue life predictions, we need to find an expression for $SWT = SWT(N_f)$, which can be easily derived from the strain-controlled data without mean stress. In other words, we can consider the mean NUREG/CR-6909 air curve that yields a relation between ε_a and N_f as:

$$\tilde{\varepsilon}_a = P(N_f)^{-\beta} + C \quad \text{or equivalently} \quad N_f = \left(\frac{P}{\tilde{\varepsilon}_a - C}\right)^{1/\beta} \quad \text{eq. 4.15}$$

with $P = \exp(\beta A)$ and $\beta = 1/B$, where A, B and C are the parameters of the Langer fatigue model (see eq. 2.1 for instance). The values of these coefficients for the NUREG/CR-6909 mean air curve (austenitic stainless steels) are: $P = 36.2$, $C = 0.112$, and $\beta = 0.5208$.

In addition, we need another relation between $\tilde{\sigma}_{max}$ and $\tilde{\varepsilon}_a$ (or N_f) that we established empirically by plotting $\tilde{\sigma}_{max}$ against $\tilde{\varepsilon}_a$ (see Figure 4.25) for all our tests obtained in air and PWR

environment. No significant difference between the two environments can be seen. A power law between $\tilde{\sigma}_{max}$ and $\tilde{\epsilon}_a$ was considered to fit the data.

$$\tilde{\sigma}_{max} = G + H\tilde{\epsilon}_a^n \quad \text{eq. 4.16}$$

The previous relation allows to write SWT as a function of $\tilde{\epsilon}_a$ only

$$SWT = \sqrt{(G + H\tilde{\epsilon}_a^n)\tilde{\epsilon}_a E} \quad \text{eq. 4.17}$$

Using eq. 4.15, SWT can be written as a function of N_f to derive a SWT-life curve:

$$SWT = \sqrt{\left(G + H \left(P(N_f)^{-\beta} + C\right)^n\right) \left(P(N_f)^{-\beta} + C\right) E} \quad \text{eq. 4.18}$$

Using the numerical values of NUREG/CR-6909 mean curve for P, C and β , and the fitted value G and H, we can calculate the SWT-life curve to check if our experimental data in air are consistent with the predictions with eq. 4.18. The results are shown in Figure 4.25 where one can clearly see that globally all data with and without mean stress, independently of the deformation mode, are well described by eq. 4.18.

The same analysis was done with the data obtained in PWR environment. To take into account the LWR environment effect, we consider the approach based on the environmental factor F_{en} that we apply on the SWT-life curve. Since F_{en} is defined as:

$$F_{en} = \frac{N_{f,air}}{N_{f,water}} \quad \text{eq. 4.19}$$

and since it is a constant for a given testing condition (T, $\dot{\epsilon}$ and DO) and the fatigue limit B is unaffected by the environment, it can be simply written as:

$$F_{en} = \left(\frac{P_{air}}{P_{water}}\right)^{1/\beta} \quad \text{or equivalently} \quad P_{water} = \frac{P_{air}}{(F_{en})^\beta} \quad \text{eq. 4.20}$$

For the analysed test conditions, the F_{en} is about 2.7, so that P_{water} is equal to 21.6. With that value, we recalculated the SWT-life curve in PWR environment and found that the PWR data are also in reasonable agreement with the SWT predictions as can be observed in Figure 4.25. The analysis shows that converting the standard NUREG/CR-6909 strain-life curve into a SWT-life appears as a powerful method to account for mean stress effect in air and PWR environments.

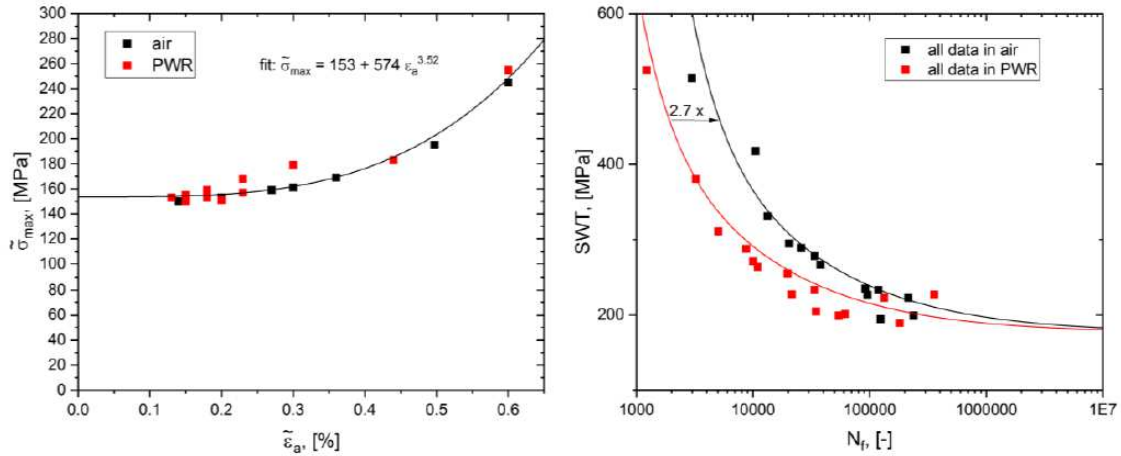


Figure 4.25 Left: empirical relation between $\tilde{\sigma}_{max}$ and $\tilde{\epsilon}_a$; right: SWT-life calculated with NUREG/CR-6909 mean curve coefficients [4.1].

The quality of the calculated SWT-life curves could have been slightly improved by fitting first the coefficients of the mean curve (eq. 4.15) to get values specific to the studied material and using them in eq. 4.18, instead of the coefficients of the mean curve. The SWT-life curves were then calculated by using the specific coefficients of the investigated 304L steel, which are: $P = 61.303$, $C = 0.115178$, and $\beta = 0.570616$. As can be seen in Figure 4.26 the quality of the fit is not significantly better than that in Figure 4.25 with the NUREG/CR-6909 mean curve coefficients. In addition, it must be recognized that the fitted curves slightly over predict the measured fatigue lives in air and PWR environments.

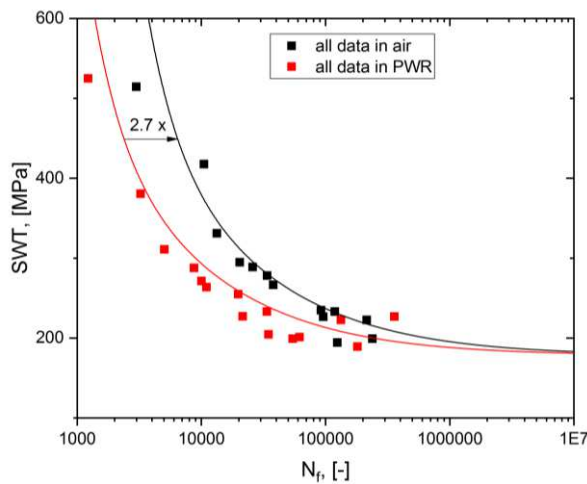


Figure 4.26 SWT-life calculated with the specific 304L mean curve coefficients.

Instead of using a SWT function given by eq. 4.18, one can fit the SWT data with simple Langer equations, keeping the power exponent and fatigue limit the same in both environments to make use of the F_{en} concept. The Langer fits yield somewhat better predictions as can be seen in Figure 4.27. Furthermore, the F_{en} factor associated with these Langer fits was found equal to 2.8, which is consistent with the expected F_{en} estimated with the NUREG/CR-6909 formula for the testing conditions.

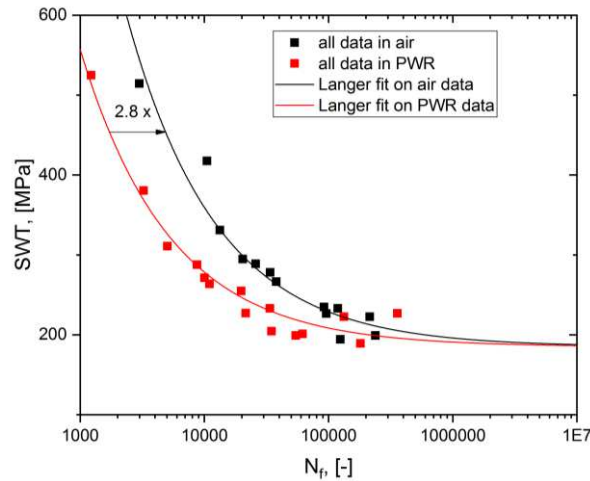


Figure 4.27 Langer fits on the SWT-data.

4.5.1.3 CONCLUSIONS FOR MEAN STRESS PROGRAMME

Mean stress (+50 MPa) effects on fatigue life and possible interactions with PWR environment were investigated with strain-controlled and load-controlled experiments. For the strain-controlled experiments and for $N_f < 10^5$, a clear reduction of fatigue life in PWR environment was found independent of the mean stress level and is in good agreement with the predictions based on the F_{en} calculations with NUREG/CR-6909 equation. This indicates that there is no synergistic effect between mean stress and PWR environments. A reduction of fatigue life due to the PWR environment was also found for the load-controlled tests and $N_f < 10^5$.

The large scatter in fatigue life for all tests performed with smaller strain or stress amplitude leading to $N_f > 10^5$ do not permit the drawing of firm conclusions on the conjugate effect of mean stress and PWR environment in the high cycle fatigue (HCF) regime. However, it seems that the environmental effect on fatigue life disappears for the lowest amplitudes (stress or strain) tested in this study without mean stress and that it becomes effective again when a non-zero mean stress is applied.

An analysis based upon the Smith-Watson-Topper parameter was considered. The NUREG/CR 6909 air curve was converted into a SWT-life curve using an empirical calibration between the maximum stress and strain amplitude at half-life. The SWT parameter was calculated for all tests of the program. The results obtained in air show that the NUREG/CR-6909 converted SWT-life curve correlates well all the data with and without mean stress. Similarly, the data obtained in PWR environment falls reasonably close to the SWT-life curve, shifted by the appropriate F_{en} . This observation also confirms that for conditions tested in this program, mean stress does not amplify the PWR environment effect.

4.5.2 ANALYSIS OF THE DATA GENERATED DURING THE HOLD TIME PROGRAMME

This subsection presents an interpretation of the results from additional testing on hold times. A series of tests that included hold times were included in Phases I and Phase II of the INCEFA-PLUS testing programme. A preliminary analysis of these results suggested that there was no

observable effect of hold times for the tested conditions, which led to the decision to reassess the test matrix prior to the commencement of Phase III [4.15].

4.5.2.1 EXPERIMENTAL PROCEDURES

Prior review identified the following main points:

- Previous work performed under the AdFaM programme [4.4] had identified that hold times were more significant at lower strain amplitudes than those used during Phases I and II of WP2 (0.3 and 0.6%). This was considered to be due to differences in the relative levels of plasticity that develop during testing at different strain amplitudes, with hold time effects being understood to be more effective when loading is predominantly elastic.
- Larger life extensions were observed for more severe hold times, specifically those performed at higher temperatures and for longer durations.
- Hold time effects are theorised to extend life by extending the time to nucleate a crack. This means that applying holds towards the start of a test, when there is a lower probability of crack nucleation having already occurred, should lead to longer test lifetimes.

These observations were used to formulate a revised testing matrix for a smaller focused testing programme on hold times that was subsequently conducted by LEI (see Section 3.2.3.2). The revised tests were designed with consideration of the factors described above in order to try and maximise the likelihood of observing clear hold time effects. This included using a lower strain amplitude (0.2%) and applying holds earlier in the test. The temperature during hold times was increased from 300 °C to 350 °C. All testing was completed at LEI using polished solid specimens⁵. The Table 4.20 summarises the test conditions:

Strain amplitude	0.2%
Environment	air
Loading rate	0.4 %/s
Control method during hold	Zero load
Cycling temperature	20 °C or 300 °C
Hold temperature	350 °C
Cycles for applying holds	10000, 20000, and 3000
Hold duration	72 h
R-ratio	-1

Table 4.20 Test matrix for hold time test carried out during Phase III.

⁵ A detailed analysis will be published later [4.30].

4.5.2.2 EXPERIMENTAL RESULTS

Figure 4.28 shows available results from tests completed during the INCEFA-PLUS programme along with additional standard endurance data on XY182 material that was reported in [4.17]. Since the majority of data collected during the INCEFA-PLUS programme was at higher strain amplitudes, the latter data was included in order to allow for an estimation of the baseline endurance behaviour at a strain amplitude of 0.2% (i.e. the strain amplitude at which the later INCEFA-PLUS hold time tests were performed). In total LEI completed hold time tests where cycling was performed at room temperature, and some other tests where cycling was completed at a higher temperature of 300 °C. In both cases holds were applied at a temperature of 350 °C. A single room temperature control test that featured no holds was also included in the testing. It is shown that material hardening (an increase in the applied stress required to obtain the original strain amplitude) occurred following the application of each hold time at both higher and lower strain amplitudes⁶.

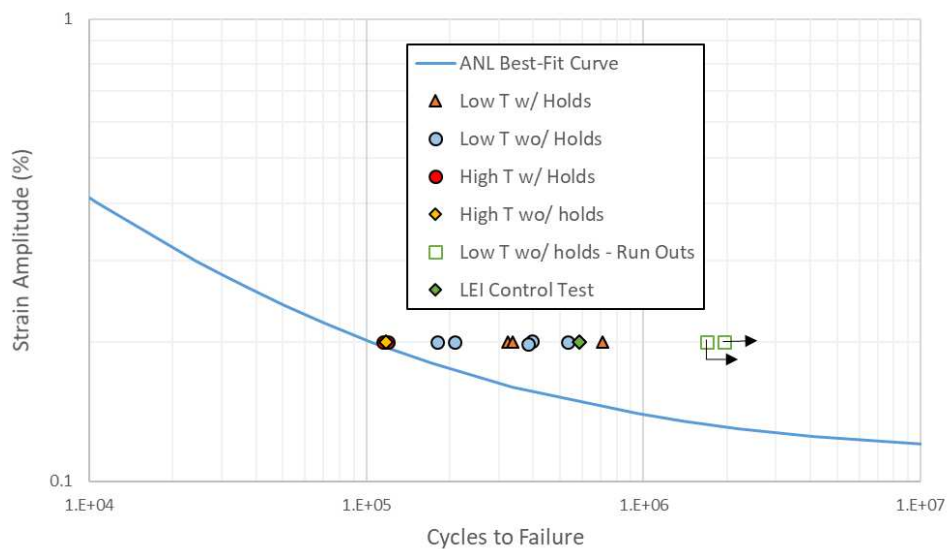


Figure 4.28 Results for endurance tests on XY182 at a strain amplitude of 0.2 %, with and without hold times [4.18].

There are only three data points representing cycling at 300 °C, where two of the points correspond to LEI hold time tests, and the third is an EDF test which was labelled as a run out. The endurance lives from all three tests are very similar. Given the small number of tests, similar lifetimes, and run-out behaviour, it is not possible to draw any strong conclusions about the effect of hold times under these conditions. It is known that temperature can have an effect on fatigue lifetimes at lower strain amplitudes, and so the remaining room temperature cycling data was analysed separately to these data.

Analysis of the room temperature tests is complicated by the relatively large amount of scatter for XY182 at a strain amplitude of 0.2%, and the relatively small number of data points. A comparison of the geometric means of tests with and without hold times (excluding run out data) suggests that the mean of tests with hold times is approximately 22% higher than those with no hold times, although a two-sample T-test on these populations showed that it was not

⁶ A detailed analysis will be published later [4.30].

possible to claim a statistically valid difference in the means at the $p = 0.05$ level. The single LEI control test with no holds had a longer life than the average of the low temperature hold time tests and was slightly longer than the equivalent literature data.

There are eleven room temperature cycling data points, three of which have holds. Of the eight remaining data points, two of these are classed as runouts. For the high temperature (300 °C) cycling data points, two have holds and one of the remaining without hold times points is a runout. These runouts and the low number of data points present an issue in determining the mean values for each of the conditions (high/low temperature and with/without hold times). By excluding or analysing these runouts as finite data, the means of the affected groups will be lower than if these data are handled as right censored data. However, the inclusion of right censored data in data sets containing few finite data points may result in the censored data being more influential than it should be. A useful exercise is to analyse a data set that includes the censored data and one that excludes it. In this way, it is possible to understand the sensitivity of the conclusions drawn from the analysis to the runout data.

Figure 4.29 displays the graphical interpretation of the distributions for the room temperature cycling data. This analysis and the Wilcoxon Homogeneity hypothesis test can be used to determine if there is a difference between two distributions. The large amount of overlap between the two lognormal distributions and the p-value greater than 0.05 (0.68 for this hypothesis test) indicates that there is no statistical difference between the tests with and without holds.

A similar analysis can be performed using the high temperature data. However, with so few data points, the use of a more qualitative assessment of the data is appropriate. The visual comparison of the two distributions in Figure 4.30 shows a large degree of overlap between the data from the two groups. Furthermore, it is clear that the two hold time data points are contained within the range of the reference data points.

Table 4.21 provides a summary of the means and associated 95% confidence intervals calculated from the lognormal distributions fitted to the groups of data. Comparison of the means for data sets containing runouts to those with only finite data points highlights the effect of including the runout data points on the calculated mean. To determine the presence of any differences between the groups of data it is necessary to compare the confidence interval values to the mean as well as the mean values themselves. Therefore, the assessment of the high temperature data investigating hold times supports the conclusion that under these test conditions there is no observable effect of hold times on the fatigue life of 304L stainless steel.

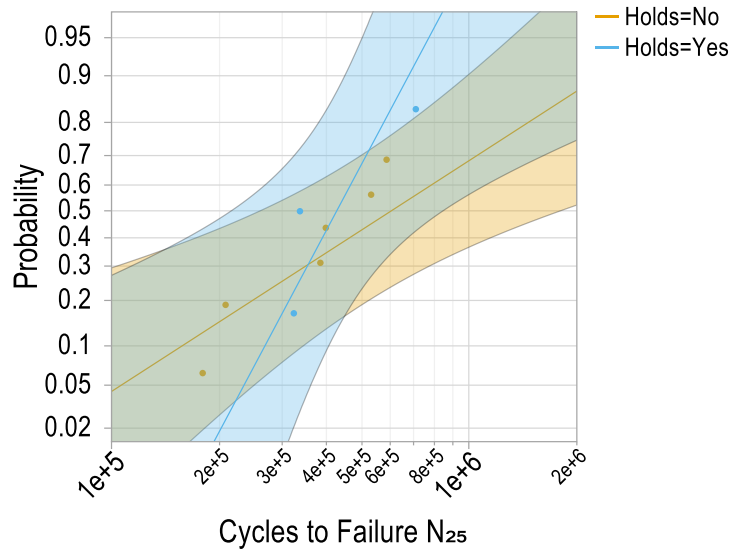


Figure 4.29 Life distribution analysis for the $\epsilon_a = 0.2\%$ room temperature data with and without holds [4.18].

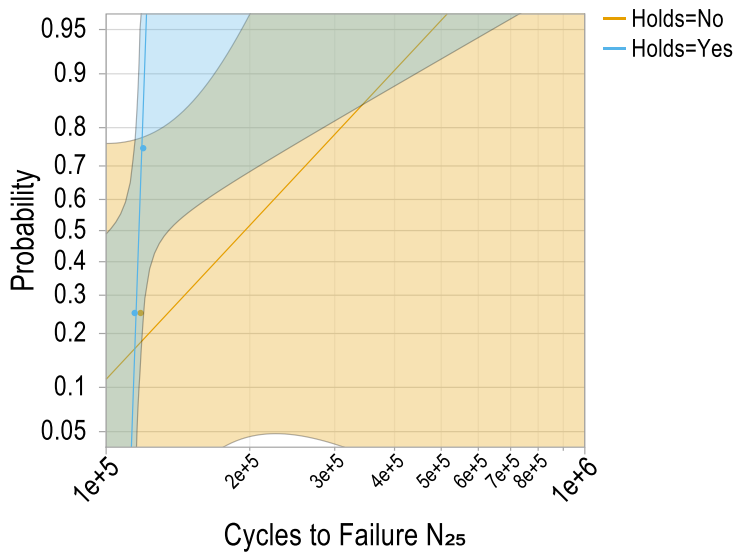


Figure 4.30 Life distribution analysis for the $\epsilon_a = 0.2\%$ high temperature (300 °C) data with and without holds [4.18].

Condition	Temperature (°C)	Mean (cycles)	Lower confidence interval	Upper confidence interval
Without holds	22	1049346	282916	3137002
With holds	22	454,453	298,006	693,031
Without holds	300	226,613	66,375	773,685
With holds	300	117,120	113,835	120,499

Table 4.21 Mean and 95% confidence interval values calculated from the lognormal distributions fitted to the data including runouts.

4.5.2.3 DISCUSSION OF THE HOLD TIME PROGRAMME

Hold times were previously investigated by the AdFaM [4.4] project and have featured prominently in the testing campaign of VTT. The project provided consistent evidence for life extensions as a result of the application of multiple hold time events in both 347 and 304L stainless steels at lower strain amplitudes (0.2 - 0.25%).

Although a full mechanistic description of the effects of hold times has not been developed, previous researchers have proposed that life extension may occur as a result of some combination of the following factors:

- 1) Material hardening following the application of holds may increase the effective endurance limit of the material and/or reduce the relative ratio of plastic to elastic strain. The precise reason for the observed hardening behaviour is not understood but is expected to be due to a dynamic strain ageing type phenomenon or some other type of reorganisation of internal dislocations and vacancies.
- 2) Higher temperatures may reduce/reverse the effective fatigue damage in the material, either through delocalisation of strain or internal stress-relief, by means of an annealing-type effect.

Both of the above factors would have a relatively larger effect on the high cycle fatigue (HCF) performance where fatigue lives are more sensitive to the material's endurance limit, a longer relative fraction of the life is taken up by crack nucleation, and a smaller proportion of the total applied strain is plastic (considered to be the main driving factor in developing fatigue damage). As discussed in Section 3.2.3.2, during Phases I and Phase II of testing the INCEFA-PLUS programme was not able to identify any significant effect (beneficial or detrimental) of hold times at strain amplitudes of 0.3 and 0.6% in air or light water reactor environments. Given the proposed explanations for hold time life extensions this is not completely unexpected, however the relatively low hold temperature of 300 °C complicates the interpretation of the results since this would most likely reduce the magnitude of any hold time effects if they were applicable across these loading ranges. Despite these complications, the INCEFA-PLUS programme has significantly increased the amount and variety of data at these loading conditions which will serve as an important contribution to the wider scientific literature surrounding these effects.

As shown in the analysis above, it was not possible to claim that hold times had a statistically significant effect on fatigue lives for the tested material. This is predominantly considered to be due to the relatively small number of tests that were able to be completed during Phase III of the programme. HCF testing is characterised by an increased amount of scatter in fatigue lives which can be seen in Figure 4.29. The amount of scatter in the available baseline data is of a similar or greater order of magnitude to the expected size of the effects being investigated. The requirement to include supplementary literature data to understand the baseline behaviour of this material is expected to have also contributed to the large amount of variation through normal lab-to-lab scatter.

The revised hold time testing in Phase III of the INCEFA-PLUS programme aimed to more closely replicate the conditions used during the AdFaM project by lowering the strain amplitude, increasing the hold temperature, and introducing holds at an earlier point in the test. Despite

these changes the test conditions were still relatively modest compared to some of the AdFaM tests where very strong hold times were observed. Many AdFaM tests featured regular applications of hold times throughout the entire test and an increased hold temperature of up to 420 °C. In reality, plant components are expected to spend long durations of time held at plant operating temperatures under static loading conditions, and these conditions are not practical to test within a laboratory. The choice of testing conditions in the INCEFA-PLUS programme was based on a combination of laboratory testing capabilities and programme partner interests relating to plant relevant operating temperatures. Overall, the conditions tested under the INCEFA-PLUS programme were generally more modest than those tested under AdFaM, but they are still considered to be of plant relevance and are complementary to the wider existing data set. Future analyses on these effects would benefit from investigating the larger global database of testing featuring hold times, and to this end the INCEFA-PLUS testing has provided a valuable contribution in this area.

4.5.2.4 CONCLUSION FOR HOLD TIME PROGRAMME

Hold time effects are still not fully understood and are an active area of research due to their potential use as an explanation for the good fatigue service history of nuclear power plant. An improved understanding of these effects could allow for these potential benefits to be claimed in the engineering justification of plant components, which would justify longer safe operational lives and reduced inspection requirements.

Testing during Phases I and Phase II of the INCEFA-PLUS programme included tests with hold times at higher strain amplitudes in air and light water reactor water environments at plant operating temperatures. Revised testing conditions in Phase III of the programme focused on lower strain amplitudes in the HCF regime, with testing conditions more closely aligned to previous hold time programmes.

Detailed analyses of the data have demonstrated that no statistically significant effect (either beneficial or detrimental) of hold times could be observed in the INCEFA+ results. A discussion on the data highlighted several complicating factors including the use of more moderate loading conditions, testing under conditions where hold time effects might not be expected, and the overall small number of available test results.

It is recommended that future investigations into hold time effects consider the wider body of test data that is now available in order to help improve the understanding of hold time effects and how they might be applied in engineering safety justifications.

4.5.3 FATIGUE DATA CONTRIBUTED BY PREUSSENELEKTRA

The INCEFA-PLUS database also includes a significant number of data points from a previous testing campaign sponsored by PreussenElektra and performed by VTT. These tests were all performed on standard uniaxial specimens under fully-reversed ($R = -1$), strain-controlled loading. All of the results correspond to polished specimens and were performed on a type 347 Nb-stabilized austenitic stainless steel (heat identifier: X6 CrNiNb1810 - 105493). Testing was performed in both air and PWR water environments, covering a range of different temperatures in air, and a range of different strain rates in PWR water. The database also contains a small

number of tests that included the application of periodic hold times, however these were not included in the scope of the current analysis.

The results from PreussenElektra were not incorporated into either of the main analyses given in Sections 4.2 and 4.3 due to the differences in material composition and test conditions. An independent analysis of the data was performed using the standard austenitic stainless steel methods outlined in NUREG/CR-6909. The main findings are summarized below.

Figure 4.31 shows the results from testing in air at a range of different temperatures along with the ANL mean curve. As per previous observations, the data indicate that temperature can have a significant effect on the fatigue lifetimes of austenitic stainless steels. This difference is predominantly manifested towards the higher cycle region of the curve and can most likely be attributed to changes in the endurance limit of the material as a result of temperature-dependent material property changes. Towards the lower cycle regime, the observed differences in fatigue life are minimal.

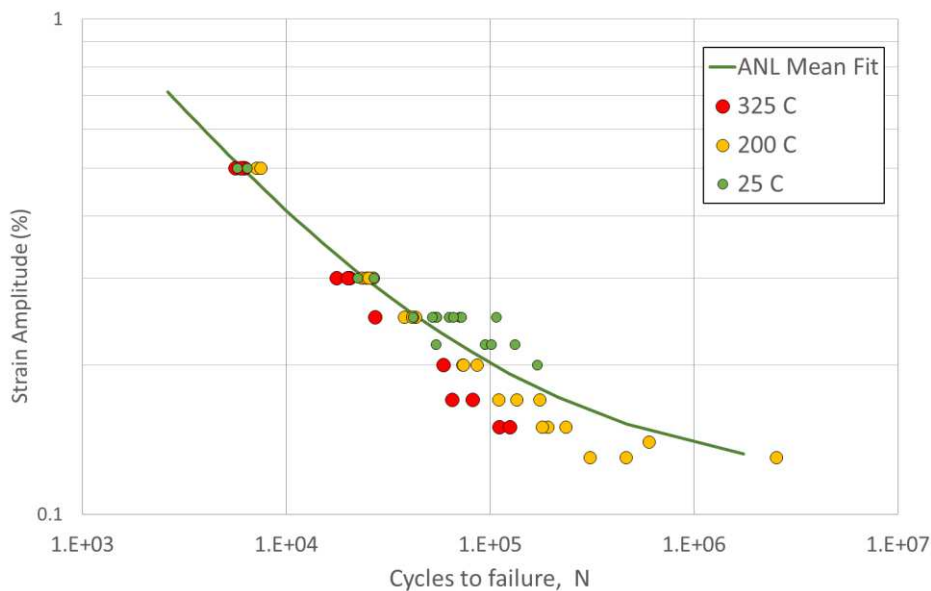


Figure 4.31 PreussenElektra fatigue endurance data in air separated according to applied test temperature [4.1].

Figure 4.32 shows a residual plot for tests conducted in PWR water as a function of the applied F_{en} . These results correspond to tests with strain amplitudes between 0.23% and 0.6% (i.e. predominantly lower cycle fatigue). F_{en} was primarily changed by altering the applied strain rate, however a small number of results correspond to testing at a lower temperature of 200 °C. The results show reasonable agreement with the NUREG/CR-6909 model at lower temperatures and for a F_{en} up to approximately 5.5. However, at higher F_{en} values (i.e. slower strain rates) the models are excessively over-conservative by approximately a factor of 2. This testing featured higher temperatures and slower strain rates than those used in the main INCEFA-PLUS campaign, but the results at lower F_{en} values are seen to be comparable to the wider database. Without further analysis and comparisons to more similar test conditions, it is difficult to determine the cause of the excess conservatism that is associated with the higher F_{en} results. It is considered that this is most likely due to some combination of inaccuracies in the description

of environmental effects at higher temperatures, and the specific environmental response of the tested material.

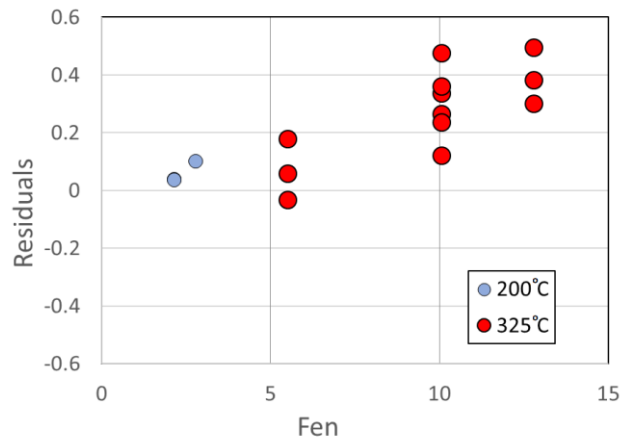


Figure 4.32 Residuals for PreussenElektra fatigue endurance data in PWR water as a function of applied F_{en} . Residuals calculated according to NUREG/CR-6909 [4.1].

4.6 CONCLUSIONS OF STATISTICAL ANALYSIS

The work presented in this section mainly deals with the statistical analysis of the data generated during the main experimental programme of the three phases of the INCEFA-PLUS Project. For this purpose, two different approaches were used to analyse the data.

1. The first one is based on a statistical linear model that allows studying the effect of all parameters at once, including interaction between parameters. In the last phase of the project, a number of tests with a reduced F_{en} were carried out. The test matrix does not allow analysing the low F_{en} data together with the data from the main test campaign. Therefore, a second model based only on the LWR tests at 0.6% strain range was formulated.
2. The second one is a more conventional and graphical approach based on residuals calculated against a best-fit curve (the F_{en} expression from NUREG/CR-6909 [4.8] is used for fatigue life prediction in PWR environment), complemented by statistical hypothesis testing. This second category of analyses does not allow assessing interactions, and for this reason, requires splitting the database into subgroups that correspond to different testing conditions.

These two independent analyses have led to the same main conclusions. Aside from the obvious (and expected) effects of strain range and environment, the only parameter amongst surface roughness, mean strain and hold time that has been identified as having a significant effect is surface roughness. Previous analyses [4.2] led on earlier versions of the database have shown an interaction between surface roughness and environment (a small impact of surface finish in air and a more deleterious impact in LWR environment); however, this interaction is not detected anymore with the current version of the database used in the present report. It is now replaced by an interaction between strain range and surface roughness. It therefore seems

difficult to draw a definitive conclusion regarding potential interactions between the effects studied. Independently of this fact, the PWR data generated on rough specimens will be further analysed in Chapter 5, in the framework of existing codified fatigue assessment procedures.

Beyond the main experimental programme, the data generated during the specific testing programme on mean stress (+50 MPa) effect on fatigue life and possible interactions with PWR environment has also been analysed.

1. For the strain-controlled experiments and for $N_f < 10^5$, a clear reduction of fatigue life in PWR environment was found independent of the mean stress level and is in good agreement with the predictions based on the F_{en} calculations with NUREG/CR-6909 equation. This indicates that there is no synergistic effect between mean stress and PWR environments. A reduction of fatigue life due to the PWR environment was also found for the load-controlled tests and $N_f < 10^5$.
2. The large scatter in fatigue life for all tests performed with smaller strain or stress amplitude leading to $N_f > 10^5$ does not permit the drawing of firm conclusions on the conjugate effect of mean stress and PWR environment in the HCF regime. However, it seems that the environmental effect on fatigue life disappears for the lowest amplitudes (stress or strain) tested in this study without mean stress and that it becomes effective again when a non-zero mean stress is applied.
3. An analysis based upon the Smith-Watson-Topper parameter was considered. The NUREG/CR-6909 air curve was converted into a SWT-life curve using an empirical calibration between the maximum stress and strain amplitude at half-life. The SWT parameter was calculated for all tests of the program. The results obtained in air show that the NUREG/CR-6909 converted SWT-life curve correlates well all the data with and without mean stress. Similarly, the data obtained in PWR environment falls reasonably close to the SWT-life curve, shifted by the appropriate F_{en} . This observation also confirms that for conditions tested in this program, mean stress does not amplify the PWR environment effect.

The analysis of the data from a specific hold time programme have demonstrated that no statistically significant effect (either beneficial or detrimental) of hold times could be observed in the INCEFA-PLUS results.

4.7 IMPACT OF USING FATIGUE DATA GENERATED FROM MULTIPLE SPECIMEN GEOMETRIES

The work presented in this section is concerned with any implications of combining multiple different specimen geometries across many different laboratories for the conclusions obtained using the INCEFA-PLUS fatigue life model presented in Section 4.2. The use of multiple specimen geometries in a single analysis could have an influence on the results of the fatigue life model proposed in the INCEFA-PLUS programme. This is especially true of the hollow specimen geometries that have been the centre of significant debate over the past few years regarding the comparability of the fatigue lives obtained from them to those of solid specimens [4.5,4.19,4.20].

4.7.1 METHODOLOGY

4.7.1.1 SPECIMEN GEOMETRIES

Two separate specimen geometries, solid (bar) and hollow (tubular) were tested in the high temperature LWR environment over the course of the INCEFA-PLUS project. A generic example of these specimen geometries is shown in Figure 4.33, with a dimensional summary provided in Table 4.22 and Table 4.23. Due to the surface of the inner bore of the hollow specimens not being accessible for the application of rough surface finishes, these specimens were solely tested in the reference conditions. The solid specimen geometries were used for both the polished and ground surface finish testing.

4.7.1.2 SOLID SPECIMEN GEOMETRIES TESTING METHODOLOGY

All INCEFA-PLUS air testing was performed to a uniaxial-strain controlled fatigue standard such as ISO 12106 [4.21]. However, uniaxial-strain-controlled fatigue testing in high temperature water environments is not explicitly covered by any of the relevant fatigue standards. Therefore, the INCEFA-PLUS LWR fatigue testing was performed to a common method agreed between the testing laboratories that was written in the spirit of ISO 12106 [4.6]. The specific areas in which the testing methods deviated from the standard were the method of strain control and loading measurements. For the majority of test laboratories, the test was controlled using shoulder displacement control and the strain on the gauge length determined using either finite elements modelling or an experimental calibration. The tests performed by 221 were controlled from the gauge length using a side contacting extensometer that was specially adapted for use in an LWR environment.

The implications and effects of the control method on the fatigue lives of specimens tested in LWR environments have been discussed in the frame of the project [4.22,4.23]. The measurements on load were obtained using an in-autoclave load cell, out-of-autoclave load cell, or a calculation based on the pressure inside a bellows. The hollow specimen geometry is also not described within the ISO 12016 standard. Therefore, this method is described in more detail in the next subsection. Alignment in all cases was performed according to the relevant ISO or national standard of the laboratory performing the testing.

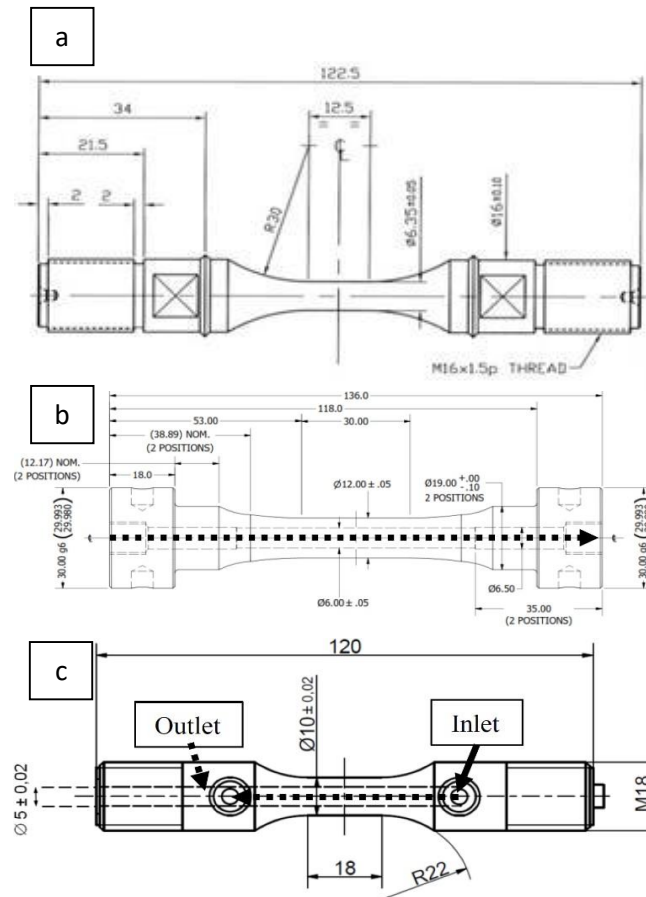


Figure 4.33 Geometry of solid bar (a), hollow specimen for 224 and 228 (b) and hollow specimen for 225 (c). Dashed arrows indicate the flow path of simulated LWR coolant through the hollow specimen [4.3].

Laboratory	Air Nominal diameter	LWR Nominal diameter
230	N/A	4
221	N/A	4.5
229	N/A	5
226	5	N/A
220	N/A	6
228	7/6.35	6.35 and Table 4.23
225	8	See Table 4.23
224	8	See Table 4.23
227	8.3	N/A
231	9	9
223	10	N/A

Table 4.22 Diameters for the solid specimens used in air and LWR environments.

Laboratory	Inner diameter (mm)	Outer diameter (mm)	Wall thickness (mm)
228	6	12	3
225	5	10	2.5
224	6	12	3

Table 4.23 Diameters and wall thicknesses for the hollow specimen geometries in LWR environment.

4.7.1.3 HOLLOW SPECIMEN TESTING METHODOLOGY

- 228: The specimen was connected to the pipe work supplying the environment and fitted into the load chain under load control in a manner consistent with ISO 12106. Prior to tightening up the grips the specimen was purged with nitrogen gas and pressurized with the water from the flow loop. The lower grip was then assembled and tightened before a compressive preload of 1 kN was applied to the specimen during tightening of the second grip. The preload was subsequently removed prior to installation of the gauge length extensometer. Once the gauge length extensometer was installed, the grips were lagged to minimize axial thermal losses through the load chain. The specimen was fully pressurised and the temperature of the water increased to the set point. Once the temperature had stabilised at the set point, the test machine was set to strain control and cycling was commenced. During testing, the temperature of the containment was recorded as being 60 °C as a result of the high temperature water flowing through the specimen. Measurements on specimens with thermocouples situated directly on the outer diameter of the specimen indicate a through wall temperature difference of 3 °C.
- 225: The specimen was mounted in the load chain under load control at zero load. Once the specimen was securely fitted, the machine was switched into position control and filled with water. A gauge length extensometer was installed and the specimen was then pressurised to 15 MPa. The load signal was balanced at -294.5 N to counter-act the pressure-induced force experienced by the specimen ends. The temperature of the water was then increased to the relevant set point. The test machine was then switched into strain control to commence the test once the temperature was proven to be stable. Measurements on specimens with thermocouples situated directly on the outer diameter of the specimen indicate a through wall temperature difference of 5 °C.
- 224: The specimen was secured into the first grip in the load chain. The specimen was then clamped into the second grip under load control using a slightly compressive preload during tightening. The specimen was then filled with the simulated LWR primary coolant. The extensometer was then installed on the specimen gauge length using a “set piece” to ensure that the extensometer probe position was correct and balanced. The temperature of the furnace and flow loop was then increased to the set point. Twenty-four hours after the set point had been achieved, the test machine was set to strain control and the cycling applied. Due to the use of a furnace to control the temperature of the outer diameter of the specimen, no through wall temperature gradient was measured for these specimens.

4.7.1.4 FEA METHOD

As the comparability of the fatigue lives of hollow specimens to those obtained on solid specimen geometries has been previously questioned [4.5], Finite Elements Analysis (FEA) was undertaken to investigate the effect of geometry, internal pressure and thermal gradient on the distribution and evolution of the strain state of each specimen.

Axisymmetric models of the hollow specimens were defined and used for the analysis. Compared to 3D models, this method allowed a finer mesh to be applied so that the stresses and strains could be predicted more accurately with a shorter running time. Axisymmetric four noded linear elements (CAX4) were used for each of the simulations. Figure 4.34 shows the mesh for the 228 specimen, as an example, along with the partitions used to ensure the mesh was structured.

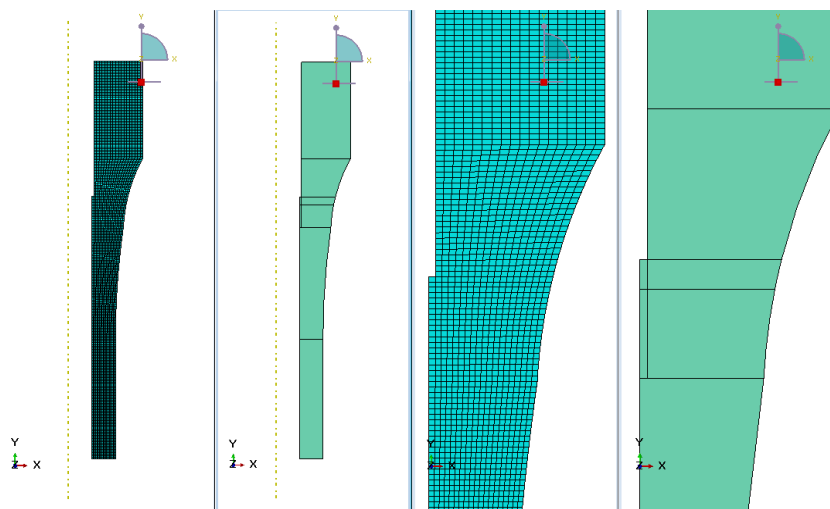


Figure 4.34 An example of the mesh and partitions used for the hollow specimens [4.3].

Displacements were applied to the end of the specimen to determine the point at which 0.6 % axial strain was reached. Each specimen was ramped to 0.3 mm and the displacements corresponding to 0.6% gauge strain were interpolated, as shown in Figure 4.35. The total axial strain was calculated by adding the elastic and plastic strain components together.

The material model considered here utilised the Abaqus Multi-Linear Kinematic Hardening model [4.5]. This was calibrated from half-life cycles of fatigue endurance tests carried out at 228.

The temperature differences of the specimens were modelled using a film coefficient. An inner temperature of 300 °C and an outer temperature of 20 °C were applied to the models. The temperature gradients are: 228 = 3 °C, 225 = 5 °C and 224 = 0 °C. The output from these thermal simulations were used as a predefined field in the structural simulations.

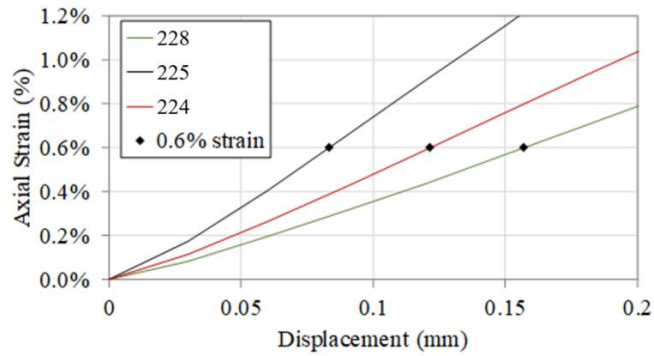


Figure 4.35 Graph of axial strain vs. displacement used to determine the displacement values corresponding to 0.6% strain [4.3].

A constant internal pressure was applied to the inner surfaces of the models (228 = 17.5 MPa, 225 = 15 MPa and 224 = 15.5 MPa). In the final simulations, the thermal gradient and internal pressure were applied to the models first, which in turn created a displacement due to the thermal stresses in the specimens. The specimens were then cycled using the displacement values calculated previously, taking into account the initial displacement from the thermal and pressure steps.

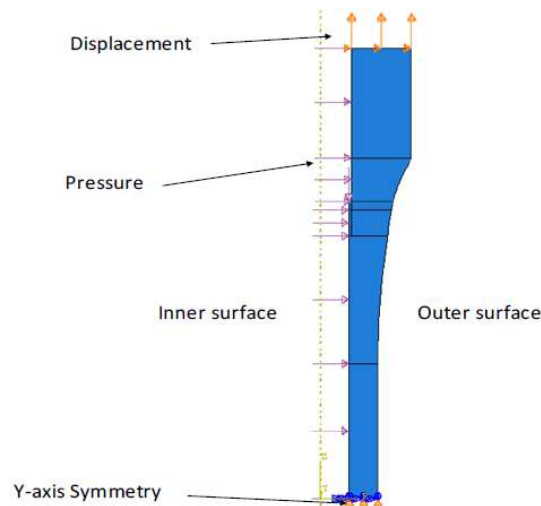


Figure 4.36 Boundary conditions that were applied to 228's model. The same conditions apply for all hollow specimens [4.3].

4.7.2 RESULTS AND DISCUSSION

4.7.2.1 DATA MODEL

The analyses presented hereafter use the INCEFA-PLUS database of fatigue testing in air and a PWR environment to investigate the potential implications of the different specimen geometries. To achieve this, a four parameter statistical linear model similar to that defined in Section 4.2 (Table 4.7 and Table 4.8) was used to interpret the database and formulate conclusions on the effect of specimen geometry. This model, based on 117 data points, only differs from that of Section 4.2 regarding the material considered. It only uses the data generated on the common material (82% of the data points used in Section 4.2 was obtained on the common material, as described in Figure 4.1(a)), in order to remove potential sources of

extra scatter due to the inclusion of several heats and grades of austenitic stainless steel (the remaining 18% of national materials). The resulting model terms are listed in Table 4.24 and Table 4.25. It is worth noting that considering only the common material does not change the parameters identified in the reduced model (Table 4.7 vs Table 4.24), and has almost no impact on the coefficients identified for the model (Table 4.8 vs Table 4.25). This is mainly due to the fact that 82% of the data points considered in Section 4.2 were generated on common material.

Source	LogWorth	PValue
norm strain range	58.478	0.00000
norm env.	54.852	0.00000
norm Rt	5.351	0.00000
norm strain range*norm Rt	1.733	0.01847

Time to event: N25 (Nf)	AICc	1985.680	Observation Used	117
Distribution: Lognormal	BIC	2001.489	Uncensored Values	114
Censored By: Test status	-2*LogLikelihood	1972.916	Right Censored Values	3

Table 4.24 List of the parameters in the reduced model with 4 parameters that only uses the common material.

Term	Estimate	Std.error
Intercept	8.33436647	0.0379713
norm strain range	-0.8508337	0.0265684
norm Rt	-0.235153	0.0488911
norm env	0.81579279	0.0275722
(norm strain range-0.01895)*(norm Rt+0.528)	0.11454159	0.0480301
σ	0.29372428	0.0194827

Table 4.25 Coefficients for the model in Table 4.24, σ is the standard deviation of $\ln(N_f)$.

The model predictions are presented against the experimental values in Figure 4.37 and demonstrate that the model provides a reasonable fit to the data.

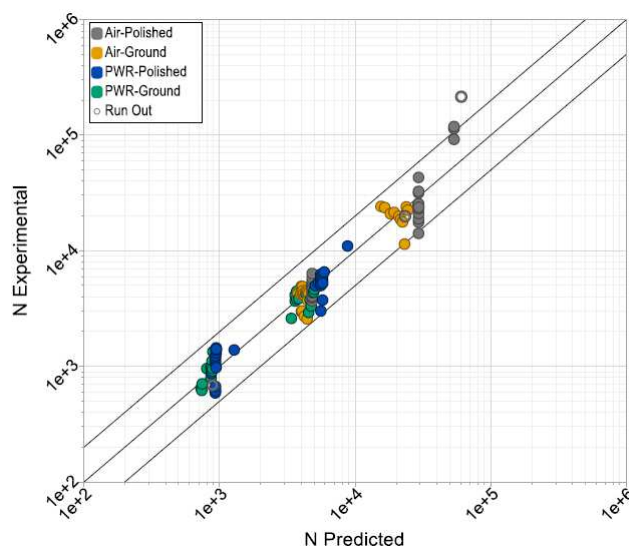


Figure 4.37 Predicted vs. experimental fatigue lives for the common material over the full range of parameters. Black diagonal lines represent the 1 to 1 line and a factor 0.5 and 2 [4.1].

4.7.2.2 VARIATION THE FATIGUE LIFE OF SOLID SPECIMEN GEOMETRIES

Due to the use of a common testing methodology and a large portion of the testing being performed by different laboratories on the common material, the INCEFA-PLUS programme is in a unique position to study fatigue endurance data scatter. The scatter of the fatigue data in the INCEFA-PLUS programme has multiple sources, which can be summarised in material, lab-to-lab, and specimen geometry.

In some respects, the specimen geometry and procedural variation could be seen as part of lab-to-lab scatter. However, the INCEFA-PLUS programme has defined the procedure in LWR environments, and the air testing is performed in accordance with applicable standards. Therefore, scatter due to procedural variation should be negligible within this programme. Additionally, the specimen geometries of each laboratory have been recorded and analysed based on diameter for both solid and hollow specimens (Table 4.22 and Table 4.23). The diameter was selected as the fundamental parameter for specimen geometry due to the standards basing all other aspects of specimen geometry on it. Furthermore, as multiple laboratories have performed analogous testing on the same material, an estimate of the lab-to-lab and within-material variation for the fatigue data should also be possible.

The diameters of the specimens used by the various laboratories are graphically presented in Figure 4.38. This shows that the range of diameters used for the testing falls between 3.5 mm and 10 mm. As indicated in Figure 4.38 several of the specimen diameters fall outside of the guidance given in ISO 12106 [4.21]. This is primarily due to space and control issues that are common in fatigue testing in LWR environments. 230, 221, and 229 all test specimens in LWR relevant conditions where the restrictions on their test equipment require diameters of less than 5 mm.

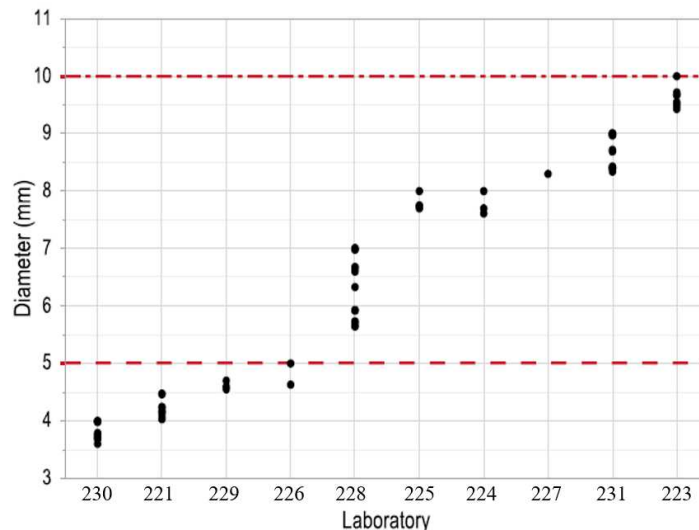


Figure 4.38 Measured diameters for each solid specimen tested by different organisations. The x-axis has been rank ordered by specimen diameter [4.1].

The air tests performed by 226 were done on specimens with a diameter of 5 mm, which is within the range defined by the ISO 12106 standard. However, due to the grinding method of producing the roughened surface condition, the single rough specimen tested by 226 has a

diameter of less than 5 mm. Given that 226 tested a single specimen with a diameter of less than 5 mm, no firm conclusions can be drawn for the effect of testing specimens with diameters less than 5 mm. The implications of comparing test results produced from specimens with smaller diameters than the nominal specified value and its interaction with shoulder control calibrations in LWR environmental testing is discussed, in detail, in [4.23].

Irrespective of the reasoning for smaller than standard defined specimen diameters, this geometrical condition could have an unintended influence on fatigue life and any model based on the data set. However, since in the case of the thinnest specimens there would be greater than 50 grains sampled during a test, it is thought that the implications for the fatigue lives determined using the solid specimen geometries are likely to be insignificant.

Considering that any potential effect is likely to be a function of the diameter, it should be possible to determine its existence by analysing the model residuals vs. diameter. The residual versus diameter plot Figure 4.39 shows that no trend is discernible from the data. The residuals have a mean of zero and a linear fit to the residual data as a function of diameter size does not differ significantly from the mean line.

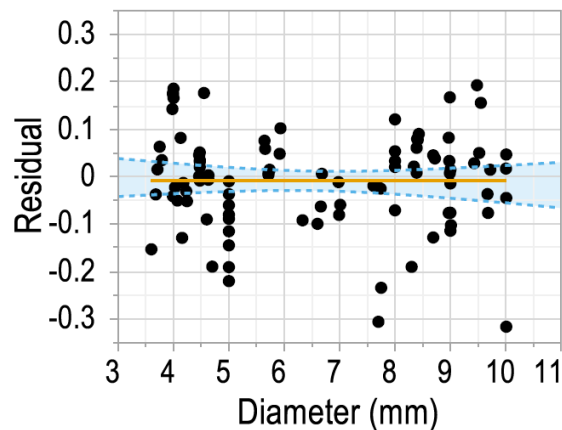


Figure 4.39 The residual vs. specimen diameter for solid specimen data. The blue shaded region bordered by a broken blue line represents the 90% confidence interval. The orange line represents the mean residual value for all datapoints [4.1].

4.7.2.3 VARIATION IN THE FATIGUE LIFE OF HOLLOW SPECIMEN GEOMETRIES

Many influential datasets that inform the current assessment method for environmental fatigue, such as NUREG/CR-6909 [4.8] contain data generated from hollow and solid specimen geometries. A review of work comparing the fatigue lives of hollow and solid specimen geometries [4.22] highlighted the conflicting position of the industry regarding the differences between hollow and solid specimens with respect to fatigue initiation and crack growth. Literature sources summarised in the review show that for fatigue initiation some testing shows a significant difference between the fatigue lives of the two specimen types, while others observe no difference at all. A similar position is found for fatigue crack growth where Bae and Lee [4.24] suggested that hollow specimens had larger internal plastic strains than solid specimens, but in contrast to these findings Kanasaki et al. [4.25] found no difference. More recent studies and reports raise questions regarding the comparability of the data generated from these two distinctly different geometries [4.5,4.19]. These sources highlight the potential

effects of strain ratcheting due to the combination of constant internal pressure and plastic deformation (because of low cycle fatigue). If a particular specimen geometry were to give consistently different lives than another, this could be a potential source of additional unaccounted for scatter. This could lead to an excessive data scatter transference factor and over-conservatism in fatigue assessments.

In the case of the work by Gill et al. [4.5] a difference between the fatigue lives of hollow and solid specimens was observed for analogous loading conditions in LWR environments. A correction factor on strain was empirically derived to account for this and subsequently supported by FEA modelling. However, there is conflicting evidence in the literature regarding the magnitude of the effect of this aspect of specimen geometry, with Asada et al. [4.20] and 225 finding a negligible difference. Therefore, it is necessary for the INCEFA-PLUS programme to investigate any potential implications for using both specimen geometries to generate data that will be analysed within one model, and the conclusions made from the analysis.

The implications of using these two specimen geometries can be determined using an equivalence test such as analysis of variance (ANOVA) [4.26,4.27] to determine if there is a significant difference between the mean residuals of the groups (Figure 4.40). The results of this test give an F ratio of 62.2 with a probability of < 0.0001 for finding a larger F ratio by chance. Therefore, the conclusion of this analysis is that there is a significant difference between the three laboratories using hollow specimens. A Tukey's honestly significant difference (THSD) test [4.28] was also run to confirm that the mean for 225 was significantly different to the other two groups. This test also confirmed that the means for 228 and 224 were not significantly different to each other. A t-test of the mean residuals for the solid and hollow specimen LWR tests performed by 228 confirmed that the hollow specimens gave significantly shorter fatigue lives than the solid ($p < t = 0.002$). This indicated that the difference between the means is not likely to be due to lab-to-lab variance.

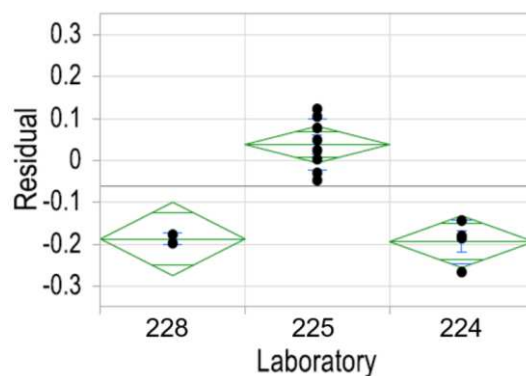


Figure 4.40 Residuals vs. laboratory for hollow specimen data. The green diamonds represent the mean value of the group at the centre line, and 95% confidence interval from upper to lower point [4.1].

Contour plots of the Von Mises and Axial (S22) stress in Figure 4.41 show little difference between the three specimens from a stress point of view. Furthermore, Figure 4.42 shows consistency between the variation of hoop and radial strain with time. This observation confirms that the higher through-wall gradient (more negative on inside surface as shown in Figure 4.43) in the 225 specimen does not significantly reduce ratcheting and, hence, cannot explain the extended lifetime of these specimens when compared to 228's and 224's specimens.

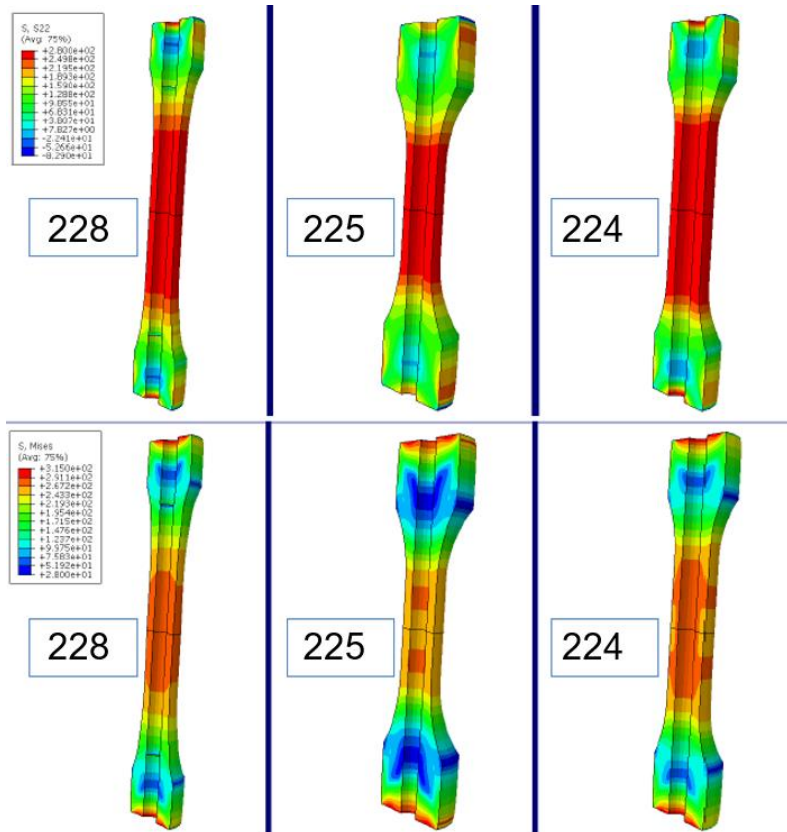


Figure 4.41 Contour maps of axial stress (top row) and Von Mises stress (bottom row) [4.3].

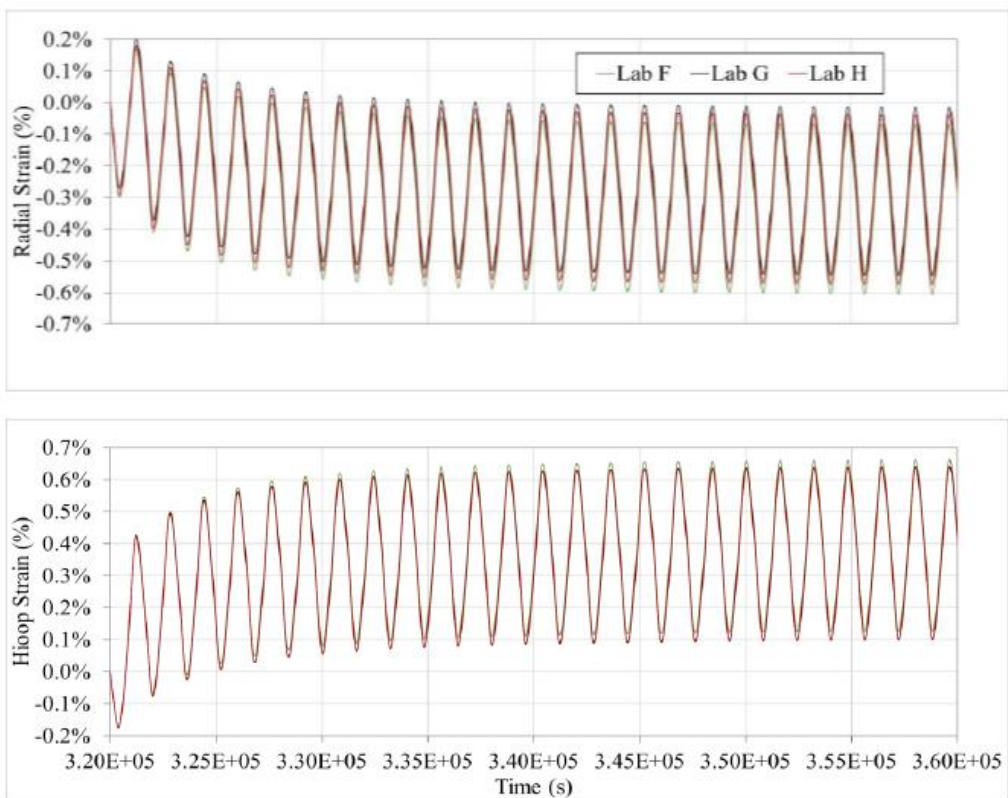


Figure 4.42 Variation of radial and hoop strain in the hollow specimens [4.3].

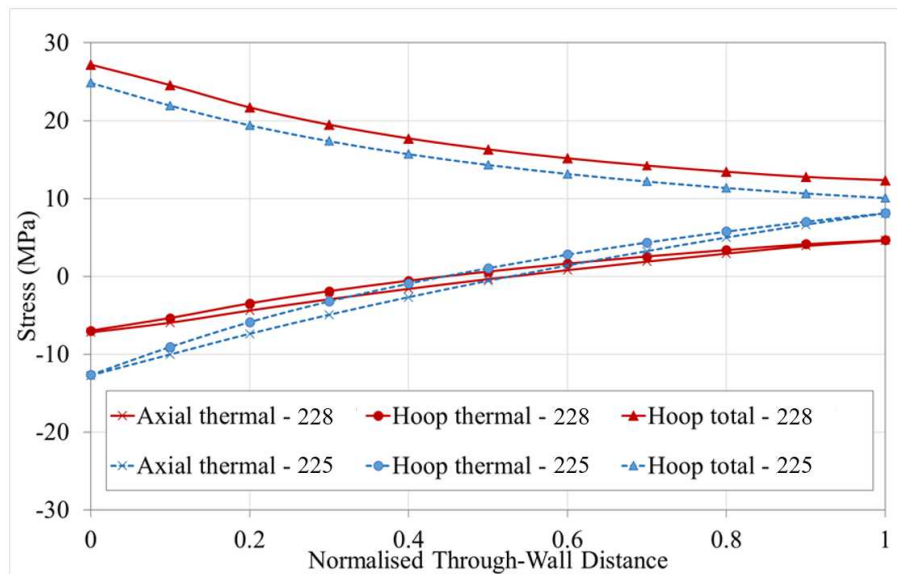


Figure 4.43 Through wall stress from the inner surface to the outer surface (from the final time point in the cycle) [4.3].

Since a significant difference between the various hollow specimen geometries has been identified, but no physical basis found, a sensitivity study was performed on the linear model defined in Table 4.24 and Table 4.25 to inform the decision on how to accommodate the hollow specimen data. By following the procedure defined in that work, a model was produced for each data set corresponding to:

- a) Including all hollow specimen data without correction.
- b) Correcting the hollow specimen data as per Gill et al. [4.5].
- c) Excluding all hollow specimen data. In each case, the model simplified down to the same four practically significant parameters shown in Table 4.25 and Figure 4.44.

The sensitivity study investigated changes to the statistically significant parameters of the model for the cases (Figure 4.44). It concluded that irrespective of how the hollow specimen data were accommodated in the data set, there was no effect on the conclusions based on the linear model defined in Table 4.24 and Table 4.25. This was due to the number of 228 and 224 tests being similar to the number of 225 tests, which effectively gave an average residual that falls within the scatter of the other solid specimen data. However, if more tests were performed this result may not hold true.

Since the hollow specimen tests were all performed on a surface condition considered equivalent to the polished surface in the INCEFA-PLUS and the average residuals being in line with those of solid specimens, these tests would not be expected to influence conclusions regarding the impact of the roughened surfaces. Therefore, the decision was made to keep these data points in the analysis until further evidence is obtained that can inform a way forward. However, it should be noted by the community that the inclusion of these test results would increase scatter and the level of conservatism shown for data scatter in the INCEFA-PLUS database. For testing campaigns that feature a significant number of hollow specimens (such as the one used to produce the ANL methods) differences due to specimen geometries could be more significant and this should be investigated in the future.

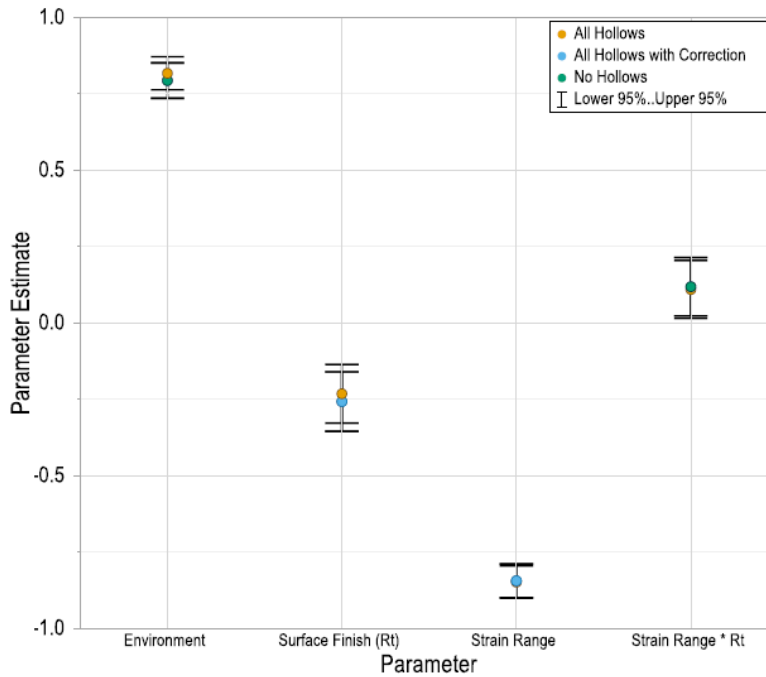


Figure 4.44 Comparison of the estimates for the practically significant parameters of the model based on data sets that include hollow specimens and hollow specimens with a correction factor applied, and exclude hollow specimens [4.1].

4.8 QUANTIFYING LAB-TO-LAB SCATTER FOR SOLID SPECIMEN DATA

To attempt to quantify the lab-to-lab variation, the model residuals were categorised by laboratory and an ANOVA test was applied. The results of this analysis showed that one or more of the laboratories' mean residual was significantly different from the others. The test calculated an F ratio of 3.4 with a probability of 0.001 of finding a greater ratio by chance. To identify the group or groups with different mean values, a comparison of all the pairs using THSD was performed. This additional test indicated that 230's results were significantly different from the data obtained from 226 (5 mm diameter). However, the mean residuals for 226 are indistinguishable from all other laboratories except 230. In addition, the THSD test showed that 230's data were also indistinguishable from the rest of the laboratories. This shows that there is a significant difference between the laboratories at the extremes of the data, but not compared to the laboratories with means closer to zero. As the fatigue data is assessed by an Expert Panel [4.29] and rated before being used in the analysis [4.1], the quality of the data for all laboratories should be of a good standard. On this basis, the fact that some laboratories produce data that has a different mean than another laboratory is not likely to be due to poor practice. Therefore, the spread of the means in this dataset should be considered a reasonable measure of lab-to-lab variation.

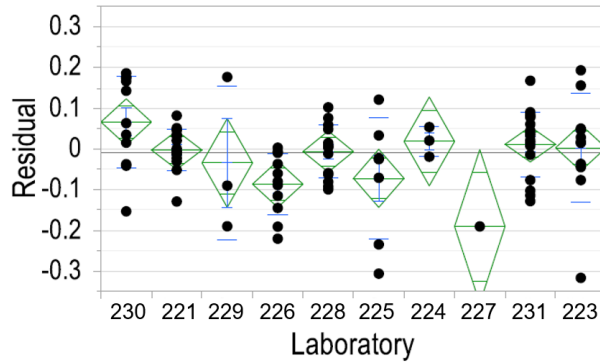


Figure 4.45 The residuals vs. laboratory for solid specimen data. The x-axis has been rank ordered by specimen diameter. The green diamonds represent the mean value of the group at the centre line, and 95% confidence interval from upper to lower point. The green lines close to each confidence bound are overlap marks that can be used to visually judge significant differences between the groups [4.1].

The mean residual values for each laboratory as calculated by the ANOVA, presented in Figure 4.45, can be rank ordered and a cumulative distribution function (a normal distribution in this case) fitted to the data. A plot of this function vs. the residuals allows a value for a residual that corresponds to the 5th percentile of the distribution to be defined (Figure 4.46). This residual value can then be expected to bound 95 % of the population of laboratory means. This value can then be converted into a factor on life depending on the percentile and confidence level of the data. Using this method, a value of 1.5 is calculated as an initial idea of the factor on fatigue life to account for lab-to-lab scatter (Table 4.26).

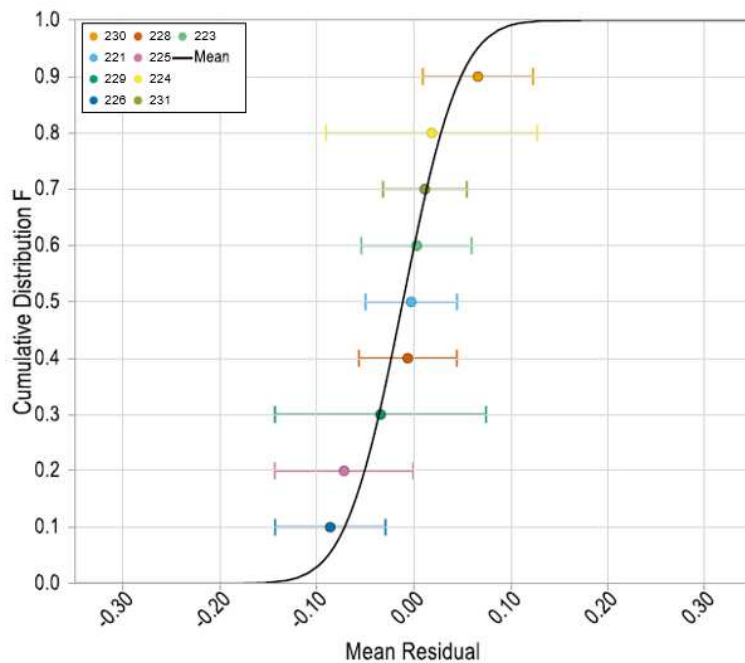


Figure 4.46 Estimated cumulative distribution of the lab-to-lab residuals as obtained from the fatigue life model. The error bars represent the 95th and 5th confidence bounds [4.1].

Confidence level (%)	% of population bounded	
	95	50
50	-0.09	-0.01
95	-0.17	-0.08
Factors on life		
50	1.2	1.0
95	1.5	1.2

Table 4.26 Values of residual in the INCEFA-PLUS fatigue life model and the factors on life as a function of confidence interval and percentage of the population bounded [4.1].

REFERENCES

- [4.1] S. Cuvilliez, M. Bruchhausen, J.-C. Le Roux, J. Mann, A. McLennan, P. Spätig, Final WP3.2 Report (D3.8); INCEFA-PLUS Internal Report, 2020.
- [4.2] M. Bruchhausen, A. McLennan, R. Cicero, C. Huotilainen, K. Mottershead, J.-C. Le Roux, M. Vankeerberghen, Incefa-Plus Project : Review of the Test Programme; PVP2020-21377, Am. Soc. Mech. Eng. Press. Vessel. Pip. Div. PVP. (2020).
- [4.3] A. McLennan, P. Spätig, J.-C. Le Roux, J. Waters, P. Gill, J. Beswick, N. Platts, INCEFA-PLUS Project: The Impact of using Fatigue Data generated from Multiple Specimen Geometries on the Outcome of a Regression Analysis; PVP2020-21422, Am. Soc. Mech. Eng. Press. Vessel. Pip. Div. PVP. (2020).
- [4.4] H.E. Karabaki, J.P. Solin, M. Twite, M. Herbst, J. Mann, G. Burke, Fatigue with hold times simulating npp normal operation results for stainless steel grades 304L and 347; PVP2017-66097, Am. Soc. Mech. Eng. Press. Vessel. Pip. Div. PVP. 1A-2017 (2017) V01AT01A031. doi:10.1115/PVP2017-66097.
- [4.5] P. Gill, P. James, C. Currie, C. Madew, A. Morley, An investigation into the lifetimes of solid and hollow fatigue endurance specimens using cyclic hardening material models in finite element analysis; PVP2017-65975, Am. Soc. Mech. Eng. Press. Vessel. Pip. Div. PVP. 1A-2017 (2017). doi:10.1115/PVP2017-65975.
- [4.6] M. Vankeerberghen, L. Doremus, P. Spätig, M. Bruchhausen, J.-C. Le Roux, M. Twite, R. Cicero, N. Platts, K. Mottershead, Ensuring data quality for environmental fatigue – INCEFA-Plus testing procedure and data evaluation; PVP2018-84081, Am. Soc. Mech. Eng. Press. Vessel. Pip. Div. PVP. 1A-2018 (2018). doi:10.1115/PVP201884081.
- [4.7] M. Bruchhausen, Collection of fatigue data from the INCEFA+ project, version 1.0, (2020). <http://dx.doi.org/10.5290/50>.
- [4.8] O.K. Chopra, G.L. Stevens, NUREG/CR-6909, Rev.1; Effect of LWR Water Environments on the Fatigue Life of Reactor Materials. Final Report, 2018.
- [4.9] ISO, Metallic Materials - Fatigue Testing - Statistical Planning and Analysis of Data; ISO 12107:2012, (2012).
- [4.10] K.P. Burnham, D.R. Anderson, Multimodel inference: Understanding AIC and BIC in model selection, *Sociol. Methods Res.* 33 (2004) 261–304. doi:10.1177/0049124104268644.

- [4.11] M. Bruchhausen, A. McLennan, R. Cicero, C. Huotilainen, K. Mottershead, J.-C. Le Roux, M. Vankeerberghen, Environmentally assisted fatigue data from the INCEFA-PLUS project; PVP2019-93085, Am. Soc. Mech. Eng. Press. Vessel. Pip. Div. PVP. 1 (2019). doi:10.1115/PVP2019-93085.
- [4.12] L. de Baglion, Comportement et endommagement en fatigue oligocyclique d'un acier inoxydable austénitique 304L en fonction de l'environnement (vide, air, eau primaire REP) à 300°C., 2011.
- [4.13] N. Huin, Environmental effect on cracking of an 304L austenitic stainless steels in PWR primary environment under cyclic loading, 2013.
- [4.14] T. Poulain, Low Cycle Fatigue of a 304L Austenitic Stainless Steel : Influence of Surface Finish and Load Signals in PWR Water Environment, 2015.
- [4.15] K. Mottershead, J. Mann, Phase 3 hold time test proposals; INCEFA-PLUS Internal Report, 2018.
- [4.16] R. Rakotomalala, Comparaison de populations: Tests paramétriques, v1.0, Lyon, 2008. http://eric.univ-lyon2.fr/~ricco/cours/cours/Comp_Pop_Tests_Nonparametriques.pdf.
- [4.17] T. Métais, S. Courtin, P. Genette, L. De Baglion, C. Gourdin, J.-C. Le Roux, Status of the French Methodology Proposal for Environmentally Assisted Fatigue Assessment, in: Vol. 1 Codes Stand., American Society of Mechanical Engineers, 2014. doi:10.1115/PVP2014-28408.
- [4.18] J. Mann, G. Dundulis, WP3 Final Hold Time Position, INCEFA-PLUS Internal Report, 2020.
- [4.19] ISO, Metallic materials - Principles and designs for multiaxial fatigue testing; ISO/TR 12112:2018, (2018).
- [4.20] S. Asada, K. Tsutsumi, Y. Fukuta, H. Kanasaki, Applicability of hollow cylindrical specimens to environmental assisted fatigue tests; PVP2017-65514, Am. Soc. Mech. Eng. Press. Vessel. Pip. Div. PVP. 1A-2017 (2017). doi:10.1115/PVP2017-65514.
- [4.21] ISO, Metallic materials - Fatigue testing - Axial-strain-controlled method; ISO/FDIS 12106:2016(E), 2016 (2016).
- [4.22] M. Twite, N. Platts, A. McLennan, J. Meldrum, A. McMinn, Variations in measured fatigue life in LWR coolant environments due to different small specimen geometries; PVP2016-63584, Am. Soc. Mech. Eng. Press. Vessel. Pip. Div. PVP. 1A-2016 (2016). doi:10.1115/PVP2016-63584.
- [4.23] M. Vankeerberghen, A. McLennan, I. Simonovski, G. Barrera, S. Arrieta, M. Ernestova, N. Platts, M. Scibetta, M. Twite, Strain Control Correction for Fatigue Testing in LWR Environments; PVP2020-21373, Am. Soc. Mech. Eng. Press. Vessel. Pip. Div. PVP. (2020).
- [4.24] K.-H. Bae, S.-B. Lee, The effect of specimen geometry on the low cycle fatigue life of metallic materials, Mater. High Temp. 28 (2011) 33–39. doi:10.1179/096034011x12982896521562.
- [4.25] H. Kanasaki, I. Satoh, M. Koyama, T. Okubo, T.R. Mager, R.G. Lott, Fatigue and Stress Corrosion Cracking Behaviors of Irradiated Stainless Steels in PWR Primary Water, in: Fifth Int. Conf. Nucl. Eng. (ICONE 5), Nice, 1997.

- [4.26] F.J. Anscombe, The Validity of Comparative Experiments, *J. R. Stat. Soc. Ser. A.* 111 (1948) 181. doi:10.2307/2984159.
- [4.27] K. Hinkelmann, *Design and Analysis of Experiments*, 2012. doi:10.1002/9781118147634.
- [4.28] J.W. Tukey, *Comparing Individual Means in the Analysis of Variance*, 1949. doi:10.2307/3001913.
- [4.29] R. Cicero, *Expert Panel Tool Proposal*; INCEFA-PLUS Internal Report, 2017.
- [4.30] M. Bruchhausen, A. McLennan, S. Arrieta, T. Austin, R. Cicero, W.J. Chitty, L. Doremus, G. Dundulis, M. Ernestova, A. Grybenas, C. Huotilainen, J. Mann, K. Mottershead, R. Novotny, F.J. Perosanz Lopez, N. Platts, J.-C. Le Roux, P. Spätig, C. Torre Celeizábal, M. Twite, M. Vankeerberghen, *Characterization of Austenitic Stainless Steels with regard to Environmentally Assisted Fatigue in Simulated Light Water Reactor Conditions (Under preparation)*, *Metals (Basel)*. 10 (2020).

CHAPTER 5 INCEFA-PLUS DATA EVALUATION AGAINST EXISTING FATIGUE ASSESSMENT PROCEDURES

This Chapter includes statistical analysis from the data obtained during INCEFA-PLUS Project. It is based in “Final Work Package 3.2 Report” [5.1], developed by INCEFA-PLUS Consortium, and “INCEFA-PLUS Project: lessons learned from the project data and impact on existing Fatigue Assessment Procedures”, by Sam Cuvilliez et al. [5.2,5.3].

5.1 INTRODUCTION

This section discusses how the outcome of the analysis of the INCEFA-PLUS data can be used to evaluate existing fatigue assessment procedures that incorporate environmental effects in a similar way to NUREG/CR-6909. A key difference between these approaches and the NUREG/CR-6909 is the reduction of conservatisms resulting from the joint implementation of the adjustment sub-factor related to surface finish effect (as quantified in the design air curve derivation) and a F_{en} penalization factor for fatigue assessment of a location subjected to a PWR primary environment. The analysis presented in this section indicates that the adjustment (sub-)factor on life associated with the effect of surface finish in air (as described in the derivation of the design air curve in NUREG/CR-6909) leads to substantial conservatisms when it is used to predict fatigue lifetimes in PWR environments for rough specimens. The corresponding margins can be explicitly quantified against the design air curve used for Environmentally Assisted Fatigue (EAF) assessment, but may also depend on the environmental correction F_{en} factor expression that is used to take environmental effects into account.

EAF is currently receiving an increased level of attention for existing NPPs as utilities are working to extend their operational life, and also for nuclear new builds. Indeed, in many countries, regulatory requirements have led to an update of fatigue analysis rules in order to take into account the effect of a LWR environment on fatigue life in stress report calculations. The most well-known example is the NUREG/CR-6909 report ([5.4–5.6]) prepared by the Argonne National Laboratory (ANL) on behalf of the United States Nuclear Regulatory Commission (US-NRC), where environmental penalization factor (F_{en}) expressions were derived for several reactor materials (stainless steels, ferritic steels and nickel based alloys) from experimental data obtained on small-scale laboratory specimens with a smooth surface finish tested in Pressurized Water Reactor (PWR) and BWR (Boiling Water Reactor) environments. These penalization factors are applied to the life predicted with the appropriate fatigue design air curve (depending on the material considered), so as to take into account the deleterious effect of environment. While the NUREG/CR-6909 guidance applies as it stands in the US through the US-NRC Regulatory Guide 1.207 [5.7], it was also declined (with certain amendments) in several international codes, for instance in the ASME Boiler and Pressure Vessel Code with the Code Case N-792-1 [5.8] or in the AFCEN RCC-M code [5.9] through the Rules in Probationary Phase “RPP-2” and “RPP-3”. Beyond codified approaches, domestic engineering methodologies were also developed on the basis of the NUREG methodologies by nuclear stakeholders, as for instance in the UK, for assessment of embarked reactor components as documented in [5.10].

On the basis of the findings reported in Chapter 4, it seems that the data generated during INCEFA-PLUS does not show any significant effect of mean strain or hold times as tested during the project, while surface finish has been identified as a parameter for which the effect can be considered as significant.

The goal of this Section is therefore to assess this data against an already existing fatigue assessment procedure that incorporates environmental effects in a similar way to NUREG/CR-6909, while reducing its conservatism associated with surface finish effects. This section focuses on the EAF assessment procedure known as the ASME “ $F_{en-threshold}$ ” Code-Case proposal [5.11]. However, there are two additional EAF assessment procedures worth noting: the AFCEN RCC-M “ $F_{en-integrated}$ ” (RPP-3 of RCC-M code) [5.12,5.13] and the “ $F_{en-incorporated}$ ” methodology as described in [5.10] (and based on testing in [5.14,5.15]). These three different approaches, all documented and compared in [5.10], are very similar but rely on different design air curves and/or F_{en} expressions. Repeating the assessment presented in this section using the other two EAF assessment procedures leads to similar conclusions. These three EAF assessment procedures highlight an over-conservatism quantified by a factor of 3 on life in fatigue assessment of a location subjected to a PWR primary environment, resulting from the joint implementation of the adjustment sub-factor related to surface finish effect in air (as quantified in the design curve translation factor on life) and a F_{en} penalization factor derived from data generated in water on small-scale specimens with a polished surface finish. Indeed, real surface finish conditions in NPP components do not correspond to such a smooth surface state, but rather to an industrially polished, ground or as-manufactured surface finish. The margins quantified in these approaches then rely on fatigue data generated in water on rough specimens.

This section is organized as follows: the theoretical prerequisites of the $F_{en-threshold}$ Code-Case proposal is first reviewed, and the INCEFA-PLUS database subset available so far is then assessed according to this approach, so as to highlight the margins that can be retrieved.

5.2 THEORETICAL BACKGROUND OF THE $F_{EN-THRESHOLD}$ CODE-CASE PROPOSAL

The purpose of this subsection is to introduce the information used in the next subsection for assessing the new experimental data according to the $F_{en-threshold}$ approach. As already mentioned in the introduction, it relies on the same theoretical framework as in NUREG/CR-6909 but contains some amendments to the original methodology.

It is first important to explain the way the design air curve is derived from the mean air curve, and more particularly how the several aggravating effects on fatigue life are embedded in a single global reduction factor on life denoted hereafter by $TC_{life-global}$. The $F_{en-threshold}$ Code-Case applies to austenitic and cast duplex stainless steels, and relies on the relevant ASME design curve of mandatory appendix I of BPVC.III (Table I-9.2). This curve has been obtained by applying on the NUREG/CR-6909 best fit air curve a reduction factor of 12 on fatigue life (N), and a reduction factor of 2 on alternating stress amplitude (S_{alt}) (a modified Goodman correction is applied to the mean air curve as a first step). The design curve then corresponds to the minimum of these two shifted curves.

The factor of 12 corresponds to the quantity denoted above as $TC_{life-global}$, and was derived in NUREG/CR-6909 [5.4] from a statistical combination of different sub-factors, each of them pertaining to an aggravating effect:

- material variability and data scatter (MVDS) effect (translation factor denoted by a),
- loading history effect (translation factor denoted by b),
- surface finish (translation factor denoted by c),
- size effect (translation factor denoted by d).

These sub-factors are illustrated on Figure 5.1, and their numerical values are listed in Table 5.1 (depending on the revision of NUREG/CR-6909).

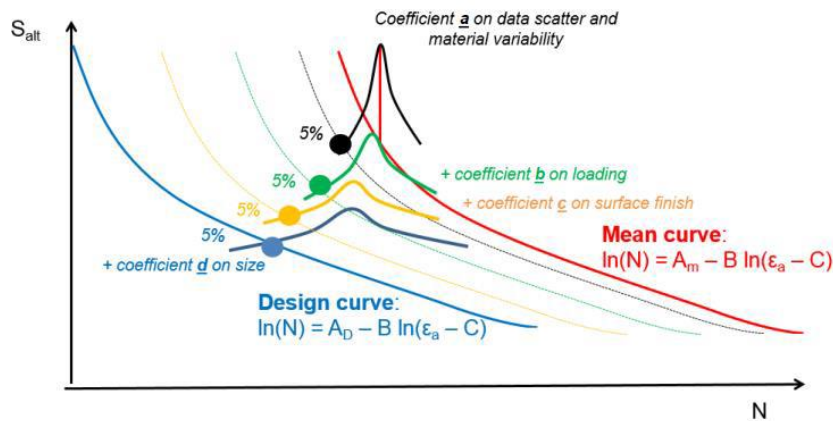


Figure 5.1 Illustration of translation sub-factors from mean air curve to design air curve [5.10].

Parameter	NUREG/CR-6909	NUREG/CR-6909,Rev.1
	[5.4]	[5.5,5.6]
MVDS (a)	$A_m = 6.891$ & $sd = 0.417$	
Loading history (b)	1.2 - 2.0	1.0 - 2.0
Surface finish (c)	2.0 - 3.5	1.5 - 3.5
Size (d)	1.2 - 1.4	1.0 - 1.4
$TC_{life-global}$ (NUREG)	11.6	9.6
$TC_{life-global}$ (recalculated)	11.7	9.4

Table 5.1 Translation sub-factors on life in successive revisions of NUREG/CR-6909.

The MVDS factor (a) plays a particular role as it is intrinsically linked to the mean air curve, which in this case is fitted using a weighted least-square regression, with a Langer equation:

$$\ln(N) = A - B \ln(\epsilon_a - C) \tag{eq. 5.1}$$

where A, B and C coefficients are respectively corresponding to the horizontal position of the curve, its slope, and the endurance limit. The A coefficient in eq. 5.1 is assumed to be a random variable (RV) following a normal distribution in the $\ln(N)$ -space with mean A_m and standard deviation sd :

$$A \sim N(A_m, sd^2) \tag{eq. 5.2}$$

where A_m is the value fitted in the mean curve equation. In order to incorporate the aggravating effects on life represented by the remaining sub-factors b , c and d , it is furthermore assumed that each of them follows a lognormal distribution (i.e. a normal distribution in the $\ln(N)$ -space):

$$\left| \begin{array}{l} \ln(X_i) \sim N(\mu_i, \sigma_i^2), i = 1, n; \text{ with:} \\ \mu_i = \frac{\ln(X_{i,5}) + \ln(X_{i,95})}{2} \\ \sigma_i = \frac{\ln(X_{i,95}) - \ln(X_{i,5})}{2t_{95}} \end{array} \right. \quad \text{eq. 5.3}$$

where X_i denotes the i^{th} RV associated with the i^{th} factor amongst b , c and d , μ_i and σ_i respectively denote the mean and the standard deviation of these normal distributions, and $t_{95} \approx 1.645$ denotes the 95th percentile of the standard normal distribution. Thanks to the lognormal hypothesis, μ_i and σ_i can be determined in eq. 5.3 using the range of values given in Table 5.1 for each parameter. The lower and upper bounds of the i^{th} range of values are assumed to be respectively the 5th percentile ($X_{i,5}$) and 95th ($X_{i,95}$) percentile of the associated lognormal distribution. The next step consists in the statistical combination itself, which reflects the successive application of each reduction factor to the life predicted with the mean air curve in the $\ln(N)$ -space:

$$A' \stackrel{\text{def}}{=} A - \sum_{i=1,n} \ln(X_i) \quad \text{eq. 5.4}$$

where the RV A' characterizes the position of the new left-shifted fatigue curve. The global translation factor on life $TC_{\text{life-global}}$ is then obtained for a given percentile of A' (5% in practice). In NUREG/CR-6909, Monte-Carlo simulations were carried out by randomly drawing values for A and X_i according to their assumed distributions in order to determine $TC_{\text{life-global}}$. However, since A' is defined as a linear combination of normal independent RVs, A' is also normally distributed with a mean μ' and a standard deviation σ' :

$$\left| \begin{array}{l} A' \sim N(\mu', \sigma'^2); \text{ with:} \\ \mu' = A_m - \sum_{i=1,n} \mu_i \\ \sigma'^2 = sd^2 - \sum_{i=1,n} \sigma_i^2 \end{array} \right. \quad \text{eq. 5.5}$$

$TC_{\text{life-global}}$ can then be calculated with the following closed-form expression, also illustrated on Figure 5.2:

$$\left| \begin{array}{l} TC_{\text{life-global}} = \exp(A_m - A'_5); \text{ with:} \\ A'_5 = \mu' - t_{95}\sigma' \end{array} \right. \quad \text{eq. 5.6}$$

where A'_5 denotes the 5th percentile of the normal distribution associated with A' .

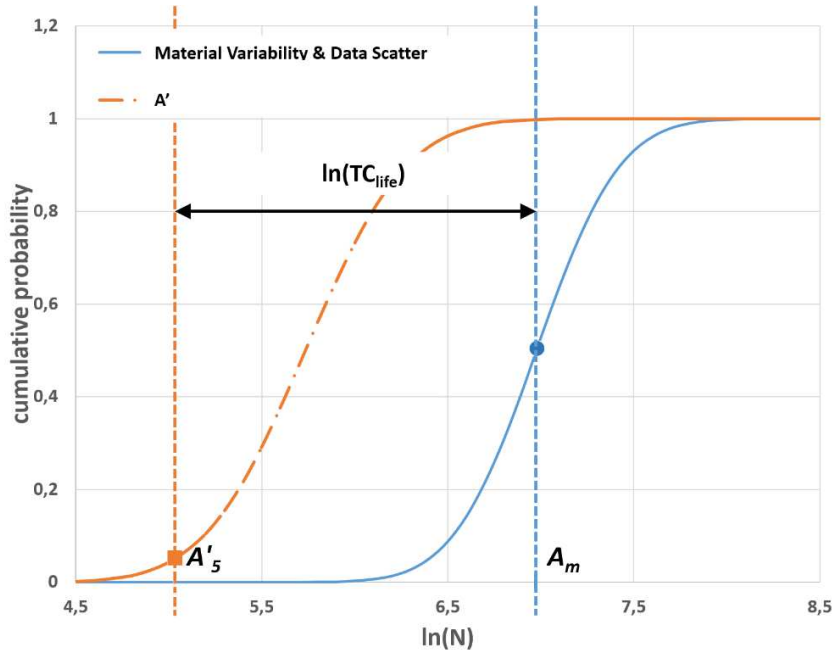


Figure 5.2 Illustration of the cumulative probability density functions associated with MVDS and A' random variable [5.3].

The $F_{en-threshold}$ is then defined as follows, so as to quantify the mismatch between experimental results obtained in a PWR environment on a rough specimen and a life prediction that uses a F_{en} factor and the design air curve translation factors:

$$F_{en-threshold} \stackrel{def}{=} \frac{F_{en-cc792} N_f}{TC_{life}} \frac{1}{N_{design}} \quad \text{eq. 5.7}$$

where $F_{en-cc792}$ is the environmental correction factor used in ASME Code-Case N-792-1 and recalled in eq. 5.8 to eq. 5.11, N_f is the experimental life of the specimen (N_{25} for instance), N_{design} is the life obtained for a strain amplitude equal to the one applied during the test using the code design curve, and TC_{life} is the translation coefficient on life (statistical combination of a given set of sub-factors amongst a , b , and d , depending on the surface condition). In eq. 5.7 TC_{life} is calculated the same way as $TC_{life-global}$ using eq. 5.2 to eq. 5.6, but the difference is that the sub-factor pertaining to surface finish has been excluded from the statistical combination in equation (3-4), since its effect is already accounted for through N_f (the test being conducted on a rough specimen). Consequently, the red part of eq. 5.7 is intended to make the water data comparable to the design curve prediction in air (blue part), as illustrated in Figure 5.3.

$$F_{en-cc792} = \exp(0.734 - T^* \varepsilon^* O^*) \quad \text{eq. 5.8}$$

$$\left| \begin{array}{ll} T^* = 0 & (T < 150 \text{ }^\circ\text{C}) \\ T^* = (T - 150)175 & (150 \text{ }^\circ\text{C} \leq T < 325 \text{ }^\circ\text{C}) \\ T^* = 0 & (T \geq 325 \text{ }^\circ\text{C}) \end{array} \right. \quad \text{eq. 5.9}$$

$$\left\{ \begin{array}{ll} \dot{\varepsilon}^* = 0 & (\dot{\varepsilon} > 0.4\%/s) \\ \dot{\varepsilon}^* = \ln(\dot{\varepsilon}/0.4) & (0.0004\%/s \leq \dot{\varepsilon} \leq 0.4\%/s) \\ \dot{\varepsilon}^* = \ln(0.0004/0.4) & (\dot{\varepsilon} < 0.0004\%/s) \end{array} \right. \quad \text{eq. 5.10}$$

$$O^* = 0.281 \quad (\text{all DO levels}) \quad \text{eq. 5.11}$$

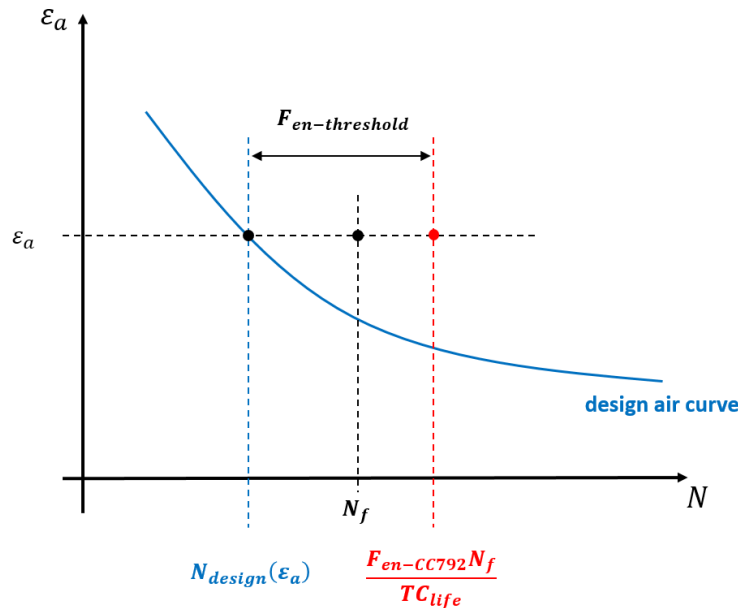


Figure 5.3 Schematic illustrating eq. 5.7, in the configuration where test conditions are such that $F_{en-CC792} > TC_{life}$ [5.3].

TC_{life} coefficient in eq. 5.7 takes two distinct values depending on the rough surface condition tested amongst industrially polished (IP) specimens and ground specimens [5.11] (the corresponding ranges of surface roughness are recalled in Table 5.2):

- For IP specimens, the sub-factors a, b, and d have to be combined (without c which is related to surface finish effect) using eq. 5.4, thus leading to a reported value of 4.5 for TC_{life} .
- For ground specimens, only the sub-factors a and b have to be combined using eq. 5.4, thus leading to a reported value of 3.5 for TC_{life} . Indeed, the size effect (d) is intricately linked to the surface finish and gets absorbed by the aggravating effect of surface finish (c) in the case of rough surface finish conditions, as reported in successive revisions of NUREG/CR-6909 [5.4–5.6].

Surface condition	R_a (μm)	R_t (μm)
Industrially polished (IP)	1.5 – 2	15 – 20
Ground	5 – 7	50 – 70

Table 5.2 Rough surface finishes tested [5.11].

Parameter	NUREG/CR-6909 [5.4]		NUREG/CR-6909,Rev1 [5.5,5.6]	
	IP specimens	Ground specimens	IP specimens	Ground specimens
MVDS (a)	$A_m = 6.891$ & $sd = 0.417$			
Loading history (b)	1.2 – 2.0		1.0 – 2.0	
Size (d)	1.2 – 1.4	N/A ¹	1.0 – 1.4	N/A ¹
TC_{life} (recalculated)	4.2	3.2	3.7	3.0

Table 5.3 Possible values of TC_{life} for F_{en-threshold} calculation, according to successive revisions of NUREG/CR-6909.

It is not specified exactly in [5.11] from which revision of NUREG/CR-6909 the reported values of 4.5 and 3.5 for TC_{life} (respectively for IP and ground specimens) have been derived, but the values recalculated in Table 5.3 using eq. 5.2 to eq. 5.6 tend to indicate that Rev.0 was used, as 4.2 and 3.2 were obtained respectively for industrially polished and ground specimens using Rev.0 sub-factors (and then probably rounded up to 4.5 and 3.5). However, as the sub-factors on life were revised in Rev.1, and since this is completely uncorrelated with the F_{en} expression used, it could be useful to take advantage of these revised sub-factors since the corresponding TC_{life} values given in Table 5.3 are lower than the ones reported in [5.11] (3.7 and 3.0 respectively for IP and ground specimens). Indeed, since the design curve remains unchanged, a lower TC_{life} leads to a higher F_{en-threshold}.

Finally, the quantified value for F_{en-threshold} can be effectively used in a fatigue usage factor calculation that accounts for environmental effects (using ASME Code-Case N-792-1) as a corrective factor that can be applied on the penalization F_{en} factor, so as to moderate its effect (see [5.11] for more details on the implementation and the scope of applicability).

5.3 QUANTIFICATION OF THE F_{EN-THRESHOLD} USING THE INCEFA-PLUS PWR DATA GENERATED ON ROUGH SPECIMENS

The experimental data used in the present analysis (and more broadly used within the INCEFA-PLUS Project for any analysis) has been previously assessed by an Expert Panel [5.16] in terms of quality and completeness. In this subsection, we consider the INCEFA-PLUS data available so far and generated in PWR environments on rough specimens. Some tests were performed under VVER conditions, where the F_{en-threshold} cannot be calculated since the F_{en} expression used in eq. 5.7 does not apply to this type of environment. These test results were therefore excluded from the analysis. With regard to surface finish, the data considered is that generated on solid bar specimens, since the surface condition of the inner wall of hollow bar specimens tested during the project corresponds to a honed finish (assimilated to a polished finish). This data has been generated by a total of six different laboratories performing tests within an autoclave, each of them using its own specimen geometry and control method [5.17], which can introduce a certain amount of scatter. The considered subset of the INCEFA- PLUS database corresponds to strain-controlled tests, with saw tooth waveforms (for several rising strain rates) under different

¹ Size effect is not taken into account because of the rough surface condition [5.4–5.6].

constant temperatures. Some of these data points have been generated by applying a mean strain and/or hold times (as reported in Chapter 4, Table 3.1) during cycling (which could also be a source of extra scatter), but according to the analysis reported in Chapter 4, these two parameters (as tested during the project) do not have a significant effect. Amongst these 50 tests, 49 were conducted on the same batch of 304L material (common material, heat identifier “XY182”), the remaining test was performed on a 304 material used in a Jacobs domestic program. The rough surface conditions tested correspond to R_t values ranging from 13.65 μm to 65.5 μm . In order to allow for a quantification of the $F_{\text{en-threshold}}$ the subset has to be split up into two parts. Consistently with the bounds given in [5.11] and recalled in Table 5.2, it is considered that $R_t \leq 20\mu\text{m}$ corresponds to an IP condition, and $R_t > 20\mu\text{m}$ corresponds to a ground conditions. The corresponding two sets of test results are then detailed in Table 5.4 and Table 5.5.

Moreover, it is important to emphasize that, at the time writing, one laboratory has reported in the database strain amplitudes that appear to be too low compared to the ones actually seen by the gauge. Revised gauge correction factors are currently being determined on the basis of refined FEA, but these are not yet available ². As the revised strain amplitudes can only be higher than those currently reported in the database, these test results can be used to calculate the $F_{\text{en-threshold}}$ in a conservative manner as the revised strain amplitudes would only decrease the quantity N_{design} in eq. 5.7, thereby increasing the $F_{\text{en-threshold}}$. This concerns 12 tests conducted on ground specimens at both 0.3% and 0.6% strain amplitude, with temperature and strain rate conditions such that a $F_{\text{en-CC792}} = 5.07$. These 12 data points have then been kept for this analysis, knowing that further correction could only improve the quantified margins.

Surface condition	ϵ_a (%)	T (°C)	Rising $\dot{\epsilon}$ (%/s)	$F_{\text{en-CC792}}$	Number of tests
IP	0.3	300	0.01	5.07	3
IP	0.32	300	0.01	5.07	1
IP	0.6	300	0.01	5.07	4

Table 5.4 Test conditions for industrially polished specimens.

Surface condition	ϵ_a (%)	T (°C)	Rising $\dot{\epsilon}$ (%/s)	$F_{\text{en-CC792}}$	Number of tests
Ground	0.3	230 or 300	0.01 or 0.1	2.91 or 3.35 or 5.07	17
Ground	0.302	300	0.01	5.07	1
Ground	0.313	300	0.01	5.07	1
Ground	0.38	300	0.008	3.07	1
Ground	0.6	300	0.01 or 0.1	2.91 or 5.07	18
Ground	0.611	300	0.01	5.07	1
Ground	0.622	300	0.01	5.07	1
Ground	1.2	300	0.01	4.9	2

Table 5.5 Test conditions for ground specimens.

² See footnote 2 in Section 4.2.3 and footnote 3 in Section 4.2.4. The revised data set is going to be published in [5.18].

This experimental data is plotted (without applying any correction on life at this stage) on Figure 5.4 per surface finish condition, against NUREG/CR-6909 mean air curve and ASME design air curve (mandatory appendix I of BPVC.III, Table I-9.2). Even if not used in the F_{en} -threshold quantification, the data obtained on polished solid bar specimens has also been reported on this chart (the test conditions are similar to those detailed in Table 5.4 and Table 5.5 but not reported here).

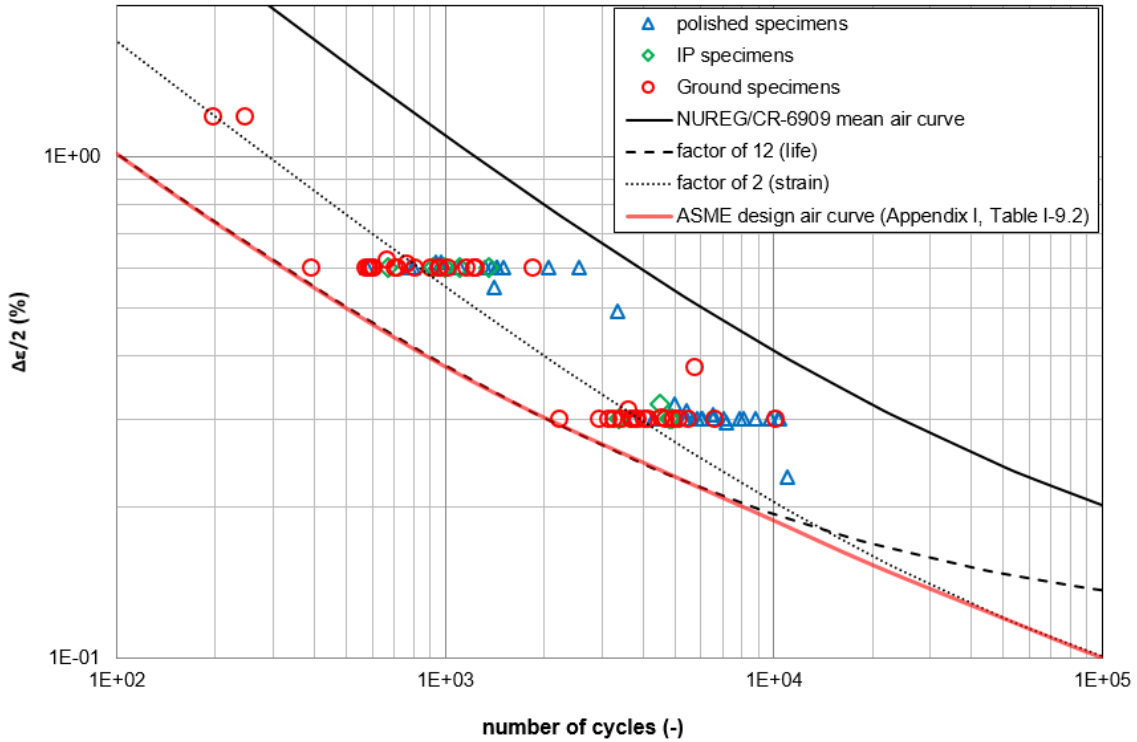


Figure 5.4 Considered subset of the INCEFA-PLUS PWR database (solid bar specimens) [5.1].

The raw data represented on Figure 5.4 does not allow to clearly visualize the potential margins associated with the joint use of the design curve translation factors and F_{en} factor. To this end, it is necessary to correct the life predicted with the design curve with the appropriate quantities that were mentioned above ($F_{en-CC792}$ and TC_{life}). This is what has been done in Figure 5.5; where the (corrected) predicted life is compared with the life. For polished specimen, life is predicted using NUREG/CR-6909 mean air and divided by the F_{en} expression from the Code-Case N-792-1. For rough specimens (industrially polished and ground specimens), life is predicted according to eq. 5.12:

$$N_{pred} = \frac{TC_{life} N_{design}}{F_{en-CC792}} \quad (\text{for rough specimens}) \quad \text{eq. 5.12}$$

where TC_{life} increases the design curve prediction by removing the aggravating effects that are not part of the test conditions. The values used for TC_{life} in Figure 5.5 are the ones reported in [5.11] (4.5 for IP specimens and 3.5 for ground specimens). This first graphical analysis helps make it clear that the model fits well for polished surface finish since the corresponding data points are located along the first bisector. By contrast, the model exhibits a certain level of conservatism for rough specimens since the corresponding data points are shifted by a factor of approximately 3 below the first bisector.

In addition to Figure 5.5, this data has also been reported relative to the NUREG/CR-6909 database used to derive the F_{en} expression, on Figure 5.6 and Figure 5.7 (respectively for polished and rough specimens).

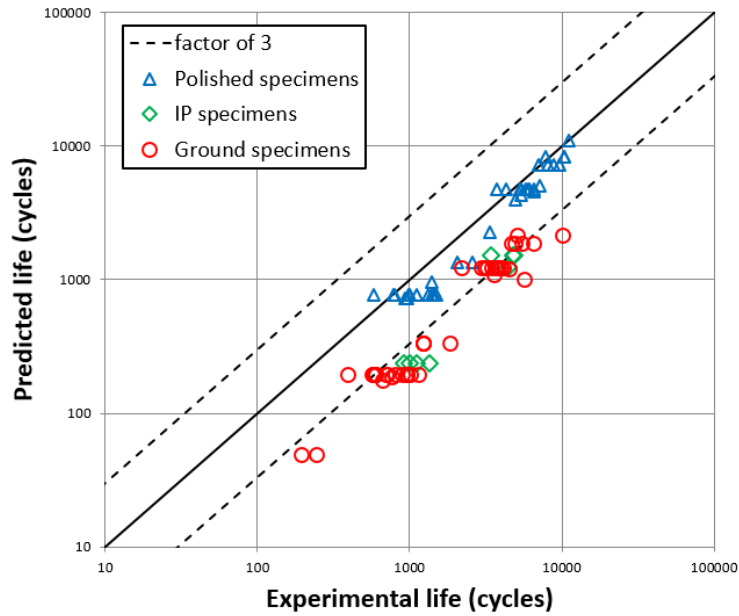


Figure 5.5 Experimental lives vs. predicted lives for the considered subset of the INCEFA-PLUS PWR database: tests conducted on polished and rough solid bar specimens [5.1].

Note: for IP and ground specimens, life is predicted according to eq. 5.12.

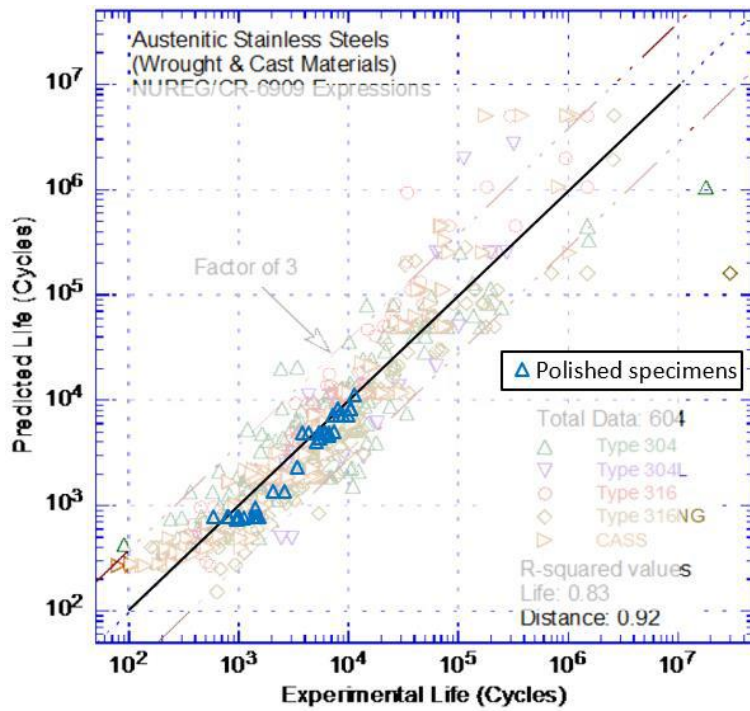


Figure 5.6 Experimental lives vs. predicted lives for the considered subset of the INCEFA-PLUS PWR database: tests conducted on polished solid specimens. Background figure originates from [5.5].

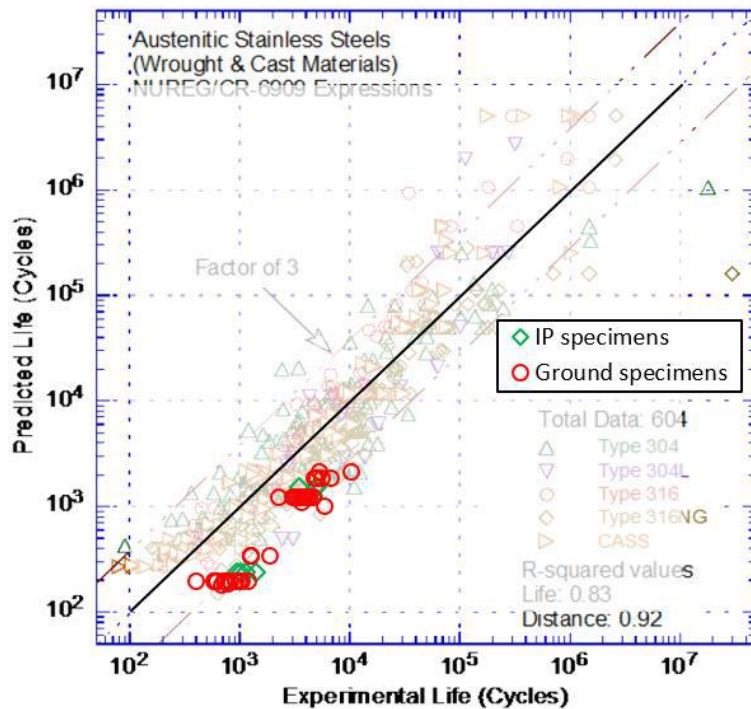


Figure 5.7: Experimental lives vs. predicted lives for the considered subset of the INCEFA-PLUS PWR database: tests conducted on industrially polished and ground specimens. Background figure originates from [5.5].

Note 1: both tests conducted at $\epsilon_a = 1.2\%$ are not plotted on this chart.

Note 2: for IP and ground specimens, life is predicted according to eq. 5.12.

Beyond this graphical analysis, an explicit quantification of the margin can be performed using eq. 5.7. The $F_{\text{en-threshold}}$ is calculated for each data point, and then averaged per strain amplitude level (regardless of the theoretical $F_{\text{en-CC792}}$ value) for both surface conditions. These calculations are reported in Table 5.6 and Table 5.7 (respectively for IP and ground specimens). A global weighted average is then calculated for all strain amplitude conditions. Two different $F_{\text{en-threshold}}$ values are given in the last columns of these tables: the first has been obtained using TC_{life} values as originally reported in [5.11] (based on NUREG/CR-6909 Rev.0 sub-factors), and the second one has been obtained using TC_{life} values based on NUREG/CR-6909 Rev.1 sub-factors (see Table 5.3). As previously reported in [5.11] on the basis of data generated on the same material, the quantified margin can reach values below 3.0 for certain levels of strain amplitude. However, the average $F_{\text{en-threshold}}$ value reported in the last row of Table 5.6 and Table 5.7 ranges from 3.09 to 3.85, depending on the surface condition and TC_{life} values used. This permits the conclusion that the INCEFA-PLUS data represents further evidence for the conservatism incorporated in the NUREG/CR-6909 approach, and quantified by a factor of 3 in several existing EAF assessment procedures [5.10].

In addition, for ground surface finishes, it is possible to split the database in two groups that correspond to high and low F_{en} conditions (respectively 5.07 and 2.91 or 3.35 using Code-Case N-792-1 expression), and then to recalculate the $F_{\text{en-threshold}}$ value associated with these two groups (for all strain amplitude conditions). These values are reported in Table 5.8, and the quantified margin does not seem to be significantly affected when these two groups are considered separately.

Surface condition	Number of tests	ϵ_a (%)	$F_{en-CC792}$	$F_{en-threshold}^3$	$F_{en-threshold}^4$
IP	3	0.3	5.07	2.38	2.89
IP	1	0.32	5.07	2.98	3.62
IP	4	0.6	5.07	3.80	4.62
Total (weighted average)				3.16	3.85

Table 5.6 $F_{en-threshold}$ values for tests on industrially polished surface finish (total of 8 tests).

Surface condition	Number of tests	ϵ_a (%)	$F_{en-CC792}$	$F_{en-threshold}^5$	$F_{en-threshold}^6$
Ground	17	0.3	2.91 or 3.35 or 5.07	2.53	2.95
Ground	1	0.302	5.07	3.24	3.78
Ground	1	0.313	5.07	2.87	3.35
Ground	1	0.38	3.07	4.94	5.76
Ground	18	0.6	2.91 or 5.07	3.41	3.98
Ground	1	0.611	5.07	3.56	4.16
Ground	1	0.622	5.07	3.22	3.76
Ground	2	1.2	4.9	3.86	4.51
Total (weighted average)				3.09	3.61

Table 5.7 $F_{en-threshold}$ values for tests on ground surface finish (total of 42 tests).

Surface condition	Number of tests	ϵ_a (%)	$F_{en-CC792}$	$F_{en-threshold}^4$	$F_{en-threshold}^5$
Ground	11	all	2.91 or 3.35 ("low F_{en} conditions")	3.21	3.74
Ground	31	all	5.07 ("low F_{en} conditions")	3.05	3.56

Table 5.8 $F_{en-threshold}$ values for tests on ground surface finish (total of 42 tests).

5.4 CONCLUSION

INCEFA-PLUS data⁷ have been investigated according to an existing EAF codified approach that allows for the quantification of the margins related to the joint implementation of a design air curve (especially its translation factor on life related to surface finish effects) and an environmental penalization factor F_{en} . Despite possible additional sources of scatter (different laboratories, different strain control methods in autoclave, different specimen geometries, application of mean strain and hold times for during several tests...) and despite the

³ TC_{life} is 4.5 for IP specimens as in [5.11].

⁴ TC_{life} is 3.7 for IP specimens, using NUREG/CR-6909, Rev.1 sub-factors as in Table 5.3.

⁵ TC_{life} is 3.5 for ground specimens as in [5.11].

⁶ TC_{life} is 3.0 for ground specimens, using NUREG/CR-6909, Rev.1 sub-factors as in Table 5.3.

⁷ INCEFA-PLUS database of experimental test results. Retrieved 16 June 2020 from <https://doi.org/10.5290/50>.

incorporation of data points for which the quantified margins are known to be slightly underestimated, the results are consistent with what has been previously reported in the literature, and underpin these conclusions.

REFERENCES

- [5.1] S. Cuvilliez, M. Bruchhausen, J.-C. Le Roux, J. Mann, A. McLennan, P. Spätig, Final WP3.2 Report (D3.8); INCEFA-PLUS Internal Report, 2020.
- [5.2] S. Cuvilliez, A. McLennan, K. Mottershead, J. Mann, M. Bruchhausen, INCEFA-PLUS Project: Lessons learned from the project data and impact on existing Fatigue Assessment Procedures; PVP2020-21106, Am. Soc. Mech. Eng. Press. Vessel. Pip. Div. PVP. (2020) 1–8.
- [5.3] S. Cuvilliez, A. McLennan, K. Mottershead, J. Mann, M. Bruchhausen, Incefa-Plus Project: Lessons Learned From the Project Data and Impact on Existing Fatigue Assessment Procedures, J. Press. Vessel Technol. 142 (2020). doi:10.1115/1.4047273.
- [5.4] O.K. Chopra, W.J. Shack, NUREG/CR-6909; ANL-06/08, Effect of LWR Coolant Environments on the Fatigue Life of Reactor Materials. Final Report, 2007.
- [5.5] O.K. Chopra, G.L. Stevens, NUREG/CR-6909,Rev.1; ANL-12/60; Effect of LWR Coolant Environments on the Fatigue Life of Reactor Materials. Draft Report for Comment, 2014.
- [5.6] O.K. Chopra, G.L. Stevens, NUREG/CR-6909,Rev.1; Effect of LWR Water Environments on the Fatigue Life of Reactor Materials. Final Report, 2018.
- [5.7] R. Tregoning, Guidelines for evaluating the effects of Light-Water Reactor Water Environments in Fatigue Analyses of Metal Components; Regulatory Guide 1.207, Rev. 1, 2018.
- [5.8] Code-Case ASME N-792-1, Fatigue Evaluation Including Environmental Effects, Section III, Division 1, 2010.
- [5.9] RCC-M, Règles de Construction et de Conception des matériel Mécaniques de l'îlot nucléaires REP, (2007) avec addenda 2008,2009 et 2010.
- [5.10] T. Métais, D. Tice, A. Morley, G.L. Stevens, L. de Baglion, S. Cuvilliez, Explicit quantification of the interaction between the PWR environment and component surface finish in environmental fatigue evaluation methods for austenitic stainless steels; PVP2018-84240, Am. Soc. Mech. Eng. Press. Vessel. Pip. Div. PVP. 1A-2018 (2018). doi:10.1115/PVP201884240.
- [5.11] T. Métais, S. Courtin, L. de Baglion, C. Gourdin, J.-C. Le Roux, ASME Code-Case Proposal to Explicitly Quantify the Interaction Between the PWR Environment and Component Surface Finish; PVP2017-65367, 2017. doi:10.1115/PVP2017-65367.
- [5.12] RCC-M, Design and Construction Rules for mechanical components of nuclear PWR islands, (2016).
- [5.13] S. Courtin, T. Métais, M. Triay, E. Meister, S. Marie, Modifications of the 2016 Edition of

the RCC-M Code to Account for Environmentally Assisted Fatigue; PVP2016-63127, 2016. doi:10.1115/PVP2016-63127.

- [5.14] J. Stairmand, N. Platts, D. Tice, K. Mottershead, W. Zhang, J. Meldrum, A. McLennan, Effect of Surface Condition on the Fatigue Life of Austenitic Stainless Steels in High Temperature Water Environments; PVP2015-63127, 2015. doi:10.1115/PVP2015-45029.
- [5.15] A. Morley, M. Twite, N. Platts, A. McLennan, C. Currie, Effect of Surface Condition on the Fatigue Life of Austenitic Stainless Steels in High Temperature Water Environments; PVP2018-84251, Am. Soc. Mech. Eng. Press. Vessel. Pip. Div. PVP. (2018) V01AT01A017. doi:10.1115/PVP2018-84251.
- [5.16] M. Bruchhausen, A. McLennan, R. Cicero, C. Huotilainen, K. Mottershead, J.-C. Le Roux, M. Vankeerberghen, Environmentally assisted fatigue data from the INCEFA-PLUS project; PVP2019-93085, Am. Soc. Mech. Eng. Press. Vessel. Pip. Div. PVP. 1 (2019). doi:10.1115/PVP2019-93085.
- [5.17] M. Vankeerberghen, A. McLennan, I. Simonovski, G. Barrera, S. Arrieta, M. Ernestova, N. Platts, M. Scibetta, M. Twite, Strain Control Correction for Fatigue Testing in LWR Environments; PVP2020-21373, Am. Soc. Mech. Eng. Press. Vessel. Pip. Div. PVP. (2020).
- [5.18] M. Bruchhausen, A. McLennan, S. Arrieta, T. Austin, R. Cicero, W.J. Chitty, L. Doremus, G. Dundulis, M. Ernestova, A. Grybenas, C. Huotilainen, J. Mann, K. Mottershead, R. Novotny, F.J. Perosanz Lopez, N. Platts, J.-C. Le Roux, P. Spätig, C. Torre Celeizábal, M. Twite, M. Vankeerberghen, Characterization of Austenitic Stainless Steels with regard to Environmentally Assisted Fatigue in Simulated Light Water Reactor Conditions, Metals (Basel). 10 (2020).

CHAPTER 6 CONCLUSIONS

INCEFA-PLUS Project is a five-year project supported by the European Commission Horizon 2020 programme. The project concluded in October 2020. Sixteen organisations from across Europe have combined forces to deliver more than 200 experimental fatigue data points on austenitic stainless steel in both air and LWR primary environment, which can be used to develop improved guidelines for assessment of environmental fatigue damage to ensure safe operation of nuclear power plants.

Within INCEFA-PLUS, the effects of mean strain and stress, hold time, strain amplitude and surface finish on fatigue resistance of austenitic stainless steels in light water reactor environments have been studied experimentally.

The data obtained have been collected and standardised in an online environmental fatigue database (MatDB by JRC [6.1]), implemented with the assistance of an INCEFA-PLUS led CEN Workshop on this aspect (FATEDA [6.2]). These data have been reviewed by Expert Panel to ensure their quality and completeness.

INCEFA-PLUS develops and disseminates methods for including the new data into assessment approaches for environmental fatigue degradation.

6.1 TEST CAMPAIGN

The test campaign was planned to occur over four of the five years of the project, divided in successive phases (Phase I, II and III [6.3–6.5]).

The programme, which covered solid and hollow specimens, focussed on the effects of parameters such as strain range, mean strain, surface roughness, hold time periods and environment, as well as their interactions on the fatigue life in strain controlled low cycle fatigue tests. Due to the continuous analysis of the obtained results throughout the experimental campaign, the three test phases had slightly different foci:

- I. During the first phase two values of each of parameters were considered: strain range, mean strain, surface finish, hold time, and environment. A single $F_{en} = 4.57$ was considered for Phases I and Phase II.
- II. Since Phase I did not show indications of an effect of mean strain on fatigue life this parameter was dropped from the main test programme in Phase II and a third higher surface roughness was introduced.
It was defined a mean strain under the assumption that it would reproduce experimentally the mean load on plant components during operation. However, an imposed mean strain initially leads to a mean stress, but this mean stress relaxes early in the fatigue test so that the imposed mean strain has no effect on fatigue life.
In parallel, a limited test programme on the effects of mean stress under strain control was carried out.
- III. The results from Phase II did not show any hold time effect, in contrast to what was observed elsewhere [6.6]. A likely reason for this discrepancy are differences between

the application of the hold time during the fatigue cycle. Consequently, no tests with hold times were included in the main programme during Phase III, but a limited programme on hold time effects was added to help elucidate why the hold times did not reveal a significant impact on fatigue life.

A reduced environmental factor $F_{en} = 2.68$ was introduced for the main test programme in Phase III (with similar parameters as those used in Phase I and II). The reduction of the F_{en} was achieved by either reducing the temperature or increasing the rising strain rate during the test.

The programme on strain-controlled testing with mean stress started in Phase II was extended in Phase III. The aim of this program to suggest a method for carrying out laboratory tests under conditions which are closer to mechanical loading conditions seen by actual plant components than either stress-controlled tests with mean stress or strain controlled tests with mean strain.

The data of the main testing campaign are shown in Figure 4.3, where the INCEFA-PLUS data points are plotted together with the NUREG/CR-6909 [6.7] air and PWR curves. The four groups of tests in air/PWR environment and with two nominal strain ranges 0.6% and 1.2% can easily be discerned. In the two test groups in air, the ground specimens are all in the lower bound which is not the case for the tests in water. This indicates a higher sensitivity to surface finish in air than in water.

To sum up, **the data analysis confirmed the following observations:**

- **Effects of environment and strain range on fatigue life are clearly visible.**
- **Subtle interactions between surface roughness and either environment or strain range have been found in different analyses.**
- **There does not seem to be a systematic difference between hollow and full specimens.**
- **No effect of hold times on fatigue life was observed.**
- **As no effect of mean strain was observed, a sub-program based on mean stress have been developed, showing no synergy between mean stress and PWR environment.**

6.2 STATISTICAL TREATMENT

The experimental data have been analysed by two statistical methods (Chapter 4):

1. Statistical linear model (Section 4.2).
2. Manual analysis by residual plots and two-sample statistical tests (Section 4.3).

The first one is based on a statistical linear model that allows studying the effect of all parameters at once, including interaction between parameters. This approach is based on a linear model of the form:

$$\ln(N_f) = \sum_i \alpha_i x_i + \sum_{i < j} \alpha_{i,j} x_i x_j + I \quad \text{eq. 6.1}$$

From this analysis, it is obtained a simplified model described by 4 parameters (see Table 4.7 and Table 4.8) which works for the main experimental programme data. This model contains

three main effects (strain range, surface roughness and environment) and one interaction (strain range and surface roughness). The resulting expression¹ is:

$$\ln(N_f) = -0.84613x_1 - 0.23010x_2 + 0.82034x_3 + 0.13308x_1x_2 + 8.32523 \quad \text{eq. 6.2}$$

In the case of low F_{en} sub-program, the linear analysis produces a model with three effects: surface roughness, positive strain rate and temperature (see Table 4.14 and Table 4.15). The low F_{en} expression² is:

$$\ln(N_f) = -0.28661x_1 + 0.20422x_2 - 0.20846x_3 + 8.64314 \quad \text{eq. 6.3}$$

The second statistical approach is a more conventional and graphical approach based on residuals analysis and two-sample statistical tests. This analysis uses an engineering method, based on Langer fatigue model (the same model used in NUREG/CR-6909 [6.7]). The best-fit curve to common material (304L, XY182) data³ is given by:

$$\ln(N) = 7.295 - 1.483 \ln(\varepsilon_a - 0.160) \quad \text{eq. 6.4}$$

Although, the data from the experimental program are in good agreement with the NUREG/CR-6909 best-fit curve, the use of a material-specific best-fit air curve further improves the agreement between predictions and experimental results (see Figure 4.8).

The analysis by residual plots (see Figure 4.12) describes the effect of surface roughness in each environment: it is minimal in air and more significant in PWR environmental. However, in both environments, the effect of surface roughness was lower than predicted by NUREG/CR-6909.

These two independent approaches (compared in Section 4.4) have led to the same main conclusions. Aside from the obvious effects of strain range and environment, the only parameter amongst surface roughness, mean strain and hold time that has been identified as having a significant effect is surface roughness.

Even if it is necessary to point that it is difficult to get a definitive conclusion regarding the potential interaction between the effects studied, both analyses point an interaction between surface roughness and strain range, in the case of current statistical linear model, and environment, in the case of current analysis by residuals plots and prior linear analysis [6.8].

Beyond the main experimental programme, the data generated during the specific testing programme on mean stress effect on fatigue life and possible interactions with PWR environment have also been analysed:

- **For the strain-controlled experiments and for $N_f < 10^5$, a clear reduction of fatigue life in PWR environment was found independent of the mean stress level** and is in good agreement with the predictions based on the F_{en} calculations with NUREG/CR-6909

¹ The normalized parameter strain range correspond to x_1 , surface roughness (R_t) to x_2 and environment to x_3 respectively. The interaction between strain range and surface correspond to x_1x_2 .

² For low F_{en} model, the normalized parameter surface roughness (R_t) correspond to x_1 , positive strain rate to x_2 and temperature to x_3 respectively.

³ The data used to fit the Langer equation have been obtained for applied strain amplitudes between 0.2% and 0.6%. It should not be considered accurate enough for high-cycle fatigue regime.

equation. This indicates that **there is no synergistic effect between mean stress and PWR environments.**

- **A reduction of fatigue life due to the PWR environment was also found for the load-controlled tests and $N_f < 10^5$.**
- The large scatter in fatigue life for all tests performed with smaller strain or stress amplitude ($N_f > 10^5$) do not permit the drawing of firm conclusions on the conjugate effect of mean stress and PWR environment in the HCF regime.
- An analysis based upon the Smith-Watson-Topper parameter was considered. The NUREG/CR-6909 air curve was converted into a SWT-life curve using an empirical calibration between the maximum stress and strain amplitude at half-life. The SWT parameter was calculated for all the tests of the program. The results obtained in air show that **the NUREG/CR-6909 converted SWT-life curve correlates well all the data with and without mean stress. Similarly, the data obtained in PWR environment falls reasonably close to the SWT-life curve, shifted by the appropriate F_{en} (Figure 4.25). This observation also confirms that for conditions tested in this program, mean stress does not amplify the PWR environment effect.**

Summarising, from the main program, the experimental data can be described by a three factor model. The three main effects of those studied are environment, strain range and surface finish (R_t). The developed model for common material 304L works for A312 steel in VVER environment.

The F_{en} values derived from both the main INCEFA-PLUS experimental programme and sub-programs have been found to be comparable to those provided by NUREG/CR-6909.

6.3 DATA SCATTERING IMPACT

The data scattering in this project is related with lab-to-lab variation and specimen geometries. From the beginning of the project, the partners agreed on a procedure [6.9] to minimize divergences in the tests performance, agreeing on common condition to carry out the tests and evaluating the obtained results to guarantee their quality [6.10].

As the solid specimen geometry is by far the dominant specimen type in the INCEFA-PLUS experimental programme, these data are used to assess the lab-to-lab variation and the effect of diameter size on fatigue life. There was no trend for the residuals as a function of diameter, indicating that **specimen diameter does not contribute to any of the significant parameters defined in the model.** The average residuals of the laboratories testing the smaller diameters did not fall outside the scatter of the other laboratories.

When considering the hollow specimen geometries that were tested by three different laboratories, the residuals show that two laboratories (that used the same hollow specimen design) generated fatigue lives that are consistently lower than other tests conducted on solid specimens by these laboratories, according to [6.11]. On the contrary, one laboratory that used a different hollow specimen design generated fatigue lives comparable to those of solid specimens. To attempt to fully understand the differences between the hollow specimen geometries and take account of the differences in through wall temperature gradients (due to

differences in test method) FEA modelling was conducted. These calculations were unable to explain the differences observed in the residuals. At least for now, there is no physical explanation behind the difference between the laboratories using different hollow specimen designs. A sensitivity study was then performed on the statistical linear model to assess the impact of inclusion or exclusion of hollow specimen data in the database. This study concluded that **the results of the INCEFA-PLUS programme are insensitive to the hollow specimen data and the hollow specimen results could be included in the analysis without any correction factor on strain amplitude.**

Since one particular feature of this project was to have several different laboratories performing fatigue testing on the same batch of material, considering the residuals of the solid specimen data (by laboratory), **it was possible to develop an approach to derive a factor on life associated with lab-to-lab variation. For the INCEFA-PLUS database (common material), a factor on life of 1.5 has been quantified.**

6.4 INCEFA-PLUS DATA EVALUATION AGAINST NUREG/CR-6909

According to the conclusions of Chapter 5, the data generated during INCEFA-PLUS does not show any significant effect of mean strain or hold times as tested during the project, while surface finish has been identified as a parameter for which the effect can be considered as statistically significant.

The magnitude of this effect, especially in PWR environment, has been compared with that currently used in NUREG/CR-6909 guidance for EAF assessment. **The INCEFA-PLUS data generated on a 304L austenitic stainless steel in PWR environment on ground specimens show that a margin corresponding to a factor of 3 on fatigue life can be claimed when the NUREG/CR-6909 prediction is used.**

Despite possible additional sources of scatter (different laboratories, different strain control methods in autoclave, different specimen geometries, application of mean strain and hold time...), which have been minimized in this project, these results are consistent with what has been previously reported in the literature [6.12–6.14], and underpin already existing fatigue procedures that have been recently developed to incorporate this margin.

REFERENCES

- [6.1] Joint Research Center, ODIN Portal - MatDB, (2020). <https://odin.jrc.ec.europa.eu>.
- [6.2] European Committee for Standardization, Engineering materials - Electronic data interchange - Formats for fatigue test data, (2017) 1–57.
- [6.3] M. Bruchhausen, Test data from testing Phase I in MatDB (D2.08 and 15); INCEFA-PLUS Internal Report, 2019.

- [6.4] M. Bruchhausen, Test data from testing Phase II in MatDB (D2.10 and 17); INCEFA-PLUS Internal Report, 2019.
- [6.5] M. Bruchhausen, Test data from testing Phase III in MatDB (D2.12 and 19); INCEFA-PLUS Internal Report, 2020.
- [6.6] H.E. Karabaki, J.P. Solin, M. Twite, M. Herbst, J. Mann, G. Burke, Fatigue with hold times simulating npp normal operation results for stainless steel grades 304L and 347; PVP2017-66097, Am. Soc. Mech. Eng. Press. Vessel. Pip. Div. PVP. 1A-2017 (2017) V01AT01A031. doi:10.1115/PVP2017-66097.
- [6.7] O.K. Chopra, G.L. Stevens, NUREG/CR-6909,Rev.1; Effect of LWR Water Environments on the Fatigue Life of Reactor Materials. Final Report, 2018.
- [6.8] M. Bruchhausen, A. McLennan, R. Cicero, C. Huotilainen, K. Mottershead, J.-C. Le Roux, M. Vankeerberghen, Environmentally assisted fatigue data from the INCEFA-PLUS project; PVP2019-93085, Am. Soc. Mech. Eng. Press. Vessel. Pip. Div. PVP. 1 (2019). doi:10.1115/PVP2019-93085.
- [6.9] M. Vankeerberghen, L. Doremus, P. Spätig, M. Bruchhausen, J.-C. Le Roux, M. Twite, R. Cicero, N. Platts, K. Mottershead, Ensuring data quality for environmental fatigue – INCEFA-Plus testing procedure and data evaluation; PVP2018-84081, Am. Soc. Mech. Eng. Press. Vessel. Pip. Div. PVP. 1A-2018 (2018). doi:10.1115/PVP201884081.
- [6.10] R. Cicero, Expert Panel Tool Proposal; INCEFA-PLUS Internal Report, 2017.
- [6.11] P. Gill, P. James, C. Currie, C. Madew, A. Morley, An investigation into the lifetimes of solid and hollow fatigue endurance specimens using cyclic hardening material models in finite element analysis; PVP2017-65975, Am. Soc. Mech. Eng. Press. Vessel. Pip. Div. PVP. 1A-2017 (2017). doi:10.1115/PVP2017-65975.
- [6.12] J. Stairmand, N. Platts, D. Tice, K. Mottershead, W. Zhang, J. Meldrum, A. McLennan, Effect of Surface Condition on the Fatigue Life of Austenitic Stainless Steels in High Temperature Water Environments; PVP2015-63127, 2015. doi:10.1115/PVP2015-45029.
- [6.13] A. Morley, M. Twite, N. Platts, A. McLennan, C. Currie, Effect of Surface Condition on the Fatigue Life of Austenitic Stainless Steels in High Temperature Water Environments; PVP2018-84251, Am. Soc. Mech. Eng. Press. Vessel. Pip. Div. PVP. (2018) V01AT01A017. doi:10.1115/PVP2018-84251.
- [6.14] T. Métais, D. Tice, A. Morley, G.L. Stevens, L. de Baglion, S. Cuvilliez, Explicit quantification of the interaction between the PWR environment and component surface finish in environmental fatigue evaluation methods for austenitic stainless steels; PVP2018-84240, Am. Soc. Mech. Eng. Press. Vessel. Pip. Div. PVP. 1A-2018 (2018). doi:10.1115/PVP201884240.

ANNEXES

Contents:

Annex A	INCEFA-PLUS Testing Protocol.....	A.1
A.1	Introduction	A.1
A.2	Principle	A.1
A.3	Specimen '	A.2
A.4	Apparatus	A.2
A.5	Testing in air.....	A.3
A.6	Testing in LWR environment.....	A.4
A.7	Stressing.....	A.4
A.8	Procedure	A.5
A.9	Test report	A.6
A.10	Fatigue-related test parameters.....	A.9
A.11	Hysteresis data.....	A.10
A.12	Hold times.....	A.10
A.13	Mean strain/stress.....	A.11
A.14	Test matrix Phase II.....	A.11
	References.....	A.12
Annex B	Review sheet of Expert Panel	B.1
B.1	Expert Panel tool.....	B.1
	References.....	B.7
Annex C	Test Matrix.....	C.1
C.1	Test Matrix Phase I.....	C.1
C.2	Test Matrix Phase II.....	C.3
C.3	Test Matrix Phase III.....	C.6
	References.....	C.8

Annex D	Summary of INCEFA-PLUS Project publications.....	D.1
	2016.....	D.1
	2017.....	D.1
	2018.....	D.1
	2019.....	D.2
	2020.....	D.3

ANNEX A INCEFA-PLUS TESTING PROTOCOL

This annex gathers the contents of the documents “Testing Protocol for INCEFA-PLUS” [A.1,A.2] and “Infopack for Phase II” [A.1,A.2] developed by Marc Vankeerberghen.

A.1 INTRODUCTION

The following standards are examples of standards relevant to environment-assisted fatigue testing in the framework of INCEFA-PLUS:

1. ASTM E606 Standard Practice for Strain-Controlled Fatigue Testing [A.3].
2. ISO/DIS 12106 Metallic materials – Fatigue testing – Axial-strain-controlled method [A.4].
3. ISO 11782-1 Corrosion of metals and alloys – Corrosion fatigue testing – Part 1: Cycles to failure testing [A.5].
4. BS 7270:2006 Metallic materials. Constant amplitude strain controlled axial fatigue. Method of test [A.6].
5. AFNOR A03-403 Produits métalliques – Pratique des essais de fatigue oligocyclique [A.7].

Testing shall be conducted, where practicable, to such (an) appropriate national or international standard(s). However, it is important to note that there is no available standard that fully covers fatigue testing in high temperature light water reactor environments. Hence, this document draws upon available standards to create a protocol for INCEFA-PLUS testing in both air and water.

A.2 PRINCIPLE

The INCEFA-PLUS fatigue test involves subjecting a series of specimens to the number of strain cycles required for a fatigue crack to initiate and grow large enough to cause failure, or a pre-agreed load drop, during exposure to a LWR environment and, for reference, to an air environment at two alternating strains (0.3% and 0.6%). The objective for both environments is to define either the fatigue strength at N cycles, from a SN diagram, or the fatigue strength limit, as the fatigue life becomes very large, and, hence, to determine the environmental correction factor F_{en} .

The INCEFA-PLUS fatigue tests are used to determine the effect of surface roughness, strain amplitude, mean stress/strain and hold time on the corrosion fatigue life of 304 stainless steel subjected to an applied strain range (or occasionally stress range) for a relatively low numbers of cycles (low cycle fatigue).

A.3 SPECIMEN ^{1,2}

- Specimens should be of a size consistent with the use, so far as practicable, of the middle to upper ranges of the strain or load calibration of the fatigue machine.
- Care must be exercised in the machining of uniform-gauge specimens to blend the shoulder radius at the specimen ends with the minimum diameter so as to avoid undercutting. So that stress concentrations are minimized, the shoulder radius should be as large as possible, consistent with limitations on specimen length (ISO: $r > 8d$, ASTM: $r = 4d \pm 2d$).
- For solid specimens the cross-sectional area of the shoulders A_{end} shall be at least four times that of the test section area A_g . Criteria will differ for hollow specimens.
- For tests run in compression, the length of the test section, L_g , shall be $3d \pm d$ in order to minimize buckling.
- A minimum cross-section diameter of 5 mm is preferred for solid specimens. For hollow specimens minimum outside diameter is 10 mm and minimum wall thickness is 2.5 mm.
- Design of specimen end connections is dependent upon user preference, fixture, or availability of material, or a combination of all three; it is constrained principally by proper considerations of axial alignment and backlash.
- Specimens should be prepared to procedures agreed by the INCEFA-PLUS consortium.

The machining and polishing processes are controlled by EDF whereas the preparation of the rough surfaces is the responsibility of Framatome. Further information can be found in D2.1 – SPECIMEN MANUFACTURING INSTRUCTIONS [A.8].

A.4 APPARATUS ³

- The fatigue testing machine shall be capable of operation at cyclic frequencies and with waveforms relevant to the application of interest and shall be equipped with adequate cycle counting and load monitoring systems. Requirements for INCEFA-PLUS include a gauge strain rate of 0.01%/s and gauge (or shoulder) strain or load control to within 1%.
- The alignment of the fatigue testing machine shall ensure axially of the applied load. The testing machine, together with any fixtures used in the test program, must meet a bending strain criteria; the maximum allowed bending strain is 5%. Alignment must be carried to a procedure specified in an appropriate standard⁴. For tests in water, labs shall strive towards such air test requirements, and any deviation from these shall be reported.
- The machine should be one in which specific measures have been taken to minimize backlash in the loading train.

¹ Nomenclature: L_g = gauge length; d = specimen diameter; r = a radius; A_g = cross-section in gauge; A_{end} = cross-section specimen end.

² Testing partners should indicate in their test reporting items mentioned here and that are not satisfied.

³ Testing partners should indicate in their test reporting items mentioned here and that are not satisfied.

⁴ E.g. BS ISO 23788 2012 Metallic materials- verification of the alignment of fatigue testing machines or ASTM E1012 – 12 Verification of testing frame and specimen alignment under tensile and compressive axial force application.

- The force transducer should be designed specifically for fatigue testing and possess the following characteristics: high resistance to bending; high axial stiffness; high linearity; accuracy and sensitivity; low hysteresis; high overturning moment stiffness; and high lateral stiffness. For best results, it is recommended that the maximum force transducer nonlinearity and hysteresis should not exceed 0.5% and 0.3% of full-scale range, respectively.
- Extensometers must pass dynamic verification. Maximum test frequencies must be consistent with the verification. Extensometers must be calibrated to a relevant standard⁵. The class of extensometer must be appropriate to the measured gauge length. It is anticipated that both gauge and shoulder extensometers will be used within INCEFA-PLUS. Strains must be measured on the gauge length for tests in air or for tests on hollow specimens. Where shoulder extensometers are necessary (for example in some tests in water), they must be calibrated to ensure reliable determination of gauge extension from the measured shoulder strain.
- If material behavior permits (for example, aging effects do not hinder), control stability should be such that the strain maximum and minimum limits are repeatable over the test duration to within 1% of the range between maximum and minimum control limits.
- For PWR environments it is not necessary to electrically insulate specimens with respect to the autoclave. However, materials must be compatible with 304 stainless steel to prevent galvanic effects. For significantly different environments electrical insulation could be required.

A.5 TESTING IN AIR

- Tests in air are done at a specified temperature (e.g. ambient, 25 °C or 300 °C), humidity and atmospheric pressure (see Table A.1).
- Factors of importance are temperature and humidity.
- The common air-test environment for INCEFA-PLUS testing can be seen in Table A.2:

Field name	Unit	Symbol	Comment
Temperature (measure on the specimen)	°C	T	Ambient or 300 °C ± 3 °C
Humidity	%	RH	@ ambient < 30 % @ 300 °C, practically irrelevant
Pressure	bar	p	atmospheric

Table A.1 Air testing conditions.

Where different conditions are used to suit national programmes this must be clearly stated.

⁵ E.g. ASTM E83 - 10a Verification and classification of extensometer systems.

A.6 TESTING IN LWR ENVIRONMENT

- Because of the specificity of metal-environment interactions, it is essential that corrosion fatigue tests be conducted under environmental conditions which are closely controlled.
- Environmental factors of importance are electrode potential, temperature, solution composition, pH, conductivity, concentration of dissolved gases, flowrate and pressure.
- The common high-temperature water test environment for INCEFA-PLUS testing shall be:

Field name	Unit	Symbol	Comment
Temperature (measured close to the specimen)	°C	T	300 °C ± 3 °C
Pressure	bar	p	<ul style="list-style-type: none"> • large enough to avoid boiling in the test environment • mandatory reporting for hollow specimen 150 bar
Lithium content	ppm	Li	2 ppm ± 0.2 ppm as LiOH
Boron content	ppm	B	1000 ppm ± 100 ppm as boric acid
Dissolved hydrogen	cc(STP)H ₂ /kg (3)	H ₂	25 ± 5 cc(STP)H ₂ /kg (3)
pH @ T (2)	-	pH300	~6.95 (indication, from calculation)
pH @ 25 °C (2)	-	pH25	~6.41 (indication, from calculation)
Conductivity @25 °C (2)	µS/cm		~30 (indication, from calculation)
Anionic contamination (1)			< 10 ppb (any one specific, not total)
Oxygen			< 5 ppb
Cationic contamination (1)			< 100 ppb (any one specific, not total)
TOC (1) (total organics carbon)			< 200 ppb

⁽¹⁾ from grab samples

⁽²⁾ @T not used, @ 25 °C for monitoring changes

⁽³⁾ STP, standard temperature and pressure, 1 atm and 25 °C

Table A.2 LWR testing conditions.

Where different water chemistries are used to suit national programmes this must be clearly stated.

A.7 STRESSING

- Cyclic frequency (or strain rate) is of far greater importance when cycles to failure tests are conducted in light water reactor environments rather than in air where cyclic frequency usually has little, if any, effect. This sensitivity to frequency is due to time-dependent processes associated with the material-environment interaction. For INCEFA-PLUS testing the reference strain rate is fixed at 0.01%/s during the up-ramp. For details please refer to the appendix on hold times.

- Hold times might be of importance for both fatigue tests in air and in light water reactor environments. However, they might be of greater importance when cycles to failure tests are conducted in light water reactor environments. This increased sensitivity to hold times would be due to time-dependent processes associated with the material-environment interaction. For INCEFA-PLUS testing hold times are as given in APPENDIX – Hold times.
- Fatigue life is affected by the waveform and sequencing of the loading cycles. This is particularly so where the cycle incorporates hold times during which time-dependent processes may influence crack initiation and growth. For INCEFA-PLUS testing the waveform is essentially triangular or sawtooth with hold time possibilities at minimum, mean and maximum strain during or subsequent to an up-ramp. For INCEFA-PLUS this information is as given in APPENDIX – Hold times.
- The nature of strain-controlled fatigue imposes distinctive requirements on fatigue testing methods. In particular, cyclic total strain should be measured and cyclic plastic strain should be determined. Furthermore, either of these strains typically is used to establish cyclic limits. For INCEFA-PLUS testing total strain is controlled throughout the cycle during strain-controlled fatigue. In stress controlled fatigue the measured load, or its fixed conversion to stress, is usually controlled throughout the cycle.

A.8 PROCEDURE ⁶

- Specimens shall be identified by an indelible marking method, ideally by vibro-etching at both ends of the specimen away from alignment surfaces but not on the gauge length. When shoulder extensometers are used marking shall not be between gauge and shoulder.
- Specimens shall be stored after appropriate cleaning under appropriate conditions prior to testing in order to avoid corrosion which may influence the test results.
- The specimen (degreased immediately prior to insertion in the test machine and handled with care) shall be mounted in the specimen grips, every effort being made to prevent the occurrence of misalignment either due to rotation of the grips or to displacement in their axes of symmetry. No torsion shall be exerted on the specimen whilst mounting.
- Prior to the (environment-assisted) fatigue test it is strongly recommended to perform a full cycle in the elastic domain to obtain both the cold and the hot moduli. The limits for this linear cycle should be up to 0.03% gauge strain and down to -0.03% gauge strain. For INCEFA-PLUS' common material this equals to up to 50 MPa in tension and down to -50 MPa in compression.
- Environment-assisted fatigue test to start as soon as possible (in principle within 24 hours) after the start of exposure and achievement of 300 °C, subject to achievement of the required water chemistry. The exposure times at ambient and elevated temperature in the water environment prior to the start of test must be recorded. Air test should start after 24 hours at 300 °C.
- If oxygen levels cannot be verified then it is strongly recommended that the electrode potential be measured with a reference electrode appropriate for the application.

⁶ Testing partners should indicate in their test reporting items mentioned here and that are not satisfied.

- All tests must start in tension.
- Total axial strain amplitude is the default control parameter for INCEFA-PLUS. Where other methods are used this must be declared.
- Testing shall be continued until the specimen fails or until a predetermined load drop is achieved. N_x failure is defined as a $x\%$ load drop from a reference cycle (or from the flatter part of the maximum load versus number of cycles plot prior to it). For INCEFA-PLUS life reporting is set at N_{25} ($x=25$) and testing should be sufficiently long to determine it. It is desirable to stop at 50% load drop (as evaluated from the flatter part of the maximum load versus number of cycles plot prior to failure), to allow for fracture surface characterization.

A.9 TEST REPORT

The test report must include the information listed below. In those cases where the item is lengthy and available in other sources, e.g. in an accessible database or document, and marked with a star, a reference may be given. Note that MatDB at JRC will store the information in a systematic way.

- Specimen design and dimension *. A technical drawing of the specimen design and dimensions is to be supplied.
- Specimen orientation * and its location with respect to the parent product from which it was removed. Product size and form * shall also be identified.
- Specimen machining processes and surface condition *. The exact procedure of specimen preparation and handling should be clearly and carefully documented. The method of stress relief shall also be identified.
- Test material characterization * in terms of, for example, chemical composition, melting and fabrication process, heat treatment, microstructure, grain size, non-metallic inclusion content and mechanical properties (obtained at the appropriate temperature: tensile or compressive yield, ultimate tensile strength, percent elongation, percent reduction of area, Poisson's ratio and Young's modulus, true fracture strength, true fracture ductility, strain hardening exponent, strength coefficient and hardness). It also would be prudent to determine and record the surface residual stresses and the residual stress profile of at least one exemplary specimen.
- Description of the test machine *, including the method of verification of dynamic load monitoring and load alignment.
- Each testing partner needs to provide a description of its environmental chamber * and all equipment used for environmental monitoring and control *.
- Temperature. All temperatures throughout the gauge section shall be the specified temperature $\pm \max\{2\text{ }^\circ\text{C}, 1\%\}$, e.g. $300 \pm 3\text{ }^\circ\text{C}$. The actual temperature variability should be reported with the test results. If the temperature cannot be maintained within limits mentioned above, then temperature deviations should be reported.
- Environmental conditions. Environmental conditions include, but are not limited to, chemical composition, pH, conductivity and electrode potential. The actual variability

should be reported with the test results. If the environmental conditions cannot be maintained within the specified limits, then deviations should be reported.

- Test loading variables, including stress and strain amplitude and stress ratio, fatigue life (or cycles to end of test), cyclic frequency, strain rate(s), hold time and waveform for each specimen.
- Unintended transients in the environment or in the loading (including test interruptions) during testing, noting the nature and duration, are to be reported.
- Failure criterion. The definition of failure may vary with the ultimate use of the fatigue life information. In principle, failure is fracture, the rupture the specimen. However, in case of a force (stress) drop, it is acceptable to define failure in a manner related to the ability to sustain a tensile force (stress). Then, failure is defined as the point at which the maximum force (stress) decreases by a given percentage (25% for INCEFA-PLUS), because of a crack or cracks being present. The exact method (the preferred one is shown in Figure A.1) and the percentage drop should be documented. Record the total accumulated cycles up to failure (and fracture) by means of a cycle counter and check against a measure of elapsed time.

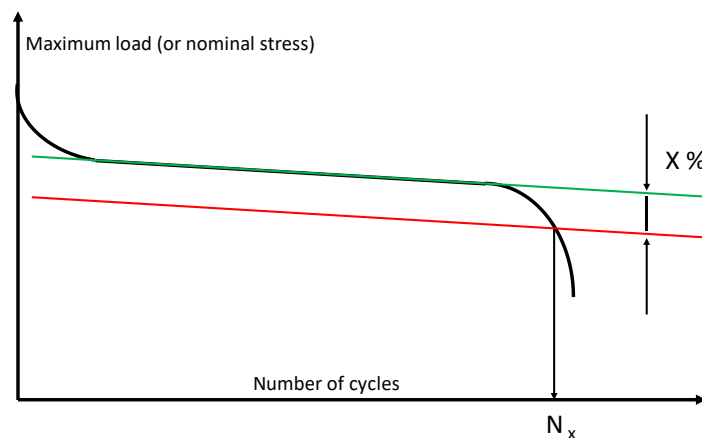


Figure A.1 Nominal stress x number of cycles.

- Original data should be reported to the greatest extent possible. Data reduction methods should be detailed along with assumptions.
- A plot of stress evolution⁷ against the cycle number. Suitable stress parameters depend on the test objective and include, but are not limited to, maximum stress, mean stress, minimum stress, stress range and/or stress amplitude. Please refer to the MatDB guide at the end of this document for guidance on the cyclic data to be uploaded to MatDB.
- A plot of strain evolution⁸ against the cycle number. Suitable strain parameters depend on the test objective and include, but are not limited to, maximum strain, mean strain, minimum strain, strain range and/or strain amplitude. Please refer to the MatDB guide at the end of this document for guidance on the cyclic data to be uploaded to MatDB.

⁷ Stress evolution is a response in strain-controlled testing.

⁸ Strain evolution is for monitoring test control in strain-controlled testing.

- A number of stress-strain hysteresis (see Figure A.2) loops should be recorded and plotted. Associated, the plastic strain range can be calculated. Please refer to the MatDB guide at the end of this document for guidance on the hysteresis data to be uploaded to MatDB.

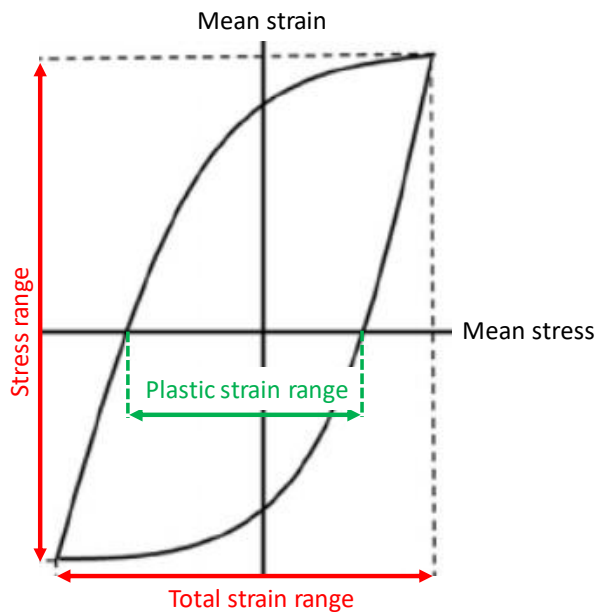


Figure A.2 Plastic strain range in hysteresis loops.

- Fatigue life data are to be plotted on a strain amplitude versus fatigue life diagram (strain-controlled tests) or stress amplitude versus fatigue life diagram (stress-controlled tests). It is conventional to plot fatigue life, N , in cycles logarithmically on the abscissa while strain (stress) is plotted arithmetically or logarithmically on the ordinate. For strain-controlled tests all data should be plotted in the diagram along with the following lines for stainless steel in air:

$$\text{NUREG/CR-6909 air curve} \quad \ln(N) = 6.891 - 1.920 \ln(\varepsilon_a - 0.112) \quad (\text{A.1})$$

$$\text{ASME Code air curve} (\leq 2008) \quad \ln N = 6.954 - 2.000 \ln(\varepsilon_a - 0.167) \quad (\text{A.2})$$

$$\text{JNES air curve} \quad \ln(N) = 6.861 - 2.188 \ln(\varepsilon_a - 0.110) \quad (\text{A.3})$$

For stress-controlled tests all data should be plotted in the diagram along with the following lines for stainless steel in air:

e.g. ASME B&PV code, Section III, Mandatory Appendix I, Table I-9.1M, Figure I-9.2.1M

- A post-mortem failure analysis should be performed to uncover any unusual causes of failure. Reporting the actual failure location is important. Inclusions, voids, defects, etc., that are not representative of the bulk material or its application may render fatigue life determination invalid. Also, consistent failures at one position may signal alignment problems or “knife-edge” failures caused by extensometer attachment. Of foremost importance is a fractographic examination of the two surfaces to determine any unusual

causes of failure that might invalidate the test results. Scanning electron microscopy and transmission electron microscopy of fracture replicas are two common methods used in such an investigation.

A.10 FATIGUE-RELATED TEST PARAMETERS

The testing parameters and cyclic data can be found in Table A.3 and A.4, respectively.

Field name	Unit	Symbol	Comment
Strain amplitude	%	$\varepsilon_a (= (\varepsilon_{\max} - \varepsilon_{\min}) / 2)$	0.3 & 0.6%
R-value	-	$R (= \varepsilon_{\max} / \varepsilon_{\min})$	-1 & tbd**
Strain rate, positive	%/s	$\dot{\varepsilon}^+$	0.01%/s
Strain rate, negative	%/s	$\dot{\varepsilon}^-$	e.g. -0.1%/s
Hold time @ maximum	h	t_{hold}^{\max}	tbd*
Hold time @ minimum	h	t_{hold}^{\min}	tbd*
Hold time @ mean(up)	h	t_{hold}^{mean+}	tbd*
Hold time @ mean(down)	h	t_{hold}^{mean-}	tbd*
Temperature during hold	°C	T_{hold}	300 °C
Number of cycles between holds	-	N_{hold}	$\varepsilon_a = 0.6\% \rightarrow 5000$ $\varepsilon_a = 0.3\% \rightarrow 20000$

* see Hold times section

** see also Mean strain/stress section

Table A.3 Testing parameters.

Field name	Unit	Symbol	Comment
Cycle number	-	N	
Strain @ maximum	%	$\varepsilon_{\max} = \varepsilon_t^+$	primary input, per cycle
Strain @ minimum	%	$\varepsilon_{\min} = \varepsilon_t^-$	primary input, per cycle
Stress @ maximum	MPa	σ_{\max}	primary input, per cycle
Stress @ minimum	MPa	σ_{\min}	primary input, per cycle
Strain range	%	$\Delta\varepsilon = \varepsilon_{\max} - \varepsilon_{\min}$	
Mean strain	%	$\varepsilon_{mean} = (\varepsilon_{\max} + \varepsilon_{\min}) / 2$	
Inelastic strain @ maximum	%	$\varepsilon_i^+ = \varepsilon_{\max} - \sigma_{\max} / E$	
Inelastic strain @ minimum	%	$\varepsilon_i^- = \varepsilon_{\min} - \sigma_{\min} / E$	
Inelastic strain range	%	$\Delta\varepsilon_i = \varepsilon_i^+ - \varepsilon_i^-$	
Elastic strain @ maximum	%	$\varepsilon_e^+ = \sigma_{\max} / E$	
Elastic strain @ minimum	%	$\varepsilon_e^- = \sigma_{\min} / E$	
Elastic strain range	%	$\Delta\varepsilon_e = \varepsilon_e^+ - \varepsilon_e^-$	

Stress range	MPa	$\Delta\sigma = \sigma_{\max} - \sigma_{\min}$	
Mean stress	MPa	$\sigma_{mean} = (\sigma_{\max} + \sigma_{\min}) / 2$	
R-value	-	$R = \varepsilon_{\min} / \varepsilon_{\max}$	

Note: Gray shaded rows are mandatory.

Non shaded rows could/should be calculated by MatDB database.

Table A.4 Cyclic data.

A.11 HYSTERESIS DATA

Hysteresis data can be found in Table A.5.

Field name	Unit	Symbol	Comment
Cycle number	-	j	
Strain	%	ε_j	detailed input, for cycle j
Stress	MPa	σ_j	detailed input, for cycle j
Young's modulus upon loading	MPa	$E_{ct} = (\partial\sigma/\partial\varepsilon)_{linear\ portion}$	
Young's modulus upon unloading	MPa	$E_{cc} = (\partial\sigma/\partial\varepsilon)_{linear\ portion}$	
Hysteresis area	MPa	$A_h = \int_{cycle} \sigma d\varepsilon$	

Note: Gray shaded rows are mandatory.

Non shaded rows could/should be calculated by MatDB database.

Table A.5 Hysteresis data.

A.12 HOLD TIMES

Below the hold time parameters for Phase I testing are posted:

- Strain-control.
- Waveform = saw tooth.
 - Positive strain rate 0.01%/s (LWR) or 0.1%/s (air).
 - Negative strain rate -0.1%/s (if it helps with test control, slower strain rates can be used).
- Strain amplitude = 0.3% and 0.6%.
- Cycling @ 300 °C.
- Hold temperature = 300 °C.
- Hold time = 72 hours.
- Hold frequency (see Table A.6).

ϵ_a (%)	Air environment		LWR environment	
	CR-6909 predicted life	3 holds	CR-6909 predicted life*	3 holds
0.3	24341	6000, 12000 and 18000	4897	1200, 2400 and 3600
0.6	3899	1000, 2000 and 3000	784	200, 400 and 600

* $F_{en} = 4.97$ (T = 300 °C, strain rate = 0.01%/s)

Table A.6 Hold frequency.

- Hold position = during positive strain rate (see Table A.7).
- Hold strain = mean strain during cycle (0%):

ϵ_a (%)	ϵ_{range} (%)	Hold ϵ (%)
0.6	-0.6 to +0.6	0
0.3	-0.3 to +0.3	0

Table A.7 Hold position.

A.13 MEAN STRAIN/STRESS

The mean strain/stress test parameters for Phase I testing can be seen in Table A.8.

The fatigue tests related to the mean strain/stress effect will be performed under strain control with mean strain for Phase I testing.

- Strain amplitude of 0.3% and 0.6%.
- Mean strain during cycling (0% or 0.5%):

ϵ_a (%)	Mean ϵ (%) for cycling	ϵ_{range} (%)
0.6	0	-0.6 to +0.6
0.6	0.5	-0.1 to +1.1
0.3	0	-0.3 to +0.3
0.3	0.5	+0.2 to +0.8

Table A.8 Mean strain/stress parameters.

A.14 TEST MATRIX PHASE II

Please note that the values -1, 0 and +1 depend on the test variable:

For strain amplitude/range:

‘-1’ = 0.3% strain amplitude, 0.6% strain range.

‘1’ = 0.6% strain amplitude, 1.2% strain range.

For hold time:

‘-1’ = no hold.

'1' = hold.

For surface roughness:

'-1' = smooth, polished/honed surface.

'0' = Phase I rough, ground surface ($R_t \sim 20 \mu\text{m}$).

'1' = Phase II very rough, ground surface ($R_t > 40 \mu\text{m}$).

REFERENCES

- [A.1] M. Vankeerberghen, Testing Protocol for INCEFA-PLUS; INCEFA-PLUS Internal Report, (2017).
- [A.2] M. Vankeerberghen, M. Bruchhausen, Information Pack INCEFA+ Phase II; INCEFA-PLUS Internal Report, 2018.
- [A.3] ASTM, Standard Test Method for Strain-Controlled Fatigue Testing, E606/E606M-12. (2004). doi:10.1520/E0606-04E01.Copyright.
- [A.4] ISO, Metallic materials - Fatigue testing - Axial-strain-controlled method; ISO/FDIS 12106:2016(E), 2016 (2016).
- [A.5] ISO, Corrosion of metals and alloys — Corrosion fatigue testing — Part 1: Cycles to failure testing, 11782-1. (1998).
- [A.6] BS, Metallic Materials. Constant Amplitude Strain Controlled Axial Fatigue. Method of Test, 7270. (2006).
- [A.7] AFNOR, Produit métalliques - Pratique des essais de fatigue oligocyclique, A03-403. (1990).
- [A.8] J.-C. Le Roux, Specimen Manufacturing Instructions (D2.1); INCEFA-PLUS Internal Report, 2016.

ANNEX B REVIEW SHEET OF EXPERT PANEL

This annex is based on an INCEFA-PLUS internal report “Expert Panel Tool Proposed” [B.1] developed by Román Cicero.

The Expert Panel reviews datasets that are validated in MatDB [B.2] by using a template whose different pages are shown below.

B.1 EXPERT PANEL TOOL

INCEFA+ Test Data Summary Report



MatDB TEST REFERENCE
 Completeness Value

TEST DETAILS

Conditions From Test Matrix (Nominal Values)		Actual Test Conditions	
Lab		Mean Lab Temp (°C)	
Environment		Mean Test/Coolant T (°C)	
Specimen Type		Specimen Diameter (mm)	
Material		R _a (µm)	
Surface Finish		R _t (µm)	
Mean Strain (%)		Mean Strain (%)	
Δε, nominal (%)		Δε, average (%)	
Hold Times		Hold Durations (s)	
Strain Waveform		Hold Positions (cycles)	
ε̇, rising (%/s)		ε̇, rising (%/s)	
ε̇, falling (%/s)		ε̇, falling (%/s)	

Nominal Specimen Gauge Length (mm)	
Extensometer Gauge Length (mm)	

Cold Modulus (GPa)	
Hot Modulus (GPa)	

Chemistry		
	first cycle	last cycle
pH		
pressure (bar)		
DH (cc(STP)H ₂ /kg)		
DO (cc(STP)O ₂ /kg)		
conductivity (uS/cm)		

Test Comments

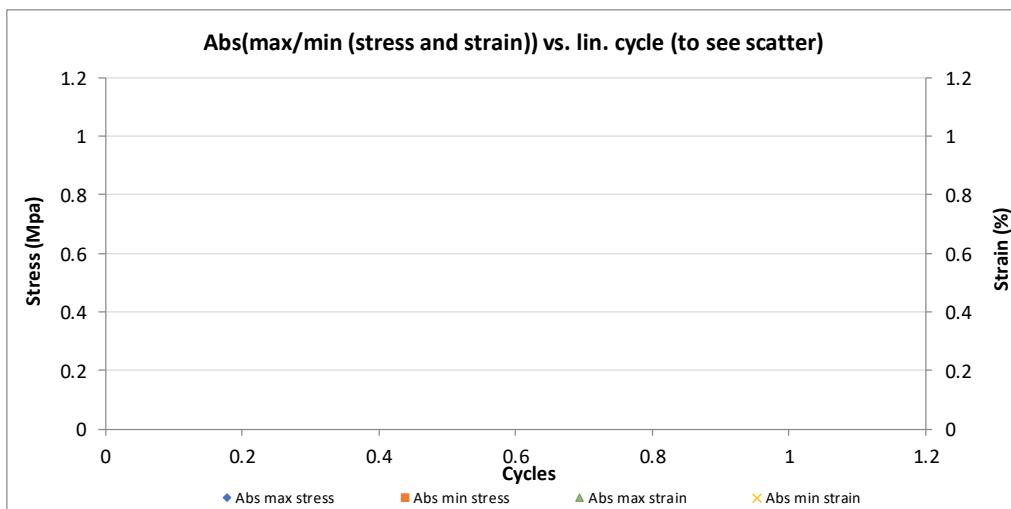
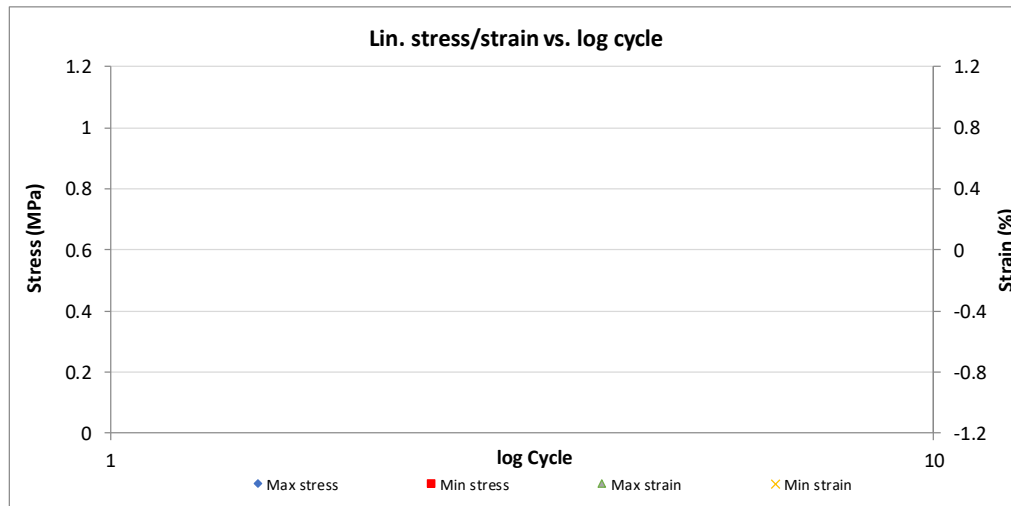
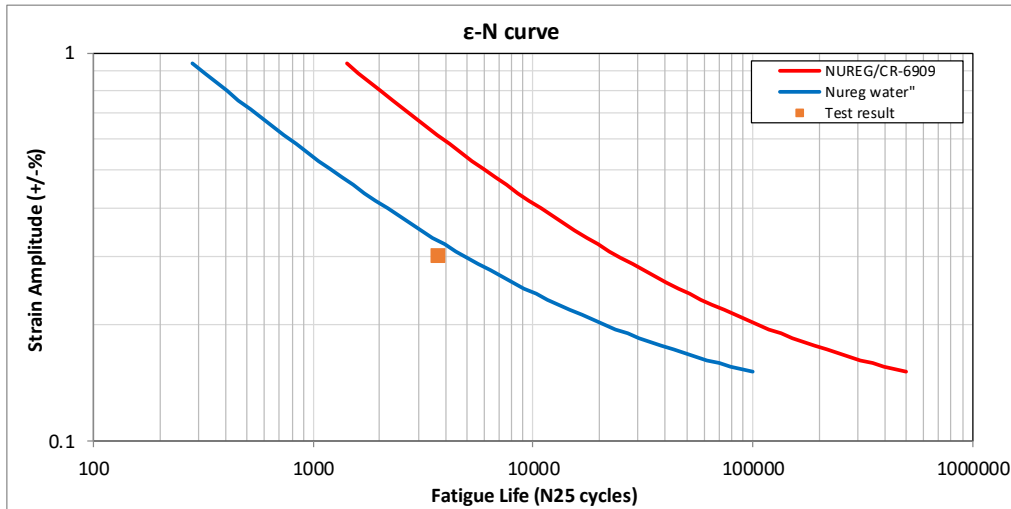
--	--

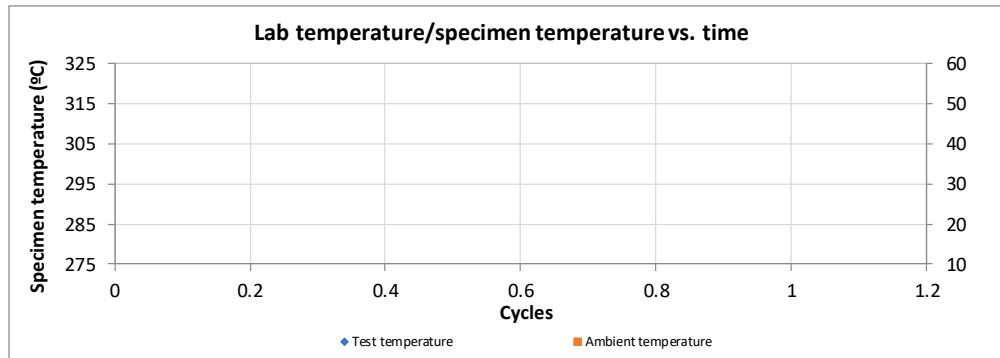
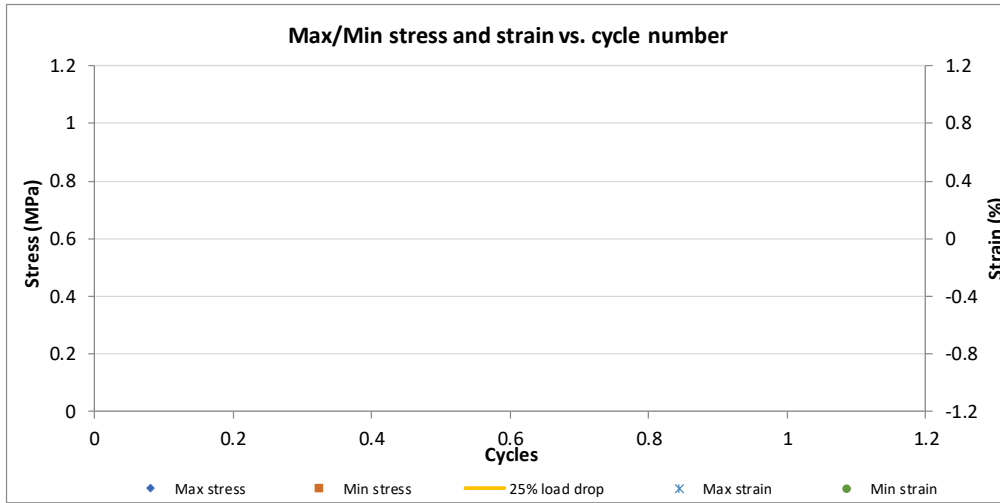
TEST RESULTS

Failure Definition	
25% load drop (cycle)	615
N25 ÷ 2	

Failure Position

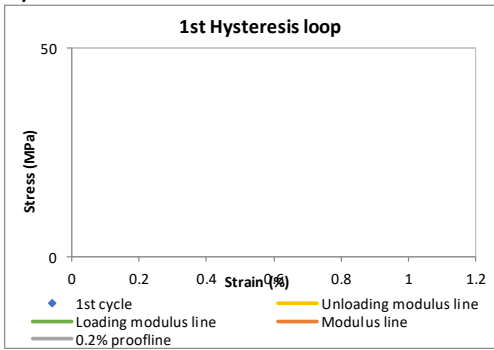
Outside measured gauge length



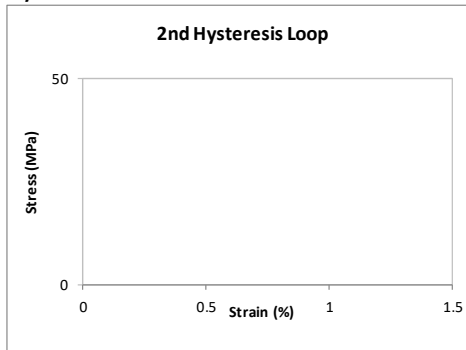


HYSTERESIS LOOPS

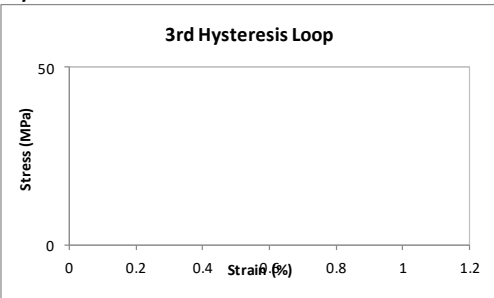
Cycle 1



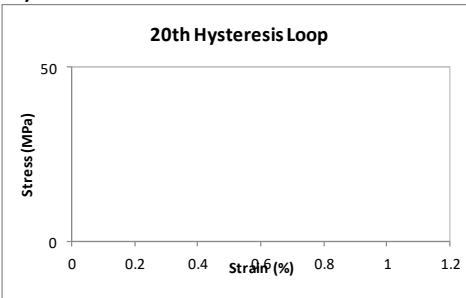
Cycle 2



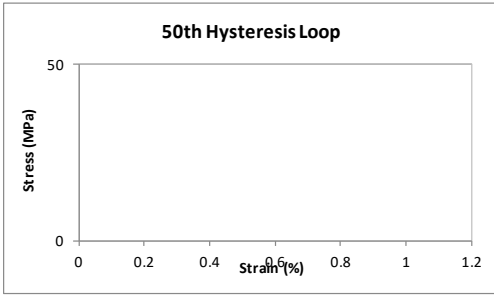
Cycle 3



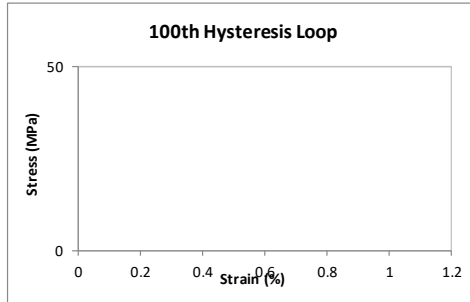
Cycle 20



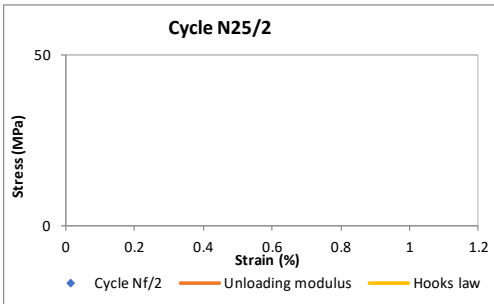
Cycle 50



Cycle 100

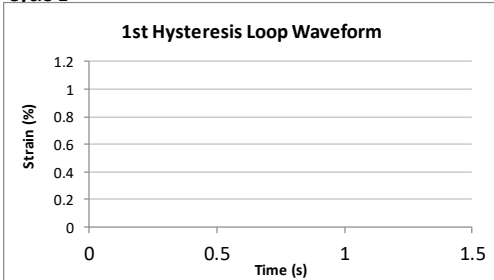


N25 ÷ 2

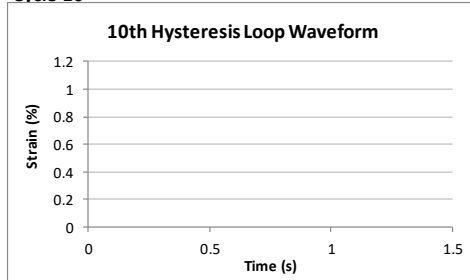


STRAIN WAVEFORMS

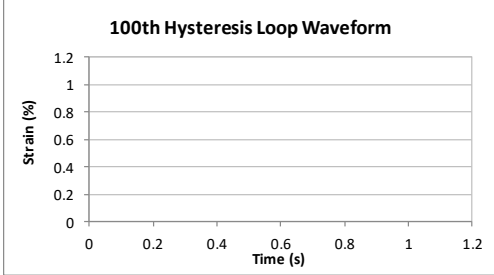
Cycle 1



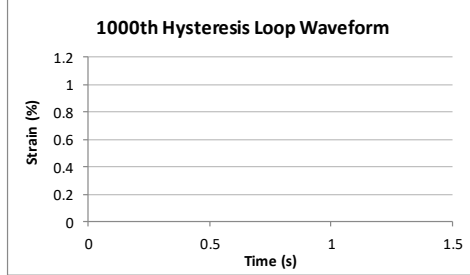
Cycle 10



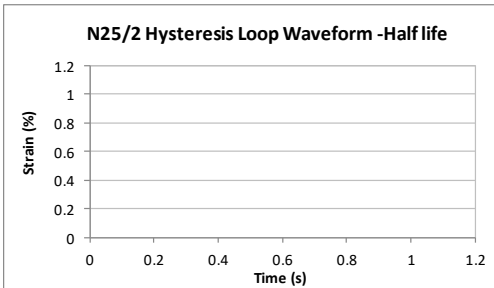
Cycle 100



Cycle 1,000

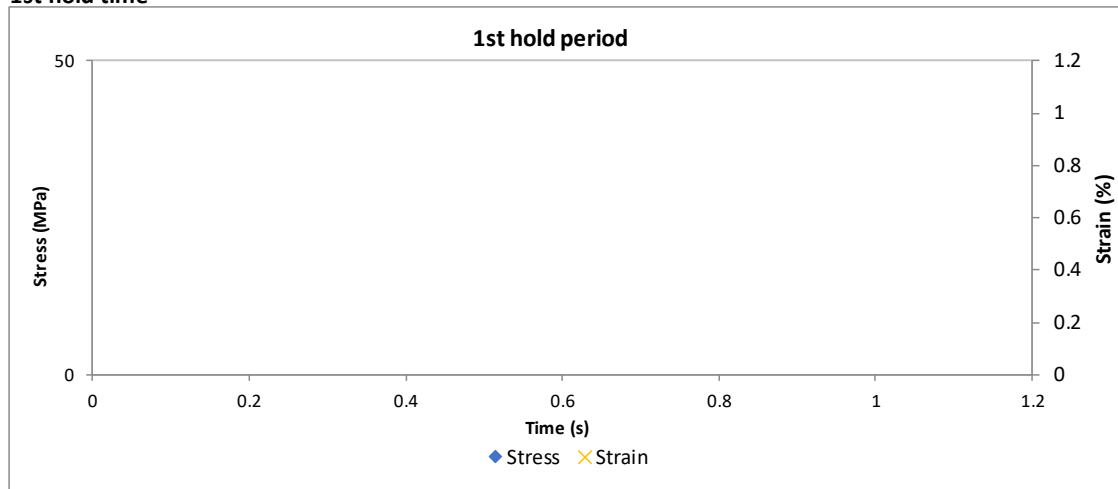


N25 ÷ 2

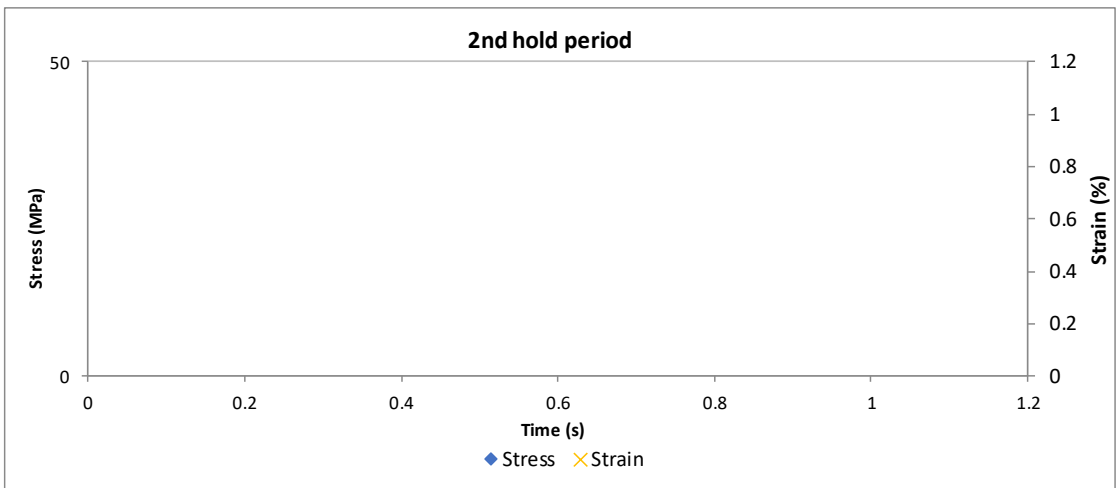


HOLD TIME CYCLES

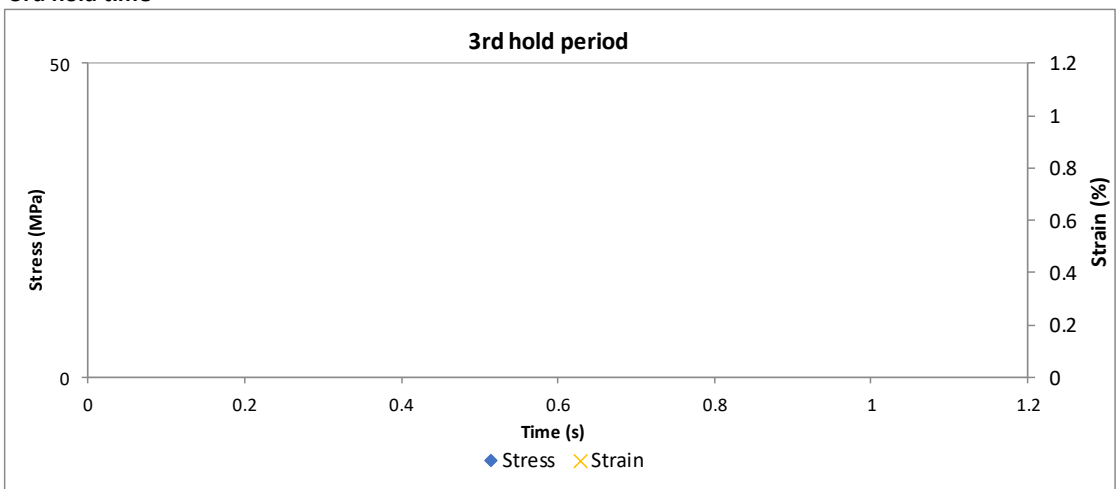
1st hold time



2nd hold time



3rd hold time



REFERENCES

- [B.1] R. Cicero, Expert Panel Tool Proposal; INCEFA-PLUS Internal Report, 2017.
- [B.2] Joint Research Center, ODIN Portal - MatDB, (2020). <https://odin.jrc.ec.europa.eu>.

This page intentionally left blank.

ANNEX C TEST MATRIX

This annex is based on successive internal reports [C.1–C.3] which define test matrixes for the three experimental phases of the project.

C.1 TEST MATRIX PHASE I

The text matrix for Phase I (both tests in air and in water) can be found in Table C.1.

Lab	Environment	Specimen Type	Material	Mean strain	Strain amplitude	Hold time	Surface Roughness
228	air @ 300°C	full	304L(EDF)	1	-1	1	-1
228	air @ 300°C	full	304L(EDF)	1	1	-1	1
228	air @ 300°C	full	304L(EDF)	-1	-1	-1	-1
228	air @ 300°C	full	304L(EDF)	-1	-1	1	1
228	air @ 300°C	full	304L (RR)	1	1	1	1
228	air @ 300°C	full	304L (RR)	-1	-1	-1	-1
231	air @ 300°C	full	304L(EDF)	1	-1	-1	-1
231	air @ 300°C	full	304L(EDF)	-1	1	-1	-1
231	air @ 300°C	full	304L(EDF)	1	-1	1	-1
226	air @ 300°C	full	304L(EDF)	1	1	-1	-1
226	air @ 300°C	full	304L(EDF)	-1	1	-1	-1
226	air @ 300°C	full	304L(EDF)	-1	1	-1	-1
226	air @ 300°C	full	304L(EDF)	1	1	-1	1
226	air @ 300°C	full	304L(EDF)	-1	-1	-1	1
224	air @ 300°C	full	304L(EDF)	-1	-1	1	1
224	air @ 300°C	full	304L(EDF)	-1	1	1	1
224	air @ 300°C	full	304L(EDF)	-1	1	-1	-1
225	air @ 300°C	full	304L(EDF)	-1	1	1	1
225	air @ 300°C	full	304L(EDF)	1	-1	-1	-1
225	air @ 300°C	full	304L(EDF)	1	-1	1	1
225	air @ 300°C	full	304L(EDF)	1	-1	-1	1
225	air @ 300°C	full	304L(EDF)	1	1	1	-1
225	air @ 300°C	full	304L(EDF)	1	1	-1	-1
225	air @ 300°C	full	304L(EDF)	-1	1	-1	1
221 >> 227	air @ 300°C	full	304L(EDF)	-1	-1	1	-1
221	air @ 300°C	full	304L(EDF)	1	1	-1	1
221 >> 227	air @ 300°C	full	304L(EDF)	1	-1	1	1
223	air @ 300°C	full	304L(EDF)	1	1	1	-1
223	air @ 300°C	full	304L(EDF)	-1	-1	-1	1
223	air @ 300°C	full	304L(EDF)	-1	1	1	1
223	air @ 300°C	full	304L(EDF)	-1	1	1	-1
223	air @ 300°C	full	304L(EDF)	1	-1	-1	1
223 (air)	air @ 300°C	full	304L(EDF)	-1	-1	1	-1
223 (air)	air @ 300°C	full	304L(EDF)	1	1	1	1
228	PWR @ 300°C	full	304L(EDF)	-1	1	-1	1
228	PWR @ 300°C	full	304L(EDF)	1	1	1	1
228	PWR @ 300°C	full	304L (RR)	1	-1	-1	1

228	PWR @ 300°C	full	304L (RR)	1	1	-1	-1
228	PWR @ 300°C	hollow	304L(EDF)	-1	1	1	-1
228	PWR @ 300°C	hollow	304L (RR)	1	-1	1	-1
230	PWR @ 300°C	full	304L(EDF)	-1	-1	1	-1
230	PWR @ 300°C	full	304L(EDF)	1	1	-1	1
230	PWR @ 300°C	full	304L(EDF)	-1	2	-1	1
230	PWR @ 300°C	full	304L(EDF)	-1	-1	-1	1
230	PWR @ 300°C	full	304L(EDF)	1	1	1	1
230	PWR @ 300°C	full	304L(EDF)	1	1	-1	1
230	PWR @ 300°C	full	304L(EDF)	1	2	1	1
230	PWR @ 300°C	full	304L(EDF)	1	1	-1	1
220	PWR @ 300°C	full	304L(EDF)	1	-1	-1	1
220	PWR @ 300°C	full	304L(EDF)	-1	-1	1	1
220	PWR @ 300°C	full	304L(EDF)	1	-1	-1	-1
220	PWR @ 300°C	full	304L(EDF)	1	-1	1	-1
220	PWR @ 300°C	full	304L(EDF)	-1	1	-1	1
220	PWR @ 300°C	full	304L(EDF)	1	1	1	1
220	PWR @ 300°C	full	304L(EDF)	-1	1	-1	1
220	PWR @ 300°C	full	304L(EDF)	-1	1	1	-1
EDF	PWR @ 300°C	hollow	304L(EDF)	1	1	1	-1
EDF	PWR @ 300°C	hollow	304L(EDF)	1	-1	-1	-1
EDF	PWR @ 300°C	hollow	304L(EDF)	-1	-1	-1	-1
229	PWR @ 300°C	full	304L(EDF)	-1	-1	1	1
229	PWR @ 300°C	full	A321 (UJV)	1	-1	-1	1
229	PWR @ 300°C	full	A321 (UJV)	-1	1	1	1
229	PWR @ 300°C	full	A321 (UJV)	-1	-1	1	-1
229	PWR @ 300°C	full	A321 (UJV)	-1	1	-1	-1
229	PWR @ 300°C	full	A321 (UJV)	1	1	1	-1
225	PWR @ 300°C	hollow	304L(EDF)	1	-1	1	-1
225	PWR @ 300°C	hollow	304L(EDF)	-1	-1	-1	-1
225	PWR @ 300°C	hollow	304L(EDF)	-1	1	1	-1
225	PWR @ 300°C	hollow	304L(EDF)	1	1	-1	-1
225	PWR @ 300°C	hollow	304L(EDF)	-1	-1	-1	-1
225	PWR @ 300°C	hollow	304L(EDF)	-1	1	-1	-1
225	PWR @ 300°C	hollow	304L(EDF)	1	1	-1	-1
221	PWR @ 300°C	full	304L(EDF)	-1	-1	-1	1
221	PWR @ 300°C	full	304L(EDF)	-1	-1	-1	-1
221	PWR @ 300°C	full	304L(EDF)	1	-1	-1	1
221	PWR @ 300°C	full	304L(EDF)	1	-1	1	1
221	PWR @ 300°C	full	304L(EDF)	1	-1	1	1

Table C.1 Test matrix for Phase I.

The conversion for the test parameters can be seen in Table C.2.

Factor	Low value (-1)	High value (+1)	High value (+2)
Mean strain	0%	0.5%	-
Strain amplitude	0.3%	0.6%	1.2%
Hold time	No	Yes	-
Surface roughness	smooth	rough	-

Table C.2 Conversion table for the low and high values of the test parameters.

C.2 TEST MATRIX PHASE II

The test matrix for Phase II for tests in air and in water can be found in Table C.3 and Table C.4, respectively.

Lab	Environment	Specimen type	Material	Strain amplitude	Surface roughness	Hold time
223	Air @ 300 °C	solid	304L(EDF)	-1	1	1
223	Air @ 300 °C	solid	304L(EDF)	1	1	1
223	Air @ 300 °C	solid	304L(EDF)	-1	1	-1
223	Air @ 300 °C	solid	304L(EDF)	-1	-1	-1
223	Air @ 300 °C	solid	304L(EDF)	1	1	-1
231	Air @ 300 °C	solid	304L(EDF)	1	1	1
231	Air @ 300 °C	solid	304L(EDF)	-1	1	1
231	Air @ 300 °C	solid	304L(EDF)	1	1	1
231	Air @ 300 °C	solid	304L(EDF)	1	1	-1
231	Air @ 300 °C	solid	304L(EDF)	1	1	-1
231	Air @ 300 °C	solid	304L(EDF)	1	1	-1
225	Air @ 300 °C	solid	304L(EDF)	1	-1	-1
225	Air @ 300 °C	solid	304L(EDF)	1	1	1
226	Air @ 300 °C	solid	304L(EDF)	1	-1	-1
226	Air @ 300 °C	solid	304L(EDF)	-1	-1	1
226	Air @ 300 °C	solid	304L(EDF)	1	-1	-1
226	Air @ 300 °C	solid	304L(EDF)	-1	-1	1
226	Air @ 300 °C	solid	304L(EDF)	-1	-1	1
228	Air @ 300 °C	solid	304L(EDF)	-1	-1	-1
228	Air @ 300 °C	solid	304L(EDF)	1	-1	1
228 >> 227	Air @ 300 °C	solid	304L(EDF)	-1	1	-1
228 >> 227	Air @ 300 °C	solid	304L(EDF)	1	0	1
228	Air @ 300 °C	solid	304L(EDF)	-1	0	-1
228 >> 227	Air @ 300 °C	solid	304L(EDF)	-1	-1	-1
224	Air @ 300 °C	solid	304L(EDF)	1	-1	1

Table C.3 Air test matrix for Phase II.

Lab	Environment	Specimen type	Material	Strain amplitude	Surface roughness	Hold time
220	PWR @ 300 °C	solid	304L(EDF)	1	1	1
220	PWR @ 300 °C	solid	304L(EDF)	1	1	-1
220	PWR @ 300 °C	solid	304L(EDF)	1	1	-1
220	PWR @ 300 °C	solid	304L(EDF)	1	1	1
220	PWR @ 300 °C	solid	304L(EDF)	1	1	-1
220	PWR @ 300 °C	solid	304L(EDF)	-1	-1	1
220	PWR @ 300 °C	solid	304L(EDF)	-1	-1	-1
220	PWR @ 300 °C	solid	304L(EDF)	-1	-1	-1
220	PWR @ 300 °C	solid	304L(EDF)	1	1	1
220	PWR @ 300 °C	solid	304L(EDF)	1	1	-1
220	PWR @ 300 °C	solid	304L(EDF)	1	-1	1
220	PWR @ 300 °C	solid	304L(EDF)	1	-1	1
220	PWR @ 300 °C	solid	304L(EDF)	-1	1	-1
220	PWR @ 300 °C	solid	304L(EDF)	1	-1	-1
220	PWR @ 300 °C	solid	304L(EDF)	1	-1	-1
229	PWR @ 300 °C	solid	304L(EDF)	1	0	1
229	PWR @ 300 °C	solid	A321 (UJV)	1	0	1
229	PWR @ 300 °C	solid	A321 (UJV)	-1	-1	-1
229	PWR @ 300 °C	solid	A321 (UJV)	-1	-1	-1
229	PWR @ 300 °C	solid	A321 (UJV)	1	1	1
229	PWR @ 300 °C	solid	A321 (UJV)	1	1	1
229	PWR @ 300 °C	solid	A321 (UJV)	-1	1	1
229	PWR @ 300 °C	solid	A321 (UJV)	1	1	-1
230	PWR @ 300 °C	solid	304L(EDF)	1	0	-1
230	PWR @ 300 °C	solid	304L(EDF)	1	-1	1
230	PWR @ 300 °C	solid	304L(EDF)	1	-1	-1
230	PWR @ 300 °C	solid	304L(EDF)	1	-1	1
230	PWR @ 300 °C	solid	304L(EDF)	1	0	-1
230	PWR @ 300 °C	solid	304L(EDF)	-1	-1	-1
230	PWR @ 300 °C	solid	304L(EDF)	-1	-1	-1
230	PWR @ 300 °C	solid	304L(EDF)	1	-1	-1
230	PWR @ 300 °C	solid	304L(EDF)	1	-1	-1
230	PWR @ 300 °C	solid	304L(EDF)	-1	0	-1
227 >> 220	PWR @ 300 °C	solid	304L(EDF)	-1	1	1
227 >> 228	PWR @ 300 °C	solid	304L(EDF)	-1	1	1
227 >> 229	PWR @ 300 °C	solid	304L(EDF)	-1	0	1
227 >> 229	PWR @ 300 °C	solid	A321 (UJV)	-1	1	-1
221	PWR @ 300 °C	solid	304L(EDF)	1	0	1
221	PWR @ 300 °C	solid	304L(EDF)	1	-1	-1
221	PWR @ 300 °C	solid	304L(EDF)	1	-1	-1
221	PWR @ 300 °C	solid	304L(EDF)	1	-1	-1
221	PWR @ 300 °C	solid	304L(EDF)	-1	-1	1
221	PWR @ 300 °C	solid	304L(EDF)	-1	-1	1

221	PWR @ 300 °C	solid	304L(EDF)	-1	0	1
221	PWR @ 300 °C	solid	304L(EDF)	1	0	-1
221	PWR @ 300 °C	solid	304L(EDF)	-1	-1	1
221	PWR @ 300 °C	solid	304L(EDF)	-1	-1	-1
221	PWR @ 300 °C	solid	304L(EDF)	-1	0	-1
221	PWR @ 300 °C	solid	304L(EDF)	-1	-1	-1
225	PWR @ 300 °C	hollow	304L(EDF)	1	-1	-1
225	PWR @ 300 °C	hollow	304L(EDF)	-1	-1	-1
224	PWR @ 300 °C	hollow	304L(EDF)	1	-1	1
228	PWR @ 300 °C	solid	304L(EDF)	-1	1	1
228	PWR @ 300 °C	solid	304L(EDF)	-1	1	-1
228	PWR @ 300 °C	solid	304L(EDF)	1	1	1
228	PWR @ 300 °C	solid	304L(EDF)	-1	1	1
228	PWR @ 300 °C	hollow	304L(EDF)	-1	-1	1
228	PWR @ 300 °C	hollow	304L(EDF)	1	-1	-1
231	PWR @ 300 °C	solid	304L(EDF)	-1	-1	-1
231	PWR @ 300 °C	solid	304L(EDF)	1	-1	-1
231	PWR @ 300 °C	solid	304L(EDF)	-1	1	-1
231	PWR @ 300 °C	solid	304L(EDF)	1	1	-1

Table C.4 LWR test matrix Phase II.

The conversion for the test parameters can be seen in Table C.5.

Factor	Low value (-1)	High value (0)	High value (+1)
Strain amplitude	0.3%	-	0.6%
Surface roughness	smooth, polished/honed surface	rough, ground surface (Rt ~ 20µm)	very rough, ground surface (Rt > 40µm)
Hold time	No	-	Yes

Table C.5 Conversion table for the low and high values of the test parameters.

The part of the test program campaign on mean stress in strain control is composed of 9 tests (plus possibly a few more if needed for determining the stress amplitude for the reference test), according to Table C.6.

Test	Lab	Environment	Specimen type	Material	Mean stress	Strain amplitude	Stress amplitude	Surface roughness
1	224	Air @ 300 °C	full	304L (EDF)	0 MPa	0.20%	-	polished
2	224	Air @ 300 °C	full	304L (EDF)	50 MPa	0.20%	-	polished
3	224	PWR @ 300 °C	hollow	304L (EDF)	0 MPa	0.20%	-	honed
4	224	PWR @ 300 °C	hollow	304L (EDF)	50 MPa	0.20%	-	honed
5	225	Air @ 300 °C	full	304L (EDF)	0 MPa	(0.36%)	169 MPa	polished
6	225	Air @ 300 °C	full	304L (EDF)	0 MPa	(0.15%)	150 MPa	polished
7	225	Air @ 300 °C	full	304L (EDF)	50 MPa	(0.11%)	150 MPa	polished
8	225	PWR @ 300 °C	hollow	304L (EDF)	0 MPa	(0.15%)	150 MPa	honed
9	225	PWR @ 300 °C	hollow	304L (EDF)	50 MPa	(0.10%)	150 MPa	honed

Table C.6 - Test matrix for the campaign on mean stress in strain control in Phase II

C.3 TEST MATRIX PHASE III

The text matrix for Phase III for tests in air can be found in Table C.7 and Table C.8.

Lab	Environment	Specimen type	Material	Strain amplitude	Surface roughness	Strain rate
227	Air @ 230 °C	solid	304L(EDF)	-1	-1	-1
227	Air @ 300 °C	solid	304L(EDF)	-1	-1	-1
227	Air @ 300 °C	solid	304L(EDF)	-1	1	-1
227	Air @ 230 °C	solid	304L(EDF)	-1	1	-1
226	Air @ 230 °C	solid	304L(EDF)	-1	-1	-1
226	Air @ 230 °C	solid	304L(EDF)	-1	-1	-1
226	Air @ 230 °C	solid	304L(EDF)	-1	1	-1
226	Air @ 230 °C	solid	304L(EDF)	-1	1	-1
226	Air @ 300 °C	solid	304L(EDF)	-1	-1	1
231	Air @ 300 °C	solid	304L(EDF)	-1	1	1
231	Air @ 300 °C	solid	304L(EDF)	1	1	1
231	Air @ 300 °C	solid	304L(EDF)	1	-1	1
231	Air @ 300 °C	solid	304L(EDF)	-1	-1	1
231	Air @ 300 °C	solid	304L(EDF)	1	-1	1
231	Air @ 300 °C	solid	304L(EDF)	1	1	1

Table C.7 Air test matrix for Phase III.

Lab	Environment	Specimen type	Material	Strain amplitude	Surface roughness	Strain rate	Holds
223	Air @ RT °C	solid	304L(EDF)	0.2	-1	0.01/0.1	Yes
223	Air @ 300 °C	solid	304L(EDF)	0.2	-1	0.01/0.1	Yes
223	Air @ RT °C	solid	304L(EDF)	0.2	-1	0.01/0.1	Yes
223	Air @ 230 °C	solid	304L(EDF)	0.2	-1	0.01/0.1	Yes

Table C.8 Air test matrix for Phase III.

The conversion for the test parameters can be seen in Table C.9.

Factor	Low value (-1)	High value (+1)
Strain amplitude	0.3%	0.6%
Surface roughness	Polished	Rough
Strain rate	0.01	0.1

Table C.9 Conversion table for the low and high values of the test parameters.

Table C.10 gathers tests performed at reduced temperature (230 °C) and Table C.11 shows the tests at increased strain rate (0,1%/s).

Lab	Environment	Specimen type	Material	Strain amplitude	Surface Roughness
221	PWR @ 230 °C	solid	304L (EDF)	0.3%	smooth
221	PWR @ 230 °C	solid	304L (EDF)	0.3%	smooth
221	PWR @ 230 °C	solid	304L (EDF)	0.3%	smooth

221	PWR @ 230 °C	solid	304L (EDF)	0.3%	smooth
221	PWR @ 230 °C	solid	304L (EDF)	0.3%	rough
221	PWR @ 230 °C	solid	304L (EDF)	0.3%	rough
221	PWR @ 230 °C	solid	304L (EDF)	0.3%	rough
221	PWR @ 230 °C	solid	304L (EDF)	0.3%	rough

Table C.10 Test matrix for reduced F_{en} at reduced temperature (fixed strain rate 0.01%/s for PWR tests).

Lab	Environment	Specimen type	Material	Strain amplitude	Surface Roughness
220	PWR @ 300 °C	solid	304L (EDF)	1.2%	smooth
220	PWR @ 300 °C	solid	304L (EDF)	1.2%	rough
220	PWR @ 300 °C	solid	304L (EDF)	1.2%	smooth
220	PWR @ 300 °C	solid	304L (EDF)	0.6%	smooth
220	PWR @ 300 °C	solid	304L (EDF)	1.2%	rough
220	PWR @ 300 °C	solid	304L (EDF)	0.6%	rough
220	PWR @ 300 °C	solid	304L (EDF)	1.2%	smooth
220	PWR @ 300 °C	solid	304L (EDF)	1.2%	rough
220	PWR @ 300 °C	solid	304L (EDF)	0.6%	rough
220	PWR @ 300 °C	solid	304L (EDF)	0.6%	rough
220	PWR @ 300 °C	solid	304L (EDF)	0.6%	smooth
220	PWR @ 300 °C	solid	304L (EDF)	1.2%	rough
220	PWR @ 300 °C	solid	304L (EDF)	0.6%	smooth
220	PWR @ 300 °C	solid	304L (EDF)	0.6%	smooth
229	PWR @ 300 °C	solid	304L (EDF)	1.2%	rough
230	PWR @ 300 °C	solid	304L (EDF)	1.2%	smooth
230	PWR @ 300 °C	solid	304L (EDF)	1.2%	smooth
230	PWR @ 300 °C	solid	304L (EDF)	0.6%	rough
230	PWR @ 300 °C	solid	304L (EDF)	0.6%	rough
228	PWR @ 300 °C	solid	304L (EDF)	0.6%	smooth
228	PWR @ 300 °C	solid	304L (EDF)	1.2%	rough
228	PWR @ 300 °C	solid	304L (EDF)	1.2%	rough
228	PWR @ 300 °C	solid	304L (EDF)	0.6%	smooth
228	PWR @ 300 °C	solid	304L (EDF)	1.2%	rough
228	PWR @ 300 °C	solid	304L (EDF)	0.6%	smooth
228	PWR @ 300 °C	solid	304L (EDF)	1.2%	smooth
228	PWR @ 300 °C	solid	304L (EDF)	0.6%	rough
229	VVER @ 300 °C	solid	national	0.6%	smooth
229	VVER @ 300 °C	solid	national	1.2%	smooth
229	VVER @ 300 °C	solid	national	0.6%	rough
229	VVER @ 300 °C	solid	national	0.6%	rough
229	VVER @ 300 °C	solid	national	1.2%	smooth

Table C.11 Test matrix at 300 °C in air and LWR environment at increased strain rate.

Finally, the test program for mean stress in strain control is listed in Table C.12.

Test	Lab	Environment	Specimen type	Material	Mean stress	Strain amplitude	Stress amplitude	Surface roughness
1	224	Air @ 300 °C	hollow	304L (EDF)	50 MPa	0.18%	-	polished
2	224	Air @ 300 °C	hollow	304L (EDF)	0 MPa	0.18%	-	polished

3	225	Air @ 300 °C	hollow	304L (EDF)	50 MPa	-	160 MPa	polished
4	225	Air @ 300 °C	hollow	304L (EDF)	0 MPa	-	160 MPa	polished
5	224	PWR @ 300 °C	hollow	304L (EDF)	50 MPa	0.18%	-	honed
6	224	PWR @ 300 °C	hollow	304L (EDF)	0 MPa	0.18%	-	honed
7	225	PWR @ 300 °C	hollow	304L (EDF)	50 MPa	-	155 MPa	honed
8	225	PWR @ 300 °C	hollow	304L (EDF)	0 MPa	-	155 MPa	honed
9	225	PWR @ 300 °C	hollow	304L (EDF)	0 MPa	-	155 MPa	honed

Table C.12 Test matrix for the campaign on mean stress in strain control.

REFERENCES

- [C.1] M. Bruchhausen, Test matrix for testing Phase I (air and LWR) (D2.07 and 14); INCEFA-PLUS Internal Report, 2016.
- [C.2] M. Bruchhausen, Test matrix for testing Phase II (air and LWR) (D2.09 and 16); INCEFA-PLUS Internal Report, 2018.
- [C.3] M. Bruchhausen, Test matrix for testing Phase III (air and LWR) (D2.11 and 18); INCEFA-PLUS Internal Report, 2019.

ANNEX D SUMMARY OF INCEFA-PLUS PROJECT PUBLICATIONS

This annex summarizes the main international publications by INCEFA-PLUS Consortium during the development of the project.

2016

ASME 2016 Pressure Vessels and Piping Conference (Vancouver, British Columbia, Canada):

- K. Mottershead, M. Bruchhausen, T. Métais, S. Cicero, D. Tice, and N. Platts, “INCEFA-PLUS: Increasing Safety in Nuclear Power Plants by Covering Gaps in Environmental Fatigue Assessment”, PVP2016-63149, ASME 2016 Pressure Vessels and Piping Conference. Vancouver, British Columbia, Canada, 2016.

XVIII International Colloquium Mechanical Fatigue of Metals; INCEFA-PLUS Special Session (Gijón, Spain):

- K. Mottershead, M. Bruchhausen, T. Métais, and S. Cicero, “INCEFA+ Programme Overview and Update”, XVIII International Colloquium Mechanical Fatigue of Metals. Gijón, Spain, 2016.

2017

ASME 2017 Pressure Vessels and Piping Conference (Waikoloa, Hawaii, USA):

- K. Mottershead, M. Bruchhausen, T. Métais, S. Cicero, and D. Tice, “INCEFA-PLUS: Increasing Safety in Nuclear Power Plants by Covering Gaps in Environmental Fatigue Assessment”, PVP2017-65256, ASME 2017 Pressure Vessels and Piping Conference. Waikoloa, Hawaii, USA, 2017.

ASTM Special Technical Publication:

- M. Bruchhausen, K. Mottershead, C. Hurley, T. Métais, R. Cicero, M. Vankeerberghen, and J. C. Le Roux, “Establishing a multi-laboratory test plan for environmentally assisted fatigue”, in STP1598-EB Fatigue and Fracture Test Planning, Test Data Acquisitions and Analysis, ASTM International, 2017.

2018

7th International Conference on Fracture Fatigue and Wear (Ghent, Belgium):

- M. Vankeerberghen, P. Marmy, and L. Bens, “PWR fatigue testing at SCK-CEN in the framework of INCEFA-PLUS”, 7th International Conference on Fracture Fatigue and Wear. Ghent, Belgium, 2018.

22nd European Conference on Fracture (Belgrade, Serbia):

- I. Procopio, S. Cicero, K. Mottershead, M. Bruchhausen and, S. Cuvilliez, “INCEFA-PLUS: Increasing Safety in Nuclear Power Plants by Covering Gaps in Environmental Fatigue Assessment”, 22nd European Conference on Fracture. Belgrade, Serbia, 2018.

ASME 2018 Pressure Vessels and Piping Conference; INCEFA-PLUS Special Session (Prague, Czech Republic):

- K. Mottershead, M. Bruchhausen, S. Cuvilliez, and S. Cicero, “INCEFA-PLUS: Increasing Safety in Nuclear Power Plants by Covering Gaps in Environmental Fatigue Assessment”, PVP2018-84034, ASME 2018 Pressure Vessels and Piping Conference. Prague, Czech Republic, 2018.
- M. Vankeerberghen, M. Bruchhausen, R. Cicero, L. Doremus, J. C. Le Roux, N. Platts, P. Spätig, M. Twite, and K. Mottershead, “Ensuring Data Quality for Environmental Fatigue: INCEFA-PLUS Testing Procedure and Data Evaluation”, PVP2018-84081, ASME 2018 Pressure Vessels and Piping Conference. Prague, Czech Republic, 2018.
- T. Austin, L. Lin, and T. Métais, “Standards-Based Technologies for Exchanging Fatigue Test Data”, PVP2018-84610, ASME 2018 Pressure Vessels and Piping Conference. Prague, Czech Republic, 2018.

2019

ASME 2019 Pressure Vessels and Piping Conference (San Antonio, Texas, USA):

- M. Bruchhausen, A. McLennan, R. Cicero, C. Huotilainen, K. Mottershead, J. C. Le Roux and, M. Vankeerberghen, “Environmentally Assisted Fatigue Data from the INCEFA-PLUS Project”, PVP2019-93085, ASME 2019 Pressure Vessels and Piping Conference. San Antonio, Texas, USA, 2019.
- K. Mottershead, M. Bruchhausen, S. Cicero and, S. Cuvilliez, “INCEFA-PLUS: Increasing Safety in Nuclear Power Plants by Covering Gaps in Environmental Fatigue Assessment”, PVP2019-93276, ASME 2019 Pressure Vessels and Piping Conference. San Antonio, Texas, USA, 2019.

FISA 2019 Conference (Pitesti, Romania):

- K. Mottershead, C. Robertson, S. Lindqvist, F. J. Perosanz, and E. Puska, “Safety assurance through advances in long-term operation”, 9th European Commission Conference on Euratom Research and Training in Safety of Reactor Systems. Pitesti, Romania, 2019.

2020

ASME 2020 Pressure Vessels and Piping Conference; INCEFA-PLUS Special Session (Virtual Conference):

- S. Cuvilliez, A. McLennan, K. Mottershead, J. Mann and, M. Bruchhausen, “INCEFA-PLUS Project: Lessons learned from the project data and impact on existing Fatigue Assessment Procedures”, PVP2020-21106, ASME 2020 Pressure Vessels and Piping Conference. Virtual Conference, 2020.
- K. Mottershead, M. Bruchhausen, S. Cicero and, S. Cuvilliez, “INCEFA-PLUS: Increasing Safety in Nuclear Power Plants by Covering Gaps in Environmental Fatigue Assessment”, PVP2020-21220, ASME 2020 Pressure Vessels and Piping Conference. Virtual Conference, 2020.
- M. Vankeerberghen, A. McLennan, I. Simonovski, G. Barrera, S. Arrieta, M. Ernestova, N. Platts, M. Scibetta, and M. Twite, “Strain Control Correction for Fatigue Testing in LWR Environments”, PVP2020-21373, ASME 2020 Pressure Vessels and Piping Conference. Virtual Conference, 2020.
- M. Bruchhausen, A. McLennan, R. Cicero, C. Huotilainen, K. Mottershead, J. C. Le Roux and, M. Vankeerberghen, “INCEFA-PLUS Project: Review of the Test Programme”, PVP2020-21377, ASME 2020 Pressure Vessels and Piping Conference. Virtual Conference, 2020.
- A. McLennan, P. Spätig, J. C. Le Roux, J. Waters, P. Gill, J. Beswick and, N. Platts, “INCEFA-PLUS Project: The Impact of using Fatigue Data generated from Multiple Specimen Geometries on the Outcome of a Regression Analysis” PVP2020-21422, ASME 2020 Pressure Vessels and Piping Conference. Virtual Conference, 2020.

METAL 2020 Conference (Conference Proceedings):

- G. Dundulis, A. Grybenas, M. Bruchhausen, R. Cicero, K. Mottershead, C. Huotilainen, J. C. Le Roux, and M. Vankeerberghen, “INCEFA-PLUS Project: Review of the test programme and main results”, 29th International Conference on Metallurgy and Materials. Brno, Czech Republic, 2020. *In press*.

Journal of Pressure Vessel Technology (ASME):

- S. Cuvilliez, A. McLennan, K. Mottershead, J. Mann, and M. Bruchhausen, “INCEFA-PLUS Project: Lessons Learned from the Project Data and Impact on Existing Fatigue Assessment Procedures”, *Journal of Pressure Vessel Technology*, 142(6), 2020.

Metals (MDPI) Special Issue; Environmental Fatigue Assessment of Met Metallic Materials and Components:

- S. Cicero, T. Métais, Y. Voloshyna, S. Cuvilliez, S. Arrieta, and R. Cicero, “Environmental fatigue analysis of nuclear structural components: Assessment procedures, loads, and a case study”, *Metals*, 10(5), 609, 2020.
- M. Vankeerberghen, M. De Smet, and C. Malekian, “Gauge-Strain-Controlled Air and PWR Fatigue Life Data for 304 Stainless Steel - Some Effects of Surface Finish and Hold Time”, *Metals*, 10(9), 1248, 2020.

- M. Bruchhausen, A. McLennan, S. Arrieta, T. Austin, R. Cicero, W. J. Chitty, L. Doremus, G. Dundulis, M. Ernestova, A. Grybenas, C. Huotilainen, J. Mann, K. Motterhshead, R. Novotny, F. J. Perosanz, N. Platts, J. C. Le Roux, P. Spätig, C. Torre Celeizábal, M. Twite and, M. Vankeerberghen, “Characterization of Austenitic Stainless Steels with regard to Environmentally Assisted Fatigue in Simulated Light Water Reactor Conditions”, *Metals*, 10, 2020. *Under preparation*.
- P. Spätig, “Mean stress effect on fatigue life of 304L austenitic steel in air and PWR environments determined with strain and load controlled experiments”, *Metals*, 10, 2020. *Under preparation*.
- C. Gourdin, G. Perez, H. Dhahri, J. C. Le Roux, and H. Matirouman, “PWR Effect On Crack Initiation Under Equi-biaxial Loading”, *Metals*, 10, 2020. *Under preparation*.
- I. Simonovski. M. Bruchhausen, R. Novotny, A. McLennan, K. Mottershead, P. Gill, N. Platts, J. L. Waters, M. Vankeerberghen, G. Barrera and, S. Arrieta, “Calculated shoulder to gauge ratio of fatigue specimens in PWR environment”, *Metals*, 10, 2020. *Under preparation*.

INCEFA-PLUS FINDINGS ON ENVIRONMENTAL FATIGUE

INCEFA-PLUS: INcreasing Safety in NPPs by Covering Gaps in Environmental Fatigue Assessment

©INCEFA-PLUS Consortium, 2020.

ISBN: 978-84-09-24496-6

<https://incefaplus.unican.es/>



This project has received funding from the Euratom Research & Training Programme 2014-2018 under grant agreement n° 662320.